UNIVERSITY OF LONDON THESIS

Degree PhD Year 2007 Name of Author EFKLIDOU, Sofia

Functions of the vFLIP protein of KSHV

Sofia Efklidou

Submitted to the University of London for the degree of Doctor of Philosophy

September 2007

Windeyer Institute, Division of Infection and Immunity

University College London

ProQuest LLC
789 East Eisenhower Parkway
P.O. Box 1346
Ann Arbor, MI 48106-1346

Abstract

KSHV infection is associated with both endothelial and B cell tumours. In KSHV the genes expressed in latency have been implicated in cell transformation. vFLIP is one of a small number of viral proteins expressed in latently infected tumour cells. In KSHV-infected primary effusion lymphoma (PEL) cells, vFLIP binds to, and persistently activates the IκB kinase complex, leading to constitutive activation of the canonical NF-κB pathway. We have previously shown in our lab that vFLIP directly interacts with the IKKγ subunit of the IKK complex (Field, *et al.*, 2003) to activate IKK. In this report, we demonstrate that vFLIP also activates the alternative NF-κB pathway, which involves processing of the p100 protein precursor and generation of the p52 subunit. Stable vFLIP expression in Jurkat cells stimulates expression of endogenous p100 and nuclear accumulation of p52 and RelB. Metabolic radiolabelling of transiently transfected 293T cells indicates that vFLIP promotes proteolysis of p100 and active generation of p52. Moreover, we show that vFLIP associates with p100 when over-expressed in Jurkat cells, or when endogenously expressed in PEL cells, and a region in the C-terminus of p100, which includes the p100 DD, is identified as the vFLIP binding region. Finally, inhibition of p100 and p52 production mediated by siRNA knockdown leads to the induction of apoptosis in PEL cells, inferring that vFLIP activation of the alternative NF-κB pathway contributes to PEL survival. These data demonstrate that vFLIP activates both canonical and alternative NF-kB pathways, a property shared with the Tax oncoprotein of HTLV-1 and LMP1 of EBV. In addition, we have examined the effect of vFLIP on primary human dermal microvascular endothelial cell (MVEC) survival, as vFLIP is expressed in the KSHV-infected cells within KS lesions. Stable vFLIP expression in MVECs induces the activation of the classical NF-κB pathway and the nuclear translocation of RelA/p65. vFLIP-mediated NF-κB activation prevents detachment-induced apoptosis (anoikis) of MVECs, but does not inhibit growth factor removal-induced apoptosis, by inducing the secretion of an additional paracrine survival factor(s). These data strongly support an important role for vFLIP in NF-κB activation, which may be crucial for cell transformation by KSHV, for the survival of infected cells, and for metastasis.

Acknowledgements

There are many people to thank for their support over the last three years. First are my two supervisors, Prof. Mary Collins and Prof. Chris Boshoff. Their guidance and encouragement has been invaluable, and I thank them both for everything. I would like to especially thank Mary Collins, for giving me the wonderful opportunity to work in her lab and learn so much by her side.

There are a number of people in Mary's lab who I should single out for their help, advice and friendship. Nigel Field, from whom I inherited the vFLIP project, was instrumental in guiding me through my first few weeks of my new project. David Escors, the king of cloning in the Collins lab, provided me with much help and ingenious solutions to problems, which made impossible cloning seem so easy in the end. Most of all I thank Ranbir, Marieke, Helen, and Emma, who have always managed to make it all seem worthwhile. Apart from great collegues, they have come to be some of my closest and dearest friends who have supported me through the best and worst of times during these four years. I cannot tell them how lucky I feel that I met them.Thanks also to everyone, past and present, in the Collins lab, to John Cheshire and everyone else in the admin office.

I have been friends with some very special people these last few years and it's made all the difference. So thanks to all the "treacles", and especially Jon, Judy, Lea, Yiannis, Lucas, and Antonis, for helping me enjoy life.

I would also like to express my gratitude to Dr Mahdad Noursadeghi for our NF-κB staining collaboration, to Dr Dimitios Lagos for the microarray analysis, to Prof. Ethel Cesarman for allowing me to work in her lab in New York, and to the Bogue Committee for granting me the Bogue Fellowship. In addition, I am indebted to the MRC for funding my studies.

Last but not least, thanks to my parents for their unwavering support, and my sister who has been my best friend and my guardian angel.

List of Contents, Figures and Tables

Contents

Figures

Tables

Abbreviations

AHV	alcelaphine herpesvirus
AIDS	acquired immuno deficiency syndrome
Aly	alymphoplasia
Ang	Angiopoietin
AP-1	activating protein-1
Apaf-1	apoptotic-protease activating factor-1
ARD	ankyrin repeat domain
ARE	AU-rich element
ATF-4	activating transcription factor-4
ATL	adult T cell leukaemia
ATP	adenosine triphosphate
BAFF	B cell activating factor
Bak	Bcl-2 antagonist/killer
Bax	Bcl-2 associated X protein
BCBL	body cavity based lymphoma
Bcl	B cell lymphoma
BCR	B cell receptor
BEC	blood endothelial cell
bFGF	basic fibroblast growth factor
BH	Bcl-2 homology
BHV	bovine herpesvirus
BIR	baculovirus IAP repeat
BLC	B lymphocyte chemoattractant
BMP	bone morphogenetic protein
bp	base pair
BR3	BAFF receptor 3
βTrCP	β-transducing repeat-containing protein
CAML	calcium-modulating cyclophilin ligand
CAMP	cyclic AMP
CARD	caspase recruitment domain
CBP	CREB-binding protein
CCR	coiled-coil region
CD	Castleman's Disease
CDC	cell division cycle
cdk	cyclin-dependent kinase
$cFLIP_{L/S}$	cellular FLIP long/short
ChIP	chromatin immunoprecipitation
CHUK	conserved helix-loop-helix ubiquitous kinase
cIL-6	cellular IL-6
cPPT	central polypurine tract
CREB	cAMP-response element-binding protein
CTAR	C-terminal activating region
C-terminus	carboxy-terminus
CTL	cytotoxic T lymphocyte
DAPI	4',6-diamidino-2-phenylindole
DED	death effector domain
DD	death domain
DISC	death inducing signalling complex
DMEM	Dulbecco's modified Eagle's medium
DMSO	dimethyl sulphoxide
DNA	deoxyribonucleic acid
dNTP	deoxynucleotide triphosphate mix

DR	death receptor
DR	direct repeat
ds	double strand
DTT	dithiothreitol
DUB	de-ubiquitinating
EBNA	Epstein-Barr nuclear antigen
EBV	Epstein-Barr virus
EC	endothelial cell
ECM	extracellular matrix
EDA-R	ectodermal dysplasia receptor
EDTA	ethylene-diamine-tetra-acetic acid
eGFP	enhanced green fluorescent protein
EHV	equine herpesvirus
ELC	Ebl-1-ligand chemokine
ELISA	Enzyme-Linked ImmunoSorbent Assay
EMCV	encephalomyocarditis virus
EMSA	electrophoretic mobility shift assay
Env	*HIV envelope*
Erk	extracellular signal-regulated kinase
E-selectin	endothelial-leukocyte adhesion molecule-selectin
EST	expressed sequence tag
Ets	E26 transformation specific sequence
FACS	fluorescent-activated cell sorter
FADD	Fas-associated death domain
FCS	foetal calf serum
Fig.	figure
FLICE	FADD-like-ICE
FLIP	FLICE-inhibitory protein
g	relative centrifugal force
gag	HIV group associated antigen
GCP	granulocyte chemotactic protein
GEM	gene expression microarray
GFP	green fluorescent protein
GM-CSF	granulocyte-macrophage colony-stimulating factor
GPCR	G-protein coupled receptor
GRR	glycine rich region
GSK-3β	glycogen synthase kinase-3 beta
GST	glutathione S-transferase
h	hours
HA	haemagglutinin
HAART	highly active anti-retroviral therapy
HAEC	human aortic endothelial cell
HAT	histone acetylase
Hax-1	HS-1 associated protein
HBSS	Hank's buffered salt solution
HCMV	human cytomegalovirus
hdMVECS	human dermal microvascular endothelial cells
HDAC	histone deacetylase
H-DNA	high GC content DNA
HED-ID	hypohidrotic ectodermal dysplasia with immune deficiency
HEK	human embryonic kidney
HGF	hepatocyte growth factor
HHV	human herpesvirus

HIV	human immunodeficiency virus
HLH	helix-loop-helix
HMG I(Y)	high mobiliy group I(Y)
HNSCC	head and neck squamous cell carcinoma
HPV	human papilloma virus
Hsp90	heat shock protein 90
HSV	herpes simplex virus
HTLV-1	human T cell leukaemia virus -1
HUVEC	human umbilical vein endothelial cell
HV	herpesvirus
HVA	herpesvirus ateles
HVS	herpesvirus saimiri
IAP	inhibitor of apoptosis
IB	immunoblot
ICAM	intercellular adhesion molecule
ICE	IL-1β converting enzyme
IFA	immunofluorescence assay
IFN	interferon
Ig	immunoglobulin
IKAP-1	IKK associated protein-1
IκB	inhibitor of κB
IKK	IκB kinase
IL	interleukin
IP	immunoprecipitation
IP	incontinentia pigmenti
IPTG	isopropylthio-β-D-galactoside
IRES	internal ribosome entry site
IRF	IFN regulatory factor
ISH	*in situ* hybridisation
ISRE	interferon stimulated response element
ISS	immunostimulatory sequences
ITAM	immuno receptor tyrosin-based motif
JNK	jun N-terminal kinase
Kb	kilobase
KDa	kilodalton
KLEC	KSHV-infected lymphatic endothelial cell
KRAB	Kruppel-associated box
K-RBP	KSHV-RTA binding protein
KS	Kaposi's sarcoma
KSHV	KS-associated herpesvirus
LANA	latent nuclear antigen
LB	Luria-Bertani
LBS	LANA binding sequence
L-DNA	low GC content DNA
LEC	lymphatic endothelial cell
LMP	latent membrane protein
LPS	lipopolysaccharide
LT	latent transcript
LTβR	lymphotoxin β receptor
LTR	long terminal repeat
LUR	long unique region
LYVE	lymphatic vessel endothelial receptor
LZ	leucine zipper
M	molar
MACH	MORT1-associated ced3 homologue

MALT	mucose associated lymphoid tissue
MAPK	mitogen activated protein kinase
MCD	multicentric Castleman's disease
mCi	mili-Curie
MCP	monocyte chemoattractant protein
MCV	molluscum contagiosum virus
Mg	microgram
MEF	mouse embryo fibroblast
MEKK	MAP/Erk kinase kinase
MHC	major histocompatibility complex
MHV	murine herpesvirus
min	minutes
MIP	macrophage inflammatory protein
MIR	modulator of immune recognition
MMP	matrix metalloproteinase
MOI	multiplicity of infection
MPC	MALT1/paracaspase
mRNA	messenger RNA
miRNA	micro RNA
MVEC	microvascular endothelial cells
NAP	neutrophil activating peptide
NBD	NEMO binding domain
nef	HIV negative regulatory factor
NEMO	NF-κB essential factor
NFAT	nuclear factor of T cells
NF-κB	nuclear factor of κ light polypeptide gene enhancer in B cells
NGF-R	nerve growth factor receptor
NIK	NF-κB inducing kinase
NLS	nuclear localisation signal
nm	nanometers
NOS	nitric oxide synthase
NP40	nonidet P-40
N-terminus	amino-terminus
OD	optical density
ORC	origin recognition complex
ORF	open reading frame
PAGE	polyacrylamide gel electrophoresis
PBS	phosphate buffered saline
PCR	polymerase chain reaction
PDGF	platelet-derived growth factor
PEL	primary effusion lymphoma
PHA	phytohaemagglutinin
PI	propidium iodide
PID	processing inhibitory domain
PI-3K	phosphatidylinositol 3-kinase
PIM	protein inhibitor mix
PKC	protein kinase C
PKR	dsRNA-activated serine-threonine protein kinase
PLC	phospholipase C
PMA	phorbal myristate acetate
PNK	polynucleotide kinase
pol	HIV polymerase
PP2A	protein phosphatase 2A

pRb	retinoblastoma protein
PRD	positive regulatory domain
PS	phosphatidyl serine
PTK	protein tyrosine kinase
RAFTK	related adhesion focal tyrosine kinase
RANK	receptor activator of NF-κB
RANTES	Regulated upon Activation, Normal T-cell Expressed, and Secreted
Rel	reticuloendotheliosis
rev	HIV regulator of virion protein expression
RFHV	retroperitoneal fibromatosis herpesvirus
RHD	rel homology domain
RIP	receptor interacting protein
RIPA	radioimmunoprecipitation lysis buffer
RNA	ribonucleic acid
RNAi	RNA-interference
RPMI	Roswell Park Memorial Institute 1640 medium
RRV	rhesus rhadinovirus
RTA	replication and transcription activator
RT-PCR	reverse transcription polymerase chain reaction
s	seconds
SAP	stress activated protein
SCF	SKP1 cullin F box
SDS	sodium dodecyl citrate
SEM	standard error of the mean
SH	src homology
SLC	secondary lymphoid tissue chemokine
Sr	super-repressor
STP	saimiri transformation-associated protein
SUMO	small ubiquitin-like modifier
SV40	simian virus 40
TAB	TAK1 binding protein
TAE	tris-acetate-EDTA
TAK1	TGFβ-activated kinase-1
tat	HIV transactivator of transcription
TBE	tris-borate-EDTA
TCR	T cell receptor
TGFβ	transforming growth factor-β
Th	T helper lymphocyte
Tip	tyrosine kinase interacting protein
TNF	tumour necrosis factor
TNF-R	TNF-receptor
TPA	tetradecanoyl phorbal acetate
TR	terminal repeat
TRADD	TNFR-associated death domain
TRAF	TNF-associated factor
TRAIL	TNF-related apoptosis-inducing ligand receptor
TRAMP	TNF-related apoptosis-mediating protein
TRIKA	TRAF6-regulated IKK activator
TWEAK	TNF-like weak inducer of apoptosis
VCAM	vascular cell adhesion molecule
vCBP	viral complement binding protein
vCLAP	viral CARD-like apoptotic protein
vcyclin	viral cyclin
VEGF	vascular endothelial growth factor

vFLIP	viral FLIP
vGPCR	viral G-protein coupled receptor
vif	HIV virion infectivity factor
VIP	variable ITAM-containing protein
vMIP	viral macrophage inflammatory protein
vpr	HIV viral protein R
vpu	HIV viral protein U
VSV-G	vesicular stomatitis virus G
WPRE	Woodchuck hepatitis virus post-transcriptional regulatory element

Chapter 1

Introduction

This study is an effort to further characterize the functions of the viral FLIP protein encoded by Kaposi's sarcoma-associated herpesvirus (KSHV). vFLIP is a multifunctional protein and one of the few proteins expressed during the latent phase of the viral life cycle. This protein was originally believed to protect virally-infected cells from death receptor-induced apoptosis, but has since been described as a unique protein among the viral FLIPs in its ability to activate the NF-κB signalling pathway. The first section of the introduction presents a review of the current literature on the biology of KSHV, with special attention paid to other KSHV genes that have important roles in viral pathogenesis and oncogenesis. The second section describes the NF-κB pathway, its mechanisms of activation, and its regulation. These sections provide the context for an account of the vFLIP protein of KSHV, its structure, and known functions, which comprises the third section.

1.2 Kaposi's sarcoma-associated herpesvirus (KSHV)

1.2.1 Discovery of KSHV

In 1981, amidst reports of an increased incidence of *Pneumocystis carinii*, a highly aggressive form of Kaposi's sarcoma (KS) was identified and termed "epidemic KS" (Borkovic and Schwartz, 1981; Gottlieb *et al.*, 1981). These two events heralded the onset of the AIDS epidemic (Service, 1981), which has killed more than 25 million people since it was first recognized on June 5, 1981, making it one of the most destructive epidemics in recorded history (UNAIDS/WHO 2006 AIDS epidemic update). Kaposi's sarcoma is an unusual neoplasm first described by the Hungarian dermatologist Moritz Kaposi in 1872, who published the case histories of five elderly male patients with "idiopathic multiple pigmented sarcomas of the skin" (Kaposi, 1872). This form of the disease, which later became known as "classical KS", affects elderly men of Mediterranean, Arabic or Jewish ancestry and is typically an indolent disease that affects the extremities and is rarely life threatening (Franceschi and Serraino, 1995). However, two other, more aggressive clinical forms of KS are now recognized. In some equatorial countries of Africa, KS has existed for many decades and has long preceded the emergence of HIV. This variant, known as "endemic KS", occurs in young children in the endemic zones in equatorial Africa and results in aggressive lymphadenopathy, rather than skin lesions (Bayley, 1984; D'Oliveira and Torres, 1972). Moreover, KS has been observed in renal transplant recipients and other patients receiving immunosuppressive therapy (similar to epidemic or AIDS-related KS), and is now known as iatrogenic or "post-transplant KS"(Harwood *et al.*, 1979).

Not until the advent of the AIDS epidemic, which drew attention to KS, did large-scale epidemiological studies of human immunodeficiency virus (HIV)-infected populations, produce strong evidence of a transmissible agent as the most likely etiological cause of KS (Beral *et al.*, 1990). Although first suspicions fell on HIV, it soon became clear that HIV infection alone could not account for KS development, as most cells, and all spindle cells, in an AIDS-

KS biopsy do not harbour the HIV genome (Staskus *et al.*, 1997). As KS most commonly develops in homosexual men with AIDS, rather than hemophiliacs with AIDS, or those who acquired the HIV virus through heterosexual contact (Beral *et al.*, 1990), it was likely that a sexually transmitted cofactor was involved in KS pathogenesis. The breakthrough in confirming the infectious nature of KS was reported in a seminal paper by Chang and colleagues in 1994. After examination of KS and normal tissue by representational difference analysis, trying to identify DNA sequences present in KS but absent in normal tissue, they discovered two DNA fragments that were uniquely present in the diseased tissue of an AIDS-KS patient, the first sighting of the KS-associated herpesvirus (KSHV) genome (Chang *et al.*, 1994). The 330 and 631 bp fragments were found to have significant amino acid identity to the capsid and tegument proteins of two primate gammaherpesviruses, Epstein-Barr virus (EBV) and herpesvirus saimiri (HVS), both capable of cellular transformation. From this point, molecular clones of the entire viral genome were developed (Moore *et al.*, 1996; Zhong *et al.*, 1996), and researchers could determine its complete DNA sequence (Russo *et al.*, 1996). Soon after, DNA belonging to KSHV was detected in cells derived from patients with primary effusion lymphoma (PEL), a rare lymphoma of B cells normally associated with AIDS (Cesarman *et al.*, 1995a; Cesarman *et al.*, 1995b). KSHV was also sequenced from a KS biopsy (Neipel *et al.*, 1998) and herpesvirus-like KSHV virions were visualized by electron microscopy (Orenstein *et al.*, 1997). Together, these data confirmed the classification of KSHV as the eighth human herpesvirus (HHV-8).

1.2.2 Viral Taxonomy

As determined by its genomic structure and sequence (Davison, 2002), KSHV has been assigned membership of the γ-herpesvirus sub-family of mammalian herpesviruses, which is characterized by the ability of the herpesviruses to replicate in lymphoblastoid cells. This can be further divided into two genera, namely the γ-1 or *Lymphocryptovirus* group, of which Epstein Barr virus (EBV) is the prototype member, and the γ-2 or *Rhadinovirus* group, of which herpesvirus saimiri (HVS) is the classic prototype (Fickenscher and Fleckenstein, 2001; Moore and Chang, 2001). KSHV is currently the single

known human member of the *Rhadinovirus* genus, its closest human relative being EBV (Alba *et al.*, 2001; McGeoch and Davison, 1999; Montague and Hutchison, 2000). The human herpesviruses are listed in Table 1.1. Although KSHV was thought to be more closely related to herpesvirus saimiri (HVS) of squirrel monkeys within the γ-2 herpesviruses, it has recently become apparent that rhadinoviruses more closely related to KSHV exist among Old World monkeys, including several macaque species and African green monkeys (Desrosiers *et al.*, 1997; Greensill *et al.*, 2000; Rose *et al.*, 1997).

Old World primate γ-2 viruses can be divided into two further groups, based on phylogenetic analysis of their available sequences. The first group is the retroperitoneal fibromatosis herpesvirus (RFHV) group, and KSHV is its only human member. The RFHV group also comprises two viruses detected by concensus PCR in retroperitoneal fibromatosis lesions of different macaque species. One of them was detected in lesions from pigtail macaques (*Macacca nemestrina*) and is termed RFHVMn, and the other in rhesus macaques (*Macacca mulatta*) and is called RFHVMm (Rose *et al.*, 1997). This group also has a member derived from African green monkeys (*Chlorocebus aethiops*), the virus ChRV1 (Greensill *et al.*, 2000). The second group is composed of another virus from rhesus macaques, called rhesus rhadinovirus (RRV) (Desrosiers *et al.*, 1997), and a virus from African green monkeys, called ChRV2 (Greensill *et al.*, 2000). KSHV seems to be more closely related to RFHVMn and RFHVMm, within the RFHV-like lineage (McGeoch, 2001), although some studies have suggested that RRV is the equivalent of KSHV in rhesus macaques (Searles *et al.*, 1999), as they have a similar genome organization and share most of the genes first identified in KSHV. An evolutionary tree for herpesviruses of the γ sub-family is shown in Figure 1.1. Moreover, KSHV-related sequences have also been detected in gorillas and chimpanzees (Lacoste *et al.*, 2000). With KSHV being the only human member of the RFHV group, the possibility remains that there is an as yet undetected human herpesvirus in the RRV group.

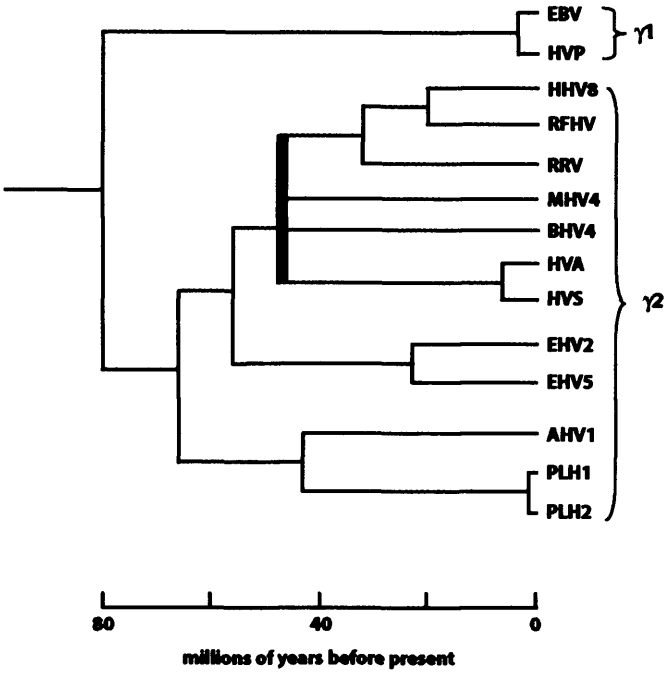

Figure 1.1 Composite phylogenetic tree for the γ-*Herpesvirinae*

The top-scoring tree for γ-*Herpesvirinae* obtained by a maximum-likelihood method (Codeml) based on eight-gene alignment (the inference of the phylogenetic tree is described in Materials and Methods of McGeoch *et al.* 2000). The region of uncertain branching around MHV4 is drawn as a multifurcation (heavy line). For purposes of presentation and for combining data from different trees, top-scoring trees were converted to a form that imposed a constant molecular clock to facilitate the interpolation of the different species. The time scale is based on a value of 47.6 Myr before present for the divergence of Old World and New World primate viruses (Kumar and Hedges, 1998). Sub-lineage designations are at the right. Figure 1.1 and the above figure legend have been generated by reproducing data from Figures 1 and 2 of McGeoch 2001, and Figure 4 of McGeoch *et al.* 2000, with the kind permission of Prof. Duncan J. McGeoch (Medical Research Council Virology Unit, Institute of Virology, University of Glasgow,). EBV, Epstein-Barr virus; HVP, *Herpesvirus papio;* HHV8, human herpesvirus 8 (or KSHV); RFHV, retroperitoneal fibromatosis herpesvirus of macaques; RRV, rhesus rhadinovirus; MHV4, murine herpesvirus 4; BHV4, bovine herpesvirus 4; HVA, *Herpesvirus ateles;* HVS, *Herpesvirus saimiri;* EHV2/5, equine herpesvirus 2/5; AHV1, alcelaphine (wildebeest) herpesvirus 1; PLH1/2, porcine lymphotropic herpesvirus 1/2.

Human Herpesviruses

Type	Synonym	Subfamily	Pathophysiology
HHV -1	Herpes simplex virus-1 (HSV -1)	α (alpha)	Oral and/or genital herpes (predominantly orofacial)
HHV -2	Herpes simplex virus-2 (HSV -1)	α	Oral and/or genital herpes (predominantly genital)
HHV -3	Varicella zoster virus (VZV)	α	Chickenpox and shingles
HHV -4	Epstein-Barr virus (EBV)	γ (gamma)	Infectious mononucleosis, Burkitts lymphoma, CNS lymphoma in AIDS patients, posttransplant lymphoproliferative syndrome (PTLD), nasopharyngeal carcinoma
HHV -5	Cytomegalovirus (CMV)	β (beta)	Infectious mononucleosis-like syndrome, retinitis
HHV -6, -7	Roseolovirus	β	Sixth disease(roseola infantum or exanthem subitum)
HHV -8	Kaposi's sarcoma associated herpesvirus (KSHV)	γ	Kaposi's sarcoma (KS), primary effusion lymphoma (PEL), a variant of multicentric Castlemans disease (MCD)

Table 1.1 Human Herpesviruses and their common infections

(Abbreviation: HV, herpesvirus)

1.2.3 Virion Structure

Herpesvirus virions are large, 200-500 nm in diameter, and share a characteristic architecture in which the double-stranded DNA genome is surrounded by a thick-walled nucleocapsid, a proteinaceous tegument layer (Steven, 1997), and a lipid bilayer envelope, which is derived from the host cell membrane but is studded with viral glycoproteins (Gibson, 1996; Homa and Brown, 1997). The genome of the virus is packaged as linearised double-stranded DNA at the core of this structure in liquid-crystalline form (Booy *et al.*, 1991). The 3D structure of the HHV-8 capsids revealed a capsid shell composed of 12 pentons, 150 hexons, and 320 triplexes arranged on an icosahedral lattice (Wu *et al.*, 2000) (Figure 1.2). This structure is similar to those of herpes simplex virus type 1 (HSV-1) and human cytomegalovirus (HCMV), which are prototypical members of α- and β-herpesviruses, respectively.

1.2.4 Genomic Organisation

The KSHV genome consists of a single long unique region (LUR) with low GC content (53.5%), which contains all of the coding sequences, flanked at each end by terminal repeats (TRs) with high GC content in excess of 84% (Russo *et al*, 1996; Schulz 1998). Similar to other rhadinoviruses, the LUR of KSHV comprises of 140.5 kb of "unique" DNA containing at least 85 open reading frames (ORFs), nearly 70 of which share sequence similarity to related gammaherpesviruses (Russo *et al*, 1996; Moore *et al*, 1996b; Neipel *et al*, 1997). The coding DNA is flanked by multiple 801 bp terminal repeats (Russo *et al*, 1996), to give a total size, estimated by native agarose gel, of 170 kb (Renne *et al.*, 1996a). The genome bears remarkable similarity to that of HVS, and the nomenclature of KSHV genes is derived from HVS, as the prototype of rhadinoviruses. The two viruses share 66 homologous genes upon which this nomenclature is based (Russo *et al.*, 1996). Within KSHV, these genes are numbered consecutively from left to right across the genome and given the prefix "ORF" (open reading frame). Novel ORFs, originally thought to be unique to KSHV, are interspaced within this structure and are designated K1 to K15. However, K3 (MIR1), K5 (MIR2), K7 (vIAP) and K13 (vFLIP) have

subsequently been found to have homologues and some additional unique genes have been added (including K4.1, K4.2, K8.1, K10.1, K10.5, K11.1, K14.1). Approximately half of the genes encoded by KSHV have now been ascribed a function, largely on the basis of sequence similarity to genes of known function (Holzerlandt *et al.*, 2002; Jenner and Boshoff, 2002). Amongst these genes are a striking number that have been pirated from the host during viral evolution, including viral homologues of interleukin-6 (vIL-6), IL-8R, Bcl-2, cyclin D, a G protein-coupled receptor and cFLIP. It has been proposed that many of these "pirated" genes were acquired because they allow the virus to directly manipulate the host cellular machinery (Choi *et al.*, 2001; Moore and Chang, 1998; Neipel *et al.*, 1997). The structure of the KSHV episome is depicted in Figure 1.3.

Although most of the LUR is highly conserved, there is marked sequence variability in the regions adjoining the terminal repeats, which manifest the contemporary evolution of KSHV. At the left end, the K1 gene, encoding a type 1 membrane glycoprotein, has evolved into four groups, whose protein sequences may vary by up to 40%. The K1 gene is therefore used to type KSHV into various subtypes (A, B, C, and D), which appear to correlate with the geographical origins of the viral isolates (Zong *et al.*, 1999). This pattern of variability is consistent with the idea that the four major KSHV clades evolved with individual populations (Cook *et al.*, 1999). At the right end of the viral genome, there is the K15 gene, expressed as a multiply spliced mRNA, which encodes a latent membrane protein, and has been substituted in some lineages by a distant homolog from an unknown herpesvirus (Glenn *et al.*, 1999; Poole *et al.*, 1999).

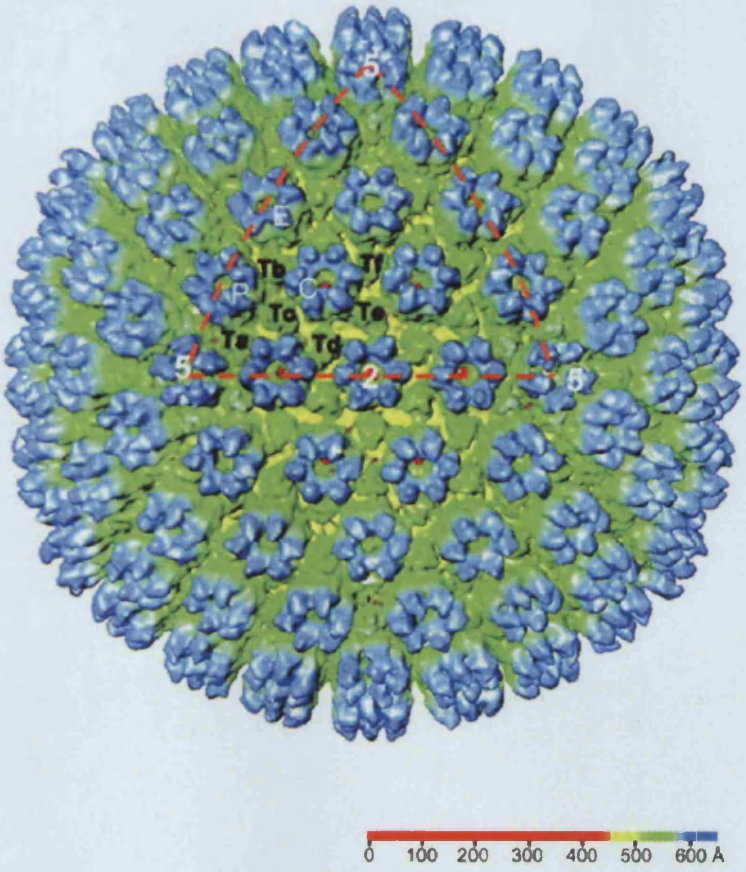

Figure 1.2 Three dimensional structure of the HHV-8 capsid

3D structure of the HHV-8 capsid at 24-Å resolution as viewed along the icosahedral twofold axis from the outside. The map is colour coded according to the particle radius (see colour bar at the bottom right), such that the upper domains of the pentons and hexons are in blue (between radii of 570 and 650 Å), the connecting triplexes are in green (between radii of 510 and 560 Å), the shell is in yellow (between radii of 460 and 510 Å), and the densities inside the capsid shell are in red (<460-Å radius). The capsid has a T=16 icosahedral symmetry (3 of the 12 fivefold axes are labelled 5, and 1 of the 20 triangular faces is outlined by a red dashed line), with the unique structural components in one asymmetric unit labelled, following the nomenclature established for HSV-1 (Steven *et al.*, 1986; Zhou *et al.*, 1994). These components include one-fifth of a penton (labelled 5), two and one-half hexons (one P, one C, and one-half of an E), and five and one-third triplexes (one each of the Ta, Tb, Tc, Td, and Te triplexes and one-third of the Tf triplex). Figure 1.2 and the above legend were generated by reproducing Figure 2 from Wu *et al.* 2000, with the kind permission of Dr. Z. Hong Zhou (Electron Imaging Center for Nanomachines, and Department of Microbiology, Immunology, and Molecular Genetics, UCLA, Los Angeles,).

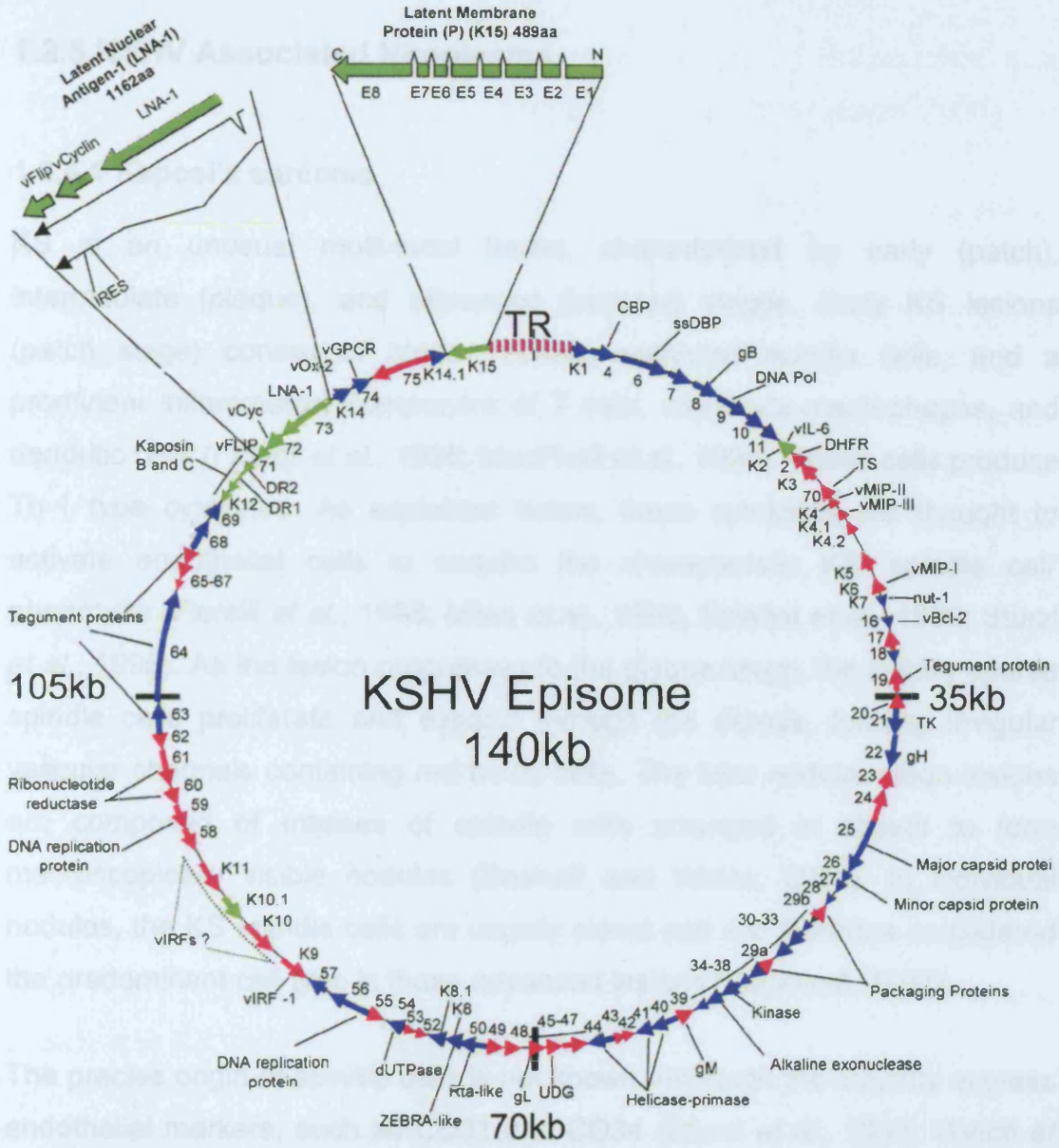

Figure 1.3 Structure of the KSHV episome

Numbers outside of the episome represent nucleotide base pairs in kilobases. Numbers within the episome indicate KSHV-encoded ORFs. Novel ORFs not present in other herpesviruses are designated K1 to K15. Blue arrows indicate ORFs encoded in a 5′ to 3′ positive polarity. Red arrows indicate ORFs encoded in a 3′ to 5′ negative polarity. Green arrows indicate ORFs encoding proteins expressed during latent infection. Annotations outside the episome indicate the putative function of each ORF. ORFs 71 to 73 are transcribed from the same promoter on a polycistronic transcript and the splice site for the intron is indicated. TR, terminal repeat DNA domains (pink stripes); CBP, complement-binding protein; ssDBP, single-stranded DNA binding protein; gB, glycoprotein B; DNA Pol, DNA polymerase; vIL-6, viral interleukin-6 homolog; DHFR, dihydrofolate reductase; vMIP, macrophage inflammatory protein; nut-1, nuclear tRNA–like transcript; vBcl-2, B-cell leukaemia/lymphoma-2; TK, thymidine kinase; TS, thymidylate synthase; gH, glycoprotein H; gM, glycoprotein M; UDG, uracil DNA glucosidase; gL, glycoprotein L; vFLIP, viral FLIP; vcyc, viral cyclin; vGPCR, viral G-protein–coupled receptor; (P), predominant form of K15; aa, amino acids; IRES, internal ribosomal entry site. Figure 1.3 and the above figure legend were generated by reproducing Figure 1 from Sharp and Boshoff, 2000, with the kind permission of Prof. Chris Boshoff (Cancer Research UK Viral Oncology Group, Wolfson Institute for Biomedical Research,).

1.2.5 KSHV Associated Neoplasms

1.2.5.1 Kaposi's sarcoma

KS is an unusual multi-focal lesion, characterized by early (patch), intermediate (plaque), and advanced (nodular) stages. Early KS lesions (patch stage) consist of blood vessels, scattered spindle cells, and a prominent inflammatory component of T cells, monocyte-macrophages, and dendritic cells (Fiorelli *et al.*, 1998; MacPhail *et al.*, 1996). These cells produce Th-1 type cytokines. As explained below, these cytokines are thought to activate endothelial cells to acquire the characteristic KS 'spindle cell' phenotype (Fiorelli *et al.*, 1998; Miles *et al.*, 1990; Sirianni *et al.*, 1998; Sturzl *et al.*, 1995). As the lesion progresses to the plaque stage, the initially sparse spindle cells proliferate and expand through the dermis, forming irregular vascular channels containing red blood cells. The later nodular stage lesions are composed of masses of spindle cells arranged in sheets to form macroscopically visible nodules (Boshoff and Weiss, 2001). In individual nodules, the KS spindle cells are usually clonal and are therefore considered the predominant cell type in these advanced lesions (Cockerell, 1991).

The precise origin of spindle cells is not known. Although the majority express endothelial markers, such as CD31 and CD34 (Sturzl *et al.*, 1992; Weich *et al.*, 1991), KS spindle cells display significant heterogeneity in marker expression. Many also express molecular markers suggesting lymphatic origin, including vascular endothelial growth factor receptor-3 (VEGF-R3), podoplanin, and lymphatic vessel endothelial receptor 1 (LYVE-1) (Dupin *et al.*, 1999; Jussila *et al.*, 1998; Weninger *et al.*, 1999). However, some cells are more characteristic of smooth muscle, macrophages and dendritic cells (Nickoloff and Griffiths, 1989; Sturzl *et al.*, 1992; Uccini *et al.*, 1994), leading researches to speculate that spindle cells may arise from pluripotent mesenchymal precursors. Another view, which is more favoured, suggests that KS spindle cells probably belong to an endothelial precursor that can differentiate into lymphatic cells, given the data on the ubiquitous expression of VEGFR-3 by spindle cells (Jussila *et al*, 1998; Dupin *et al*, 1999), and the

observation that clinical KS virtually never arises in tissues that lack lymphatics (e.g. the central nervous system) (Herndier and Ganem, 2001).

In early KS lesions, only a small proportion (<10%) of spindle and endothelial cells are positive for KSHV (Dupin *et al.*, 1999), and although KSHV can transform primary human endothelial cells *in vitro* (Flore *et al.*, 1998), KSHV genomes are not found in every transformed cell. This indicates that a paracrine contribution, such as the exchange of cytokines between cancer and host cells, is important spindle cell formation and the progression of KS lesions(Dupin *et al*, 1999). Both spindle cells, and the infiltrating inflammatory cells, express high levels of cellular IL-6 (cIL-6), basic fibroblast growth factor (bFGF), VEGF, IL-1β, TNFα and IFNγ (Fiorelli *et al.*, 1998; Miles *et al.*, 1990; Salahuddin *et al.*, 1988). cIL-6 promotes growth of KS cells *in vitro* (Miles *et al*, 1990), and IFNγ induces a spindle cell-like phenotype in endothelial cells (Fiorelli *et al*, 1998) and also reactivates latent virus (Chang *et al.*, 2000b). VEGF functions in synergy with bFGF as a KS cell growth factor, enhancing the development of KS-like lesions when human AIDS-KS cells were injected into mice (Ensoli *et al.*, 1989). Therefore it appears that unlike classical tumour cells, KS spindle cells are highly dependent upon paracrine growth signals, and KS lesions are "cytokine driven" tumours.

In nodular lesions, >90% of the spindle cells contain latent KSHV (Boshoff *et al.*, 1995; Dupin *et al.*, 1999; Staskus *et al.*, 1997). The KSHV latent proteins have the ability to induce cell growth, to block apoptosis and host immune responses, and to induce neoangiogenesis. These data infer that, unlike many of the classical tumours such as breast or colon cancer, KS begins as a polyclonal hyperplasia in which infected cells have a growth advantage (An *et al.*, 2002; Dupin *et al.*, 1999; Radkov *et al.*, 2000). This conclusion is supported by analyses of tumour clonality. Studies of X chromosome inactivation patterns suggest that both monoclonal and polyclonal patterns of inactivation exist (Delabesse *et al.*, 1997; Rabkin *et al.*, 1995; Rabkin *et al.*, 1997). A study of size heterogeneity in KSHV terminal repeats in nodular lesions demonstrated monoclonal, oligoclonal and polyclonal patterns of

infection, implying that KSHV infection preceded tumour expansion (Judde *et al.*, 2000).

1.2.5.2 Primary Effusion Lymphoma

Primary Effusion Lymphoma (PEL) is a rare malignant effusion of the peritoneal, pleural or pericardial cavities (hence originally called body cavity-based lymphoma, BCBL), usually without significant tumour mass or lymphadenopathy (Arvanitakis, 1996). These lymphomas occur predominantly in HIV-infected individuals with advanced stages of immunosuppression, but are also seen occasionally in HIV seronegative patients (Boshoff and Weiss, 1998; Schulz, 1998). The lymphoma cells combine features of immunoblastic and anaplastic large cell lymphomas (Gaidano *et al.*, 1996). They display a large cytoplasm, irregular and pleomorphic nuclei with prominent nucleoli, and significant size heterogeneity (Schulz, 2001).

Studies of rearrangements of immunoglobulin genes have indicated a B cell origin for these lymphoma cells (Knowles *et al.*, 1989; Walts *et al.*, 1990), although rare cases of KSHV-positive PEL expressing T cell markers have been described (Said *et al.*, 1999). The presence of clonal immunoglobulin gene rearrangement and monoclonal terminal repeats, demonstrate a monoclonal origin in most cases (Cesarman *et al.*, 1995b; Knowles *et al.*, 1989). A recent study, using microarrays to group B cell tumours by comparing their expression profiles, found that PEL gene expression was most similar to that of plasma cell tumours (Jenner *et al.*, 2003). These data support previous observations that PEL cells frequently express CD138 (Gaidano *et al.*, 1999), an adhesion molecule selectively associated with late stages of B-cell differentiation. Southern blot analysis of PEL cells has shown that the KSHV genome is present at a high copy number, 50-150 copies per cell, which is substantially higher than that observed in KS-infected spindle cells (Arvanitakis *et al.*, 1996; Cesarman *et al.*, 1995b; Gessain *et al.*, 1997; Renne *et al.*, 1996a). PEL is a distinct neoplasm that is strongly associated with KSHV infection (Carbone *et al.*, 1996; Karcher and Alkan, 1997; Pastore *et al.*, 1995). Nonethesless, co-infection with EBV is found in most PEL cases (Cesarman *et al*, 1995a; Cesarman *et al*, 1995b) and PEL is rarely found in

the absence of AIDS. Thus EBV infection and immunosuppression probably contribute to the pathogenesis of PEL. However, the expression of EBV latent genes such as EBNA 2, EBNA 3 and LMP1 is restricted in these cells (Callahan *et al.*, 1999; Horenstein *et al.*, 1997; Szekely *et al.*, 1998), making it less likely that EBV is driving their proliferation. Furthermore, examples of PEL containing only KSHV have been reported, from which cell lines have been derived (Arvanitakis *et al.*, 1996; Boshoff *et al.*, 1998; Carbone *et al.*, 2000; Carbone *et al.*, 1998; Said *et al.*, 1996). When injected into nude mice, such cells can induce PEL-like lymphomas (Boshoff *et al.*, 1998; Said *et al.*, 1996). PEL is unusual amongst B cell malignancies in the absence of an association with any consistent genetic lesion such as mutations of genes encoding c-myc, ras or p53 (Cesarman *et al.*, 1995a; Gaidano *et al.*, 1999; Karcher and Alkan, 1997). The absence of a common mutation and the discovery of PEL in the absence of EBV support the concept that KSHV is directly responsible for transformation in these lymphomas.

1.2.5.3 Multicentric Castleman's Disease

Multicentric Castleman's Disease (MCD) is a systemic variant of Castleman's disease (CD), a rare lymphoproliferation often diagnosed in HIV patients (Castelman, 1956), and is associated with the development of secondary B-cell lymphoma, multiple organ involvement, and systemic symptoms such as weight loss and fever (Frizzera *et al.*, 1983). KSHV is linked with a subgroup of MCD. KSHV infection is found in more than 90% of AIDS patients with MCD, but only 40% of HIV-seronegative MCD patients (Chadburn *et al.*, 1997; Grandadam *et al.*, 1997; Soulier *et al.*, 1995). In affected lymph nodes, KSHV is present in plasmablasts belonging to the B-cell lineage that localise to the mantle zone of B cell follicles (Dupin et al, 1999; Katano et al, 2000). These plasmablasts are not present in KSHV-negative MCD (Dupin *et al.*, 1999). Since the presence of plasmablasts in MCD is specifically associated with KSHV infection, a distinct plasmablastic variant of MCD is now recognised (Dupin *et al*, 2000). Unlike PEL cells, co-infection with EBV has not been detected in plasmablasts (Du *et al.*, 2001; Dupin *et al.*, 2000).

The KSHV-positive plasmablasts in MCD invariably express high levels of cytoplasmic IgM λ (Dupin *et al.*, 2000), whether occurring as isolated cells, in

microscopic aggregates, or in the plasmablastic lymphomas, suggesting that these cells are a monotypic. However, Ig gene rearrangement analysis has since shown that these monotypic cells are polyclonal (Du *et al.*, 2001). KSHV-infected plasmablasts do not harbour somatic mutations in the rearranged Ig gene, indicating that they originate from naïve B cells, despite they mature phenotype. KSHV-positive plasmablasts express high levels of viral IL-6 (Moore *et al.*, 1996), and it is possible that vIL-6 plays a role in the proliferation of these KSHV-infected B cells by autocrine and paracrine mechanisms.

1.2.6 Patterns of Gene Expression in KSHV

Like all herpesviruses, KSHV can adopt either of two replicative programs, which are known as latency and lytic replication. In latency, viral gene expression is heavily restricted, with only a small subset of viral genes being expressed (Cohrs and Gilden, 2001). During latent infection the virus exists as a multicopy circular episomal DNA in the nucleus, and no progeny virions are produced (Boshoff *et al.*, 1995). Most KS spindle cells can be shown to be latently infected, with only a small subpopulation of spindle cells (1%-3%) displaying lytic replication (Dupin *et al.*, 1999; Staskus *et al.*, 1997). Examination of late KS (nodular KS) lesions, shows that virtually all spindle-like cells are latently infected (Dupin *et al.*, 1999), which implies that latently infected cells have a growth or survival advantage in vivo by establishing persistent infection and avoiding immune surveillance. In contrast, lytic replication involves the temporally regulated expression of virtually the entire viral genome, with viral DNA replication and production of infectious progeny, in the course of which the host cell dies (Jenner *et al.*, 2001). Hence the lytic cycle has traditionally been thought not to contribute directly to oncogenesis because cells that enter this program invariably die. The genes expressed in latency are therefore predicted to play a major role in the tumourigenesis associated with KSHV infection (Chang and Moore, 1996). However, accumulating evidence suggests that the expression of latent proteins may not be sufficient to initiate Kaposi's sarcoma. Conversely, expression of the KSHV-encoded lytic gene viral G-protein-coupled receptor (vGPCR) by endothelial-specific retroviral infection is sufficient to induce Kaposi's

sarcoma-like tumours in mice (Montaner *et al.*, 2003). Therefore, lytic replication is now believed to play a critical role in tumorigenesis, since it is possible that continuous low-level reactivation leads to efficient viral transmission and disease development in infected cells. Moreover, it is likely that cellular and viral cytokines produced during the lytic cycle, provide a favourable environment for the proliferation of infected cells (Chang *et al.*, 2000b; Deng *et al.*, 2002; McCormick and Ganem, 2005; Nicholas *et al.*, 1997). Lytic replication can be induced from the latent state by the expression of a single viral gene from ORF50, which encodes the "replication and transcription activator" (RTA) (Lukac *et al.*, 1998; Sun *et al.*, 1998). RTA functions as a transcription factor, activating the expression of multiple downstream target genes, as well as that of its own gene (Deng *et al.*, 2000a; Ragoczy and Miller, 2001). In vitro, this can be achieved by the treatment of cells with tetradecanoyl phorbal acetate (TPA) or sodium butyrate (Arvanitakis *et al.*, 1996; Renne *et al.*, 1996b), or transfection with constitutively active RTA alleles, and these methods have been used to assign KSHV genes to lytic and latent phases. More recently, a genome-wide cell-based screen on latently infected PEL cells, utilizing an arrayed cDNA expression library, was used to investigate the cellular pathways involved in regulating transcription and expression of RTA, and therefore KSHV reactivation. The screen revealed that the Raf/MEK/ERK/Ets-1 pathway mediates Ras-induced reactivation by activating the RTA promoter, and the same pathway seems to be responsible for mediating the spontaneous KSHV reactivation (Yu *et al.*, 2007). Moreover, the KSHV-RTA binding protein (K-RBP), a cellular protein that acts as a transcriptional repressor due to its Kruppel-associated box (KRAB) and adjacent zinc-finger motifs, was recently shown to be responsible for suppressing RTA-mediated transactivation and KSHV lytic replication (Yang and Wood, 2007). It seems that KSHV utilizes this cellular protein as a regulator to maintain a balance between latency and lytic replication.

The first genome-wide analysis of KSHV gene expression was made using the BC-1 PEL cell line (EBV and KSHV infected) (Sarid *et al.*, 1998). Using DNA probes across the viral genome, Northern analysis was made of cells during normal culture (i.e. latent infection) and following TPA treatment (Sarid *et al.*, 1998). On this basis, the genes were divided into three classes:

Class I Expressed in normal culture (latency) and unaffected by TPA treatment

Class II Expressed in normal culture but upregulated by TPA treatment

Class III Expressed only upon TPA treatment

This study was the first to recognise the Class I "latency associated cluster" of LANA, v-cyclin and vFLIP (Sarid *et al.*, 1998). The latent classification of this cluster has been confirmed by their expression in a range of KSHV-infected tissues (Dittmer *et al.*, 1998; Low *et al.*, 2001). The Class II genes included small polyadenylated RNAs and most of the pirated viral genes (viral cytokines and signal transduction genes) (Sarid *et al.*, 1998). The Class III genes largely consisted of viral structural and replication-associated genes. The kaposin (K12) gene was initially identified as Class III (Sarid *et al.*, 1998), however, in-situ hybridisation of spindle cell populations demonstrated expression of kaposin in >85% of spindle cells, and confirmed its classification as a latent gene (Staskus *et al.*, 1997). More recently, microarrays have been used to study the kinetics of gene expression during induction of lytic replication, and these studies have largely confirmed the original classifications (Jenner *et al.*, 2001; Paulose-Murphy *et al.*, 2001).

1.2.7 KSHV latent genes implicated in viral pathogenesis

Altogether, six proteins are known to be expressed in latently infected KS cells. All have the ability to modulate growth of infected cells, and may therefore have a role in viral pathogenesis (Table 1.2). Their functions are discussed in detail below.

1.2.7.1 The latency associated cluster

The adjacent ORFs 71, 72 and 73 encode vFLIP, v-cyclin and the latent nuclear antigen (LANA) respectively. They are transcribed as two differentially spliced and polycistronic mRNAs from the same locus and their expression is controlled by a single constitutively active promoter (Cesarman *et al.*, 1996; Dittmer *et al.*, 1998; Grundhoff and Ganem, 2001). Latent transcript 1 (LT1) encodes LANA, v-cyclin and vFLIP, and LT2 encodes v-cyclin and vFLIP (Grundhoff and Ganem, 2001; Low *et al.*, 2001; Renne *et al.*, 2001; Talbot *et al.*, 1999). LANA is translated from LT1, while both vFLIP and v-cyclin are translated from LT2 by means of an internal ribosome entry site (IRES) within ORF72 (Bieleski and Talbot, 2001; Grundhoff and Ganem, 2001; Low *et al.*, 2001). The promoter region is bi-directional, regulating constitutive expression of LT1 and LT2 to the left and expression of the lytic genes, K14 and vGPCR, to the right (Dittmer et al, 1998; Sarid et al, 1999; Talbot et al, 1999; Jeong et al, 2001). The K12 locus, which codes for kaposin, is separated from the latency transcript (LT) cluster by a ~4Kb intergenic region that includes one or two origins of lytic replication (AuCoin *et al.*, 2004; Lin *et al.*, 2003). Within this region, recent studies have identified a cluster of 12 microRNA (miRNA) genes, which code for a total of 17 miRNAs in PEL cells (Cai and Cullen, 2006; Cai *et al.*, 2005; Pfeffer *et al.*, 2005; Samols *et al.*, 2005). Since KSHV miRNAs are co-ordinately expressed with the genes for LANA, v-cyclin, vFLIP, and kaposin, which all modulate the host cellular environment as described below, it is thought that they target host gene expression and, as a result, play a role in viral pathogenesis (Gottwein *et al.*, 2006; Sullivan, 2007). Figure 1.4 shows a schematic representation of the latency gene cluster of KSHV with its array of overlapping transcripts.

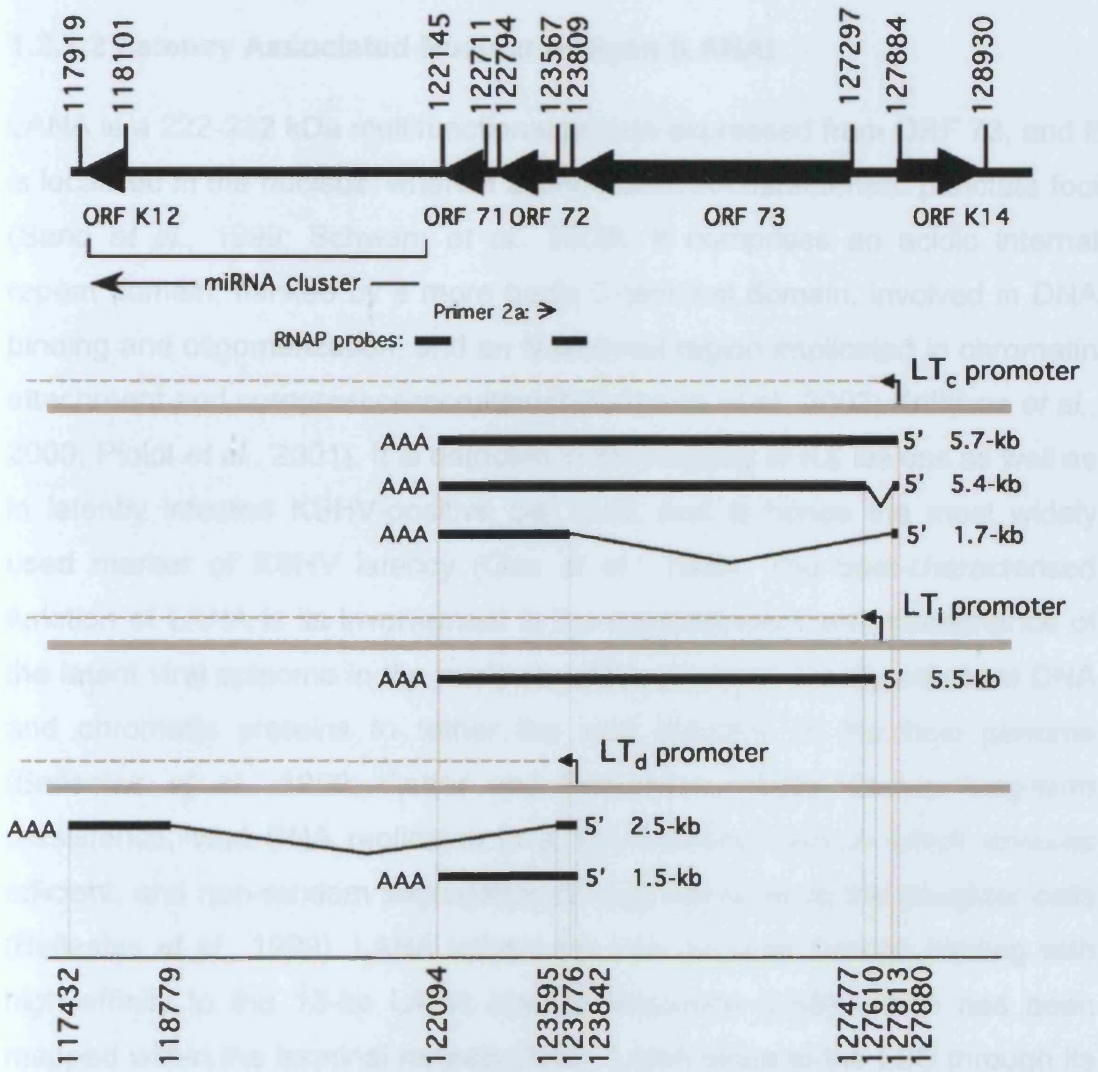

Figure 1.4 The latency gene cluster of KSHV

Organisation of known ORFs, miRNAs, and mRNA transcripts within the major latency cluster of KSHV, which is expressed via a network of overlapping transcripts. Coordinates are based on the prototype BC-1 sequence (Russo *et al.*, 1996) and correspond to initiation/termination codons (upper set) and exon sequences (lower set). A cluster of 11 miRNA genes, orientated in the direction indicated by an arrow, are located between the body of the K12 ORF (nucleotide 117,970) and the 3' end of ORF 71 (nucleotide 121,911) (Cai *et al.*, 2005; Pfeffer *et al.*, 2005; Samols *et al.*, 2005). RNAP, RNase protection assay probe. A constitutively active promoter (LTc) gives rise to a precursor RNA (dotted line) that undergoes polyadenylation/cleavage and alternative splicing to produce ~5.7-kb and ~5.4-kb tricistronic (ORFs 71, 72, and 73) and ~1.7-kb dicistronic (ORFs 71 and 72) mRNAs (Dittmer *et al.*, 1998; Sarid *et al.*, 1999; Talbot *et al.*, 1999). Expression of the lytic activator RTA induces a second promoter (LTi) located between ORF 73 and LTc, giving rise to a 5.5-kb mRNA spanning all three ORFs (Matsumura *et al.*, 2005). A 2.3- to 2.5-kb spliced mRNA corresponding to ORF K12, encoding multiple isoforms of kaposin, is transcribed during latency from a promoter at the 3' end of ORF 73 (LTd) and is induced further during lytic replication (Li *et al.*, 2002; Sadler *et al.*, 1999). Shorter K12 transcripts initiating at 118,758 have also been reported (Sadler *et al.*, 1999). Figure 1.4 and the above legend were generated by reproducing Figure 1 from Pearce *et al.* 2005, with the kind permission of Dr. Angus Wilson (Department of Microbiology and NYU Cancer Institute, NYU School of Medicine,).

1.2.7.2 Latency Associated Nuclear Antigen (LANA)

LANA is a 222-232 kDa multifunctional protein expressed from ORF 73, and it is localised in the nucleus, where it accumulates in characteristic punctate foci (Sarid *et al.*, 1999; Schwam *et al.*, 2000). It comprises an acidic internal repeat domain, flanked by a more basic C-terminal domain, involved in DNA binding and oligomerization, and an N-terminal region implicated in chromatin attachment and corepressor recruitment (Krithivas *et al.*, 2002; Krithivas *et al.*, 2000; Piolot *et al.*, 2001). It is detected in the majority of KS lesions as well as in latently infected KSHV-positive cell lines, and is hence the most widely used marker of KSHV latency (Gao *et al.*, 1996). The best-characterised function of LANA is its involvement in the establishment and maintenance of the latent viral episome in the nucleus. LANA interacts directly with host DNA and chromatin proteins to tether the viral episome to the host genome (Ballestas *et al.*, 1999; Cotter and Robertson, 1999). During long-term persistence, viral DNA replicates in a synchronized fashion which ensures efficient, and non-random segregation of viral episomes to the daughter cells (Ballestas *et al.*, 1999). LANA tethers the viral genome through binding with high affinity to the 13-bp LANA binding sequence (LBS), which has been mapped within the terminal repeats (TRs). LANA binds to the LBS through its carboxy-terminal DNA binding domain (996-1139 amino acids), and C-terminal LANA oligomerises to bind the TR DNA, a process which is critical for DNA binding (Ballestas and Kaye, 2001; Cotter *et al.*, 2001; Garber *et al.*, 2002; Garber *et al.*, 2001; Komatsu *et al.*, 2004; Lim *et al.*, 2002; Renne *et al.*, 2001; Schwam *et al.*, 2000). Additionally, the amino terminus of LANA is responsible for nuclear targeting and binding to human chromosomes (Piolot *et al.*, 2001), and has been shown to bind histone H1, tethering the viral episomes to the host chromatin (Cotter and Robertson, 1999). LANA contains two independent chromosome association regions, one within its N-terminus, and another in the C-terminus. The 1-22 N-terminal residues of LANA bind directly to an acidic patch on the core histone dimers H2A-H2B (Barbera *et al.*, 2006), whereas a short 15aa region in the C-terminal part is responsible for the association with heterochromatin (Viejo-Borbolla *et al.*, 2003).

LANA also associates directly with DNA replication origin recognition complexes (ORC) 1 and 2, which are primarily associated with the terminal repeat of the KSHV genome (Verma *et al.*, 2006b). Binding of LANA to the TR confers transcriptional silencing on the promoter of the neighbouring lytic gene K1 (Verma *et al.*, 2006a), and LANA can also suppress the activity of the key lytic regulator RTA, by directly binding to the recombination signal sequence-binding protein Jkappa (RBP-Jkappa), whose interaction with RTA activates the expression of lytic viral genes (Lan *et al.*, 2005). Therefore, LANA is believed to play an important role in the suppression of lytic viral genes and maintenance of viral latency.

The secondary structure of LANA suggests that there are potential sites for interactions with various cellular factors involved in transcription, and hence LANA is capable of both activating and repressing transcription (An *et al.*, 2002; Lim *et al.*, 2002; Renne *et al.*, 2001; Verma *et al.*, 2007). LANA specifically activates the AP-1 response element to induce expression of cellular interleukin-6 (IL-6) (An *et al.*, 2002; An *et al.*, 2003). It also activates the human telomerase reverse transcriptase promoter, as well as the HIV LTR cooperating with the Tat protein expressed by HIV-1 (Hyun *et al.*, 2001; Knight *et al.*, 2001); these data imply a role for LANA in maintaining the proliferative potential of KSHV-infected cells. In transfected cells, LANA binds p53, blocking its ability to act as a transcriptional activator and conferring increased resistance to p53-dependent apoptosis (Friborg *et al.*, 1999). LANA has also been reported to bind the tumour suppressor Rb (Radkov *et al.*, 2000), and in transfected cells this leads to enhanced expression of E2F-dependent reporter genes. This indicates that Rb binding by LANA is associated with loss of Rb function and progression through the G1 cell cycle check-point. LANA also binds a number of cellular proteins involved in transcriptional regulation such as CBP (Lim *et al.*, 2001), RING3 and DEK1 (Platt *et al.*, 1999), ATF4/CREB2 (Lim *et al.*, 2000), EC_5S Ubiquitin Complex (Cai *et al.*, 2006), and members of the mSin3 corepressor complex (Krithivas *et al.*, 2000). The interactions between LANA and chromatin remodelling proteins indicate a role for LANA in regulating global transcriptional activity of the infected cell as an

epigenetic modifier, which results in altered host gene expression, and may contribute to viral oncogenesis.

Another potential role for LANA in tumourigenesis derives from its interaction with GSK-3β, a kinase that inactivates β-catenin (Fujimuro *et al.*, 2003). When LANA binds GSK-3β, it relocates the kinase from the cytosol to the nucleus, which allows stabilization and cellular accumulation of β-catenin. Oligomerisation of β-catenin with the transcription factor LEF activates a proliferative program that includes expression of cyclin D, c-Myc, and c-jun. Apart from β-catenin, GSK-3β phosphorylates numerous substrates, including c-Myc (Jope and Johnson, 2004), and therefore regulates their turnover. It was recently shown that PEL cells have abnormally stable c-Myc protein, due to LANA-mediated inhibition of GSK-3β phosphorylation of the T58 residue of c-Myc (Bubman *et al.*, 2007). Inability to phosphorylate c-Myc on T58 leads to increased oncogenisity (Henriksson *et al.*, 1993; Pulverer *et al.*, 1994), and defects in apoptotic death (Chang *et al.*, 2000a; Conzen *et al.*, 2000). Therefore LANA's inhibition of c-Myc T58 phosphorylation seems to contribute to transformation by prolonging the c-Myc half-life and inhibiting its pro-apoptotic functions in PEL cells.

These findings indicate that LANA is a multifunctional protein, involved in modulating activation and repression of transcription, and these activities are important for the regulation of cell proliferation and apoptosis in KSHV-infected cells.

1.2.7.3 Viral Cyclin (v-cyclin)

KSHV-encoded v-cyclin, ORF72, is the viral homologue to cellular cyclin, most closely related to cyclin D2 (32% identity and 54% similarity) (Li *et al.*, 1997). The v-cyclin gene is located immediately downstream of that for LANA, and, like LANA, is expressed during latency in PEL cell lines (Dittmer *et al.*, 1998; Talbot *et al.*, 1999). It shares a number of functional properties with its cellular counterpart; it binds to, and activates cdk6 (Chang *et al.*, 1996), which then phosphorylates pRb, releasing the transcription factor E2F. E2F in turn, activates the transcription of S-phase genes and promotes G1-S phase cell

cycle progression (Godden-Kent *et al.*, 1997). However, unlike its cellular counterpart, the activity of v-cyclin/cdk6 complexes cannot be limited by the CDK inhibitors $p16^{INKa}$, $p21^{CIP1}$ and $p27^{KIP1}$ (Ellis *et al.*, 1999; Mann *et al.*, 1999; Swanton *et al.*, 1997). In fact, the v-cyclin/cdk6 complex appears to inactivate $p27^{KIP1}$, by phosphorylation-mediated degradation and mislocalisation in the cytoplasm (Ellis *et al.*, 1999; Mann *et al.*, 1999; Sarek *et al.*, 2006), and $p21^{CIP1}$, by phosphorylation on serine 130, which is then unable to bind cdk2 (Jarviluoma *et al.*, 2006). Thus, exogenous expression of v-cyclin from the infecting viral genome prevents CDK inhibitors-imposed G1 arrest, and stimulates entry into S-phase. Moreover, the v-cyclin/cdk6 complex shows broader substrate specificity than cellular cyclin/cdk6. v-cyclin/cdk6 can phosphorylate cdk2 substrates, including ORC1, CD26, $p27^{KIP1}$, and histone H1 (Verschuren *et al.*, 2004).

However, in the presence of v-cyclin, cells that express elevated levels of cdk6 undergo apoptosis (Ojala *et al.*, 1999) due to the phosphorylation and inactivation of the cellular antiapoptotic factor Bcl-2 (Ojala *et al.*, 2000). It is unclear how this problem of apoptosis is mitigated in vivo, but the low levels of v-cyclin expressed in latency may provide one explanation, and the antiapoptotic effects of other latency proteins (LANA, vFLIP) may represent another. Relevant to this hypothesis is the observation that v-cyclin induces p53-dependent growth arrest in primary cells, but causes lymphomas in p53-null mice (Verschuren *et al.*, 2002). Since LANA can disrupt p53 function and is expressed in conjunction with v-cyclin, this may explain how the virus can benefit from a protein that is apparently pro-apoptotic. Moreover, the KSHV-encoded vBcl-2, a homologue to the cellular gene, interacts with and inhibits the proapoptotic function of the cellular Bcl-2 family member (discussed below) (Ojala *et al.*, 2000).

Viral FLIP (vFLIP)

VFLIP is discussed in great detail elsewhere

1.2.7.4 Kaposin

The kaposin transcript is the most abundantly expressed transcript in KSHV latent infection, and in situ hybridisation analysis detected this transcript in the majority of KS spindle cells (Staskus *et al.*, 1997), and in PEL cells (Sturzl *et al.*, 1999). In addition, the promoter of the kaposin locus, which is separate from the LANA promoter, is strongly induced during lytic replication owing to the presence of at least one high-affinity binding site for the lytic switch protein RTA (Chang *et al.*, 2002b; Song *et al.*, 2003). The single 2.5 kb kaposin mRNA, located at the K12 locus, encodes at least three proteins, expressed via translation of alternative reading frames, and utilization of non-AUG codons upstream of K12 in addition to the AUG codon that defines the start of the K12 ORF (Li *et al.*, 2002; Sadler *et al.*, 1999) (Figure 1.4). The 3' end of the transcript has a small ORF that codes for kaposin A, a 60 amino acid hydrophobic membrane polypeptide (Tomkowicz *et al.*, 2002), which has been shown to mediate cell transformation in Rat-3 cell/nude mouse models (Muralidhar *et al.*, 1998). Kaposin A can bind cytohesin-1, a guanine nucleotide exchange factor for ARF GTPases, and a regulator of integrin-mediated cell adhesion. This binding triggers anchorage independent growth and loss of contact inhibition (Kliche *et al.*, 2001). Kaposin B is translated from the most 5' CUG codon (in frame 2) in the major kaposin transcript and comprises 23 amino acid repetitive sequences derived from direct repeat (DR1 and DR2) elements but contains no K12-derived amino acids; kaposin C is translated from a downstream CUG codon (in frame 1) and comprises a fusion of DR1/DR2 and K12-encoded sequences (Sadler *et al.*, 1999). Kaposin B functions as an adapter protein in signal transduction, by binding to and activating a kinase, MK2, that is normally a target of p38 phosphorylation (McCormick and Ganem, 2005). MK2 appears to be a central regulator of mRNA stabilisation for cytokines (IL-1/3/4/6, TNF, GM-CSF), growth factors (VEGF), and oncoproteins (myc and fos) that harbour AU-rich elements (AREs) in their 3' UTRs, rendering the transcripts unstable (Shaw and Kamen, 1986). Activated MK2 stabilises these mRNAs, and hence kaposin B expression blocks the degradation of ARE-containing mRNAs and substantially enhances cytokine release (McCormick and Ganem, 2005). It

was recently shown that this mRNA stabilization function of kaposin B requires both the DR1 and DR2 elements, and that kaposin B itself, is a target for direct phosphorylation by p38 MAPK on a putative serine residue in DR1 (McCormick and Ganem, 2005).

1.2.7.5 K15

K15 is situated at the right end of the unique coding region of the KSHV genome, between ORF75 and the TRs. The alternatively spliced K15 gene encodes multiple transcripts. The most prominent one encompasses eight exons and is predicted to encode a membrane protein with 12 transmembrane domains and a C-terminal cytoplasmic segment (Choi *et al.*, 2000; Glenn *et al.*, 1999; Poole *et al.*, 1999). The cytoplasmic domain of K15 contains a number of putative domains associated with signal transduction including: an SH2 domain, an SH3 domain and a TRAF-binding site (Choi *et al.*, 2000; Glenn *et al.*, 1999; Poole *et al.*, 1999). The location of the K15 gene, its predicted structure, and the presence of putative SH2 and SH3 domains, are all features found in latent membrane protein 2A (LMP2A) of Epstein-Barr virus, and therefore K15 is thought to be the positional homologue of LMP2A, which provides a survival signal for latently infected B cells and controls viral latency (Brinkmann and Schulz, 2006). Latent K15 protein expression has been detected in PEL cells and MCD B cells (Sharp *et al.*, 2002). However, northern blot analysis, RT-PCR, and gene array studies have shown weak K15 expression in PEL cells, which was upregulated upon TPA treatment (Choi *et al.*, 2000; Glenn *et al.*, 1999).

Yeast-two-hybrid analysis identified Hax-1, a Bcl-2-related anti-apoptotic protein, as an interacting partner of K15. This interaction was confirmed *in vivo*, and may play a role in inhibition of apoptosis (Sharp *et al.*, 2002). In reporter assays, K15 strongly activated the mitogen-activated protein kinase (MAPK) pathway Ras/MEK/Erk2 and the c-Jun N-terminal kinase (JNK), and weakly activated the NF-κB pathway (Brinkmann *et al.*, 2003). This activation involved the phosphorylation of the SH2-binding motif Y^{481}EEV by members of the Src family of protein tyrosine kinases (PTKs) (Brinkmann *et al.*, 2003). More recently, DNA microarray analysis revealed the downstream target

genes of K15 signalling. It appears that K15 signalling can induce the expression of multiple cytokines and chemokines, including IL-8, IL-6, CCL20, CCL2, CXCL3, and IL-1α/β, which have been show to play a major role in KSHV pathogenesis (Brinkmann *et al.*, 2007).

1.2.7.6 vIRF3

KSHV encodes four homologues of cellular interferon (IFN) regulatory factor (IRF), namely vIRF1-4 expressed from ORF K9 and ORFs K10, K10.5 and K11 spliced to upstream sequences (Cunningham *et al.*, 2003; Jenner *et al.*, 2001; Jenner and Boshoff, 2002; Lubyova and Pitha, 2000). ORF K10.5 encodes vIRF3, a protein that is expressed during latency in PEL cell lines, whereas the remaining vIRFs appear to be expressed exclusively or predominantly as lytic genes (Cunningham *et al.*, 2003; Fakhari and Dittmer, 2002; Jenner *et al.*, 2001; Paulose-Murphy *et al.*, 2001; Rivas *et al.*, 2001). vIRF3 is expressed in the nucleus of PEL cell lines, and this has lead to its naming by some investigators as latency-associated nuclear antigen 2 (LANA2). Interestingly, while vIRF3 is a latent protein in PEL cell lines and has also been detected in lymphocytes from MCD tissue, it is not expressed in KS cells and tissue (Rivas *et al.*, 2001). Therefore, it seems that while vIRF3 may play a role in KSHV pathogenesis, this is restricted to infected B cell populations and is not of significance with respect to KS.

The main function of vIRF3 in KSHV pathogenesis appears to be the blocking of cellular IRF functions and IR-stimulated pathways that lead to apoptosis. vIRF3 can inhibit the activities of IRF3 and IRF7 and, as a consequence, suppress the interferon induction in response to virus infection (Lubyova and Pitha, 2000). In fact, vIRF3 can interact either with the DNA-binding domain, or the central IRF-association domain of IRF7, which results in the inhibition of IRF7 DNA binding activity, and subsequently the suppression of IFN-α production and IFN-mediated immunity (Joo *et al.*, 2007). vIRF3 can also mediate protection against apoptosis, by inhibiting p53-dependent transactivation, possibly through direct interactions with the tumour suppressor (Rivas *et al.*, 2001), and it also prevents apoptosis triggered by double-stranded RNA (dsRNA)-activated serine-threonine protein kinase

(PKR) (Esteban *et al.*, 2003). vIRF3 can interfere with immune responses via inhibition of the NF-κB-activating IκB kinase β (IKKβ) (Seo *et al.*, 2004). These findings suggest a role for vIRF3 in protection of infected haematopoietic cells from immune surveillance and apoptosis in latency. The function of vIRF3 is probably related to deregulation of the immune system to promote survival of infected cells, which could contribute to KSHV malignancies involving B cells, such as PEL and MCD, where vIRF3 is expressed.

1.2.8 The Lytic Cycle in KS Pathogenesis

The latent genes of KSHV have profound effects on growth-regulation and survival, suggesting a significant contribution to viral pathogenesis. However, several lines of evidence suggest that lytic replication also plays a pivotal role in KS development. Treatment of AIDS-KS patients with gancyclovir, a drug that blocks lytic but not latent KSHV infection, results in a dramatic decline in the incidence of new KS tumours (Martin *et al.*, 1999). Furthermore, regression of AIDS-KS due to highly active anti-retroviral therapy (HAART) is associated with reduced KSHV viral load (Sirianni *et al.*, 1998; Wilkinson *et al.*, 2002). Moreover, post-transplant KS usually results from reactivation from reservoirs of latent virus (Frances *et al.*, 2000; Jenkins *et al.*, 2002). Finally, most KS spindle cells, and MCD plasmablasts, sustain latent KSHV infection, but in up to 20% of cells the virus undergoes spontaneous reactivation (Staskus *et al.*, 1999; Staskus *et al.*, 1997; Zhong *et al.*, 1996). These data suggest that lytic reactivation is required to enhance the dissemination of the virus and may also modulate growth through paracrine mechanisms as a result of lytic gene expression. Examination of the KSHV genome reveals numerous viral genes whose products are secreted signalling molecules, many of which are cellular cytokines or chemokines (Nicholas, 2003). The majority of these are lytic cycle genes, including the three viral CC chemokines (**vMIP-I, vMIP-II, and vMIP-III**) and v-IL6. Several of the viral chemokines are chemotactic for Th2 cells, raising the possibility that they can dampen antiviral Th1 responses by favouring Th2 polarization of the immune response (Sozzani *et al.*, 1998; Stine *et al.*, 2000). Some of the key viral genes expressed during lytic replication, and their potential roles in KSHV pathogenesis (Table 1.2) are described in more detail below.

1.2.8.1 K1-Variable ITAM-containing Protein (VIP)

KSHV VIP is encoded by ORF K1, at the far left end of the unique coding region. Transforming γ-herpesviruses HVS and EBV have genes at analogous positions, which encode signalling membrane proteins STP (saimiri transformation-associated protein) (Jung *et al.*, 1999), and LMP-1 (latency membrane protein-1) (Eliopoulos *et al.*, 2001) respectively, and these function as transforming proteins. Although neither of these proteins is homologous to KSHV VIP, all three are constitutively active signal transducers (Jung and Desrosiers, 1995; Lagunoff *et al.*, 1999; Lee *et al.*, 1999; Lee *et al.*, 1998a; Li and Chang, 2003; Moorthy and Thorley-Lawson, 1993). Like STP and LMP-1, KSHV VIP can induce plasmablastic lymphomas and sarcomatoid tumours in transgenic mice expressing K1 (Lee *et al.*, 1998b; Prakash *et al.*, 2002). Interestingly, although K1 and STP do not share sequence homology, K1 can substitute for STP in *in vitro* and *in* vivo transformation assays in the context of the HVS genome and virus infection (Douglas *et al.*, 2004; Lee *et al.*, 1998b). However, it should be noted that Tip, a related transforming gene belonging to HVS, was not removed from the recombinant virus. Nonetheless, when K1 was introduced into the murine γ-2-herpesvirus MHV-68, it independently induced salivary gland adenocarcinomas in 25% of infected animal (Douglas *et al.*, 2004; Lee *et al.*, 1998b). These findings suggest that VIP may play a role in KSHV-induced malignancies via direct cellular transformation.

Evidence from Northern analyses have revealed that K1 transcripts expressed in PEL cell lines are upregulated following TPA treatment (Lagunoff *et al.*, 1999; Samaniego *et al.*, 2001), and in KS tumour cells (Samaniego *et al.*, 2001). A recent study using monoclonal antibodies raised against K1 confirmed early lytic expression in PEL cells and in MCD tissue, but K1 was not detected in KS samples (Lee *et al.*, 2003a). These data suggest there is an essential difference between K1 and STP/LMP1, because both are expressed in latency.

K1 is a 46 kDa type 1 transmembrane glycoprotein (289aa) that resembles a single-domain Ig superfamily receptor (Lagunoff and Ganem, 1997; Lee *et al.*, 1998a; Russo *et al.*, 1996). Its extracellular N-terminal domain contains several *N*-glycosylation sites and displays a high degree of genetic variability between different KSHV isolates. These have been used to classify the virus into four clades (A, B, C and D) (Hayward, 1999; McGeoch, 2001; Zong *et al.*, 1999). Apparently, these regions were found to be targeted by CTLs, and therefore their hypervariability may be attributed to positive selection rather than drift (Stebbing *et al.*, 2003). These data suggest that K1 might act as an immune decoy, providing some evolutionary advantage to the virus. The cytoplasmic domain of K1 contains an immunoreceptor tyrosine-based motif (ITAM), which is highly conserved between different K1 subtypes and is similar to the one found in LMP2A (Lee *et al.*, 1998a).

Similar to LMP2A, K1 downregulates the expression of the B cell receptor at the cell surface of BJAB cells, by binding to the heavy chains of the BCR complex through its extracellular domain, thereby preventing their expression on the plasma membrane (Lee *et al.*, 2000). This function may indirectly prevent the display of KSHV viral antigens on B cell MHC class II, and may therefore represent an immune escape strategy of the virus. K1 expression has been reported to both switch on (Lagunoff *et al.*, 2001), and switch off (Lee *et al.*, 2002) lytic replication, thereby acting as a lytic/latent switch, and/or a latency maintenance protein.

K1 constitutively activates B cell signalling pathways via its C-terminal ITAM. VIP is known to activate SH2 domain-containing Src-family kinases, the p85 subunit of PI3K, and PLCγ, in order to initiate a range of downstream signalling cascades (Lagunoff *et al.*, 2001; Lee *et al.*, 2005; Lee *et al.*, 1998a; Samaniego *et al.*, 2001; Tomlinson and Damania, 2004). It can stimulate the nuclear factor of T cells (NFAT) (Lagunoff et al, 1999), the Akt signalling pathway (Tomlinson and Damania, 2004) and NF-κB (Prakash *et al.*, 2002; Samaniego *et al.*, 2001). Transfected K1 activates NF-κB in reporter based assays (Samaniego *et al.*, 2001), while B lymphocytes from transgenic mice expressing K1 show increased NF-κB activity and the mice develop tumours

that resemble spindle cell sarcomas (Prakash *et al.*, 2002). VIP can also induce cytokine expression via Akt-mediated NF-κB activation (Samaniego *et al.*, 2001), and these include IL-6, IL-12, and GM-CSF. The angiogenic factors VEGF and matrix metalloproteinase 9 (MMP-9) are also induced by VIP (Wang *et al.*, 2004b). These pro-inflammatory and angiogenic factors are likely to contribute to KSHV pathogenesis by establishing the conditions for endothelial and B cell growth, as well as promoting the infiltration of inflammatory cells into sites of infection (Aoki *et al.*, 2000; Ensoli *et al.*, 2000).

1.2.8.2 vGPCR

ORF74 encodes the viral G-protein coupled receptor (vGPCR), which is most closely related to the IL-8 receptors CXCR1 and CXCR2 (Kirshner *et al.*, 1999). Unlike its cellular counterparts, vGPCR is constitutively active (Arvanitakis *et al.*, 1997), but can be modulated by chemokine binding (Geras-Raaka *et al.*, 1998; Gershengorn *et al.*, 1998; Rosenkilde *et al.*, 1999).

vGPCR is known to activate a range of pro-inflammatory, growth, and angiogenic factors. It stimulates the MAPK, PI-3-kinase, and p38 pathways (Smit *et al.*, 2002; Sodhi *et al.*, 2000), as well as the NF-κB pathway (Pati *et al.*, 2001). NF-κB activation leads to the expression of NF-κB-dependent genes, including pro-angiogenic factors (VEGF, bFGF), chemokines (IL-1β, IL-6, IL-8, TNFα), and adhesion molecules (VCAM, ICAM-1, E-selectin) (Couty *et al.*, 2001; Montaner *et al.*, 2004; Pati *et al.*, 2001; Schwarz and Murphy, 2001), which potentially contribute to KS, PEL, and MCD. vGPCR also activates NFAT (Pati *et al.*, 2003), related adhesion focal tyrosine kinase (RAFTK), and lyn (Munshi *et al.*, 1999). More recently, vGPCR was shown to cause upregulation of Ang-2, a proangiogenic and lymphangiogenic secreted molecule, in lymphatic endothelial cells infected with KSHV. This upregulation occurred in a paracrine manner through the vGPCR-mediated activation of the MAPK pathway (Vart *et al.*, 2007).

In addition to its broad signalling effects, vGPCR expression has been shown to slow the growth of PEL cells in culture, which reflects a role for a vGPCR-mediated cell cycle arrest during the lytic phase (Cannon *et al.*, 2003). This

subversion of the cell cycle is mediated by a p53-independent transcriptional upregulation of the CDK inhibitor $p21^{CIP1}$, and results in a delay of KSHV replication (Cannon *et al.*, 2006). Therefore, expression of vGPCR may ensure a delay or even a block of full lytic transcription and cell death, which would allow sufficient time for the proliferative and angiogenic potential of vGPCR to be biologically significant in the tumour microenvironment (Cannon *et al.*, 2006).

Functional studies have provided the evidence that vGPCR contributes to KS, and possibly also to PEL and MCD, through its angiogenic and cytokine-induced activities. vGPCR transforms NIH3T3 cells (Bais *et al.*, 1998), enhances survival of primary endothelial cells (Couty *et al.*, 2001; Montaner *et al.*, 2001) and can immortalise human umbilical vein endothelial cells (HUVECs) (Bais *et al.*, 2003). The strongest evidence for a pathogenic role of vGPCR comes from the finding that transgenic mice expressing vGPCR develop multiple tumours that resemble KS lesions (Guo *et al.*, 2003; Yang *et al.*, 2000). Interestingly, vGPCR is expressed in only a minority of cells within these lesions, but elevated levels of VEGF in these lesions have been noted. Therefore, the KS phenotype appears to be supported by vGPCR-induced paracrine signalling, presumably via VEGF and other cytokines induced in the vGPCR-expressing cells. These data support the concept that a paracrine component is important in the pathogenesis of KS tumours. It seems likely that vGPCR is an important component in KSHV pathogenesis, which can act in a paracrine manner in concert with latent KSHV genes expressed in neighbouring cells (Montaner *et al.*, 2003).

1.2.8.3 vIL-6

Cellular IL-6 has been known to act as a growth factor, and to be implicated in KS and MCD, even before the discovery of KSHV (Miles *et al.*, 1990; Yoshizaki *et al.*, 1989). High levels of clL-6 have been observed in the tissues of patients with each of the KSHV-associated neoplasms (Ensoli *et al.*, 1989; Foussat *et al.*, 1999; Leger-Ravet *et al.*, 1991), which suggests that clL-6 plays an important role in KSHV pathogenesis. Therefore, it was interesting to

discover that KSHV encoded its own version of this cytokine, in the form of a viral IL-6 homologue. The viral IL-6 (vIL-6) is encoded by ORF K2 and its amino acid sequence is 25% identical to human IL-6 (Neipel *et al.*, 1997). The cIL-6 receptor consists of two subunits, gp130 and IL-6Rα, and cIL-6 has an absolute requirement for both subunits (Taga and Kishimoto, 1997). Common with its cellular counterparts, vIL-6 supports the growth of IL-6-dependent murine B9 cells (Moore *et al.*, 1996), and mediates signalling through the gp130 signalling-transducer subunit to activate Jak/STAT (primarily 1 and 3), and the Ras/MAPK pathways (Molden *et al.*, 1997; Osborne *et al.*, 1999). However, in contrast to cIL-6 proteins, vIL-6 does not require the IL-6Rα subunit for the formation of stable signalling complexes (Molden *et al.*, 1997; Wan *et al.*, 1999). This may allow for a broader spectrum of target cells since IL-6Rα has a restricted expression profile and is downregulated by the IFN response, while gp130 is ubiquitously expressed (Taga and Kishimoto, 1997).

While vIL-6 is abundantly expressed during lytic replication, it is also expressed at low levels in uninduced latently infected PEL cell cultures, in the absence of other lytic gene expression. It has been demonstrated that vIL-6 was specifically induced when PEL cells were treated with IFNα, and it blocked the cell cycle arrest and apoptotic activities of IFNα in these cells (Chatterjee *et al.*, 2002). This suggests that vIL-6 also plays a role during latency, as well as during lytic replication, in protecting latently infected cells against anti-viral host defences mediated by IFN. vIL-6 can also stimulate the production of VEGF (Aoki *et al.*, 1999; Liu *et al.*, 2001), and along with vGPCR, is responsible for upregulating the expression of Ang-2, thereby contributing to the initial stages of KSHV infection through paracrine effects that promote angiogenesis (Vart *et al.*, 2007). Moreover, vIL-6 is able to induce endothelial expression of PTX3, an acute-phase protein, which would be expected to promote the infiltration of inflammatory cells into sites of infection and contribute to the cytokine milieu supporting KS cell growth (Klouche *et al.*, 2002). When injected into nude mice, NIH3T3 cells stably expressing vIL-6 and secreting high levels of VEGF are tumourigenic, and PEL cells introduced into nude mice develop lymphomatous effusions in a VEGF-dependent manner (Aoki *et al.*, 1999; Chatterjee *et al.*, 2002).

Furthermore, vIL-6 is a mitogenic factor for PEL cells and could directly be contributing to PEL development (Jones *et al.*, 1999). Therefore, vIL-6 expression during reactivation, could mediate mitogenic and angiogenic activities of relevance to KSHV-associated malignancies.

1.2.8.4 vBcl-2

KSHV ORF16 encodes a viral homologue of human Bcl-2 , vBcl-2 (Sarid *et al.*, 1997), which is expressed early in the lytic replication cycle. The Bcl-2 family regulates apoptosis through association with other pro-apoptotic family members such as Bad, Bak and Bax, and plays an important role in tissue homeostasis, embryogenesis, and the immune response (Chao and Korsmeyer, 1998). The KSHV-encoded vBcl-2 is highly homologous to Bcl-2, especially at the BH1 and BH2 domains (Sarid *et al.*, 1997), which are required for inhibition of apoptosis and heterodimerization with Bax (Yin *et al.*, 1994). vBcl-2 is also anti-apoptotic, and can inhibit apoptosis induced by several stimuli, including Bax overexpression, and vcyclin overexpression (Ojala *et al.*, 1999), ensuring that the cell survives to allow for production of viral progeny. Therefore, it appears that vBcl-2 contributes to the evasion of host cell apoptosis induced by viral infection, which is caused when the virus activates endogenous machinery during the lytic cycle. This is advantageous to the virus, as it prevents premature lysis, and promotes viral expansion and survival.

1.2.8.5 Viral inhibitor of apoptosis protein (vIAP)

Apoptotic pathway deregulation is also achieved by the expression of viral products related to the inhibitor-of-apoptosis proteins (IAPs). ORF K7 encodes a viral inhibitor of apoptosis protein (vIAP) that is structurally related to survivin-ΔEx3, a splice variant of human survivin that inhibits apoptosis (Wang *et al.*, 2002). vIAP localises to the mitochondria via a putative mitochondrial-targeting domain in its N-terminus (Wang *et al.*, 2002), where it can inhibit apoptosis induced by multiple stimuli including Fas, TRAIL, Bax, TNFα plus cyclohexamide, staurosporine and ceramide (Feng *et al.*, 2002; Wang *et al.*, 2002). Mechanistically, the vIAP N-terminal BIR (baculovirus IAP repeat)

domain interacts with caspase-3 and inhibits its activity, and the vIAP BH2 (Bcl-2 homology) domain binds to Bcl-2. Therefore, vIAP acts as an adaptor protein and bridges an interaction between cellular Bcl-2 and caspase-3, thereby promoting the anti-apoptotic activity of Bcl-2 against active caspase-3 (Wang *et al.*, 2002). vIAP also directly interacts with the cellular calcium-modulating cyclophilin ligand (CAML) and mediates the increase of cytosolic Ca^{2+} concentration during an apoptotic stimulus. This increase in cytosolic Ca^{2+} by vIAP was found to protect cells from mitochondrial damage and apoptosis (Feng *et al.*, 2002).

1.2.8.6 vIRF1, vIRF2 and vIRF4

During lytic replication, KSHV encodes three proteins that show homology with the cellular interferon-regulatory factors (IRFs), vIRFs 1, 2, and 4 (Cunningham *et al.*, 2003; Neipel *et al.*, 1997). The IRFs are a large family of transcription factors, which together with the transcriptional activator p300, regulate IFN signal transduction through binding to interferon-stimulated response elements in the promoter of interferon-responsive genes. The IFNs stimulate the anti-viral defence in cells by activating various signal transduction pathways, and modifying the expression of a number of antiviral genes. Among these genes is double-stranded RNA-activated protein kinase R (PKR), a key mediator of antiviral and antiproliferative effects (Clemens and Elia, 1997). ORF K11.1 represents the first exon of viral-IRF2 and encodes a 20kDa protein (Burysek *et al.*, 1999b), which exerts its anti-IFN effects by physically interacting with, and suppressing the activity of PKR (Burysek and Pitha, 2001). vIRF2 also binds to a consensus NF-κB binding site and suppresses the cellular IRF-1- and IRF-3-driven activation of IFN-α. Moreover, vIRF2 has been shown to interact with cellular IRF-1, p300/CBP, p65, IRF-2, and IFN consensus sequence binding protein/IRF-8 (Burysek *et al.*, 1999b). More recently, it was found that the vIRF2 gene encodes a 2.2kb spliced transcript representing the two exons of ORFs K11.1 and K11, from which the full-length vIRF2 protein is translated (Cunningham *et al.*, 2003; Jenner *et al.*, 2001). This full length vIRF2, could inhibit IFN-α- and IFN-λ-driven transactivation of a reporter promoter containing the interferon stimulated

response element (ISRE), and suppressed transactivation of the ISRE promoter by IRF-1. Moreover, full length vIRF2 inhibited transactivation of a full-length IFN-β reporter promoter by either IRF-3 or IRF-1 (Fuld *et al.*, 2006).

ORF K9 encodes vIRF1, which directly interacts with cellular IRF1 and IRF3 (Burysek *et al.*, 1999a), p300 (Burysek *et al.*, 1999a; Li *et al.*, 2000), CRB (Seo *et al.*, 2000), and p53 (Nakamura *et al.*, 2001). Therefore, through effects on transcription mediated via these interactions, vIRF1 negatively regulates the IFN-mediated gene expression and anti-viral effects. A recent study demonstrated that vIRF1, along with vFLIP, can also regulate the transcription and expression of antigen presenting genes in lymphatic endothelial cells (LECs) (Lagos *et al.*, 2007). vIRF1 expression in LECs resulted in the downregulation of MHC-I expression, and this was dependent on a domain in the N-terminus of vIRF1 (amino acids 1-82) (Lagos *et al.*, 2007), which has been shown to be responsible for binding to the coactivator p300 (Li *et al.*, 2000). Furthermore, LECs expressing vIRF1 were found to be less responsive to IFN-α-mediated induction of MHC-I expression. Thus, vIRF1, through its downregulation of MHC-I transcription, might contribute to KSHV-infected cells' immune evasion. Moreover, vIRF1 has been shown to transform NIH3T3 and Rat-1 cells, by reducing intracellular levels of the CDK inhibitor $p21^{WAF1/CIP1}$ (Gao *et al.*, 1997; Li *et al.*, 1998). Finally, vIRF4 is encoded within K10.1 and also blocks IFN- and IRF-mediated transcriptional activation (Jenner and Boshoff, 2002).

KSHV genes involved in viral pathogenesis			
ORF	**Protein Product**	**Function**	**Expression**
K1	**vIP**	Cellular transformation. Constitutively activates B-cell signalling pathways (NFAT, NF-κB, Akt). Downregulates the B-cell receptor (immune decoy). Induces cytokine and angiogenic factor secretion.	Lytic replication
K2	vIL-6	Activates Jak/STAT and Ras/MAPK pathways. Acts as autocrine growth factor in PEL cells. Angiogenic by inducing VEGF and Ang-2 production.	Lytic replication
K4, K4.1, K6	vMIP-II, vMIP-III, vMIP-I (respectively)	Dampen antiviral Th1 responses. Angiogenic.	Lytic replication
K7	vIAP	Inhibits apoptosis induced by Fas, TRAIL, Bax, TNFα. Increases cytosolic Ca^{2+} and protects from mitochondrial damage and apoptosis.	Lytic replication
ORF16	vBcl-2	Inhibits Bax-mediated and virally-induced apoptosis	Lytic replication
K9	vIRF1	Blocks IFN- and IRF-mediated transcriptional activation. Downregulates MHC-I transcription (immune decoy). Cellular transformation.	Lytic replication
K10	vIRF4 (when spliced to K10.1)	Blocks IFN- and IRF-mediated transcriptional activation.	Lytic replication (Latent ?)
K10.5	vIRF3	Blocks IFN- and IRF-mediated transcriptional activation. Blocks apoptosis by inhibiting p53-dependent transactivation.	Latent. Also induced in lytic replication
K11	vIRF2 (when spliced to K11.1)	Blocks IFN- and IRF-mediated transcriptional activation. Suppresses PKR.	Lytic replication (Latent ?)
K12	Kaposin A, B, C	Cell transformation. Kaposin A promotes anchorage independent growth. Kaposin B mediates mRNA stabilisation for cytokines, growth factors, and oncoproteins through the activation of MK2 kinase.	Latent and induced in lytic replication
ORF71	**vFLIP**	Cell transformation. Blocks DR-mediated apoptosis. Activation of classical and alternative NF-κB pathways. Induction of cytokine secretion.	Latent
ORF72	v-cyclin	Promotes cell cycle progression by constitutively activating cdk6.	Latent
ORF73	LANA (latent nuclear antigen)	Tethers the viral episome to the host genome. Binds p53 and pRb. Acts as a transcriptional regulator.	Latent
ORF74	vGPCR	Cell transformation. Activates MAPK, p38, PI3K, NF-κB. Induces the secretion of pro-angiogenic factors, chemokines, and adhesion molecules.	Lytic replication
K15	-	Blocks apoptosis by interacting with Hax-1. Activates MAPK, Ras/MEK/Erk2, JNK, NF-κB via TRAF binding. Induces the secretion of cytokines.	Latent and induced in lytic replication

Table 1.2 KSHV genes involved in viral pathogenesis

List of KSHV genes involved in viral pathogenesis, their protein products, and their expression pattern. Highlighted (bold) genes are those capable of NF-κB activation. Each KSHV ORF is named according to the system of Russo *et al.* 1996. Gene function is based on experimental evidence and is referenced and described in more detail in the text of Chapter 1, sections 1.2.7 and 1.2.8.

1.3 Regulation of NF-κB transcription factors

1.3.1 Rel and IκB protein families

Rel or nuclear factor of κB (NF-κB) proteins comprise a family of dimeric transcription factors, which exist in virtually all cell types and regulate the expression of a wide range of genes involved in immune and inflammatory responses, developmental processes, cellular growth, apoptosis, and survival (Pahl, 1999). Active NF-κB promotes the expression of over 150 target genes. The majority of the NF-κB target genes participate in the host immune response. These include, for example, an array of cytokines, chemokines, and adhesion molecules, as well as receptors required for immune recognition, such as MHC molecules, and proteins involved in antigen presentation (Ghosh and Karin, 2002). It also includes molecules involved in migration, differentiation and maturation of lymphocytes. Finally, it contains genes that regulate cell growth and apoptosis (Zhong *et al.*, 2002).

NF-κB was first described in 1986 as a protein that bound to a specific decameric DNA sequence within the intronic enhancer of the immunoglobulin kappa light chain in mature B- and plasma cells, but not pre B-cells (Sen and Baltimore, 1986b). Later, NF-κB was demonstrated by the same authors as an inducible transcription factor in a range of other cells (Sen and Baltimore, 1986a). NF-κB dimers are composed of different combinations of the five mammalian reticuloendotheliosis (Rel) family proteins. The Rel family share a conserved N-terminal Rel homology domain (RHD) of 300 amino acids (Figure 1.5), which resembles two Ig domains (May and Ghosh, 1997). The RHD mediates the DNA binding and dimerisation of NF-κB subunits, and is also the binding domain for a family of inhibitory proteins, termed inhibitors of κB (IκB) (Ghosh *et al.*, 1998). The IκB family share a domain containing six or seven ankyrin repeats (Figure 1.5), through which they bind the RHDs (Whiteside and Israel, 1997). The c-Rel, RelB, and RelA proteins also have a C-terminal non-homologous transactivation domain, which strongly activates transcription from NF-κB binding sites in target genes (Blair *et al.*, 1994; Bull *et al.*, 1990; Ryseck *et al.*, 1992; Schmitz and Baeuerle, 1991; Schmitz *et al.*, 1994; Schmitz *et al.*, 1995) (Figure 1.5). Two classes of Rel proteins are

recognised. Class I members (RelA/p65, RelB and c-Rel) are synthesised as mature molecules, and class II members (p105/NF-κB1 and p100/NF-κB2) are synthesised as large precursor proteins containing an N-terminal RHD and a C-terminal ankyrin repeat domain (Figure 1.5). Prior to processing, p105 and p100 function as IκB-like molecules (Dobrzanski *et al.*, 1995; Mercurio *et al.*, 1993; Rice *et al.*, 1992; Solan *et al.*, 2002). Proteolytic processing cleaves their inhibitory C-terminus to produce the mature NF-κB subunits p50, and p52 respectively (Whiteside and Israel, 1997).

1.3.2 NF-κB Dimers

NF-κB is now known to exist in most cell types, binding to the common consensus sequence 5'-GGGRNNYYCC-3' (where R is purine and Y is pyrimidine) (Kunsch *et al.*, 1992; Parry and Mackman, 1994), which may regulate more than 150 genes (Pahl, 1999). The RelA/p50 heterodimer is the most abundant NF-κB complex, but almost all combinations of Rel/NF-κB homo- and heterodimers have been identified *in vivo* (Ganchi *et al.*, 1993; Hansen *et al.*, 1994a; Kang *et al.*, 1992; Molitor *et al.*, 1990; Parry and Mackman, 1994). One exception is RelB, which only forms heterodimers with p50 and p52 (Ryseck *et al.*, 1992; Ryseck *et al.*, 1995). Almost all dimers are transcriptionally active, with the exception of p50 and p52, neither of which contain the C-terminal transactivating regions present in RelA, RelB and c-Rel (Ghosh *et al.*, 1998). However, p50 and p52 still bind to NF-κB consensus sites in DNA, and are therefore thought by some to act as transcriptional repressors (Brown *et al.*, 1994; Hansen *et al.*, 1994a; Hansen *et al.*, 1994b; Kang *et al.*, 1992; Plaksin *et al.*, 1993). The mechanism by which p50 and p52 mediate transcriptional repression is not yet clear, but it may be through passive occupancy of κB sites that might otherwise be bound by transactivating NF-κB molecules (Kang *et al.*, 1992), competition with other transcriptionally active NF-κB dimers (May and Ghosh, 1997), or through the recruitment of specific corepressor complexes (Zhong *et al.*, 2002). Interestingly, p50 and p52 homodimers also specifically associate with the IκB-like proto-oncogene, Bcl-3, to form transcriptionally active complexes

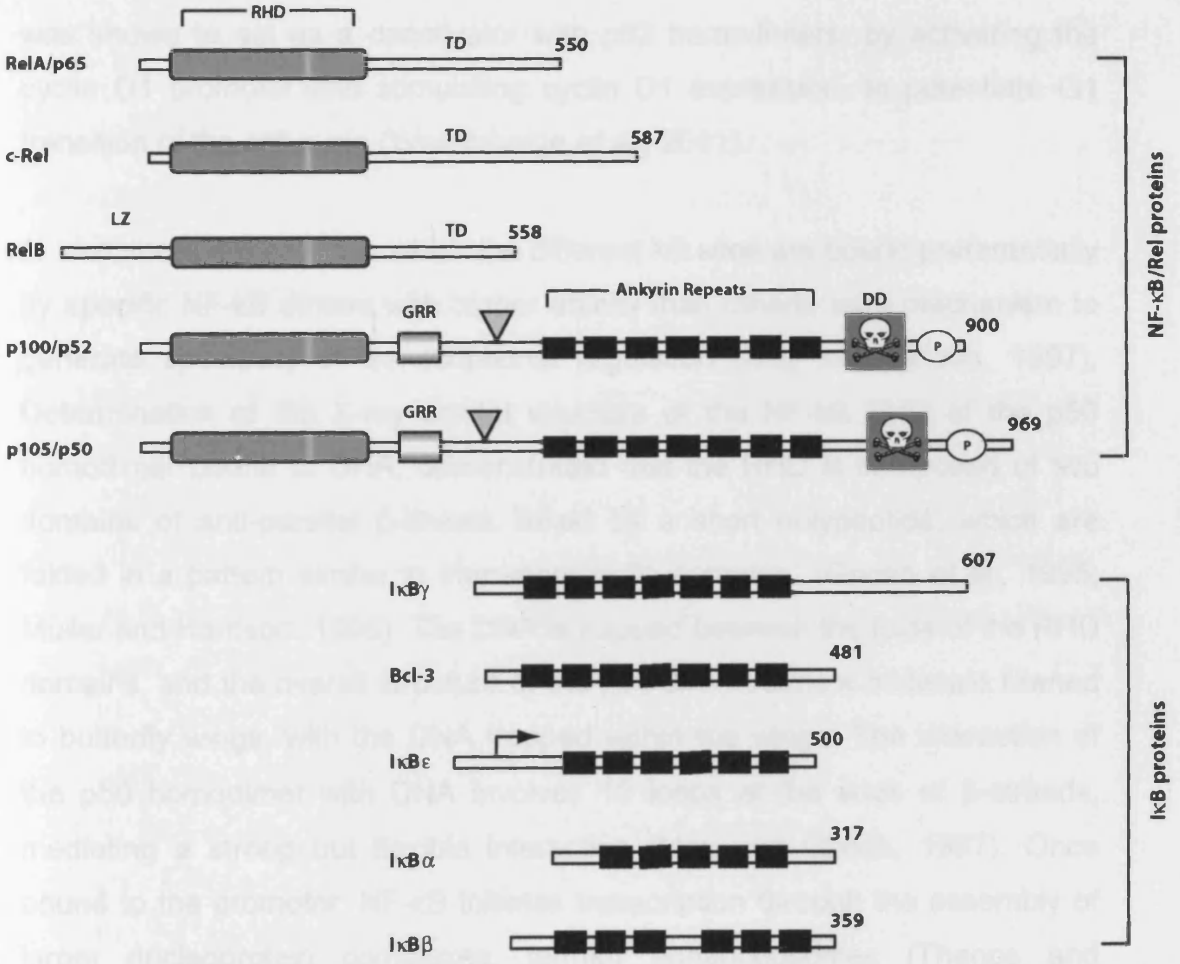

Figure 1.5 Members of the NF-κB/Rel protein family and their IκB regulators

Members of the NF-κB/Rel and IκB families of proteins are shown. NF-κB proteins contain an N-terminal Rel-homology domain (RHD), and a C-terminal transactivation domain (TD). p105 and p100 are the precursors for p50 and p52, respectively. Both p105 and p100 contain a glycine-rich region (GRR) followed by C-terminal ankyrin repeats, which are also present in the IκB family of proteins, and a death domain (DD). The grey triangular arrows point to the endoproteolytic cleavage sites of p100/p52 and p105/p50. The number of amino acids in each protein is shown on the right. LZ, leucine zipper domain of RelB; P, phosphorylation site of p100/p52 and p105/p50.

(Bours *et al.*, 1993; Fujita *et al.*, 1993). In human breast epithelial cells, Bcl-3 was shown to act as a coactivator with p52 homodimers, by activating the cyclin D1 promoter and stimulating cyclin D1 expression, to potentiate G1 transition of the cell cycle (Westerheide *et al.*, 2001).

In vivo, there are cases in which the different kB sites are bound preferentially by specific NF-kB dimers with higher affinity than others, as a mechanism to generate specificity of transcriptional regulation (May and Ghosh, 1997). Determination of the X-ray crystal structure of the NF-kB RHD of the p50 homodimer bound to DNA, demonstrated that the RHD is composed of two domains of anti-parallel β-sheets linked by a short polypeptide, which are folded in a pattern similar to immunoglobulin domains (Ghosh *et al.*, 1995; Muller and Harrison, 1995). The DNA is trapped between the folds of the RHD domains, and the overall structure of the p50 dimer forms a molecule likened to butterfly wings, with the DNA trapped within the wings. The interaction of the p50 homodimer with DNA involves 10 loops at the ends of β-strands, mediating a strong but flexible interaction (May and Ghosh, 1997). Once bound to the promoter, NF-κB initiates transcription through the assembly of larger nucleoprotein complexes, termed enhanceosomes (Thanos and Maniatis, 1995). Studies on the IFN-β promoters have demonstrated transcriptional synergy imparted by the interaction between Rel proteins with other factors. These protein-protein interactions have been proposed to bend the promoter DNA to form a higher order transcriptional complex (Thanos and Maniatis, 1995). In the case of the IFN-β gene, its enhancer element contains DNA-binding sites for three transcription factors, NF-κB, a heterodimer of ATF-2/c-jun, and IRF proteins, which bind on three positive regulatory domains (PRDs), PRDII, PRDIV and PRDIII-1, respectively (Thanos *et al.*, 1993). The IFN-β enhancer element also contains a sequence that allows the binding of the DNA-remodelling protein HMG I(Y) to the minor groove. Binding of HMG I(Y) to the central region of PRDII (Thanos and Maniatis, 1992), bends the DNA and facilitates the cooperative DNA binding of NF-κB and ATF-2/c-Jun (Yie *et al.*, 1999). Once bound to a κB motif, the Rel proteins can interact with various other DNA-associated transcription factors, and can

recruit IRF, and the co-activator p300/CBP into the complex (Munshi *et al.*, 1998). Co-activators are non-DNA binding proteins that couple transcription factors to the basal transcription machinery and induce chromatin remodelling (Blobel, 2000). The process of chromatin remodelling is the first step in promoter activation. It is therefore significant that RelA directly recruits p300/CBP through an interaction with its C-terminal transactivation domain (Perkins *et al.*, 1997; Wadgaonkar *et al.*, 1999).

In most cells, NF-kB is present as a latent, inactive complex with the IkB inhibitors, which bind NF-kB and mask its nuclear localisation signal, thus sequestering it in the cytoplasm. There are several pathways that regulate the activation of NF-κB. The most common one is termed the classical or canonical pathway, and regulates the degradation of IkB to release dimers composed of RelA, c-Rel and p50 (Bonizzi and Karin, 2004). In brief, the canonical NF-κB pathway is activated when inflammatory signals induce proteolytic degradation of the IκB inhibitory proteins, which then release NF-κB (Henkel *et al.*, 1993). NF-κB dimers then migrate to the nucleus and activate transcription. A second pathway, which is activated by distinct stimuli and termed the alternative pathway, controls the processing of p100. Full-length p100 preferentially sequesters RelB in the cytoplasm of cells (Dobrzanski *et al.*, 1995; Solan *et al.*, 2002), and specific stimuli can activate processing of p100, which generates the active subunit p52, and releases RelB heterodimers to translocate to the nucleus. The regulation of the canonical and alternative NF-κB pathways will be the subject of discussion in this section.

1.3.3 Classical NF-κB Pathway

The canonical or classical NF-κB pathway (Figure 1.6), is induced by a variety of proinflammatory stimuli including bacterial LPS, negative strand viruses, ds-RNA, immunostimulatory sequences (ISS) of DNA, TNFα, IL-1, and antigens (Ghosh and Karin, 2002). Stimulation of the classical pathway leads to the activation of the β subunit of the IκB kinase (IKK) complex, which then phosphorylates IκB proteins on two N-terminal serine residues (Ser32 and 36 for IκBα, and Ser19 and 23 for IκBβ) (DiDonato *et al.*, 1997; Mercurio *et al.*, 1997; Regnier *et al.*, 1997; Woronicz *et al.*, 1997; Zandi *et al.*, 1997). In the classical NF-κB signalling pathway, IKKβ is necessary and sufficient for phosphorylation of IκBα and IκBβ. Phosphorylated IκB proteins are recognised and ubiquitinated by members of the Skp1-Culin-Roc1/Rbx1/Hrt-1-F-box (SCF/SCRF) family of ubiquitin ligases (Ben-Neriah, 2002). The β-TrCP receptor protein of the SCF family ubiquitin ligase complex, recognizes and binds directly to the phosphorylated E3 recognition sequence (DS*GXXS*) founds on IκB molecules (Fuchs *et al.*, 1999; Hatakeyama *et al.*, 1999; Kroll *et al.*, 1999; Spencer *et al.*, 1999; Suzuki *et al.*, 1999; Winston *et al.*, 1999; Wu and Ghosh, 1999; Yaron *et al.*, 1997; Yaron *et al.*, 1998). IκBs are in turn targeted for poly-ubiquitination at two conserved N-terminal arginine acceptor sites on IκB, Lys 21 and Lys 22, by an E3 ubiquitin ligase enzyme (Alkalay *et al.*, 1995b; Yaron *et al.*, 1997). Phosphorylated and ubiquitinated IκB is thus targeted for degradation by the 26S proteosome (Brown *et al.*, 1995; Chen *et al.*, 1995). This process is rapid, such that all IκBα can be degraded within a few minutes (Alkalay *et al.*, 1995a; DiDonato *et al.*, 1995). The classical pathway therefore ensures a rapid response that is crucial for effective inflammatory and immunoregulatory processes. Following degradation of IκB, the released NF-κB translocates to the nucleus, where it is able to bind promoter and enhancer regions containing the κB consensus binding motif and regulate gene transcription.

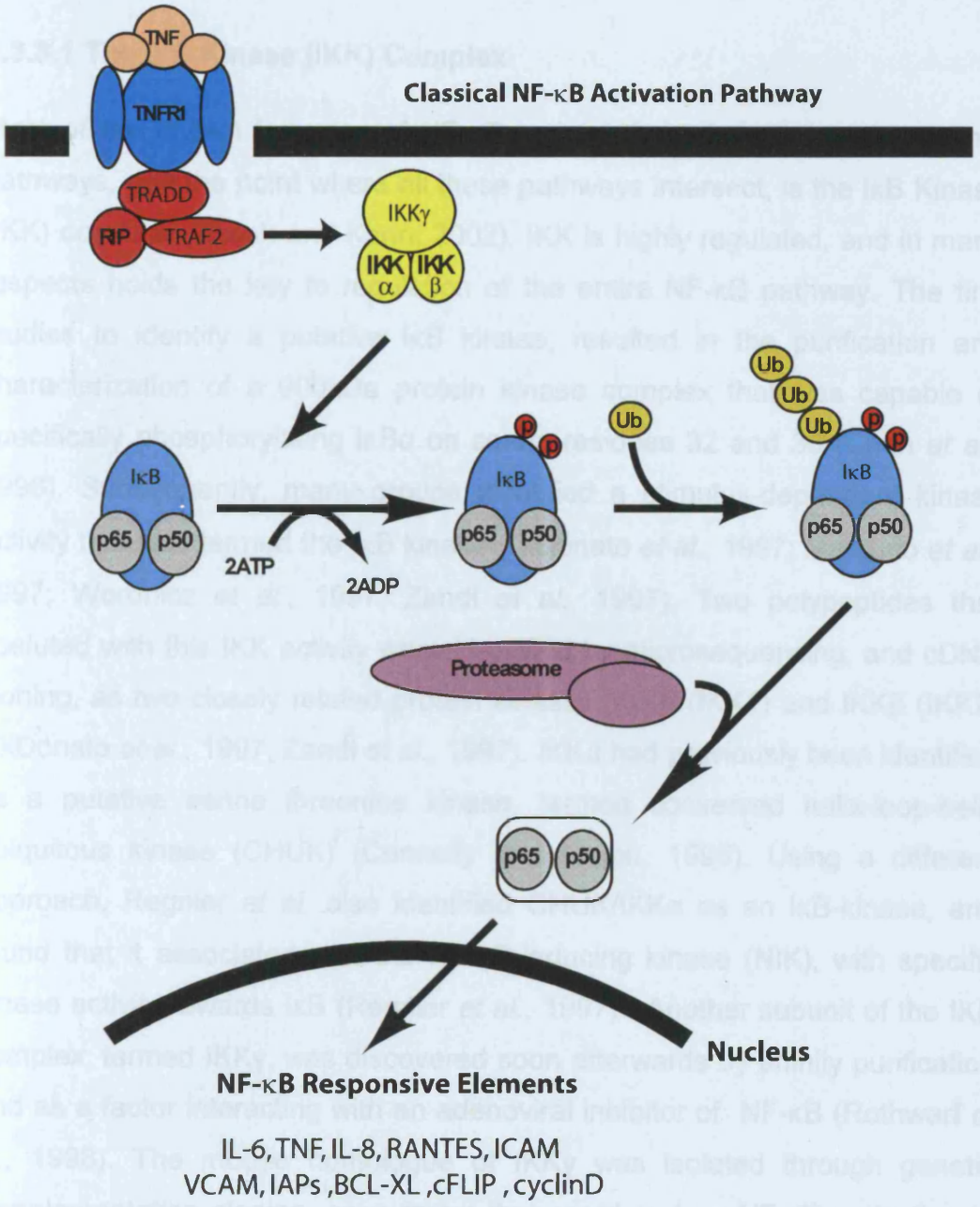

Figure 1.6 The classical pathway of NF-κB activation

The classical pathway is triggered by pro-inflammatory stimuli and genotoxic stress, including the following: cytokines, such as tumour-necrosis factor (TNF) and interleukin-1 (IL-1); bacterial cell-wall components, such as lipopolysaccharide (LPS); viruses; and DNA-damaging agents. Activation of this pathway leads to the IKK-(inhibitor of NF-κB (IκB) kinase) dependent phosphorylation of IκBs, which induces their rapid proteasomal degradation. This results in the liberation of NF-κB dimers (which are mostly p50:p65 dimers) and their subsequent translocation into the nucleus, where they transactivate genes involved in immune responses, inflammation, and promoting cell survival. Ub, ubiquitin; P, phosphorylation.

1.3.3.1 The IκB Kinase (IKK) Complex

Most of the known inducers of NF-κB convey their signals through distinct pathways, and the point where all these pathways intersect, is the IκB Kinase (IKK) complex (Ghosh and Karin, 2002). IKK is highly regulated, and in many respects holds the key to regulation of the entire NF-κB pathway. The first studies to identify a putative IκB kinase, resulted in the purification and characterization of a 900kDa protein kinase complex that was capable of specifically phosphorylating IκBα on serine residues 32 and 36 (Chen *et al.*, 1996). Subsequently, many groups identified a stimulus-dependent kinase activity that was termed the IκB kinase (DiDonato *et al.*, 1997; Mercurio *et al.*, 1997; Woronicz *et al.*, 1997; Zandi *et al.*, 1997). Two polypeptides that coeluted with this IKK activity were identified by microsequencing, and cDNA cloning, as two closely related protein kinases, IKKα (IKK1) and IKKβ (IKK2) (DiDonato *et al.*, 1997; Zandi *et al.*, 1997). IKKα had previously been identified as a putative serine threonine kinase, termed conserved helix-loop-helix ubiquitous kinase (CHUK) (Connelly and Marcu, 1995). Using a different approach, Regnier *et al.* also identified CHUK/IKKα as an IκB-kinase, and found that it associated with the NF-κB-inducing kinase (NIK), with specific kinase activity towards IκB (Regnier *et al.*, 1997). Another subunit of the IKK complex, termed IKKγ, was discovered soon afterwards by affinity purification and as a factor interacting with an adenoviral inhibitor of NF-κB (Rothwarf *et al.*, 1998). The mouse homologue of IKKγ was isolated through genetic complementation cloning, as a factor that could restore NF-κB activation in two cell lines defective in this activity, and was subsequently termed NF-κB essential factor (NEMO) (Yamaoka et al, 1998).

IKKα and IKKβ are 85 and 87 kDa proteins, which constitute the catalytic component of the IKK complex. They share 52% overall sequence identity and 65% identity within the catalytic domain. Both can be inactivated by the mutation of Lysine 44 within the predicted ATP-binding site (Mercurio *et al.*, 1997; Woronicz *et al.*, 1997; Zandi *et al.*, 1997). They are serine/threonine kinases that are characterised by the presence of an N-terminal kinase domain, a C-terminal helix-loop-helix (HLH) domain, and a leucine zipper (LZ)

domain (DiDonato *et al.*, 1997; Zandi *et al.*, 1997). Immunoprecipitation studies have shown that IKKα and IKKβ can form homo- or heterodimers, and these interactions are mediated by binding between the LZ domains, which are therefore required for kinase activity (Hansen *et al.*, 1994a; Mercurio *et al.*, 1997; Ryseck *et al.*, 1995). IKKγ, the regulatory subunit of the IKK complex, is a 48kDa protein that is not related to IKKα and IKKβ, and contains a C-terminal zinc finger-like domain, a leucine zipper, and N-terminal and C-terminal coiled-coil domains. NEMO is non-catalytic, but essential for the assembly and activation of the high molecular weight complex (Li *et al.*, 2001; Rothwarf *et al.*, 1998; Rudolph *et al.*, 2000; Yamaoka *et al.*, 1998). The HLH domain is required for full IKKβ activity, and this is mediated through direct interaction between the C-terminal HLH domain and the N-terminal kinase domain (Delhase *et al.*, 1999). More recently, it has been shown that removing the HLH domain of IKKα and IKKβ, abolishes the binding of IKK to NEMO, and therefore the HLH domain may be necessary for the assembly of functional IKK-NEMO complexes (May *et al.*, 2002). IKKα and IKKβ associate with IKKγ through a C-terminal hexapeptide sequence (Leu-Asp-Trp-Ser-Trp-Leu), termed the NEMO binding domain (NBD) (May *et al.*, 2002). NEMO binding to IKK requires residues 135-231, located at the N-terminus within the first coiled-coil motif, and can interact with the NBD of both IKKα and IKKβ (May *et al.*, 2002; Mercurio *et al.*, 1999; Poyet *et al.*, 2000; Rothwarf *et al.*, 1998; Ye *et al.*, 2000). In addition, the C-terminus of NEMO is required for binding to ubiquitin or the deubiquitinase CYLD, or for the oligomerization of NEMO (Agou *et al.*, 2002; Ea *et al.*, 2006; Rothwarf *et al.*, 1998; Saito *et al.*, 2004; Schomer-Miller *et al.*, 2006; Tegethoff *et al.*, 2003; Wu *et al.*, 2006a; Ye *et al.*, 2000). More recently, a group identified and characterized the counterpart of the NEMO-binding domain, the IKK-binding domain (IBD) in NEMO. Various reports have demonstrated that the domain of NEMO necessary and sufficient for the interaction with IKKs is located in the amino-terminal portion of NEMO (Harhaj and Sun, 1999; Iha *et al.*, 2003; May *et al.*, 2000; Tegethoff *et al.*, 2003; Ye *et al.*, 2000). Marienfeld *et al.* demonstrated that IKKα and IKKβ bound on the region from amino acid 40 to 120 of NEMO. Moreover, they found that a coiled-coil domain spanning amino acids 47 to 80 within the IBD of NEMO, and consisting of three α-helical subdomains, is

crucial for both dimerisation as well as binding to IKKs. The study further demonstrated that this amino-terminal dimerisation domain in NEMO is required for robust, inducible NF-κB activation (Marienfeld *et al.*, 2006).

The composition of the IKK complex is still debated, and this is driven by the discrepancy between the apparent molecular weight observed during gel filtration, which is 700-900 kDa, and its predicted size, which is 200-350 kDa, based on the actual molecular weights of its individual components. So far, the only definitive members of the complex are IKKα, IKKβ, and NEMO, with many groups supporting the idea of a heterodimer of IKKα and IKKβ, which associates with NEMO (Miller and Zandi, 2001; Rothwarf and Karin, 1999). More recently, several proteins have been shown to interact with the IKK complex. The chaperone protein Hsp90 and a cochaperone called Cdc37 have been shown to be constitutively associated with the IKK complex (Chen *et al.*, 2002), and they may function in maintaining the complex during assembly or regeneration following signalling. Moreover, ELKS, a 105 kDa regulatory protein has also been recently demonstrated as an IKK-interacting protein (Ducut Sigala *et al.*, 2004). siRNA-mediated knockdown of ELKS blocked the early activation of NF-κB mediated by TNF-α and IL-1, and in the absence of ELKS, the IKK complex failed to associate with IκBα, suggesting a potential role for ELKS in mediating the interaction between the IKK complex and IκBα (Ducut Sigala *et al.*, 2004).

1.3.3.2 The Functions of the IKK Subunits

In order to study the roles of the three IKK subunits, knockouts of each one have been generated. IKKβ$^{-/-}$ mice exhibited embryonic lethality caused by liver degeneration, a phenotype highly analogous to p65$^{-/-}$ mice, supporting an argument for a central role for IKKβ in mediating NF-κB signalling via TNFα (Li *et al.*, 1999a; Li *et al.*, 1999b; Tanaka *et al.*, 1999). Therefore, it appears that there is no partial compensation for IKKβ by IKKα or any other kinase. In contrast, IKKα$^{-/-}$ mice were born live, but died perinatally from severe morphogenetic defects in keratinocyte proliferation and differentiation (Hu *et al.*, 1999). Interestingly, IκB degradation by proinflammatory stimuli was

virtually unaffected, but despite normal IκB degradation and nuclear translocation of NF-κB, IKKα$^{-/-}$ mice were deficient in inducing several NF-κB-dependent mRNAs in response to IL-1 and TNFα (Li *et al.*, 1999a; Li *et al.*, 2002). These findings indicate that IKKα plays a minor role in NF-κB signalling, but is perhaps required for development, as knockout mice exhibit altered limb bud morphology (Hu *et al.*, 1999; Li *et al.*, 1999a; Takeda *et al.*, 1999). Moreover, it was recently shown that in response to TNFα, IKKα in conjunction with RelA, is recruited to the promoter regions of NF-κB responsive genes including IkBα, IL-8, and IL-6, and mediates the inducible phosphorylation of Histone H3 at Ser10 (Anest *et al.*, 2003; Yamamoto *et al.*, 2003). IKKα was also found to interact with the transactivation domain of the transcriptional coactivator cAMP-response-element-binding protein (CREB)-binding protein (CBP), and enhance CBP-dependent transcription and histone H3 acetylation (Yamamoto *et al.*, 2003). This function was antagonised by IKKγ, which was also found to shuttle between cytoplasm and nucleus and compete with RelA and IKKα for binding to CBP (Verma *et al.*, 2004). These studies indicate that IKKα has an important downstream role in augmenting NF-κB-dependent gene expression by forming a complex with p65 or CBP on these promoter regions and, thus, regulating initial histone H3 phosphorylation and subsequent acetylation by CBP. IKKγ$^{-/-}$ mice exhibited embryonic lethality from severe liver apoptosis, and cells from NEMO$^{-/-}$ mice were refractory to NF-κB activation by proinflammatory stimuli (Makris *et al.*, 2000; Rudolph *et al.*, 2000; Schmidt-Supprian *et al.*, 2000). Studies using deletion mutants of NEMO demonstrate that the C-terminal portion is required for stimulus-induced activation of IKK through interaction with upstream adapters, whereas binding to IKKα and IKKβ occurs using sequences from the N-terminus (Makris *et al.*, 2002; Rothwarf *et al.*, 1998). Therefore, it appears that only IKKβ and NEMO are required for signalling through the classical NF-κB pathway.

1.3.3.3 Activation and Regulation of IKK

Numerous signalling pathways lead to the induction of the canonical NF-κB pathway, and almost all of these pathways proceed via the activation of IKK. Activation of the IKK complex is dependent on phosphorylation of the IKKβ catalytic subunit, which is phosphorylated on Ser177 and Ser181 within the activation loop of the kinase domain (Delhase *et al.*, 1999). The activation of the canonical NF-κB pathway is best characterised for TNFα, which recruits the IKK complex to the TNFR1 upon receptor binding (Chen *et al.*, 2002; Devin *et al.*, 2000; Zhang *et al.*, 2000). Genetic experiments have identified critical molecules in this process, including TRAF2 (Kelliher *et al.*, 1998; Tada *et al.*, 2001), TRAF5 (Tada *et al.*, 2001) and the protein kinase RIP1 (Devin *et al.*, 2000). Ligation of TNFR1 by trimeric TNFα causes aggregation of the receptor and binding of the TNFR-associated death domain protein (TRADD) (Jiang *et al.*, 1999). TRADD subsequently recruits the downstream adapter TRAF2, which in turn recruits the IKK complex through a direct interaction with the leucine zipper of IKKα or IKKβ (Devin *et al.*, 2000). TRAF2 also interacts with the serine/threonine kinase RIP1, which can bind also directly to NEMO and thereby recruit IKK to the TNFR1 signalling complex independent of TRAF2 (Zhang *et al.*, 2000). RIP has a role in addition to or independent of simple recruitment of the IKK complex. It may nucleate the assembly of a signalling complex that induces IKK activation through oligomerisation of NEMO and subsequent autophosphorylation of IKK (Delhase *et al.*, 1999). Although these findings fail to explain exactly how the IKK complex is activated, it seems most likely that IKKβ is either phosphorylated by upstream kinases that may be recruited by the C-terminus of IKKγ, or that a transautophosphorylation mechanism is responsible for its activation.

Key elements of another important pathway that is required for B cell and T cell receptor-mediated activation of IKK have recently been elucidated. TCR ligation induces phosphorylation of key residues on ITAMs present on the TCRζ and CD3. Phosphorylated ITAMs recruit SH2-domain-containing adapters, such as the Syk family tyrosine kinases Lck and ZAP70. Recent studies have implicated several potential signalling intermediates that appear to comprise a novel signalling pathway including PKCθ, CARMA1/CARD11,

Bcl-10, and MALT1 (Lucas *et al.*, 2004; Simeoni *et al.*, 2004; Thome, 2004). PKCθ is essential for activation of NF-κB by TCR (Sun *et al.*, 2000). PKCθ is capable of directly interacting with the IKK complex in primary T cells (Khoshnan *et al.*, 2000), and it is possible that PKCθ might act as a scaffold/adapter to link events in the synapse with the other essential components in this pathway, namely, CARMA1/CARD11, Bcl-10, and MALT1. CARMA1/CARD11 is required for PKCθ-mediated activation of NF-κB following TCR ligation (Gaide *et al.*, 2002; Hara *et al.*, 2003). Bcl-10, which interacts with MALT1 and cIAPs, is also critical for NF-κB activation via the BCR (Ruland *et al.*, 2001). Bcl-10 interacts with CARMA-1 and undergoes CARMA-1-dependent phosphorylation, although CARMA-1 lacks kinase activity (Bertin *et al.*, 2001; Gaide *et al.*, 2001). It has been shown that Bcl-10 and CARMA-1 can induce E3 activity of TRAF6, which is necessary for IKK activation in Jurkat T cells after TCR ligation, as demonstrated by RNAi against TRAF6 and TRAF2 (Sun *et al.*, 2004). Moreover, MALT1 triggers the K63 ubiquitination of Lys399 in the C-terminal zinc-finger domain of NEMO, and mutation of this residue inhibits NF-κB activation mediated by BCL10 (Zhou *et al.*, 2004). BCL10 in turn, can induce the oligomerization of MALT1 (Lucas *et al.*, 2001), which might enhance its ubiquitin ligase activity.

Recent studies seem to suggest a crucial role for the K63-linked polyubiqitination of NEMO in the activation of the IKK complex, and a deubiquitinating (DUB) enzyme, termed CYLD, has been shown to negatively regulate IKK (Brummelkamp *et al.*, 2003; Kovalenko *et al.*, 2003; Trompouki *et al.*, 2003). In contrast to K48-linked ubiquitination, which results in proteasomal degradation, K63-linked ubiquitination of NEMO facilitates the binding of other proteins with ubiquitin-binding domains that are required for activation of the IKKβ catalytic subunit (Burns and Martinon, 2004; Chen, 2005; Krappmann and Scheidereit, 2005). The adapter protein, transforming growth factor [TGF]-β-activated kinase (TAK)-1, which has been proposed to link TRAF6 with IKK (Takaesu *et al.*, 2000; Takaesu *et al.*, 2003), has been shown to have a critical role in TNF-, IL-1-, Toll-like receptor (TLR)-, and TCR-mediated activation of NF-kB (Chen, 2005; Chen *et al.*, 2006; Krappmann and Scheidereit, 2005). These findings support *in vitro* observations that TAK1

could activate IKK via a ubiquitination mechanism (Deng *et al.*, 2000b; Wang *et al.*, 2001). A ubiquitin-conjugating complex containing the E2 enzyme Ubc13/Uev1, termed TRAF6-regulated IKK activator (TRIKA) 1, was biochemically purified and found to ubiquitinate TRAF6 on lysine 63, leading to its activation. Polyubiquitinated and activated TRAF6 can then recruit a second complex, TRIKA2, containing TAK1, and the TAK1-binding proteins TAB2 and TAB3, which are themselves K63-linked polyubiquitin-binding proteins, and recruitment of this complex activates TAK1(Wang *et al.*, 2001). This allows TAK1-mediated phosphorylation of IKKβ at Ser177 and Ser181 within its activation loop (Wang *et al.*, 2001), which results in activation of the IKK complex. It has therefore become progressively clearer that posttranslational modifications of NEMO play a critical role in the activation of the IKK complex.

Another pathway of NEMO-dependent IKKβ activation occurs during NF-κB activation in response to genotoxic stress. DNA damage elicits a complex cellular response, and the product of the gene mutated in ataxia-telangiectasia (ATM), a PI3-kinase-related kinase, plays a central role in sensing DNA damage and activating the DNA repair machinery (Yang *et al.*, 2004). Recently, cellular exposure to DNA damaging agents has been shown to result in the modification of NEMO with the small ubiquitin-like modifier (SUMO-1) (Huang *et al.*, 2003). NEMO translocates to the nucleus, where it is sumoylated on Lys227 and Lys309 (Huang *et al.*, 2003; Wu *et al.*, 2006b), and this results in NEMO phosphorylation by ATM on Ser85. ATM-mediated NEMO phosphorylation leads to the replacement of NEMO sumoylation by mono-ubiquitination, which promotes the nuclear export of NEMO in a complex with ATM. Finally, the cytoplasmic NEMO-ATM complex associates with an IKK regulator rich in glutamate, leucine, lysine, and serine (ELKS), which causes the activation of the IKK complex (Wu *et al.*, 2006b).

On the basis of overexpression studies, many candidate IKKβ kinases have been suggested (Ghosh and Karin, 2002), but only a few have stood the test of genetic ablation or RNA interference. MAP/ERK kinase kinase (MEKK) $3^{-/-}$ MEFs were unable to degrade IκBα following TNF-α stimulation, and MEKK3

can induce IKK activation in RIP-deficient cells (Yang *et al.*, 2001). However, it is not yet clear whether MEKK3 can directly phosphorylate IKK following TNF stimulation. Moreover, the protein kinase C PKCζ, has been implicated as a potential IKK kinase (Lallena *et al.*, 1999; Sanz *et al.*, 2000), since it was found to be required in TNFα-mediated IKK activation in mouse lung cells, but not in MEFs (Leitges *et al.*, 2001).

A different mechanism by which IKKβ may be activated is via induced proximity and trans-autophosphorylation. Indeed, many of the proposed IKK kinases have been found to play the role of adaptors instead of kinases. It has been shown that enforced oligomerisation of the N-terminus of NEMO, or truncated IKKα and IKKβ mutants lacking their C-terminus, can activate IKK, and it is proposed that RIP1 may mediate the oligomerisation of IKK *in vivo* (Inohara *et al.*, 2000; Poyet *et al.*, 2000). Overexpression of active IKKβ leads to activation via autophosphorylation (Woronicz et al., 1997; Zandi *et al.*, 1998), and it is suggested that the ability of IKKβ to oligomerise and trans-autophosphorylate is essential for IKK activation (Tang *et al.*, 2003). It is also possible that the two mechanisms are not mutually exclusive. Recent data suggest that NEMO interacts with IKKα and IKKβ as a tetramer (Tegethoff *et al.*, 2003), which holds the kinase subunits in a position that facilitates transautophosphorylation. Most studies agree that in the assembly of the IKK signalsome, NEMO binds to both IKKα and IKKβ, and this tripartite complex can optimise the positioning of the IKKβ reactive loop for activation. However, a more recent report has indicated that in unstimulated cells, NEMO can be found as a monomer, or a heterodimer with either IKKα or IKKβ (Fontan *et al.*, 2007). In this model, in response to stimulation by IL-1β, or the oncoprotein Tax from HTLV-1, NEMO dimerises thereby recruiting IKKα or IKKβ in a high molecular weight complex with increased IKK activity (Fontan *et al.*, 2007). It is also possible that the post-translational modification of IKK subunits might trigger a conformational change within the complex that facilitates IKKβ autophosphorylation. Indeed, IKKβ activation-loop phosphorylation at Ser177 and Ser181 has been shown to lead to mono-ubiquitination of IKKβ at Lys163, and mutation of Lys163 abolishes IKKβ trans-autophosphorylation of further C-terminal serine residues (Delhase *et al.*, 1999; Schomer-Miller *et al.*, 2006).

1.3.4 Alternative NF-κB Pathway

Research over the last few years has characterised a novel signalling pathway, which regulates the processing of p100/NF-κB2 to p52. This is distinct from the classical NF-κB pathway and is now known as the "alternative" or "non-canonical" NF-κB pathway (Pomerantz and Baltimore, 2002) (Figure 1.7). The first indication that p100 processing may be regulated came from the observation that overexpression of NIK in 293 cells was sufficient to induce p100 processing, independently of IKKα and IKKβ (Senftleben *et al.*, 2001). Splenocytes derived from the alymphoplasia (*aly/aly*) mice, which contain a point mutation in NIK that blocks its ability to induce p100 processing, displayed a dramatic reduction in p52 levels, although p100 levels were normal, as compared to the control *aly/+* heterozygous cells (Xiao *et al.*, 2001b; Yamada *et al.*, 2000). Consistent with the hypothesis that p100 and NIK might be part of the same pathway, *aly/aly* and *nik*$^{-/-}$ mice (Koike *et al.*, 1996; Yin *et al.*, 2001) display a phenotype that bears remarkable similarity to that of *nfkb2*$^{-/-}$ mice (Caamano *et al.*, 1998; Franzoso *et al.*, 1998). These mice are characterised by the systemic absence of lymph nodes and Peyer's patches, disorganised splenic and thymic architectures, lack of germinal centres, and defective B-cell mediated responses, resulting in immunodeficiency. Soon afterwards, Senftleben et al, demonstrated a role for IKKα in this pathway, using IKKα$^{-/-}$ haematopoietic stem cells to reconstitute lethally irradiated mice (Kaisho *et al.*, 2001; Senftleben *et al.*, 2001). These chimeras displayed similar defects in B cell maturation and lymphoid architecture to those of aly/aly, NIK$^{-/-}$ and *nfkb2*$^{-/-}$ mice. Moreover, B cells derived from IKKα$^{-/-}$ mice exhibited a specific deficiency in p100 processing that could not be rescued by the ectopic expression of NIK (Senftleben *et al*, 2001). *In vitro* kinase assays suggested that IKKα can phosphorylate p100 directly, leading to ubiquitin-dependent generation of p52 (Senftleben *et al*, 2001). IKKβ and NEMO are not required for NIK-induced p100 processing (Senftleben *et al.*, 2001; Xiao *et al.*, 2001a), raising the possibility that the pool of IKKα regulating p100 processing may

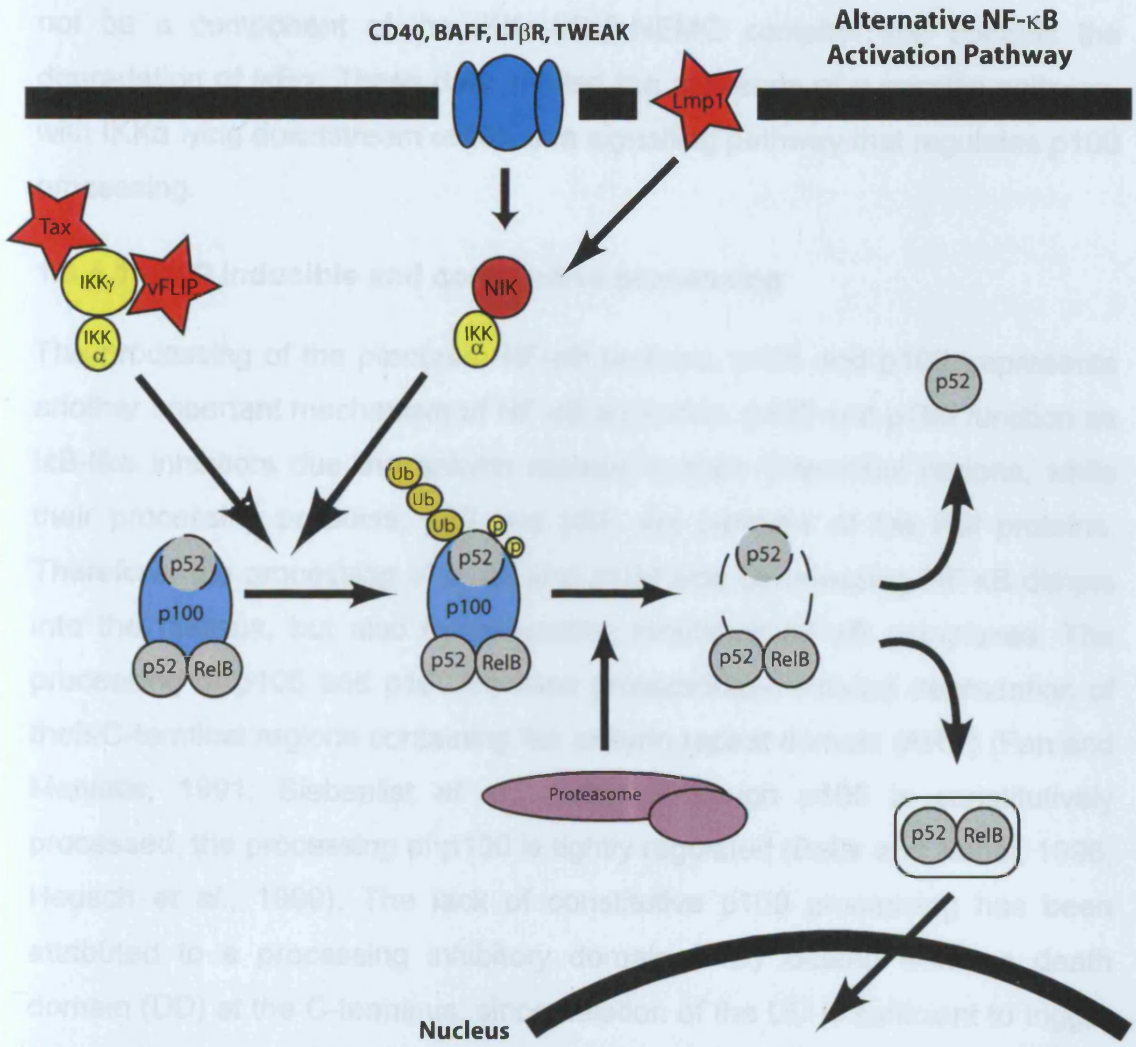

Figure 1.7 The alternative pathway of NF-κB activation

The alternative pathway involves activation of the NIK (NF-κB inducing kinase) protein kinase and the IKKα catalytic subunit of the IKK complex via membrane-bound receptors of the TNF-R superfamily. Phosphorylation by IKKα results in p100 ubiquitination by the SCF ubiquitin ligase complex, and its partial processing from p100 to p52 by the 26S proteasome. NF-κB dimers containing RelB are then released and are free to translocate into the nucleus. The alternative NF-κB pathway is important for secondary lymphoid organ development, maturation of B-cells, and adaptive humoral immunity. Three viral oncoproteins have also been shown to activate the alternative NF-κB pathway. The Tax oncoprotein from HTLV-1, and vFLIP from KSHV, act via IKKα and IKKγ, while LMP1 from EBV mimics CD40 signalling and therefore requires NIK and IKKα. Ub, ubiquitin; P, phosphorylation.

not be a component of the IKKα-IKKβ-NEMO complex that controls the degradation of IκBα. These data implied the existence of a specific pathway, with IKKα lying downstream of NIK in a signalling pathway that regulates p100 processing.

1.3.4.1 p100 inducible and constitutive processing

The processing of the precursor NF-κB proteins, p105 and p100, represents another important mechanism of NF-κB activation. p105 and p100 function as IκB-like inhibitors due the ankyrin repeats in their C-terminal regions, while their processing products, p50 and p52, are partners of the Rel proteins. Therefore, the processing of p105 and p100 acts by releasing NF-κB dimers into the nucleus, but also by generating functional NF-κB complexes. The processing of p105 and p100 involves proteasome-mediated degradation of their C-terminal regions containing the ankyrin repeat domain (ARD) (Fan and Maniatis, 1991; Siebenlist *et al.*, 1994). Although p105 is constitutively processed, the processing of p100 is tightly regulated (Betts and Nabel, 1996; Heusch *et al.*, 1999). The lack of constitutive p100 processing has been attributed to a processing inhibitory domain (PID) located within a death domain (DD) at the C-terminus, since deletion of the DD is sufficient to trigger constitutive processing of p100 (Xiao *et al.*, 2001b). Processing of p100 is also regulated by a glycine-rich region (GRR) at amino acid 346-377 (Heusch *et al*, 1999). Translocation of this GRR alters the site of proteasomal processing (Heusch *et al.*, 1999). Inducible activation of NIK, leads to activation of downstream IKKα by NIK (Senftleben *et al.*, 2001), which also recruits IKKα into a complex with p100 via two C-terminal serines, S866 and S870, of p100 (Xiao *et al.*, 2004). Formation of this complex is followed by the phosphorylation of N- and C-terminal serines of p100, namely Ser99, 108, 115, 123, 872, which results in p100 ubiquitination (Fong and Sun, 2002; Fong *et al.*, 2002; Xiao *et al.*, 2004). The DD of p100 is required for the phosphorylation-induced recruitment of β-transducing repeat-containing protein (β-TrCP), a component of the SKP1-cullin-F box (SCF) ubiquitin ligase complex which catalyses p100 polyubiquitination (Fong *et al.*, 2002a). β -TrCP has been demonstrated to bind to a phosphorylated sequence in the p100, which represents a polypeptide sequence enriched in proline (P), glutamic

acid (E), serine (S), and threonine (T), and is termed the PEST region. This region has been shown to be related to the β -TrCP binding site on IκBα, and is thought to be directly phosphorylated by IKKα (Senftleben *et al.*, 2001). More recently, it was shown that NIK/IKKα-dependent phosphorylation of p100 at serines 866, 870, and possibly 872, creates a binding site for β -TrCP, thereby regulating p100 ubiquitination (Liang *et al.*, 2006). The amino acid residue Lys855, which is located on an N-terminal region to the β-TrCP binding site, serves as the major ubiquitin-anchoring residue in p100 (Amir *et al.*, 2004). Yeast two-hybrid analysis identified S9, a non-ATPase subunit in the 19S subcomplex of the 26S proteasome, as an interacting partner of the C-terminus of p100 (Fong *et al.*, 2002b). In mammalian cells, this interaction was NIK-inducible and led to the partial processing of p100 to generate p52. The most recent data suggest that besides that C-terminal sequences, multiple functional regions, including the dimerisation domain, the nuclear localization signal, and the glycine-rich region, which are located in the N terminus of p100, may also play important roles in the constitutive and inducible processing of p100 (Qing *et al.*, 2005).

Constitutive processing of p100, which occurs due to the loss of its C-terminal PID domain and part of the ARD domain, has been detected in various lymphomas associated with *nfkb2* gene rearrangements (Xiao *et al.*, 2001b). Both common and different mechanisms have been implicated in the regulation of physiological, and the constitutive pathogenic processing of p100. Inducible and constitutive processing of p100 require IKKα, and involve the same regions of the N-terminus of p100, suggesting a common mechanism (Qing *et al.*, 2005; Qing and Xiao, 2005). Nevertheless, the mechanisms for signal-induced and constitutive p100 processing appear to be different. In contrast to inducible p100 processing, which relies on β-TrCP for p100 poly-ubiquitination, β-TrCP is dispensable for the constitutive processing of p100, which is not associated with ubiquitination either, but rather is regulated by the nuclear translocation of p100 (Fong and Sun, 2002; Liao and Sun, 2003; Qing *et al.*, 2005; Xiao *et al.*, 2001b). Moreover, the subcellular localization of induced and constitutive p100 processing is distinct. NIK-induced processing of p100 occurs in the cytoplasm, while the constitutive

processing of p100 occurs in the nucleus in association with κB-containing promoter elements (Qing *et al.*, 2005; Qing and Xiao, 2005). In the nucleus, the C-terminal truncated p100 mutants (p100ΔCs) bind to the κB motifs of the promoters and subsequently recruit the proteasome, to form a stable proteasome/p100ΔC/DNA complex, which mediates the processing of p100ΔCs. The constitutive processing of the p100ΔCs is initiated by a proteasome-mediated endoproteolytic cleavage at amino acid D415 (Qing *et al.*, 2007), whereas inducible processing of p100 seems to be mediated by proteasomal exoproteolytic degradation from the C-terminal end.

1.3.4.2 Activation and Regulation of the Alternative Pathway

It is now known that the alternative NF-κB pathway is not activated by most of the stimuli that induce the classical NF-κB pathway (Xiao et al., 2001a; Xiao et al., 2001b). The full picture of inducible p100 processing was obtained through studies of signalling that occurs downstream of four independent receptors belonging to the TNF receptor superfamily, which have been shown to induce p100 processing. Treatment of lymphotoxin-β receptor (LTβR)-expressing MEFs with an anti-LTβR antibody has demonstrated that LTβR signalling induces processing of p100 to p52 in MEFs. Moreover, studies on knockout MEFs have shown that NIK and IKKα are required for LTβR-induced p100 processing, but IKKβ and NEMO seem to be dispensable in this process (Dejardin *et al.*, 2002; Mordmuller *et al.*, 2003; Muller and Siebenlist, 2003; Saitoh *et al.*, 2002). LTβR is expressed on stromal cells, and analysis of LTβR knockout mice has suggested a crucial role for this receptor in peripheral lymphoid tissue organogenesis, since mice lacking LTβR fail to form lymph nodes and Payer's patches (Gommerman and Browning, 2003; Shakhov and Nedospasov, 2001). Two distinct receptors have been shown to regulate p100 processing in B-cells, namely B-cell activating factor receptor (BAFF-R) (Claudio *et al.*, 2002; Kayagaki *et al.*, 2002), and CD40 (Coope *et al.*, 2002). B-cell activating factor (BAFF) is critical for the development and survival of peripheral B cells (Gross *et al.*, 2001; Schiemann *et al.*, 2001). BAFF receptor 3 (BR3) is the only specific receptor for BAFF and it has been demonstrated to trigger p100 processing via a NIK-dependent pathway (Claudio *et al.*, 2002; Kayagaki *et al.*, 2002). BAFF-induced p100 processing has been shown to

play an important role in promoting the survival and maturation of transition-1-stage splenic B-cells (Claudio et al., 2002; Mackay *et al.*, 2003). Interestingly, transgene mediated overexpression of BAFF leads to B cell hyperplasia and a systemic lupus erythematous-like condition in mice (Gross *et al.*, 2000; Khare *et al.*, 2000; Mackay *et al.*, 1999). CD40 is expressed on B cells and triggers their clonal expansion and differentiation (Calderhead *et al.*, 2000). Treatment of CD40-expressing B cells with CD40 ligand also induces p100 processing (Coope *et al.*, 2002). Comparison between *nfkb2*$^{-/-}$ and wild-type splenic B cells has suggested that CD40 activation of the alternative pathway is important for optimal promotion of cell survival and homotypic aggregation (Zarnegar *et al.*, 2004). TWEAK (TNF-like weak inducer of apoptosis), which is expressed on human monocytes, can also induce p100 processing (Saitoh *et al.*, 2002). Therefore, it appears that the alternative pathway activates a transcriptional programme that is essential to B cell function. Finally, RANKL (receptor activator of NF-κB ligand), which is involved in osteoclast differentiation (Teitelbaum, 2000), has also been shown to induce p100 processing to p52 in osteoclast precursors in a NIK-dependent manner (Novack *et al.*, 2003). Moreover, NIK knockout, or expression of a non-processable p100, blocks induction of osteoclastogenesis by RANKL, and it therefore seems that alternative pathway activation also plays a role in bone formation (Novack *et al.*, 2003). These biochemical studies have highlighted several similarities in the mechanisms employed by stimuli for the activation of the alternative NF-κB pathway. Induction of p100 processing by all of these inducers is dependent on NIK and IKKα, but IKKβ and IKKγ were not required for p100 processing, suggesting that an alternative IKKα-containing complex might transmit the signal for p100 processing (Claudio et al., 2002; Coope et al., 2002; Dejardin et al., 2002; Kayagaki et al., 2002; Novack et al., 2003; Saitoh *et al.*, 2003). Moreover, activation of p100 processing by LTβR, BAFF-R, and CD40 is blocked by pre-treatment of cells with cycloheximide, an inhibitor of protein synthesis, indicating a requirement for *de novo* protein synthesis prior to the induction of the alternative pathway (Claudio et al., 2002; Muller and Siebenlist, 2003; Regnier et al., 1997). NIK and p100 are likely candidates altered by the use of cycloheximide sine it has been shown that induction of the alternative pathway by BAFF-R and CD40 upregulates

the expression of NIK protein (Liao *et al.*, 2004), and it has been proposed that LTβR induces p52 generation by a co-translational mechanism (Mordmuller et al., 2003). It appears that the non-canonical stimuli employ a novel mechanism that accounts for the increase in NIK levels. They stabilize NIK by specifically preventing basally translated NIK protein from undergoing degradation (Qing et al., 2005), which appears to be based on an inhibition of TRAF3-mediated NIK degradation (Liao *et al.*, 2004). Indeed, TRAF3 seems to be a negative regulator of CD40- and BAFF-induced p100 processing, through its association with a novel-sequence motif at the N-terminus of NIK (Liao *et al.*, 2004). TRAF3 binding targets NIK for ubiquitination and subsequent proteasomal degradation, whereas stimulation of M12 B-cells with either an agonist anti-CD40 antibody, or with recombinant BAFF, which both activate the alternative NF-κB pathway, induces stabilization of NIK and enhancement of NIK protein levels through endogenous degradation of TRAF3 (Liao *et al.*, 2004). On the other hand, TRAF2 and TRAF5 seem to be positive regulators for CD-40- and TWEAK-induced p100 processing (Hauer *et al.*, 2005; Saitoh et al., 2003). The cytoplasmic tail of CD40 has been shown to carry a binding site for TRAF2, which is essential for CD40-induced p100 processing (Coope et al., 2002; Grammer and Lipsky, 2000), while mutation of the TRAF-binding site in the cytoplasmic tail of the TWEAK receptor Fn14 (fibroblast-growth-factor-inducible 14) is capable of blocking TWEAK-induced p100 processing (Saito *et al.*, 2003). Moreover, TWEAK fails to induce p100 processing in cells deficient in TRAF2 and TRAF5 (Hauer et al., 2005; Saito et al., 2003).

Another common feature of the inducers of the alternative NF-κB pathway is that both classical and alternative pathways were activated by these stimuli. Time course studies have indicated that receptor induction of p100 processing is very slow, whereas the activation of IκBα degradation by the same stimuli occurs within minutes (Muller and Siebenlist, 2003; Saccani, 2003). Analysis of knockout MEFs has also demonstrated distinct patterns of gene expression in $IKK\alpha^{-/-}$ and $IKK\beta^{-/-}$ mice (Dejardin et al., 2002; Senftleben et al., 2001). LTβR activation of the canonical NF-κB pathway induced the expression of proinflammatory molecules, including macrophage inflammatory factor (MIP)-

1β, MIP2, and VCAM-1, which was dependent on IKKβ, whereas LTβR-mediated activation of the alternative pathway induced the expression of a set of distinct factors, such as secondary lymphoid tissue chemokine (SLC), B lymphocyte chemoattractant (BLC), EBV-induced gene (EBI)-1-ligand chemokine (ELC), and BAFF, which were dependent on IKKα (Dejardin *et all*, 2002). These findings suggest that the alternative and classical pathways can operate independently, and are distinct in time course and the genes that they regulate, which may depend on cell type, stimulus, and the target gene involved. However, there is also a certain level of cross-talk between both pathways. LTβR stimulation of wild-type MEFs initially leads to the nuclear translocation of dimers like p50/p65, released from IκBα degradation, which results in transcription of its target genes, one of them being *nfkb2* (Dejardin et al., 2002; Liptay *et al.*, 1994). In contrast, LTβR-activated MEFs deficient in p65 or IKKβ, display reduced levels of p100 and subsequently p52 proteins. Thus the canonical NF-κB pathway seems to be indirectly linked to the alternative NF-κB pathway, so that classical activation may be necessary to feed the alternative pathway, in order to ensure sufficient production of p100 for the efficient generation of its p52 processing product.

1.3.4.3 Viral Activation of the Alternative Pathway

Aberrant processing of p100 and overproduction of p52 has been associated with three viral oncoproteins, which can activate both classical and alternative NF-κB pathways. These are the Tax transforming protein of Human T cell leukaemia virus (HTLV)-1, the latent membrane protein 1 (LMP1) encoded by EBV, and the viral FLIP (vFLIP) protein of KSHV (Figure 1.7). HTLV-1 is associated with an acute and fatal T-cell malignancy termed, adult T-cell leukaemia (ATL) (Poiesz *et al.*, 1980; Yoshida *et al.*, 1982), EBV is the etiological agent for several malignancies including Burkitt's lymphoma, classical Hodgkin's lymphoma and nasopharyngeal carcinoma, and KSHV has been associated with neoplasms such as Kaposi's sarcoma, primary effusion lymphoma (PEL), and multicentric castelman's disease (MCD) (discussed in section 1.2.5). LMP1 is one of five latent genes of EBV essential and sufficient for inducing transformation of B cells, and its oncogenic ability requires NF-κB activation (Kaye *et al.*, 1995). LMP1 has six membrane-

spanning domains with a long C-terminal cytoplasmic tail that oligomerises in the plasma membrane (Saito et al., 2003). It is a functional homologue of CD40 (Kilger *et al.*, 1998; Zimber-Strobl *et al.*, 1996), but has ligand-independent constitutive activity (Gires *et al.*, 1997). Via its C-terminus, LMP1 activates both NF-κB and AP-1 transcription factors, and this domain is required for transformation by LMP1 (Eliopoulos and Young, 2001). Along the cytoplasmic tail of LMP1 there are subdomains, termed carboxy-terminal activating regions (CTARs), which are responsible for recruiting adapter molecules and activating NF-κB (Devergne *et al.*, 1996; Huen *et al.*, 1995; Mitchell and Sugden, 1995). CTAR1 is responsible for triggering IκBα degradation and therefore classical pathway activation, and CTAR2 is required for the induction of p100 processing and the translocation of RelB and p52 in the nucleus (Atkinson *et al.*, 2003; Eliopoulos *et al.*, 2003; Saito *et al.*, 2003). LMP1 mimics CD40 and other TNFR members in their mechanism of activation of the alternative NF-κB pathway, and genetic models have demonstrated the requirement of a TRAF-binding site in its C-terminal cytoplasmic tail, NIK and IKKα (Coope et al., 2002), but not IKKβ and IKKγ (Saito et al., 2003).

HTLV-1 can transform T-cells through its regulatory protein Tax, which potently induces the aberrant expression of a large number of cellular genes involved in T-cell growth and survival (Ressler *et al.*, 1996), many of which are also regulated via NF-κB (Sun and Ballard, 1999). Tax is a potent intracellular stimulator of NF-κB, and this activity is essential for its oncogenic action (Jeang, 2001). Furthermore, Tax can activate NF-κB through a direct interaction with IKKγ that requires two homologous leucine zipper domains located within IKKγ (Chu *et al.*, 1999; Harhaj and Sun, 1999; Jin *et al.*, 1999; Xiao *et al.*, 2000). The function of this interaction is to recruit Tax to the IKK catalytic subunits, IKKα and IKKβ, which can induce persistent IKK activation and subsequent degradation of IκBs (Chu *et al.*, 1998; Geleziunas *et al.*, 1998; Uhlik *et al.*, 1998; Xiao and Sun, 2000; Yin *et al.*, 1998). Subsequently, Tax has been demonstrated to induce p100 processing (Xiao *et al.*, 2001a). In contrast to other known activators of p100 processing, Tax functions independently of NIK and requires IKKα but not IKKβ, although IKKγ and its

adaptor function are also required (Xiao *et al.*, 2001a). By directly binding to both p100 and IKKγ, Tax specifically recruits IKKα to p100, and triggers p100 processing (Xiao *et al.*, 2001a).

vFLIP of KSHV is one of three proteins encoded by the latency associated cluster. It has unique functional properties, amongst which the ability to block death receptor-mediated apoptosis (Thome *et al.*, 1997). vFLIP can also activate the classical NF-κB pathway by virtue of its ability to physically associate with IKKγ (Field *et al.*, 2003) and activate the IKK complex (Chaudhary *et al.*, 1999; Field *et al.*, 2003). More recently, expression of vFLIP was shown to constitutively upregulate p100 expression and processing to p52 (Matta and Chaudhary, 2004). Similar to Tax of HTLV-1, activation of the alternative pathway depends on IKKα, whereas IKKβ and NIK are dispensable for this process (Matta and Chaudhary, 2004).

The most recent data indicate that the Saimiri transforming protein (STP)-A11, an oncoprotein of *Herpesvirus saimiri* (HVS), is the fourth viral protein that can activate the alternative NF-κB pathway leading to processing of p100 to p52 (Cho *et al.*, 2007). HVS, a member of the γ-2 herpesvirus family and one of the most closely related viruses to KSHV, naturally infects squirrel monkeys without any disease, but has been associated with the incidence of rapidly progressive fulminant lymphomas in marmoset, owl monkeys, and other species of New World primates (Damania *et al.*, 2000; Jung et al., 1999). Previous reports have demonstrated that STP-A11 can interact with TRAF2, TRAF3, and TRAF5, leading to activation of NF-κB and cell survival (Lee *et al.*, 1999). More recently, STP-A11 was shown to induce the proteasome-mediated processing of p100 to p52, and the translocation of p52 to the nucleus. A dominant negative mutant of NIK resulted in a decrease in the p52 levels generated in the presence of STP-A11, but this was not drastic, indicating that STP-A11can induce p100 processing through a NIK-dependent, as well as a NIK-independent mechanism. Moreover, analysis of STP-A11 mutants, carrying mutations on the TRAF6-binding site and Src-binding site of the protein, revealed a requirement for only the TRAF6-binding site for STP-A11-mediated p100 processing (Cho *et al.*, 2007).

1.4 KSHV-Encoded vFLIP

1.4.1 Apoptosis

ORF71/K13 in the KSHV genome encodes the vFLIP protein. In order to explain the discovery and function of vFLIP it is helpful to understand the pathways involved in apoptosis.

Apoptosis is a cellular response that regulates important processes such as tissue homoeostasis, defense against certain pathogens and elimination of unwanted cells. Apoptosis is a highly regulated process characterised by cytoskeleton disruption, shrinking of cells, condensation of nuclei and internucleosomal degradation of DNA (Kerr *et al.*, 1972). The ordered series of biochemical events that culminate in apoptosis can be triggered either at the cell membrane (extrinsic pathway) or through various forms of intracellular stress (intrinsic pathway). In each case, large multi-protein complexes are formed and a family of proteins called caspases are activated (Bratton *et al.*, 2000). The extracellular death stimuli (Fas/CD95 ligand) directly activate the death receptors (DRs) through ligand-induced assembly of a death-inducing signalling complex (DISC) at the plasma membrane (Peter and Krammer, 2003). The assembly of DISC results in the activation of caspase-8, which subsequently activates the effector caspases, caspase-3 and –7 (Riedl and Shi, 2004). Death receptors (DRs) are a family of transmembrane proteins that belong to the TNF family of receptors (Strasser *et al.*, 2000). The activated death ligands are homo-trimeric and thus induce oligomerisation of the death receptors upon binding. The death receptors then recruit the adaptor protein FADD through homophilic interaction between the death domains (DD) present on both proteins (Chinnaiyan *et al.*, 1995). FADD, in turn, uses its death effector domain (DED) to interact with the N-terminal tandem DEDs of procaspase-8 or –10, thereby linking them to the activated death receptors within the DISC (Kischkel *et al.*, 2001). Apoptosis is tightly regulated and can be inhibited at the receptor level by receptor endocytosis, soluble ligands, and decoy receptors. Apoptosis is also regulated at effector stage by three groups of inhibitors, the inhibitor of apoptosis family (IAP), the Bcl-2 family, and the FLIP (FADD-like interleukin-1-β-converting enzyme

[FLICE/caspase 8]-inhibitory protein) family. The IAPs bind directly to caspases-3, -6, -7, and -9 to inhibit their function. The anti-apoptotic Bcl-2 family members regulate the intrinsic pathway of apoptosis, which is activated to eliminate cells in response to ionising radiation, cytotoxic drugs, growth factor withdrawal and other forms of intracellular damage (Boatright and Salvesen, 2003). A different, more direct mechanism of apoptosis inhibition is mediated by the FLIP family (Thome *et al.*, 1997), which along with KSHV-encoded vFLIP, is the main focus of this section. It is interesting to note that KSHV encodes a viral homologue of each member of the three groups of inhibitors of apoptosis. ORF K7 encodes a viral IAP (vIAP) (section 1.2.8.5) protein, ORF16 encodes a viral homologue of human Bcl-2 (vBcl-2) (section 1.2.8.4), and ORF71 encodes a viral FLIP protein. NF-κB can also inhibit apoptosis by controlling the expression of some of these antiapoptotic inhibitory proteins.

1.4.2 The FLIP Family-Inhibitors of Apoptosis

To evade the host immune response, a number of viruses express distinct families of inhibitory proteins to suppress apoptosis and to promote their replication and survival in host cells (Thome and Tschopp, 2001). One important family of such proteins are the viral FLICE-inhibitory proteins (v-FLIPs). The FLIP family was discovered in 1997 through data-base mining to identify viral genes containing DEDs and therefore related to apoptosis (Bertin *et al.*, 1997; Thome *et al.*, 1997). The first FLIP genes were discovered within two oncogenic γ-herpesviruses and a human poxvirus associated with benign neoplasms of the skin: ORF71 of HVS (HVS-FLIP), ORF E8 of equine herpesvirus 2 (EHV-2) and ORF MC159L of molluscum contagiosum virus (MCV) respectively (Thome *et al.*, 1997). Other members include bovine herpervirus-4 (BHV-4) and ORF71/K13 from KSHV (Hu *et al.*, 1997a). The hallmark of all vFLIP proteins is two DED domains in tandem, linked by an intervening short linker, which are also present in the prodomains of caspase-8 and –10. The presence of DEDs in vFLIP immediately suggests potential interaction with FADD and caspase-8. Initial experiments transfected these viral FLIP proteins into cells to demonstrate protection against CD95- and TNFR1-induced apoptosis. Indeed, the DEDs of MC159 and E8 have been

shown to interact with the DED of FADD and the prodomain of caspase-8 (Bertin et al., 1997; Hu et al., 1997a; Shisler and Moss, 2001; Thome et al., 1997). Therefore, through homotypic DED interactions, some vFLIPs are thought to hinder efficient recruitment and subsequent activation of caspase-8 at the death receptors, enhancing lytic production of the virus.

1.4.3 Cellular FLIP

The cellular homologue, cFLIP, was subsequently identified (Irmler *et al.*, 1997). Several differentially spliced forms of cFLIP exist, but only two forms have been identified as proteins *in vivo*: short cFLIP ($cFLIP_S$) of 26 kDa and long cFLIP ($cFLIP_L$) of 55 kDa. $cFLIP_S$ is similar in structure to the herpesvirus FLIP proteins with an extended C-terminus of 20 amino acids. The N-terminus of $cFLIP_L$ is identical to that of $cFLIP_S$, but the C-terminus consists of a caspase-homologous domain that is catalytically inactive and contains cysteine and histidine residue substitutions within the enzymatic active site (Irmler *et al.*, 1997; Rasper *et al.*, 1998). In overall structure, $cFLIP_L$ is therefore similar to caspase-8 and -10. Both forms of cFLIP are recruited to the DISC and interfere with the function of caspase-8, although their mechanism of action is different. Like the viral FLIPs, $cFLIP_S$ is recruited by FADD and prevents the processing and release of active caspase-8 (Bin *et al.*, 2002; Krueger *et al.*, 2001). The role of $cFLIP_L$ is more controversial.

$cFLIP_L$ has been shown to have both pro- and anti-apoptotic activities. $cFLIP_L$ binds directly to caspase-8 via DED and caspase domains (Han *et al.*, 1997; Irmler *et al.*, 1997; Rasper *et al.*, 1998; Srinivasula *et al.*, 1997), and both proteins are partially processed at the DISC (Krueger *et al.*, 2001; Scaffidi *et al.*, 1999). Furthermore, $cFLIP^{-/-}$ mice showed deficient heart development that is similar to those of $FADD^{-/-}$ and $caspase\text{-}8^{-/-}$ mice (Yeh *et al.*, 2000), suggesting that cFLIP shares function with caspase-8 and FADD, rather than antagonising their activity. On the other hand, overexpression of both forms of cFLIP has been shown to have a protective effect against apoptosis induced by DRs including Fas, TNFR1, TRAIL-R1, TRAIL-R2 and TRAMP (Goltsev *et al.*, 1997; Hu *et al.*, 1997b; Irmler et al., 1997; Rasper et al., 1998; Schneider *et al.*, 1997; Srinivasula et al., 1997). Moreover, gene knockout studies

suggest that MEFs from cFLIP$^{-/-}$ mice (deficient in cFLIP$_L$ and cFLIP$_S$) are more sensitive CD95-induced apoptosis than their wild type counterparts (Yeh *et al.*, 2000). Because cFLIP$^{-/-}$ causes deficiency of both cFLIP$_L$ and cFLIP$_S$, these studies cannot rule out the possibility that cFLIP$_L$ has proapoptotic function. Although the majority of reports seem to support the notion that cFLIP$_S$ is antiapoptotic, the function of cFLIP$_L$ remains controversial. Although overexpression of transfected cFLIP$_L$ inhibits apoptosis, recent studies have demonstrated that cFLIP$_L$ can form catalytically active heterodimeric complexes with caspase-8 (Micheau *et al.*, 2002), and that ectopic expression of cFLIP$_L$ at physiological levels enhances procaspase-8 processing in the CD95 DISC and promotes apoptosis (Chang *et al.*, 2002a). In this complex, c-FLIP$_L$ contains a C-terminal loop that actually activates the enzymatic pocket of caspase-8 (Chang et al., 2002a; Micheau et al., 2002). However, the most recent data suggest that endogenous cFLIP$_L$ functions primarily as an inhibitor of DR-mediated apoptosis, since selective knockdown of cFLIP$_L$ using siRNA, enhanced DISC recruitment and activation of caspase-8, leading to apoptosis (Sharp *et al.*, 2005). Therefore, it appears that cFLIP$_L$ can act as a molecular switch, which can either promote cell death or growth signals transmitted by Fas.

cFLIP is not only involved in DR-mediated apoptosis, but also activates NF-κB. Activation of NF-κB by cFLIP requires its DEDs for function (Chaudhary *et al.*, 2000; Hu *et al.*, 2000; Kataoka *et al.*, 2000). In the case of Fas stimulation, which results in increased proliferation of CD3-activated human T lymphocytes, there is recruitment of cFLIP$_L$ to the receptor. Fas-recruited cFLIP can then interact with TRAF1 and TRAF2, and with the kinases RIP and Raf-1, leading to the activation of NF-κB and Erk, which results in increased production of IL-2 (Kataoka *et al.*, 2000). More recently, a yeast two-hybrid screen identified p105 as a cFLIP$_L$-interacting protein. cFLIP$_L$ interacts with p105 in 293T cells and inhibit its processing to p50 (Li *et al.*, 2003). Domain mapping experiments indicated that either the DEDs or the caspase-like domain of cFLIP$_L$ can independently interact with p105, although only the caspase domain can inhibit p105 processing. Moreover, overexpression of p105 potentiated cFLIP$_L$-induced apoptosis, probably due

to the p105-mediated inhibition of $cFLIP_L$-induced NF-κB activation (Li *et al.*, 2003). In addition, a novel cFLIP isoform, p22-cFLIP, which is an N-terminal cleavage product of cFLIP, was recently shown to be able to strongly induce the canonical NF-κB pathway, by interacting with the IKKγ subunit of the IKK complex (Golks *et al.*, 2006). These findings add a new mechanism to the complex FLIP-mediated regulation of apoptosis and the NF-κB pathway.

1.4.4 vFLIP Structures

KSHV vFLIP is 188 amino acids in length, with an apparent molecular weight of 23 kDa. It is a bipartite molecule composed of two DEDs of approximately 90 amino acids each with an intervening linker domain. DEDs belong to the DD superfamily (Weber and Vincenz, 2001) that includes the DD, caspase recruitment domain (CARD), involved in the intrinsic cell death pathway, and Pyrin domain, involved in inflammatory signalling (Kohl and Grutter, 2004; Reed *et al.*, 2004). These domains form strong homophilic interactions and facilitate the formation of the DISC, as well as of the apoptosome, by recruiting adaptor and effector molecules (Acehan *et al.*, 2002). Structural studies of the first DD (Huang *et al.*, 1996), DED (Eberstadt *et al.*, 1998), CARD (Chou *et al.*, 1998), and PYD (Hiller *et al.*, 2003) have all revealed a common fold, which is composed of an antiparallel six-α-helical bundle structure. A number of DEDs shares a conserved RXDL motif in α-helix 6, which has been implicated in apoptosis regulation mediated by the viral FLIP MC159 (Garvey *et al.*, 2002). Structure-based alignment of the DED sequences revealed a region of high diversity in α-helix 3, and this was used to classify the DEDs into two separate classes (Kaufmann *et al.*, 2002). Class I DEDs contain a stretch of basic residues in α-helix 3, which influences the binding and recruitment of caspase-8 and cFLIP to the DISC, and include the DED of FADD, both DEDs of caspase-8, and the C-terminal DED of cFLIP. Class II DEDs have a shortened or absent α-helix 3, and include most of the viral FLIP DEDs and the N-terminal DED of cFLIP (Kaufmann *et al.*, 2002). Consequently, both DEDs of vFLIP of KSHV fall into class II. Despite their biological importance, there have been no reported structures of tandem DEDs up to now, and therefore the molecular basis for the recruitment of caspase-8, caspase-10, and FLIPs remained to be revealed.

Recently, two groups reported a high-resolution crystal structure of MC159, a vFLIP derived from the molluscum contagiosum virus, and revealed significant insights into the function of vFLIPs (Li *et al.*, 2006; Yang *et al.*, 2005). They found that the full length MC159 protein consists of two tandem DEDs and a C-terminal extension. The DEDs of MC159 adopt a dumbbell-shaped structure, with the two DEDs at opposing ends (Figure 1.8). The first DED domain (DED1) of MC159 is highly divergent from DED2 and only contains five α helices, representing a departure from the canonical death motif. In contrast, DED2 is a bona fide DED and shows extensive structural homology with the known DED structure of FADD. They are connected by a stretch of 14 amino acids and, surprisingly, the DEDs of MC159 rigidly associate with one another through a hydrophobic interface. The close stacking of the two DEDs creates a deep surface that encircles the molecule and is lined with a number of acidic amino acids, which give rise to a highly negatively charged surface (Li *et al.*, 2006; Yang *et al.*, 2005). Structural and sequence analysis indicates that the interactions at the DED1-DED2 interface are highly conserved among all proteins that contain tandem DED domains, strongly suggesting that the rigid structure of MC159 and its interface determinants are representative of vFLIPs, c-FLIP, caspase-8 and –10. Unexpectedly, the packing interactions between the two DEDs were found to be significantly homologous to those between the CARD domains of Apaf-1 and caspase-9 (Qin *et al.*, 1999). Mutations of MC159 that render it incapable of protecting cells from apoptosis, mostly mapped to four distinct surface patches in the interface of DED1 and DED2, most likely involved in binding to FADD, caspase-8, and other proteins, which are well conserved among all tandem DED containing proteins. These findings allowed the two groups to generate hypothetical models describing how the DEDs of MC159, caspase-8, and FADD would assemble onto each other. In these models, MC159 uses the conserved surface binding elements to interact with the DEDs of caspase-8 and FADD. This arrangement allows the DEDs of FADD and caspase-8 to interact with each other in a way similar to that of DED1 and DED2 of MC159. Thus, by forming a ternary complex with FADD and caspase-8, MC159 disrupts the interactions between FADD and caspase-8 that are required for the appropriate activation of caspase-8.

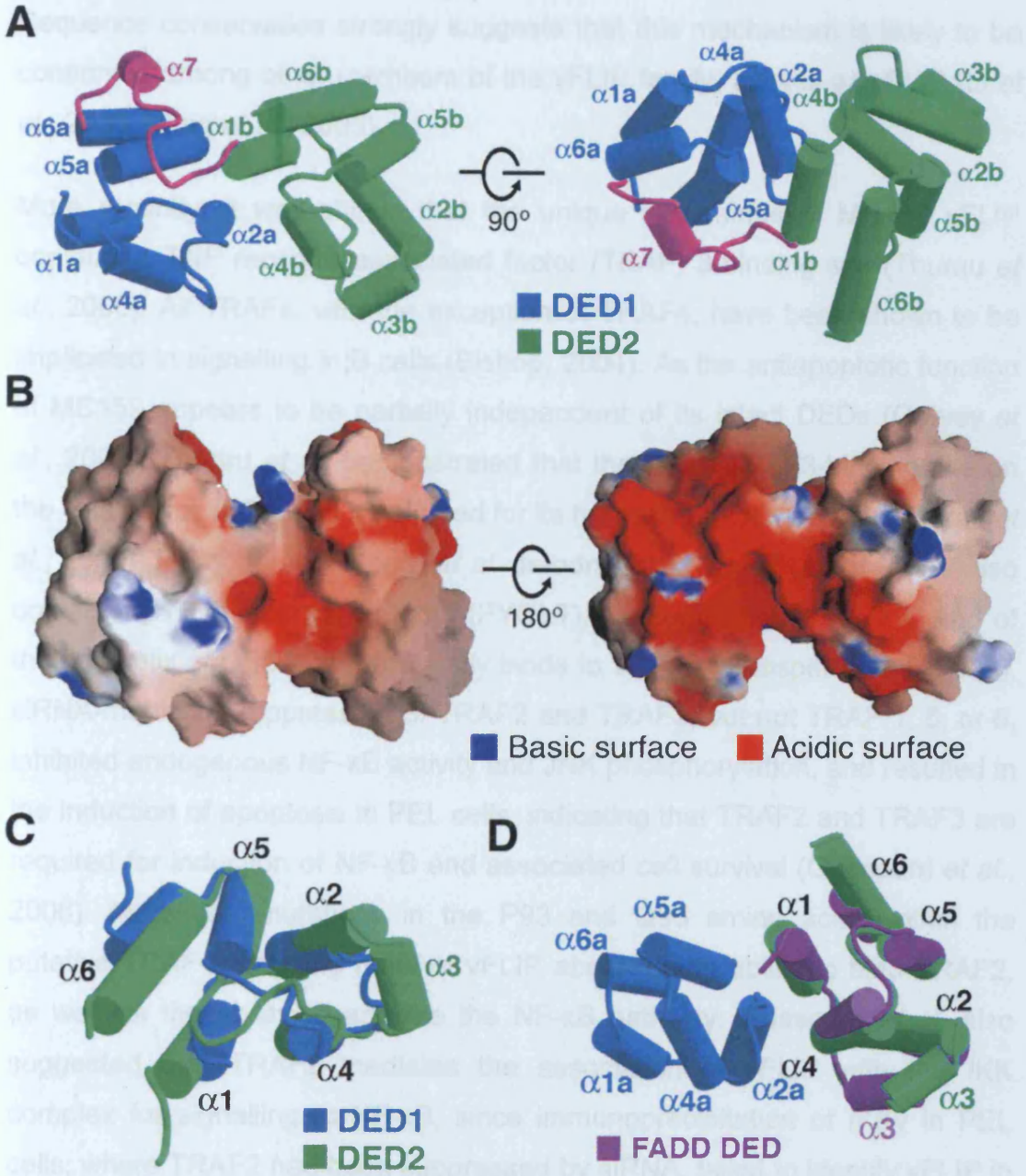

Figure 1.8 Crystal structure of vFLIP MC159 (residues 7-183)

(A) Schematic representation of the structure of the MC159 protein (residues 7-183). The first and second DED domains are coloured blue and green, respectively. The linker region is coloured magenta. **(B)** Surface representation of the MC159 structure. The acidic and basic surfaces are identified by red and blue colours, respectively. MC159 in the right panel is shown in the same orientation as that in the right panel of panel A. **(C)** Structure overlay of the two DED domains of MC159. The third helix in DED1 is reduced to a surface loop. **(D)** Structure overlay of the FADD DED with DED2 of MC159. FADD DED is shown in purple. DED, death effector domain; FADD, Fas-associated death domain. Figure 1.8 and the above figure legend have been reproduced exactly from Figure 1 from Li *et al.* 2006, with the kind permission of Prof. Z. Yigong Shi (Department of Molecular Biology, Princeton University, Lewis Thomas Laboratory,).

Sequence conservation strongly suggests that this mechanism is likely to be conserved among other members of the vFLIP family, as well as cFLIP (Li *et al.*, 2006; Yang *et al.*, 2005).

More recently, it was shown that the unique C-terminus of MC159 vFLIP contains a TNF receptor associated factor (TRAF) 3-binding site (Thurau *et al.*, 2006). All TRAFs, with the exception of TRAF4, have been shown to be implicated in signalling in B cells (Bishop, 2004). As the antiapoptotic function of MC159 appears to be partially independent of its intact DEDs (Garvey *et al.*, 2002), Thurau *et al.* demonstrated that the intact TRAF3-binding site on the C-terminus of MC159 is required for its full antiapoptotic activity (Thurau *et al.*, 2006). Moreover, Guasparri *et al.* demonstrated that vFLIP of KSHV also contains a TRAF-interacting motif (PYQLT), located in the N-terminal end of the first helix of DED2, which directly binds to TRAF2 (Guasparri *et al.*, 2006). siRNA-mediated suppression of TRAF2 and TRAF3, but not TRAF 1, 5, or 6, inhibited endogenous NF-κB activity and JNK phosphorylation, and resulted in the induction of apoptosis in PEL cells, indicating that TRAF2 and TRAF3 are required for induction of NF-κB and associated cell survival (Guasparri *et al.*, 2006). Moreover, mutations in the P93 and Q95 amino acids within the putative TRAF-interacting motif of vFLIP abolished its ability to bind TRAF2, as well as the ability to activate the NF-κB pathway. Guasparri *et al.* also suggested that TRAF2 mediates the association of vFLIP with the IKK complex for signalling to NF-κB, since immunoprecipitation of IKKγ in PEL cells, where TRAF2 had been suppressed by siRNA, failed to identify vFLIP in the precipitate. However, a more recent study re-examining the role of TRAFs in vFLIP signalling, has contradicted these findings. Matta *et al.* found that the P93 and Q95 mutations in the TRAF-interacting motif of vFLIP have absolutely no impact on the ability of vFLIP to interact with IKK, or activate the NF-κB pathway (Matta *et al.*, 2007). Moreover, they showed that endogenously expressed TRAF2 and TRAF3 do not interact with vFLIP, and do not play any role in vFLIP-mediated NF-κB activation. There are a number of differences in the way the two studies were conducted, which might explain some, but not all, of the discrepancies between the two studies. For example, the two groups used different computer models to identify the putative TRAF-

interacting motif of vFLIP. While Guasparri *et al.*'s model was based only on DED2 of vFLIP, and showed that the TRAF-interacting motif was exposed on the surface of the molecule available for interaction with TRAFs (Guasparri *et al.*, 2006), Matta *et al.*'s model was generated using comparative modelling to generate a 3D model of the complete vFLIP molecule based on the recently resolved structure of vFLIP MC159 (Matta *et al.*, 2007). Their model mapped the TRAF-interacting motif buried in the interface between DED1 and DED2, suggesting the motif is not available for surface interactions (Matta *et al.*, 2007). Several TRAFs have been shown to interact with the Epstein-Barr virus (EBV) latent membrane protein 1 (LMP1), with TRAF6 (Luftig *et al.*, 2003) and TRAF3 (Xie *et al.*, 2004) being essential for NF-κB activation by LMP1. In contrast, the Tax oncoprotein from HTLV-1 can activate NF-κB by bypassing the upstream components of the NF-κB pathway, and directly interacting with the IKK complex via NEMO (Sun and Xiao, 2003). Therefore, It appears that vFLIP of KSHV is similar to Tax in this respect, and can directly interact with the IKK complex through NEMO (Field et al., 2003), to specifically activate NF-κB (Matta *et al.*, 2007).

1.4.5 KSHV vFLIP Functions

vFLIP of KSHV is a viral homologue of the FLICE inhibitory protein and is the third coding region expressed from the LANA promoter. vFLIP is the downstream gene in a spliced, bicistronic mRNA in which v-cyclin is the upstream gene. vFLIP translation is made possible by the presence of an internal ribosomal entry site (IRES) embedded within the v-cyclin coding region (Bieleski and Talbot, 2001; Grundhoff and Ganem, 2001; Low *et al.*, 2001). The IRES elements seem to ensure efficient translation of mRNA throughout the cell cycle, and particularly during G_2/M phase when there is a general loss of cap-dependent translation (Bonneau and Sonenberg, 1987; Huang and Schneider, 1991). It is suggested that IRES-mediated expression of vFLIP guarantees protein expression at times during the cell cycle when translation is limited (Bieleski and Talbot, 2001). The fact that KSHV has acquired such a mechanism to regulate the expression of vFLIP points to an important role for this protein in KSHV infection.

By analogy with other viral FLIPs, vFLIP of KSHV was originally believed to protect virally infected cells from DR-induced apoptosis by blocking the recruitment and activation of caspase-8 (Thome *et al.*, 1997). Some groups reported findings showing that KSHV vFLIP could also function in this fashion. Overexpression of vFLIP in HeLa cells blocked procaspase-8 cleavage and reduced caspase-3 and caspase-8 activity (Belanger *et al.*, 2001). Consistent with these findings, vFLIP of KSHV was shown to act as a tumour progression factor, by promoting tumour growth *in* vivo (Djerbi *et al.*, 1999). After injection of immunocompetent mice with murine B lymphoma cells expressing vFLIP, the transduced B lymphoma cells developed into aggressive tumours showing a high rate of survival and growth (Djerbi *et al.*, 1999). However, when the same vFLIP-expressing cells were injected into immunodeficient mice, the tumour promoting property of vFLIP was not sufficient to allow tumour establishment, suggesting that vFLIP can protect KSHV-infected cells against T cell immunity (Djerbi *et al.*, 1999). These experiments defined inhibitors of DR-mediated apoptosis as a new class of tumour progression factor (Djerbi *et al.*, 1999), suggesting an important role for vFLIP in KSHV-mediated oncogenesis. However, these findings have not been consistently replicated by all groups, and there is growing evidence that KSHV vFLIP may have additional or alternative functions.

In addition to its DR-inhibitory activity, vFLIP has been implicated in the modulation of transcriptional pathways. Expression of KSHV vFLIP in 293T and NIH3T3 cells led to the activation of NF-κB driven reporter constructs, whereas E8 and MC159 failed to do so (Chaudhary *et al.*, 1999). Consistent with this, vFLIP was shown to interact with and activate a 700kDa signalsome complex consisting of IKKα, IKKβ, and NEMO, when expressed in a non-small-cell lung carcinoma cell line (Liu *et al.*, 2002). Indeed, a yeast two-hybrid screen identified the regulatory component of the IKK complex, IKKγ, as an interacting partner of vFLIP (Field *et al.*, 2003). The domain in IKKγ required for contact with vFLIP is between amino acids 150-272, in the third coiled-coil region (CCR3) and first section of CCR4. Therefore, vFLIP interacts directly with IKKγ to activate IKK, and the majority of endogenous vFLIP in a KSHV-infected PEL cell line can be found associated with IKK ~~in a KSHV-infected~~

(Field *et al.*, 2003). This interaction subsequently led to phosphorylation of IκBα and activation of the NF-κB pathway (Liu *et al.*, 2002). Moreover, An et al, showed that vFLIP of KSHV activates the JNK/AP1 pathway in a TRAF-dependent fashion (An *et al.*, 2003), contradicting findings by Chaudhary *et al.* that suggest it doesn't (Chaudhary *et al.*, 1999). The dual activation of the NF-κB and JNK/AP-1 pathways by vFLIP was shown to drive cIL-6 expression in synergy with LANA (An *et al.*, 2003). As discussed previously (section 1.2.8.3), IL-6 is an angiogenic and mitogenic factor that is likely to play a significant role in KSHV-associated neoplasms, and therefore this suggests an important role for vFLIP in KSHV pathogenesis.

Subsequently, it was shown by Matta *et al.* that stable expression of vFLIP from KSHV in a variety of cell lines, but not other FLIPs, constitutively up-regulates p100/NF-κB2 expression, and leads to its processing into the p52 subunit (Matta and Chaudhary, 2004), which implied that vFLIP of KSHV is also capable of activating the alternative NF-κB pathway. This process was dependent on the interaction of vFLIP with endogenous p100 and IKKα, but did not require the activity of NIK or IKKβ (Matta and Chaudhary, 2004) (Figure 1.7). In the same report, siRNA-mediated suppression of vFLIP in PEL cells inhibited p100 processing and cellular proliferation. Since the alternative NF-κB pathway was shown to be constitutively active in KSHV-infected PEL cell lines and vFLIP is responsible for this activation, it seems that vFLIP-induced p100 processing plays a key role in the growth and proliferation of KSHV-infected cells (Matta and Chaudhary, 2004).

NF-κB activation by vFLIP has been linked to a range of biological activities in KSHV-mediated pathogenesis. Expression vFLIP in a growth factor-dependent TF-1 leukaemia cell line protected cells against growth factor withdrawal-induced apoptosis (Sun *et al.*, 2003a). This protective effect of vFLIP was associated with its ability to induce NF-κB activation, and was accompanied by increased expression of the pro-survival Bcl-2 family member Bcl-x_L (Sun *et al.*, 2003a). NF-κB regulates a number of anti-apoptotic genes, which include members of the anti-apoptotic Bcl-2 family (Bcl-2, Bcl-X_L, Bfl-1), the IAP family (XIAP, cIAP1, cIAP2), and cFLIP (Burstein and Duckett, 2003).

These observations suggest that activation of NF-κB may account for the anti-apoptotic properties of vFLIP (Belanger *et al.*, 2001; Djerbi *et al.*, 1999). Interestingly, vFLIP expression failed to protect cells against TNFα-mediated apoptosis, suggesting that the protective ability of vFLIP does not extend to all forms of cell death (Matta *et al.*, 2002; Sun *et al.*, 2003a). Therefore, although it has previously been suggested that the main function of vFLIP from KSHV might be to protect cells against DR-mediated apoptosis, as is the case with HVS-FLIP, E8 and MC159L (Thome *et al.*, 1997), it now seems that vFLIP from KSHV may have a different biological function to other FLIP proteins, and that is to activate NF-κB. Moreover, it has been shown that KSHV vFLIP, but not E8 or MC159L, has the ability to transform Rat-1 and Balb/3T3 cells fibroblast cells (Sun *et al.*, 2003b). Expression of vFLIP in these cells led to loss of contact inhibition, growth in soft agar, and formation of tumours in nude mice. The transforming ability of vFLIP was found to be associated with the activation of NF-κB, and was effectively blocked by molecular and chemical inhibitors of this pathway (Sun *et al.*, 2003b). More recently, it was reported that although transgenic expression of vFLIP failed to protect thymocytes from Fas-induced apoptosis, vFLIP-expressing transgenic mice displayed constitutive activation of classical and alternative NF-κB pathways, enhanced proliferation of thymocytes in response to mitogen stimuli, and increased incidence of lymphoma (Chugh *et al.*, 2005). This study further supports the transforming ability of KSHV vFLIP and the hypothesis that, rather than function as an inhibitor of DR-mediated apoptosis, vFLIP acts through constitutive NF-κB activation to enhance cellular proliferation.

It is important to note that the activation of NF-κB signalling by vFLIP is not only important for transformation and cell survival, but can also have other significant consequences. Recently, vFLIP was shown to constitutively upregulate IL-8 secretion in 293T, HeLa, and primary human umbilical vein endothelial (HUVEC) cells, by transcriptional upregulation of its promoter (Sun *et al.*, 2006). vFLIP-induced IL-8 promoter activation was dependent on an intact NF-κB binding site and was associated with increased binding of classical NF-κB pathway subunits p65, c-Rel, and p50, respectively (Sun *et al.*, 2006). IL-8 plays a pivotal role in the pathogenesis of KS (Wang *et al.*,

2004a) and has been shown to stimulate angiogenesis and tumour growth (Koch *et al.*, 1992; Sparmann and Bar-Sagi, 2004). As previously mentioned, vFLIP can also induce the expression of cIL-6 in PEL cells through the activation of both NF-κB and JNK/AP-1 (An *et al.*, 2003), and this might play a significant role in KS, PEL, and MCD. Moreover, latent KSHV infection of HUVECs led to significant upregulation of a number of chemokines that are normally produced in the ground state, including MCP-1 (monocyte chemoattractant protein-1), NAP-2 (neutrophil activating peptide-2), RANTES, and especially CXCL16, which was nearly undetectable in the basal medium (Xu and Ganem, 2007). This induction was mainly associated with the expression of vFLIP and was mediated by its ability to activate NF-κB, since expression of the IκB super-repressor reduced the induction of CXCL16 substantially. CXCL16 is associated with the chemotaxis of activated T cells (Matloubian *et al.*, 2000), whose products have been shown to promote the survival and proliferation of KS cells in cell culture systems. Therefore, vFLIP-mediated induction of CXCL16 may play a paracrine role in promoting the inflammatory phenotype of KS, and enhancing the survival and expansion of the tumour (Xu and Ganem, 2007). Finally, latent KSHV infection of primary cultures of HUVECs, lymphatic endothelial cells (LECs), and blood endothelial cells (BECs), led to a dramatic elongation of cells, to the spindle cell shape characteristic of KS tumour cells (Grossmann *et al.*, 2006). This spindling phenotype was attributed to vFLIP expression and the subsequent activation of NF-κB, since the use of Bay 11-7082, a selective pharmacologic NF-κB inhibitor, inhibited the development of the spindle cell phenotype. Moreover, supernatants from HUVECs expressing only vFLIP were found to have increased amounts of interleukin-6 (IL-6) (consistent with previous findings by An *et al.*, 2003), IL-8 (consistent with previous findings by Sun *et al.*, 2006), GRO, RANTES, GCP2 (granulocyte chemotactic protein 2), and MIP3α (macrophage inflammatory protein 3), which are likely to contribute to the inflammatory component of KS lesions (Grossmann *et al.*, 2006).

In PEL, vFLIP is the major factor promoting tumour cell survival. siRNA-mediated elimination of vFLIP expression results in significantly decreased NF-κB activity, downregulation of essential NF-κB-regulated cellular prosurvival factors, such as cFLIP, cIAP-1, cIAP-2, and IL-6, induction of

apoptosis, and enhanced sensitivity to external apoptotic stimuli (Godfrey *et al.*, 2005; Guasparri *et al.*, 2004; Keller *et al.*, 2000). Furthermore, inhibition of NF-κB by Bay 11-7082 has been shown to induce apoptosis in PEL cells (Keller *et al.*, 2000), and in a murine system of EBV- and KSHV-associated lymphomas, it prevented or delayed tumour growth, and prolonged disease-free survival (Keller *et al.*, 2006).

Apart from its role in extending cell survival, NF-κB activation may also play a role in the maintenance of KSHV latency. Brown and colleagues recently reported that activation of NF-κB inhibits lytic-cycle gene expression and that inhibition of NF-κB activation, leads to lytic reactivation. If so, vFLIP expression could help maintain the latent state by preventing inappropriate lytic induction owing to transient exposure to inducing stimuli (Brown *et al.*, 2003). Finally, vFLIP has recently been implicated in regulating the transcription and expression of genes involved in immunity, which is thought to play a major role in establishing host-pathogen equilibrium (Lagos et al., 2007). Array analysis of LECs expressing a number of KSHV genes by way of lentiviral transduction, revealed that two viral genes, namely vFLIP and vIRF1, are responsible for regulating MHC-I transcription. vFLIP was shown to significantly upregulate MHC-I at the transcriptional level, while vIRF1 inhibited the vFLIP-induced MHC-I transcription and surface expression. MHC-I upregulation by vFLIP was attributed to its ability to activate NF-κB, since the effect was significantly reduced in the presence of the NF-κB inhibitor Bay 11-7082 (Lagos et al., 2007). Moreover, vFLIP expression led to significant upregulation of ICAM-1, also involved in class I antigen presentation, and induced allogeneic cytotoxic-T lymphocyte (CTL) proliferation. It is likely, that transcriptional modulation of antigen presentation by vFLIP has important functional implications, since the oncoprotein LMP-1 from EBV has also been shown to enhance antiviral immune responses (Cahir-McFarland *et al.*, 2004; Rowe *et al.*, 1995). It is thought that LMP-1-mediated upregulation of MHC-I promotes the transition to latency I-infected B cells, which establishes latency and therefore, host-pathogen equilibrium. Thus, vFLIP may also employ the regulation of MHC-I expression, as a

mechanism to control the levels of viral dissemination during persistent infection.

Combined, these data indicate that vFLIP is necessary for the growth and survival of KSHV-transformed cells and it may contribute significantly to KSHV neoplasia through its multitude of functions, most of which can be attributed to its ability to persistently activate the NF-κB pathway.

1.5 Aims of this study

vFLIP is one of seven known latent genes expressed by KSHV that regulate viral latent infection and may be essential for KSHV-mediated cell transformation. At the time this study was initiated published data relating directly to the function of vFLIP pointed to an important role for this protein in KSHV pathogenesis, due to its capacity as a direct inhibitor of DISC activity (Djerbi *et al.*, 1999), and its ability to activate the classical NF-κB pathway (Chaudhary *et al.*, 1999).

The initial aim of this project was to pursue the pathways of cellular signal transduction modulated by vFLIP, and more specifically, to investigate whether vFLIP could also activate the so-called alternative NF-κB pathway. Following this, we set out to determine the mechanism by which vFLIP of KSHV activates the alternative NF-κB pathway, and whether activation of this pathway by vFLIP plays a significant role in PEL cell survival. Finally, we wanted to examine the effect of vFLIP expression on the survival of primary endothelial cells, as they are very close to the cell type targeted naturally for infection by KSHV. Chapter 3 describes the discovery that vFLIP stimulates the alternative pathway of NF-κB activation and provides some insight into the mechanism by which it does so. Chapter 4 focuses on the effects of vFLIP on the survival of microvascular endothelial cells and demonstrates how vFLIP can rescue these cells from detachment-induced apoptosis. Finally, in Chapter 5 these results are brought together to update the current understanding of vFLIP function and to suggest how vFLIP may contribute to the pathogenesis associated with KSHV infection.

Chapter 2

Materials and Methods

2.1 Buffers and solutions

Deoxynucleotide triphosphate mix (dNTPs)	100 mM deoxyadenosine triphosphate (dATP), deoxythymidine triphosphate (dTTP), deoxyguanosine triphosphate (dGTP) and deoxycytidine triphosphate (dCTP)
6x DNA loading buffer	60 mM Tris pH 7.4, 6 mM ethylenediaminetetraacetic acid (EDTA) (pH 8.0), 30% (v:v) glycerol, 0.25% (w:v) Orange G
Luria-Bertani (LB) agar	1% (w:v) bacto tryptone, 0.5% (w:v) bacto yeast, 0.5% (w:v) sodium chloride (NaCl), pH 7.0 with 15g/L bacto-agar
Luria-Bertani (LB) broth	1% (w:v) bacto tryptone, 0.5% (w:v) bacto yeast, 0.5% (w:v) NaCl, pH 7.0
TFB-I Buffer (For competent bacteria preparation)	30mM potassium acetate, 100mM RbCl, 10mM $CaCl_2$, 50mM $MgCl_2$, 15% glycerol, pH 5.5 with acetic acid
TFB-II Buffer (For competent bacteria preparation)	10mM MOPS, 75mM $CaCl_2$, 10mM RbCl, 15% glycerol, pH 6.5 with KOH
Nonidet P-40 (NP40) lysis buffer	20 mM Tris pH 7.5, 150 mM NaCl, 0.2% (v:v) NP40, 1 mM EDTA, 1 mM ethylenedioxy nitrilotetraacetate (EGTA), 1 mM DTT, 20 mM sodium fluoride (NaF), 1 mM sodium pyrophosphate ($Na_4P_2O_7$), 1 mM Na_3VO_4, 5% (v:v) glycerol, 1 mM PMSF and PIM
Nuclear lysis buffer	20 mM HEPES pH 7.6, 0.2 mM EDTA, 0.1 mM EGTA, 25% (v:v) glycerol, 0.42 mM NaCl, 1 mM DTT, 20 mM NaF, 1 mM $Na_4P_2O_2$, 1 mM Na_3VO_4, 1 mM PMSF and PIM
Phosphate-buffered saline (PBS)	137 mM NaCL, 2 mM potassium chloride (KCl), 10 mM sodium hydrogen phosphate (dibasic), 2 mM potassium hydrogen (dibasic), pH 7.4
Polyacrylamide resolving gel	12% (v:v) acrylamide (37.5 acrylamide: 1 bis), 125 mM Tris pH 8.8, 0.1% (w:v) sodium dodecyl sulphate (SDS), polymerised with 0.05% (w:v) APS and 0.1% (v:v) TEMED
Polyacrylamide stacking gel	5% (v:v) acrylamide (37.5 acrylamide: 1 bis), 125 mM Tris pH 6.8, 0.1% (w:v) SDS, polymerised with 0.05% (w:v) APS and 0.1% (v:v) TEMED
6x Protein sample buffer	6% (w:v) SDS, 125 mM Tris pH 6.8, 36% (v:v) glycerol, 15% (v:v) β-mercaptoethanol with bromophenol blue
Radioimmuno-precipitation (RIPA) lysis buffer	150 mM NaCl, 50 mM Tris pH 7.5, 1% (v:v) Triton, 0.5% (w:v) sodium deoxycholate (DOC), 0.1% (w:v) SDS, 1 mM EDTA, 1 mM EGTA, 1 mM DTT, 20 mM NaF, 1 mM $Na_4P_2O_7$, 1 mM N_3VO_4, 1 mM PMSF and PIM

SDS-polyacrylamide gel electrophoresis (PAGE) running buffer	25 mM Tris pH 8.5, 200 mM glycine, 0.1% (w:v) SDS
Transformation buffer	250mM PIPES, 2.5mM calcium chlorohydrate ($CaCl_2.2H_2O$), 60 mM KCl, adjusted to pH 6.7 using potassium hydroxide (KOH) before addition of 55 mM manganese chloride ($MnCl_2$)
1xTris-acetate-EDTA (TAE)	40 mM Tris pH 7.8, 20 mM sodium acetate, 1 mM EDTA
5x Tris-borate-EDTA (TBE)	450 mM Tris pH 8.0, 450 mM boric acid, 10 mM EDTA

Table 2.1 Constituents of buffers and solutions

2.2 Subcloning and Plasmid Preparation

2.2.1 Preparation of heat-shock competent XL/1 Blue E. coli.

E.coli bacteria (HB101 strain, from GibCoBRL) were grown in unselective LB (Luria-Bertani) medium for the preparation of competent cells. 1 ml of an overnight culture was diluted 1:100 in fresh LB medium and shaken at 37°C to an OD_{600}=0.3-0.6. Cells were then cooled on ice for 5 minutes, and pelleted at 4°C in a pre-cooled centrifuge. The cell pellet was gently suspended in ice-cold TFB-I buffer (50ml per 100ml culture) and left on ice for 5 minutes. Cells were then centrifuged at 1500 x g for 10 minutes at 4°C, and resuspended in ice-cold TFB-II buffer (4ml per 100ml culture), before being left on ice for at least 15 minutes. 50µl aliquots of competent cells were dispensed into sterile eppendorf tubes, keeping them on ice at all times, before being stored at –70°C.

2.2.2 Transformation of heat-shock competent E. coli.

Cells were defrosted on ice for 20 minutes. 10-50ng of plasmid were mixed with 50µl of heat shock competent *E. coli* XL/1 Blue and incubated on ice for 20 minutes. The bacteria were then shocked for 90 seconds at 42°C, or for 2 minutes at 37°C, and immediately placed on ice for 1 or 1.5 minutes respectively. The transformed bacteria were then plated onto LB-agar containing the appropriate antibiotic and incubated overnight at 37°C.

2.2.3 Plasmid DNA mini-preps

To obtain small quantities (5-25µg) of plasmid DNA, mini-preps were produced from 1-5ml overnight cultures of transformed bacteria using a QIAprep Spin Miniprep Kit (Qiagen) as per the manufacturer's instructions.

2.2.4 Plasmid DNA midi-preps

Larger quantities (200µg) of pure plasmid DNA were extracted from a 100ml bacterial culture. Midi-preps were produced from this culture using the Plasmid Midi Kit (Qiagen) as per the manufacturer's instructions. The concentration of purified DNA was calculated from the UV absorbance at 260 nm using a UV spectrophotometer (Camlab). An absorbance of $1cm^{-1}$ was taken to be equivalent to 50 $\mu g.ml^{-1}$ DNA.

2.2.5 Polymerase Chain Reaction (PCR) Amplification

PCR is used to amplify a segment of DNA by using primers specific for sequences flanking the segment. The template DNA is first heated to denature it and then the reaction is cooled to allow the primers to anneal. Finally, the primers are extended by DNA polymerase. The product is amplified by repeat cycles of these three steps. PCR depends on the activity of *Taq* polymerase, a heat stable DNA polymerase extracted from *Thermus aquaticus*. In our reactions we used HotStarTaq DNA polymerase from Qiagen, which is provided in an inactive state with no polymerase activity at ambient temperatures. This prevents the formation of misprimed products and primer–dimers at low temperatures. HotStarTaq DNA Polymerase is activated by a 15-minute, 95°C incubation step. PCR was carried out using a Hybaid thermal cycler.

PCR was used to generate the full length p100, as well as the ΔN and ΔC deletion mutants of p100, from the expression vector pcDNA3.1-myc-p100. Moreover, PCR was used to amplify vFLIP (567bp) from the pcDNA3.1-vFLIP vector plasmid, using primers designed to introduce a *BamHI* and a *NotI* site at the 5' and 3' ends respectively. The reactions were prepared using the reagents listed below. Primers are listed in Table 2.2.

The constituents of each reaction were:	
10 x PCR buffer	5μl
DMSO	5μl (10%)
Magnesium Chloride (25mM stock)	4μl (2.5mM)
dNTPs	2μl (2.5mM of each)
DNA template	1μl (~200ng)
Forward primer	1μl (100pmoles)
Reverse primer	1μl (100pmoles)
HotStarTaq polymerase	0.3μl (1.5 unit/reaction)
dH_2O	30.7μl
Total	**50μl**

dNTPs, deoxyribonucleoside triphosphates; 10x PCR buffer, $MgCl_2$, HotStarTaq from Qiagen PCR kit; 10x PCR buffer contains 15mM $MgCl_2$; DMSO was added to reduce non-specific primer binding and to enhance yield.

The program used to amplify the DNA fragments in the Hybaid thermal cycler was as follows: 1 cycle at 95°C for 15 minutes to activate the polymerase, followed by 35 cycles of denaturing at 94°C for 45 seconds, annealing at 55°C for 45 seconds and extension at 72°C for 30 seconds, and up to 2 minutes, depending on the size of the fragment to be extended (30 seconds is enough to extend fragments of ~500bp. These cycles were followed by 1 final extension cycle at 72°C for 7 minutes and the reactions were held at 4°C until the analysis of DNA products by gel electrophoresis.

Amplified fragment	**Forward (F) and reverse (R) primer sequence**
p100FL	F: 5'-GGATCCGCCACCATGGCCGAGAGTTGCTAC R: 5'-GGGTCGGAGTCCACGTGATCCGCCGGCG
p100ΔN	F: 5'-GGATCCGCCACCATGCTGAAGAAGGTGATGGATCT R: 5'-GGGTCGGAGTCCACGTGATCCGCCGGCG
p100ΔC	F: 5'-GGATCCGCCACCATGGCCGAGAGTTGCTAC R: 5'-GCGGCCGCCTAGCTGGGCGGGGTCAGGGG
vFLIP	F: 5'-GAGGGATCCATGGCCACTTACGAGGTTCTCTGT R:5'-GAGGCGGCCGCCTATGGTGTATGGCGATAGTGTTG

Table 2.2. PCR primers

2.2.6 Restriction enzyme digests

Restriction enzyme digests were used for excising and subcloning DNA fragments into a desired vector and to subsequently screen for correct insertion and orientation. All restriction enzymes were purchased from Promega and used as per manufacturer's instructions, depending on the combination of enzymes used. The reaction was stopped by the addition of the appropriate volume of 6x DNA loading buffer.

2.2.7 Agarose gel electrophoresis and gel extraction

The products of PCR amplification and restriction enzyme digests were separated on the basis of size by electrophoresis on a 1% agarose (Sigma) gel, made by dissolving agarose in TAE buffer containing 0.5μg/ml ethidium bromide (Sigma). A 1kb DNA ladder (GibCo) was run in parallel to identify the sizes of the bands, which were visualized using a UV lamp. When necessary, specific bands were excised with a scalpel and DNA subsequently purified from the agarose using a QIAquick gel extraction kit (Qiagen) as per the manufacturer's instructions.

2.2.8 Ligations

Ligation reactions were used to anneal new DNA fragments (isolated by restriction digest) into linearized plasmids bearing the corresponding ends. This processes whereby new phosphodiester bonds are formed to seal the plasmid, is catalysed by the enzyme DNA ligase. Using a weight ratio of 1 vector: 4 insert, 8μl of vector plus insert were mixed with 1μl of pGEM-T Easy DNA ligase solution (Promega), and 1μl of Rapid Ligation Buffer for a final volume of 10μl, and incubated at room temperature for 1h. Ligation solutions were transformed by heat shock into *E. coli* and plated onto LB-agar. Eight single colonies were picked and screened by PCR amplification with the relevant primers, restriction enzyme digest, and sequencing at the Windeyer Institute sequencing service.

2.2.9 Precipitation and purification of DNA

PCR products were routinely purified by phenol extraction, followed by DNA precipitation, which was also used to precipitate plasmid DNA from midi-preps. First, the reaction volume was made up to 200µl with TE buffer and then an equal volume of phenol was added. The mixture was vortexed and centrifuged at high speed (14,000 x g) for 10 minutes and the upper phase was transferred to a new tube. Following this, 1/10 of the volume of sodium acetate was added (3M) and the mixture was vortexed and spun at high speed for 10 minutes. Next, 2.5 volumes of 100% ethanol was added and the mixture was vortexed and left at -20°C for >10 minutes. The DNA was pelleted and washed three times with 70% ethanol, before resuspending it in water and storing it at -20°C.

2.3 Plasmids

2.3.1 Mammalian expression vectors

The expression vector pcDNA3.1-Myc-p100, encoding a myc-tagged full-length p100, was a kind gift from Dr. S. Ley (Mill Hill, UK). The pCMV4-p100ΔαA/B (Figure 3.2A), which harbours deletions at amino acids 151-160 and 170-181 (Xiao et al., 2001a), was a kind gift from Dr. Gutian Xiao (Pennsylvania State University College of Medicine), and was generated by site-directed mutagenesis using pCMV4-p100 (Sun *et al.*, 1994). The plasmid RSV IκBα-MSS super-repressor (Chapter 3, Figure 3.5) was a kind gift from Dr. N. Perkins (Dundee, UK). To obtain the p100 deletion mutants ΔN and ΔC, PCR primers were used to amplify and subclone p100 fragments from pcDNA3.1-Myc-p100 into the pcDNA3.1 (Promega) expression vector.

2.3.2 HIV-1 based plasmids

HIV-1 based plasmids were kindly provided by D. Trono (Geneva, Switzerland) and are described elsewhere (Naldini *et al.*, 1996; Zufferey *et al.*, 1997). The packaging plasmid phCMVΔR8.9 supplies the viral proteins in *trans* and expresses *gag*, *pol*, *tat*, and *rev*, but and does not express the accessory genes *env, vif*, *vpr*, *vpu* or *nef* (Zufferey *et al.*, 1997) (Figure 2.1).

The transfer vector plasmid pHR'-hCMV-eGFP contains the reporter gene, enhanced green fluorescent protein (eGFP), under the control of the human cytomegalovirus (hCMV) immediate early promoter. It also provides the *cis*-acting sequences necessary for packaging, reverse transcription, and integration. This plasmid was modified within our laboratory to express both vFLIP and eGFP from the internal ribosome entry site (IRES) of encephalomyocarditis virus (EMCV) (Figure 2.1). The envelope plasmid pMD-G encodes the vesicular stomatitis virus G (VSV-G) envelope glycoprotein (Zufferey *et al.*, 1997), which allows vector concentration by ultra-centrifugation, as it is very stable, and which has broad tropism, making it suitable for use with a variety of target cell types (Figure 2.1). The vector plasmid pHR'-CSIW-pUb-Em (double promoter vector), is based on the plasmid pHSIN-CSGW (Demaison *et al.*, 2002), and contains the reporter gene eGFP under the control of the spleen focus forming virus promoter (SFFV). This plasmid has been engineered to be self-inactivating (SIN) upon reverse transcription due to a deletion of the 3' LTR U3 region (ΔU3). The SIN vector also contains a central polypurine tract (cPPT) from the HIV pol gene, which enhances second strand synthesis, and the Woodchuck hepatitis virus post-transcriptional regulatory element (WPRE), which enhances viral titre. This plasmid was modified by our lab to express vFLIP by placing it in the position of the original eGFP, under the control of SFFV, and also to express emerald GFP (EmGFP), by cloning the EmGFP gene under the control of the ubiquitin promoter after the WPRE in the original backbone (Figure 2.1 and 4.1).

pHCMVΔR8.91 Packaging plasmid

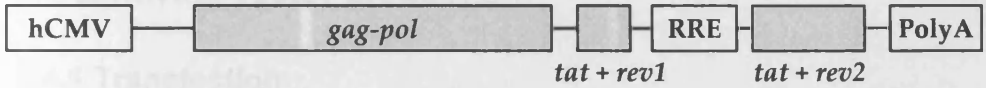

pHR'-hCMV-vFLIP-IRES-eGFP Vector plasmid

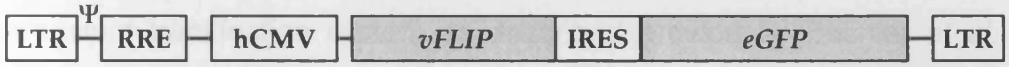

pHR'-CSIW-pUb-Em Vector plasmid

pMD-G Envelope plasmid

Figure 2.1 HIV packing, vector and envelope plasmids

Transcription of gag-pol in pHCMVDR8.91 is controlled by hCMV. pHCMVDR8.91 also encodes tat and rev. Transcription of the pHR'hCMV-vFLIP-IRES-eGFP and the pHR'-CSIW-pUb-Em vector transcripts is controlled by the LTR at the 5' end and terminates in the 3' LTR. The transgene cassette for pHR'hCMV-vFLIP-IRES-eGFP, encoding vFLIP and eGFP, is controlled by the internal hCMV promoter, while the transgene casette for pHR'-CSIW-pUb-Em, encoding vFLIP and EmGFP, is controlled by the SFFV and ubiquitin promoters, respectively . The positions of the packaging signal (ψ) and rev responsive elements (RRE) are shown. Transcription of the VSV-G envelope is also controlled by hCMV. Regions encoding protein products within the mRNA are shown in grey and regions encoding cis-acting elements in white.

2.4 Lentiviral vector production

2.4.1 Transfection

293T cells were grown to 80% confluence on the day of transfection in 20cm^2 circular plates (Nunc). Lentivirus was produced using a three plasmid transient transfection system as described previously (Besnier *et al.*, 2002; Naldini et al., 1996; Zufferey et al., 1997) (Fig. 2.1). For each plate, DNA plasmids were mixed as follows: 2.5µg of the packaging plasmid (phCMVΔR8.9), were mixed with 2.5µg of the envelope plasmid (pMD-G), and 3.75µg of the transfer vector plasmid, and the volume was up to 37.5µl with TE buffer. 45µl of the transfection reagent Fugene-6 (Roche) were diluted in 500µl OptiMEM (serum free medium, GibCo) and this mixture was added to the DNA mix and incubated at room temperature for 15 minutes. Meanwhile, the medium on the cells (complete DMEM, see section 2.5.1) was changed, and then the transfection mixture was added drop-wise, at the same time swirling the plates to ensure even distribution. 24 hours later, the medium on the cells was changed again (to remove Fugene-6).

2.4.2 Virus harvesting

The virus-containing supernatant was harvested 48-72 hours post transfection and passed through a 0.45µm filter, to remove any cells. The virus was concentrated by ultra-centrifugation at 20,000 x g for 1.5 hours, and resuspended in 1ml Optimem, aliquoted, and stored at -80°C. A small aliquot of virus was used to determine the titre.

2.4.3 Determination of the titre

Serial dilutions of the virus were made in OptiMEM (to contain 5, 1, 0.2, and 0.04µl of virus) and used to infect 293T cells that were plated at 2x10^5 cells/well in 24 well plates. The cells were assayed 2 days post infection for the expression of the reporter gene GFP by flow cytometry, in order to determine the titre (i.e. the approximate number of "infectious units" per ml). Uninfected cells were passed through a FACSCaliber and analysed using CELL QUEST software (Becton Dickinson, Franklin Lakes, USA) to determine

side vs. forward scatter characteristics and select the region in which live cells could be found. For each infection, $1x10^4$ cells in this region were recorded and analysed for eGFP expression. The side scatter vs. green fluorescence (FL-1) plot of uninfected cells determines the region in which cells not expressing eGFP fall. A gate was placed in FL-1 to record the percentage of cells with higher fluorescence than the uninfected controls. Virus titre (infectious units/ml) was calculated from the percentage of cells infected and the number of cells per well on the day of infection using the equation: (%-infected cells x number of cells at infection / 100) x dilution factor.

2.4.4 Confocal microscopy

Cells in culture were directly viewed under a Zeiss confocal microscope with a U.V. lamp to visualize GFP expression after transfection or viral transduction. A laser along with Lasersharp software (Bio-Rad) was used for more sensitive fluorescence analysis and to record and save images of the cells.

2.5 Cell culture techniques

2.5.1 Cells and culture conditions

Cell culture medium and foetal calf serum were obtained from GibCoBRL. Human embryonic kidney (HEK) 293T cells were cultured in Dulbecco's modified Eagle's medium (DMEM) with 10% foetal calf serum (FCS), penicillin and streptomycin in a 10% CO_2 humidified incubator at 37°C. Cells were passaged 1:10 every 2-3 days to ensure optimal cycling. Human B cell lines included the KSHV-transformed and EBV negative PEL cell line, BC3 (Arvanitakis *et al.*, 1996). Human $CD3^{+ve}$ Jurkat 3T8 T cells were obtained from S. Ley (Mill Hill, UK) by kind permission from A. Ting (New York, USA). All non-adherent cell lines, including BCE and Jurkat, were cultured in Roswell Park Memorial Institute (RPMI) 1640 medium with 10% FCS, penicillin and streptomycin in a 5% CO_2 humidified incubator at 37°C, and cell density was kept within the range $1x10^5$-$1x10^6$ cells/ml. Human adult dermal microvascular endothelial cells (HMVEC-d) were purchased from Lonza (Clonetics-Primary Cell and Media Systems) and cultured in EGM-2MV Bulletkit medium (Clonetics), in a 5% CO_2 humidified incubator at 37°C.

2.5.2 Transduction of tissue culture cells with concentrated lentivirus

For infection of Jurkat cell lines, $5x10^4$ cells were pelleted and resuspended in 1ml OptiMEM containing virus at a multiplicity of infection (MOI) of 10 infectious units per cell. 293T cells were infected for experimental purposes exactly as described above (section 2.4.3). For infection of MVECs, $1x10^5$ cells were plated in a 24-well plate and virus supernatant was diluted and added to the wells at an MOI of 30. After 6h, the medium on the cells was toped-up to dilute the concentrated virus, and cells were cultured as described. For all cells, transduction efficiency was measured by flow cytometry exactly as described above for 293T cells (section 2.4.3).

2.5.3 Anoikis assay

Anoikis is a form of apoptosis induced by the disruption of cell-matrix interactions. In this study, the protocol used was based on the one described by Frisch and Francis (Frisch and Francis, 1994). MVECs were grown to ~70% confuency in 24 well plates and were either not transduced, or transduced with a lentivirus encoding GFP alone, or a lentivirus encoding GFP and vFLIP. 48 hours post transduction, cells were trypsinized and equal numbers either re-plated immediately and allowed to adhere, or maintained in suspension for 16 hours by plating them in wells which had been coated with the anti-adhesive polymer polyHEMA (Fukazawa *et al.*, 1995; Fukazawa *et al.*, 1996). Briefly, polyHEMA plates were made by applying 200µl of a 12mg/ml solution of polyHEMA (diluted 1:10 in 95% ethanol from a 120mg/ml stock), and leaving the plates to dry in the tissue culture hood. This process was repeated 3 times for sufficient coating of the wells. Following coating, the wells were washed twice with PBS and once with Hank's Buffered Salt Solution (HBSS) and left to air dry. After 16 hours, cells in suspension were collected by pipetting, and adherent cells were trypsinized. All cells were then replated in 96-well plates for 4 hours and cell survival was measured by an MTT assay (section 2.5.3), while apoptosis was measured using a Death Detection ELISA (Roche) (section 2.5.3).

2.5.4 Cell viability and apoptosis assays

The viability of MVEC populations was measured using a colorimetric method based on the conversion of 3-[4,5-dimethylthiazol-2-yl]-2,5-diphenyltetrazolium bromide (MTT) to a formazan product (Hansen *et al.*, 1989). Non-viable cells are unable to reduce the MTT reagent and hence the degree of optical absorbance at 570nm gives a measure of the proportion of live cells in the mixture. Briefly, 100µl of EGM-2MV medium containing 5 x 10^4 cells was placed into each well of a flat-bottomed 96 well plate in triplicate. The MTT reagent (Sigma-Aldrich) (diluted from a 5mg/ml solution in PBS) was then added to all the wells at a final concentration of 0.5mg/ml and the cells were incubated with the MTT reagent for 4 hours at 37°C. The reaction was terminated by adding 100µl/well of 10% SDS. The plates were left overnight in the dark at room temperature, following which the absorbance was read at 570nm using an ELISA plate reader.

Cell viability was also determined using a Trypan Blue exclusion assay. Trypan Blue is a dye that is used to determine the number of viable cells in a cell suspension. Living cells possess intact cell membranes and therefore exclude the dye, whereas dead cells do not and take up the blue dye. The blue stain is easily visible, and cells can be counted using a light microscope. Cells were collected by centrifugation and resuspended in 1ml of HBSS (~5x10^5 cells/ml). 1 part of 0.4% trypan blue was mixed with 1 part of cell suspension, and the mixture was allowed to incubate for 3 minutes at room temperature. A drop of the solution was placed on a haemocytometer and examined under the light microscope. Unstained (viable) and stained (non-viable) cells were counted separately. To obtain the total number of viable cells per ml of aliquot, the number of viable cells was multiplied by 2 (the dilution factor for trypan blue). To obtain the total number of cells per ml of aliquot, the total number of viable and nonviable cells was added up and multiplied by 2. The percentage of viable cells was calculated as follows:
Viable cells (%) = (Total number of viable cells/ml of aliquot / Total number of cells/ml of aliquot) x 100.

For the detection of apoptosis, cells were stained with the Annexin V reagent. Annexin V allows the identification of cell surface changes that occur early during the induction of apoptosis using flow cytometry (explained in more detail in section 4.2.4). For the Annexin V binding assay, $1x10^6$ cells were collected by centrifugation and washed once in cold (4°C) phosphate buffered saline (PBS) before staining with TACS™ Annexin V-FITC Apoptosis detection kit (Trevigen) (in the case of BC3 cells transfected with siRNA, section 3.2.7), or TACS™ Annexin V-Biotin Apoptosis detection kit (Trevigen) (in the case of MVECs during anoikis, section 4.2.4), as per the manufacturer's instructions. Analysis was performed by FACScan using CELL QUEST software. Side scatter vs. forward scatter was used to exclude cell debris, and $1x10^4$ cells within this region were recorded to determine the percentage of Annexin V staining.

Moreover, apoptosis was also measured using a Cell Death Detection ELISA^{PLUS} kit (Roche), which is based on a quantitative sandwich-enzyme-immunoassay principle, using monoclonal antibodies directed against cytoplasmic histone-associated DNA fragments, and is a measure of DNA fragmentation after induced cell death (section 4.2.5). Briefly, 100µl of medium containing $1x10^4$ cells were plated into each well of a round-bottomed 96 well plate in triplicate. Cells were then lysed and the supernatants analysed for the presence of fragmented DNA by the addition of the immunoreagent responsible for capturing cytoplasmic histone-associated-DNA fragments as per the manufacturer's instructions. After 2 hours of incubation, the reactions were developed by the addition of the ABTS substrate and optical density was measured at 405nm against ABTS solution as a blank using an ELISA plate reader.

2.5.5 RNA interference

The protocol used to inhibit the expression of p100/p52 via RNA interference was kindly provided by Prof. Ethel Cesarman (Weill Cornell Medical College) and has previously been described by Guasparri *et al.* (Guasparri *et al.*, 2004). The RNA duplexes used in this study were purchased from Dharmacon's ON-TARGETPlus pre-designed siRNA reagents, and consisted of four highly functional duplexes that target different regions of the target gene. A scramble siRNA duplex (siCONTROL Non-Targeting siRNA #2) was also purchased from Dharmacon, and was used as a negative control as a control for non-sequence-specific effects since it doesn't target any known genes. The siRNA duplexes were delivered to BC3 cells by transient transfection using the Oligofectamine transfection reagent (Invitrogen). For the transfection, we used the guidelines for 24 well plate formats provided by the manufacturer of Oligofectamine (see Invitrogen website). In brief, cells were plated in 24 well plates in triplicate (to allow for enough cells for the apoptosis and survival assays, as well as for assaying for silencing by Western Blot) at a density of $3x10^5$ cells/well. For each well of the 24 well plate we used 0.84µg of siRNAs. We mixed 3µl of 20µM siRNA pool with 50µl of OptiMEM. In another tube, we diluted 3µl of Oligofectamine Reagent with 12µl of OptiMEM, and this mix was incubated for 15 minutes at room temperature. The solutions were then combined, mixed gently by inversion, and incubated for a further 25 minutes at room temperature. We then added 38µl of fresh OptiMEM to the solution to obtain a final volume of 106µl, which was then added to the cultured cells. We assayed for silencing 3 days post transfection by Western Blot to confirm the knockdown of the target gene at the protein level. For the extended study described in section 3.2.7, BC3 cells were transfected every 3 days, for a total of four transfections and a 12 day time course. Knockdown of the target gene, apoptosis, and survival, were evaluated by western blot, Death Detection ELISA and Annexin V staining, and Trypan Blue exclusion respectively, at 3 day intervals (days 3, 6, 9, and 12).

2.5.6 Immunofluorescence assay

The majority of the immunofluorescence assay and the data analysis were performed by Dr. Mahdad Noursadeghi, who also provided the protocol that follows. Our contribution involved growing the cells on cover slides, transducing them with the relevant lentivectors (section 4.2.3), and fixing them with paraformaldehyde.

2.5.6.1 Antibodies and blocking sera

Rabbit polyclonal affinity purified antibodies to RelA (C-20), RelB (C-19) and p52 (K-27) were purchased from Santa Cruz Biotechnology and used at a concentration of 2µg/ml for immunostaining. Alexa Fluor® (AF)633-conjugated $F(ab')_2$ goat anti-rabbit IgG (Invitrogen) was used at 4µg/ml for immunofluorescent detection of primary antibody staining. 10% normal goat serum (Sigma Aldrich) was used to block non-specific binding of the secondary antibody.

2.5.6.2 Immunostaining

MVECs were grown on 24 well chamber cover slips (VWR) to ~60% confluency, and were either not transduced or transduced with a lentivector encoding GFP alone, or vFLIP and GFP. 48 hours post transduction, the cells were fixed with 3.7% paraformaldehyde for 15 minutes at room temperature and washed with Tris-buffered saline (TBS) before immunostaining. This was performed by inverting each coverslip onto 50µl of solution placed on impermeable Nesco film (VWR). All reagents were diluted in TBS. Coverslips were incubated sequentially with 0.2% Triton-X100 (Sigma) for 10 minutes at room temperature to permeabilize cells, blocking buffer for 30 minutes at room temperature, 1° antibody (diluted in blocking buffer) overnight at 4°C, and 2° antibody (diluted in blocking buffer) for 1 hour at room temperature. Nuclei were then counterstained with 2µg/ml of the nuclear stain DAPI (Sigma Aldrich) for 5 minutes and coverslips were mounted onto glass slides (VWR) using Vectashield hard-set mounting media (Vector). Coverslips were washed by immersion into TBS between each staining step. Fluorescence images were captured on a Leica SP2 confocal microscope. DAPI, GFP and Alexa

Fluor AF633 fluorescence was captured using sequential acquisition to give separate image files for each. The excitation and emission spectra for each fluorochrome is given in Table 2.3. A pin hole of 1 Airy (114.5μm), scan speed of 400Hz, and 4-frame averaging was used. Photomultiplier tube gain and offset were adjusted to give sub-saturating fluorescence intensity with optimal signal to noise ratio.

Fluorochrome	Laser	Excitation wavelength (nm)	Emission wavelengths (nm)
DAPI		405	400-450
GFP	Argon	488	500-540
AF633	HeNe	633	650-700

Table 2.3 Excitation and emission spectra of fluorochromes

2.5.6.3 Image analysis

Image analysis was performed using ImageJ software (http://rsb.info.nih.gov/ij). For each high power field image masks were created of GFP, AF633 and DAPI positive staining. This was done by applying a median filter (3x3 pixel radius) to remove noise, automatic thresholding (using the IsoData algorithm)[1] to remove background fluorescence and conversion to binary image. The DAPI staining mask was used to define nuclear localisation. Subtraction of the DAPI mask from the AF633 was performed to create a staining mask defining cytoplasmic localisation and the GFP staining mask was used to identify cells with and without lentiviral encoded gene expression. Each of these staining masks (Figure 2.2 A-D) were then applied to the original AF633 images (Figure 2.2 E) to separate NF-κB subunit staining in the nuclei and cytoplasms of lentiviral vector-transduced and untransduced cells within each high power field. Quantitative fluorescence data were then exported from ImageJ-generated histograms into Graphpad Prism 5 software for further analysis and presentation. Nuclear:cytoplasmic ratios NF-κB subunit staining were then calculated by comparison of median values from histogram data of GFP negative (Figure 2.3A) and GFP positive cells (Figure 2.3).

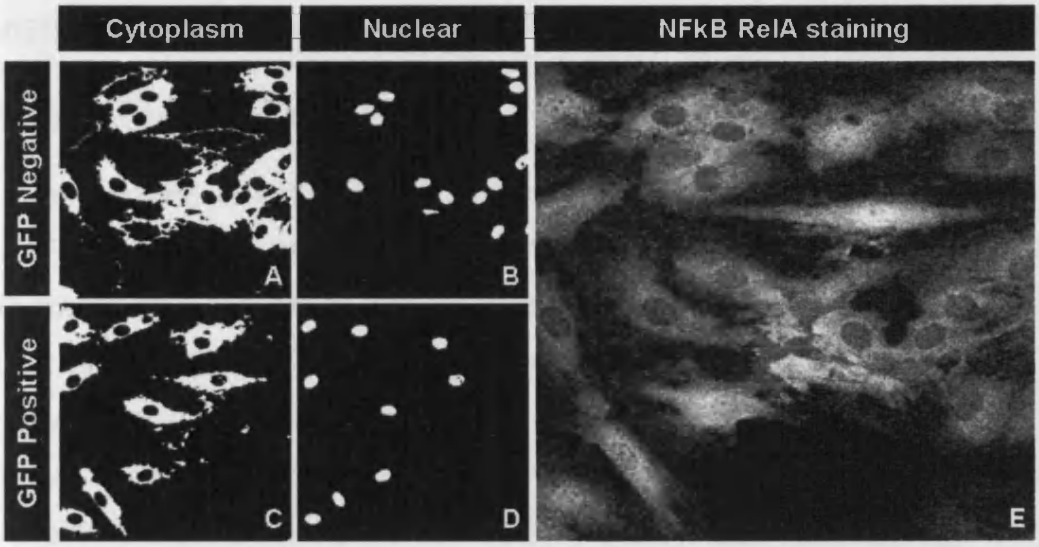

Figure 2.2 Generation of staining masks for nuclear and cytoplasmic localization (A and B), and lentiviral gene expression (C and D).

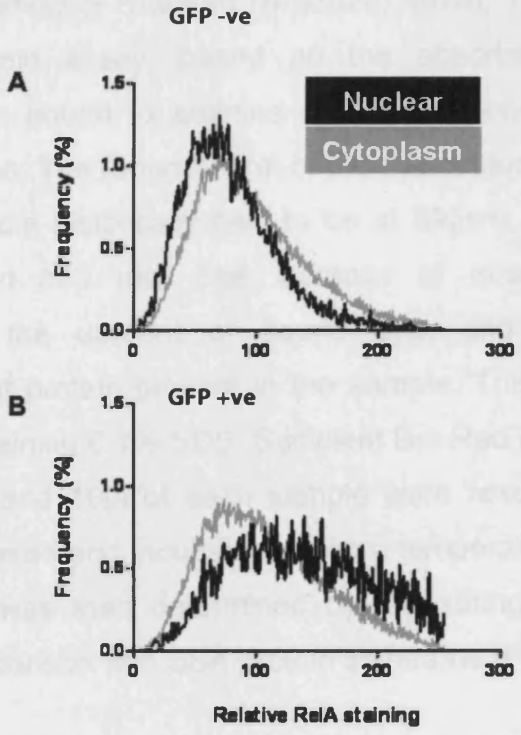

Figure 2.3 Histograms of relative nuclear and cytoplasmic NF-κB staining from GFP negative (A) and GFP positive (B) cells. Median values from these histograms were used to generate nuclear:cytoplasmic ratios

2.6 Analysis of mammalian cell extracts

2.6.1 Preparation of cell extracts

Cells were washed in PBS, pelleted by centrifugation and resuspended in either RIPA lysis buffer, or NP40 lysis buffer. The suspension was incubated at 4°C for 30 minutes on a rotating wheel before insoluble material was removed by centrifugation at 14,000 x g at 4°C for 5 minutes. At this point aliquots were removed for protein assay (section 2.6.2). The supernatants were either used as described below, or the appropriate quantity of 6x protein sample buffer was added. These samples were then heated to 95°C for 4 minutes and stored at -80°C until required.

2.6.2 Protein assay

Total protein per sample was estimated by using the Bio-Rad Protein Assay based on the method of Bradford (Bradford, 1976). The Bradford assay is a colorimetric protein assay, based on the absorbance shift in the dye Coomassie when bound to arginine and hydrophobic amino acid residues present in proteins. The (bound) form of the dye is blue and has an absorption spectrum maximum historically held to be at 595nm. The anionic (unbound) forms are green and red. The increase of absorbance at 595nm is proportional to the amount of bound dye, and thus to the amount (concentration) of protein present in the sample. This method is compatible with buffers containing 0.1% SDS. Sufficient Bio-Rad dye reagent was diluted 1:5 in H_2O. 5µl and 10µl of each sample were resuspended in 1ml of the diluted dye, vortexed and incubated at room temperature for 5 minutes. Total protein content was then determined by measuring the optical density at 595nm and comparison with BSA protein standards (Promega).

2.6.3 Preparation of nuclear and cytoplasmic fractions

Cells were washed in cold PBS, pelleted and resuspended in cold NP40 lysis buffer lacking NP40. Following 15 minutes incubation at 4°C, NP40 was added to a final concentration of 0.6%. The tubes were then mixed by vortexing and incubated for a further 4 minutes. The lysate was then

underlayered with lysis buffer containing 30% sucrose and centrifuged for 5 minutes at 14,000 x g at 4°C. The supernatant was removed as 'cytoplasmic extract', assayed for protein concentration and stored at -80°C. The nuclei were washed twice by overlayering and removing lysis buffer and then resuspended in nuclear lysis buffer. Nuclear proteins were released using 3 freeze-thaw cycles by transferring the tubes from liquid nitrogen to a 37°C water bath. The supernatant, following centrifugation for 10 minutes at 14,000 x g at 4°C, was diluted 1:2 in lysis buffer, assayed for protein concentration, and stored at -80°C as 'nuclear extract'.

2.6.4 Pulse Chase Assay

Plasmid DNA was introduced into 293T cells by transient transfection using the Fugene-6 transfection reagent (Roche), using a Fugene-6 reagent : DNA ratio of 6:1. Cells were plated at a density of $2x10^6$ cells per 10cm plate 24 hours before transfection. On the day of transfection, 1µg of vFLIP plasmid was mixed with 0.1µg of p100 plasmid, and made up to a total volume of 15µl with TE buffer. 9µl of Fugene-6 were diluted in 100µl OptiMEM and this mixture was added to the DNA mix and incubated at room temperature for 15 minutes. Meanwhile, the medium on the cells was changed, and then the transfection mixture was added drop-wise, at the same time swirling the plates to ensure even distribution. Cells were incubated for 24 hours before performing the pulse chase assay.

Cells were washed once with HBSS and starved for 1 hour by the addition of 2ml of Eagle Minimum Essential Medium (without Cystein and Methionine) containing 0.5% dialysed FCS. Cells were then pulsed for 2 hours with 1mCi/well of ^{35}S-Cysteine/^{35}S-Methionine Promix (Amersham). The reaction was then stopped immediately by the addition of complete DMEM, the hot medium collected, and the cells washed once with HBSS. Cells were then chased with 4ml of complete DMEM with 10% FCS supplemented with cold methionine and cysteine. After each time point, (0 and 6 hours of chase), cells were washed once with HBSS and lysed in 1ml of complete RIPA buffer supplemented with protease inhibitors. The radiolabelled p100 and p52 were isolated by immunoprecipitation using a rabbit polyclonal anti-p100 antibody

(Upstate Biotech), separated by SDS-PAGE and visualized by autoradiography. The radiolabelled protein bands were also quantitated using a Phosphorimager STORM 860 instrument (Molecular Dynamics).

2.6.5 Immunoprecipitation / Co-immunoprecipitation

Cell extracts were obtained by lysing cells in RIPA buffer supplemented with protease inhibitors. Protein G sepharose (Sigma) was prepared by washing the beads twice with ice-cold PBS and resuspending them in 100µl of ice-cold RIPA buffer/sample for equilibration. Following this, the cell lysate was pre-cleared by adding Protein G Sepharose (20µl of packed beads per sample) and incubating at 4°C for 30 minutes on a rotating wheel. Protein G Sepharose bound to non-specific proteins was removed by centrifugation at 14,000 x g at 4°C for 10 minutes, and the pre-cleared supernatant was transferred to a new tube. Rabbit polyclonal anti-p100 antibody (5µg antibody/500µg of cell lysate) was then added to the pre-cleared lysate and rotated at 4°C overnight. The immunocomplex was captured by adding 20µl of packed G sepharose and gently rotating the mixture at 4°C for 1 hour. The sepharose beads were then collected by pulse centrifugation (14,000 x g for 5 seconds) and the supernatant, containing unbound proteins, was either discarded or kept for further analysis (Figure 3.1). The complexes were washed three times in 800µl of RIPA buffer and all liquid was removed. Precipitated proteins were eluted from the matrix by addition of 60µl of 2x protein sample buffer, and heated to 95°C for 4 minutes to dissociate the immunocomplexes from the beads. The beads were then collected by centrifugation and the supernatant containing the immunocomplexes was analysed by SDS-PAGE.

2.6.6 SDS-polyacrylamide gel electrophoresis (SDS-PAGE) and immunoblot analysis

Proteins were separated by SDS-PAGE and transferred to hybond ECL nitrocellulose membranes (Amersham) for immunoblot analysis. All blots were incubated for 1 hour at room temperature in blocking solution (PBS containing 2.5% low-fat milk and 0.1% Tween 20), followed by overnight incubation with primary antibody in blocking solution at 4°C. Primary antibodies are listed in Table 2.4. Bound antibodies were detected with appropriate peroxidase-conjugated secondary antibodies (1:2000 dilution) and visualised by ECL chemiluminescence reagents (Amersham).

Antigen/Reference	Source	Dilution	Supplier
p100/p52	Rabbit pAb	1:200	Upstate Biotech (06-413)
p100/p52	Mouse mAb	1:1000	Upstate Biotech (05-361)
RelB	Rabbit pAb	1:200	Santa Cruz (SC-226)
RelA/p65	Rabbit pAb	1:200	Santa Cruz (SC-372)
Sp1	Rabbit pAb	1:200	Santa Cruz (SC-59)
TAT-1 tubulin (Woods *et al.*, 1989)	Mouse mAb	1:1000	Gift: S. Ley (Mill Hill, UK)
IκBα	Rabbit pAb	1:200	Santa Cruz (SC-371)
β-actin	Mouse mAb	1:5000	AbCam (ab6276-100)
vFLIP 6/14 (Low *et al.*, 2001)	Rat mAb	1:100	Gift: W.Low (UCL, UK)

Table 2.4 Primary antibodies

CHAPTER 3

vFLIP induces p100 processing

3.1 Introduction

The alternative pathway of NF-κB activation induces the processing of the p100 precursor to generate p52. This pathway involves the phosphorylation of p100 via NIK and IKKα, leading to its ubiquitination through the SCF ubiquitin ligase complex and subsequent processing to p52 (section 1.3.4). This process is tightly regulated (Xiao *et al.*, 2001b) for good reason; chromosomal translocations at the 10q24 locus that truncate the C-terminus of p100 leading to aberrant processing, are associated with lymphomas (Chang *et al.*, 1995; Fracchiolla *et al.*, 1993), and genetically manipulated mice expressing p52, but not p100, develop gastric and lymphoid hyperplasia (Ishikawa *et al.*, 1997). Physiological stimuli that regulate the processing of p100 to p52 include BAFF ligand, CD40 activation, lymphotoxin β, LPS and TWEAK (Chapter 1). Without exception, all have important roles in the development and regulation of the immune system, and in particular, B cell function. It is therefore of great interest that deregulated p100 processing has been found in leukaemic T cells transformed by HTLV-1, in which the Tax protein induces this processing (Xiao *et al.*, 2001a), and that the EBV transforming protein LMP-1is also able to induce p100 processing (Eliopoulos *et al.*, 2003). Constitutive NF-κB activation within lymphoid cells is central to the transforming activity of both viral oncoproteins (section 1.3.4.3). As a constitutive activator of NF-κB, expressed by a lymphotropic and oncogenic virus, we speculated that vFLIP might also activate this alternative NF-κB pathway, and that activation of this pathway might play a key role in the survival of KSHV-infected cells.

3.2 Results

3.2.1 vFLIP induces p100 expression and p52 generation in Jurkat cells. In these cells and BC3 PEL cells, vFLIP also physically associates with endogenous p100

To avoid the constitutive p100/p52 expression found in many B cell lines, Jurkat 3T8 T cells were used to investigate vFLIP induction of p100 processing in a lymphoid cell line. Xiao *et al.*, demonstrated that both the Tax protein from HTLV-1, and mitogen stimulation increased p100 expression in Jurkat cells, however only Tax led to increased p52 generation (Xiao *et al.*, 2001a). Jurkat 3T8 cells were therefore transduced with a lentivirus encoding vFLIP and GFP (vFLIP_IRES_GFP), or not transduced, followed by analysis of endogenous p100 expression and p52 generation by western blot. A KSHV-infected primary effusion lymphoma (PEL) cell line, BC3, was used as a positive control for vFLIP expression and constitutive activation of NF-κB. As shown in Figure 3.1, analysis of the total cell lysate of Jurkat cells transduced with the vFLIP_IRES_GFP lentivector revealed that expression of vFLIP led to a significant increase in p100 expression and generation of the p52 subunit (Figure 3.1.Total lysate lanes). The upregulation of p100 expression indicates activation of the classical NF-κB pathway by vFLIP, and is consistent with previous studies demonstrating p100 as an NF-κB target gene (Liptay *et al.*, 1994; Sun *et al.*, 1994). In these earlier studies, activation of NF-κB was associated with increased p100, but not p52 expression. More importantly, the generation of the p52 subunit indicates that the p100 precursor is being processed into p52 by the activity of the alternative NF-κB pathway. Low levels of p100 and undetectable p52 expression were observed in untransduced Jurkat cells. These data are therefore consistent with the activation of both classical and alternative pathways of NF-κB by vFLIP.

It is known that the canonical NF-κB pathway is constitutively active in PEL cell lines (Keller *et al.*, 2000; Liu *et al.*, 2002). Through using KSHV-infected BC3 cells as a positive control in the above experiment, we were able to investigate the status of the alternative NF-κB pathway in a PEL cell line, by

examining their cell lysates for the expression of p100 and the generation of its p52 subunit. As shown in figure 3.1 (top panel, BC3/PEL lanes), in the case BC3 cells, we observed high expression levels of both p100 and p52, which suggests constitutive activation of the alternative NF-κB pathway in a PEL cell line.

The mechanism of Tax-induced p100 processing has been partially explained by the ability of Tax to bind p100 (Beraud *et al.*, 1994) and recruit it to the IKK complex (Xiao *et al.*, 2001a). Since vFLIP, like Tax, is present in a complex with NEMO (Field *et al.*, 2003), it was an intriguing possibility that vFLIP might also be in a complex with p100. Lysates were made from untransduced 3T8 Jurkat T cells, or transduced with a lentivirus encoding vFLIP and GFP, (as described above), and these were used in a co-immunoprecipitation experiment to examine whether vFLIP forms a complex with endogenous p100 in Jurkat cells. p100 and its p52 subunit were immunoprecipitated from the cellular lysates by using a rabbit polyclonal p100/p52 antibody, and co-immunoprecipitated vFLIP was detected by immunoblotting with a rat monoclonal vFLIP antibody. As shown in figure 3.1(middle panel, IP lane at the far right), we detected an interaction between vFLIP and full-length p100 which indicates that vFLIP associates with endogenous p100 in Jurkat cells. We also observed that there is a significant amount of vFLIP in the unbound fraction, in contrast to results obtained from NEMO (IKKγ)/vFLIP co-immunoprecipitations in PEL cells, where the whole population of vFLIP was shown to associate with NEMO (Field *et al.*, 2003).

We also sought to determine whether endogenous vFLIP, expressed in KSHV-infected BC3 PEL cells, as opposed to ectopically expressed vFLIP in Jurkat cells, can interact with endogenous p100 in PEL cells. We analysed the cell lysates derived from BC3 cells by co-immunoprecipitation as described above. As shown in Figure 3.1 (middle panel, IP lane in the middle), vFLIP expressed by KSHV in PEL cells interacted specifically with endogenous p100, confirming our previous findings. Moreover, Figure 3.1 demonstrates that only a fraction of endogenous vFLIP is pulled down with endogenous p100/p52 by the anti-p100 antibody, while the rest remains in the unbound

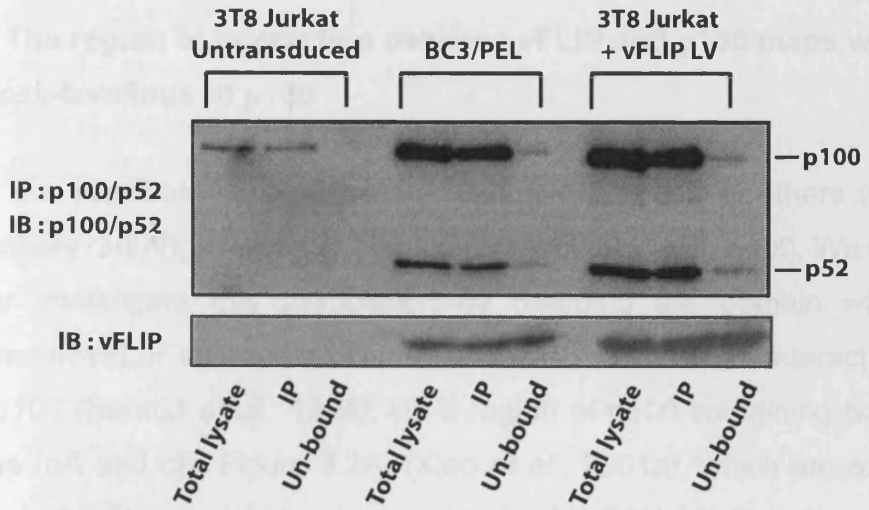

Figure 3.1 vFLIP associates with endogenous p100 in BC3 PEL cells and 3T8 Jurkat cells

Whole cell lysate (RIPA) from $5x10^6$ BC3 cells, or Jurkat 3T8 cells not infected, or infected with a lentivirus encoding vFLIP and GFP, was immunoprecipitated 48 hours post-transduction using a polyclonal anti-p100/p52 antibody (Upstate). The immunoprecipitate (IP) and 5% of both the original whole cell extract (Total Lysate) and the supernatant from the immunoprecipitation (Unbound) were then separated on a 12% SDS-polyacrylamide gel and analysed by immunoblot using an anti-vFLIP and a mouse monoclonal p100/p52 antibody (Upstate). Transduction efficiency of the lentivectors was measured by FACScan analysis of cells expressing GFP. 94% of cells expressed GFP after infection with the vFLIP lentivirus, and 87% of cells were GFP positive when infected with the GFP lentivirus.

fraction as with the Jurkat cells. This may suggest that only a subset of p100 is recruited by vFLIP to the IKK complex, as demonstrated for Tax (Xiao *et al.*, 2001a). These data demonstrate the expression of both vFLIP and p100 in the context of KSHV infection, and show the interaction between these two proteins under physiological conditions.

3.2.2 The region of interaction between vFLIP and p100 maps within the Carboxy-terminus of p100

From our previous findings (section 3.2.1), and those of others (Matta and Chaudhary, 2004), it is known that vFLIP associates with p100. We decided to further investigate this association by mapping the domain within p100 involved in vFLIP interaction. Tax from HTLV-1 is known to interact physically with p100 (Beraud *et al.*, 1994), via a region of p100 containing two short α-helices (αA and αB, Figure 3.2A) (Xiao *et al.*, 2001a), which are exposed on the surface of the protein but are not involved in DNA binding, dimerization, or folding of p52 (Cramer *et al.*, 1997). Xiao *et al.* demonstrated that deletion of both α-helices abolishes the interaction of Tax with p100 and blocks processing of p100 to p52 (Xiao *et al.*, 2001a). We speculated that the same region of p100 might be involved in the association with vFLIP, since Tax and vFLIP exhibit striking similarities in their ability and mechanism to activate the alternative NF-κB pathway. We also hypothesized that vFLIP might be binding through its death effector domain (DED) to an alternative region within the C'-terminus of p100, and more specifically its death domain (DD). Both DDs and DEDs are members of the DD superfamily, which contains homotypic protein-protein interaction modules, and it is possible that either of the two DEDs of vFLIP might be recruiting p100 to a complex via a homotypic interaction with its C'-terminal DD. To this effect, we attempted to engineer two truncation mutants of p100, one lacking a portion of the N'-terminus containing the two α-helices, and another lacking a portion of the C'-terminus containing the DD, in order to assess their role in the interaction with vFLIP. We were successful in creating and expressing a p100 construct with a truncated C'-terminus (p100ΔC, 1-753aa) by designing primers that introduced a stop codon just before the region that codes for the death domain of p100. However, although

we engineered a p100 construct with a truncated N'-terminus (p100ΔN, 181-900aa), we were never able to express it in mammalian cells. It is possible that by excluding the first 181 amino acids from the N'-terminus of our construct, we interfered with the DNA binding, dimerization, and folding of the p100 protein, since the region we deleted includes the Rel Homology Domain (RHD), which is necessary for these to occur (Ghosh *et al.*, 1998). We therefore obtained the p100 ΔαA/B deletion mutant, which was kindly provided by Prof. Gutian Xiao (Xiao *et al.*, 2001a). This was generated by site-directed mutagenesis using pCMV4-p100 (Sun *et al.*, 1994) as template, and carries combined deletions of amino acids 151-160 (ΔαA) and 170-181 (ΔαB). Figure 3.2A shows a schematic representation of the three p100 constructs used to map the area of interaction between vFLIP and p100.

293T cells were co-transfected with expression vectors encoding vFLIP together with a full length p100, or p100ΔαA/B, or p100ΔC. The p100 proteins were isolated from the cell lysates by immunoprecipitation using a polyclonal p100/p52 antibody, and co-immunoprecipitated vFLIP was detected by immunoblotting using a monoclonal vFLIP antibody. The cell lysates were also analysed by immunoblotting to check p100 expression and processing, and vFLIP expression. As seen in Figure 3.2B (middle panel), we successfully expressed the three p100 constructs in 293T cells. p100ΔαA/B yielded a lower molecular weight p52 processing product as a result of the deletion of 20 amino acids from its N'-terminus, which are part of the p52 subunit after processing. p100ΔC in turn, yielded a lower molecular weight p100 precursor due to the deletion of 147 amino acids from its C'-terminus, but its p52 subunit was the same molecular weight as that of the full length p100, since the deletions lie outside the region of p100 that gets processed into active p52.

As seen in Figure 3.2B (top panel, lane 4), the two α-helices do not seem to be necessary for the interaction between p100 and vFLIP, since their deletion had no effect on the ability of the mutant p100 to pull down vFLIP in the co-immunoprecipitation. However, deletion of the C'-terminal region of p100 almost entirely abolished the p100-vFLIP interaction (Figure 3.2B, top panel, lane 5), since p100ΔC co-immunoprecipitated with a barely detectable amount

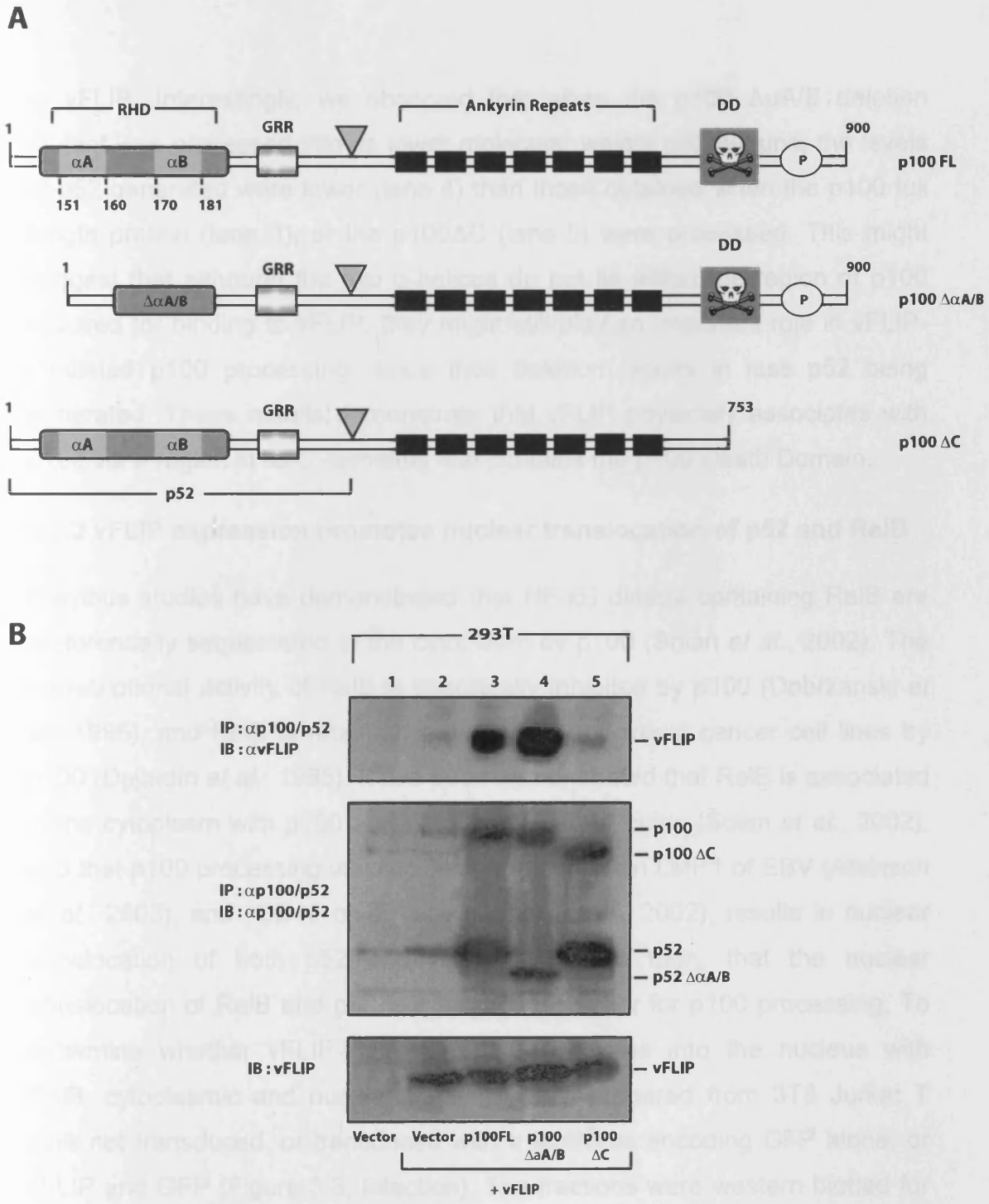

Figure 3.2 (A, B) Interaction of vFLIP with p100 occurs via a C′-terminal region of p100, which includes the Death Domain

(A) Schematic picture of p100 full length (p100 FL) and its deletion mutants p100 ΔαA/B, with the two α-helices indicated in the diagram within the Rel Homology Domain (RHD) deleted, and p100 ΔC, with the C-terminus of p100, including the Death Domain (DD), deleted. GRR, glycine-rich region; P, phosphorylation site. **(B)** 293T cells were transfected with vFLIP (1.5μg) together with the full length p100 or the indicated mutant forms of p100. The p100 proteins were isolated from cell lysates by IP using a p100/p52 rabbit polyclonal antibody (Upstate), followed by detection of the co-precipitated vFLIP by IB (upper panel). The cell lysates were also subjected to IB to monitor p100 processing and expression using a p100/p52 mouse monoclonal antibody (Upstate) (middle panel), and vFLIP expression (lower panel).

of vFLIP. Interestingly, we observed that when the p100 ΔαA/B deletion mutant was processed into its lower molecular weight p52 subunit, the levels of p52 generated were lower (lane 4) than those obtained when the p100 full length protein (lane 3), or the p100ΔC (lane 5) were processed. This might suggest that although the two α-helices do not lie within the region of p100 required for binding to vFLIP, they might still play an important role in vFLIP-mediated p100 processing, since their deletion results in less p52 being generated. These results demonstrate that vFLIP physically associates with p100 via a region in its C'-terminus that contains the p100 Death Domain.

3.2.3 vFLIP expression promotes nuclear translocation of p52 and RelB

Previous studies have demonstrated that NF-κB dimers containing RelB are preferentially sequestered in the cytoplasm by p100 (Solan *et al.*, 2002). The transcriptional activity of RelB is specifically inhibited by p100 (Dobrzanski *et al.*, 1995), and RelB is retained in the cytosol of breast cancer cell lines by p100 (Dejardin *et al.*, 1995). It has been demonstrated that RelB is associated in the cytoplasm with p100 and not other IκB molecules (Solan *et al.*, 2002), and that p100 processing induced by the oncoprotein LMP1 of EBV (Atkinson *et al.*, 2003), and CD40 on B cells (Coope *et al.*, 2002), results in nuclear translocation of both p52 and RelB. It follows then, that the nuclear translocation of RelB and p52 is a surrogate marker for p100 processing. To determine whether vFLIP-induced p52 translocates into the nucleus with RelB, cytoplasmic and nuclear fractions were prepared from 3T8 Jurkat T cells not transduced, or transduced with a lentivirus encoding GFP alone, or vFLIP and GFP (Figure 3.3, Infection). The fractions were western blotted for endogenous p100, p52 and RelB. Immunoblotting for tubulin (cytoplasmic marker) and SP1 (nuclear marker) confirmed cell fractionation. In untransduced and GFP-transduced cells, no p52 and very little RelB was detected in the nuclear fraction (Figure 3.3, nuclear panel, lanes 3 and 5). However, vFLIP expression in Jurkat cells, led to a dramatic increase in nuclear p52 and accumulation of nuclear RelB (Figure 3.3, nuclear panel, lane 6), a good indication that vFLIP stimulates p100 processing resulting in the

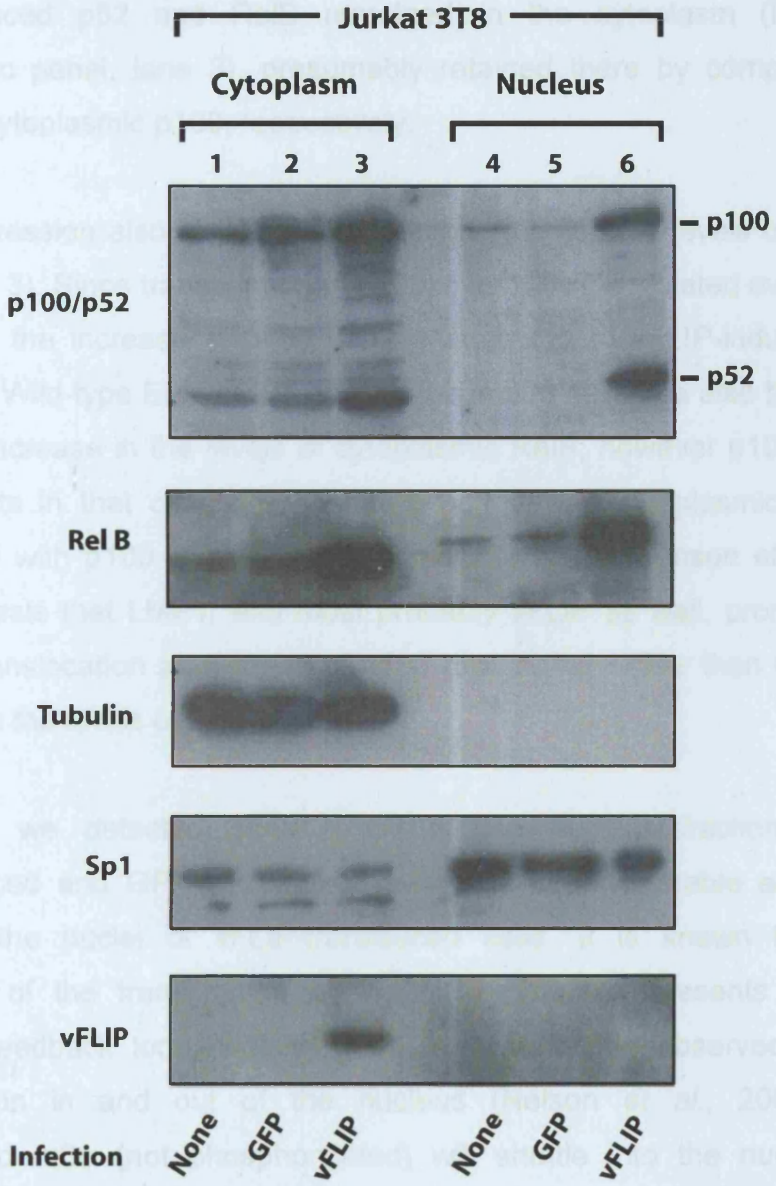

Figure 3.3 vFLIP expression induces nuclear translocation of p100, p52 and RelB

Nuclear and cytoplasmic extracts were prepared from $5x10^6$ Jurkat 3T8 cells not transduced, or transduced with lentivirus encoding either GFP, or vFLIP plus GFP, 48 hours post-transduction. 20μg of cytoplasmic extract (2%) and 30μg of nuclear extract (10%) were separated on a 12% SDS-polyacrylamide gel and analysed by immunoblotting using the monoclonal anti-p100/p52, anti-RelB, anti-Sp1, anti-tubulin, and anti-vFLIP antibodies. Transduction efficiency of the lentivectors was measured by FACScan analysis of cells expressing GFP. 98% of cells expressed GFP after infection with the vFLIP lentivirus, and 83% of cells were GFP positive when infected with the GFP lentivirus.

release of RelB, which translocates to the nucleus with p52. A portion of vFLIP-induced p52 and RelB remained in the cytoplasm (Figure 3.3, cytoplasmic panel, lane 3), presumably retained there by complexing with IκBs and cytoplasmic p100, respectively.

vFLIP expression also resulted in increased steady state levels of p100 and RelB (lane 3). Since transcription of p100 is an NF-κB regulated event (Sun *et al.*, 1994), the increase in p100 can be attributed to vFLIP-induced NF-κB activation. Wild-type EBV LMP1 expression in 293 cells has also been shown to cause increase in the levels of cytoplasmic RelB, however p100 depletion experiments in that case demonstrated that all the cytoplasmic RelB was associated with p100 in LMP1-transfected 293 cells (Atkinson *et al.*, 2003). This suggests that LMP1, and most probably vFLIP as well, promotes RelB nuclear translocation as a result of p100 processing rather than through the increase in the levels of RelB protein.

Moreover, we detected some p100 in the nuclear fractions of both untransduced and GFP-transduced cells, and a considerable amount was found in the nuclei of vFLIP-transduced cells. It is known that NF-κB regulation of the transcription of the IκBα protein represents a delayed negative feedback loop, which drives the oscillations observed in NF-κB translocation in and out of the nucleus (Nelson *et al.*, 2004). Newly synthesized IκBα (not phosphorylated) will shuttle into the nucleus as a negative feedback signal to stop NF-κB activation by binding to active Rel molecules and restoring them to the cytoplasm. It is possible, that in the same way as for IκBα, there is a p100 negative feedback loop, which causes p100 to oscillate in and out of the nucleus in order to restore the alternative NF-κB pathway by binding to nuclear RelB and sequestering it back to the cytoplasm. Indeed, the carboxyl-portion of p100 contains a nuclear export signal, which is required for effective retrieval of RelB from the nucleus (Solan *et al.*, 2002).

It has also been suggested that the nuclear shuttling of p100 is the mechanism which is required for regulating its constitutive processing (Fong and Sun, 2002; Liao and Sun, 2003; Qu *et al.*, 2004). More importantly, the

Tax protein from HTLV-1 induces a significant nuclear localisation of p100 (Qing *et al.*, 2005), which suggests that nuclear shuttling might be the β-TrCP-independent mechanism for Tax-induced p100 processing. Therefore, it is possible that vFLIP might be adopting a similar mechanism for p100 processing, as observed by the presence of significant amounts of p100 in the nuclear fraction (lane 6).

3.2.4 The induction of p100 processing and the subsequent nuclear translocation of p52 and RelB are mediated specifically by vFLIP

As previously discussed, Xiao *et al.* demonstrated that both Tax from HTLV-1, and mitogen stimulation can lead to increased p100 expression in Jurkat cells, by activating the classical NF-κB pathway (Xiao *et al.*, 2001a). However p52 was only detected in cells expressing Tax due to its ability to also activate the alternative NF-κB pathway (Xiao *et al.*, 2001a). We set out to examine whether the nuclear accumulation of p52 and RelB, observed in Jurkat cells transduced with the vFLIP lentivector, was a direct result of vFLIP-induced p100 processing and therefore alternative pathway activation, or it simply occurs through the increase in the levels of p100. Jurkat 3T8 T cells were transduced with a control lentivector expressing only GFP, or with a lentivector expressing both vFLIP and GFP. A fraction of the transduced cells was activated by mitogen stimulation for 16 hours by the addition of 10ng/ml PMA and 500ng/ml ionomycin (PMA/I), which results in the activation of the classical NF-κB pathway. Nuclear and cytoplasmic extracts were prepared from KSHV-infected BC3 cells (used as a positive control for alternative NF-κB pathway activation), and the transduced Jurkat T cells that had either been stimulated with PMA/I (Figure 3.4, lanes 4, 5, 9, 10), or not (lanes 1, 2, 7, 8). As expected, BC3 cells accumulated significant levels of nuclear p52 and RelB, indicating alternative pathway activation in the context of KSHV infection (Figure 3.4, nuclear panel, lane 6). Immunoblot analysis of cytoplasmic and nuclear fractions from the transduced Jurkat cells without mitogen stimulation, confirmed that vFLIP expression leads to higher levels of p100 expression and generation of p52 (Figure 3.4, cytoplasmic panel, lane 3), and to a significant increase in nuclear p52 and RelB (nuclear panel, lane

8). In Jurkat cells transduced with the control GFP-only lentivector, no p52 or RelB could be detected in the nucleus (Figure 3.4, nuclear panel, lane 7).

Mitogen stimulation led to heightened expression of p100 and RelB in the GFP-transduced cells (Figure 3.4, cytoplasmic panel, lane 4). This upregulation was likely due to p100 and RelB being transcriptional targets of the canonical NF-κB pathway (Liptay *et al.*, 1994; Sun *et al.*, 1994), which was activated by the mitogen stimulation in this case. Mitogen treatment had little effect on the levels of p100 and p52 in Jurkat cells transduced with the vFLIP lentivector (Figure 3.4, cytoplasmic panel, lane 5). However, consistent with the inability of p100 to respond to cellular activation signals (Sun *et al.*, 1994), mitogen stimulation in GFP-transduced cells failed to induce generation of p52, and levels of p52 in these cells were extremely low and only detectable after prolonged exposure of the western blot films (Figure 3.4, cytoplasmic panel, lane 4). Only vFLIP expression was capable of inducing increased p52 generation in Jurkat cells (Figure 3.4, cytoplasmic fraction, lanes 3 and 5), as was the case for the Tax oncoprotein of HTLV-1 (Xiao *et al.*, 2001a).

Mitogen stimulation in GFP-transduced cells did not result in p52 translocation to the nucleus, and the p52 nuclear levels in these cells were almost undetectable (Figure 3.4, nuclear panel, lane 9). Interestingly, some RelB was detected in the nuclear fraction of GFP-transduced / stimulated cells (Figure 3.4, nuclear panel, lane 9). It has been demonstrated that in the cytoplasm, RelB is mostly associated with p100 (Solan *et al.*, 2002). However, secondary to this interaction, which regulates the constitutive nuclear pool of NF-κB transcriptional activity in myeloid and lymphoid cells, it is also believed that RelB can have weak interactions with the classical NF-κB inhibitor proteins, the IκBs (Solan *et al.*, 2002). Presumably then, there is a subset of RelB which is associated with other IκBs in the cytoplasm, and when these are degraded upon mitogen stimulation, this subset of RelB is free to translocate to the nucleus, as seen in this experiment (Figure 3.4, nuclear panel, lane 9). In contrast to GFP transduced cells, expression of vFLIP in activated Jurkat cells led to a potent accumulation of p52 and RelB in the nucleus. However, the levels of p52 and RelB translocating to the nucleus in vFLIP-transduced

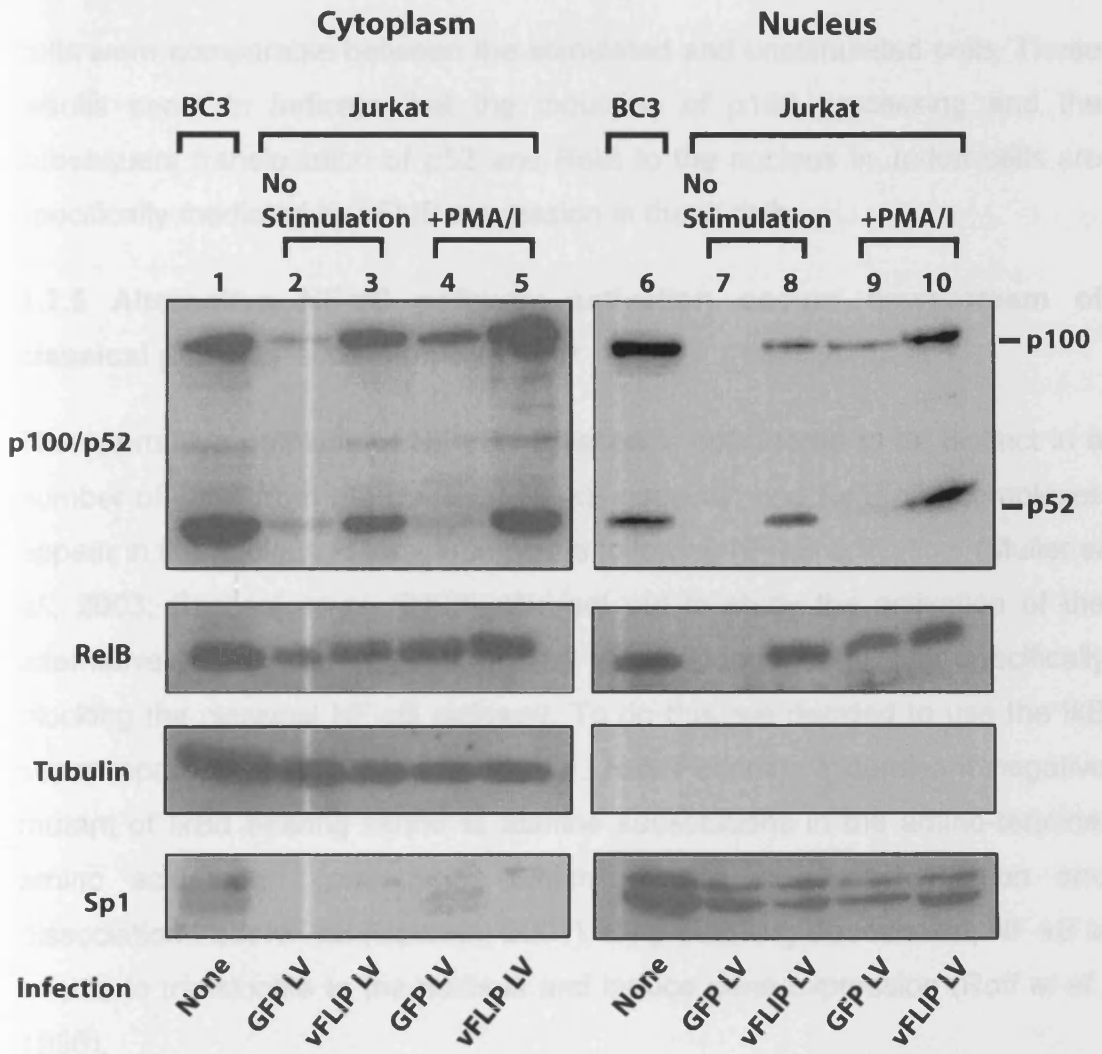

Figure 3.4 p100 processing, and the nuclear translocation of p52 and RelB, is specifically mediated by vFLIP

Nuclear and cytoplasmic extracts were prepared from $5x10^6$ BC3 cells, or Jurkat 3T8 cells, not infected or infected with a lentivirus encoding vFLIP plus GFP, on day 3 post-infection. A fraction of the Jurkat 3T8 cells were activated for 16h by addition of 10ng/ml PMA and 500ng/ml ionomycin (Lanes labelled PMA/I). 20μg of cytoplasmic extract (2%) and 30μg of nuclear extract (10%) were separated on a 12% SDS-polyacrylamide gel and analysed by immunoblotting using the monoclonal anti-p100/p52, anti-RelB, anti-Sp1, anti-tubulin, and anti-vFLIP antibodies. Transduction efficiency of the lentivector was measured by FACScan analysis of cells expressing GFP. 87% of cells expressed GFP after transduction with the vFLIP lentivirus, and 93% of cells were GFP positive when transduced with the GFP lentivirus.

cells were comparable between the stimulated and unstimulated cells. These results seem to indicate that the induction of p100 processing and the subsequent translocation of p52 and RelB to the nucleus in Jurkat cells are specifically mediated by vFLIP expression in these cells.

3.2.5 Alternative NF-κB pathway activation occurs downstream of classical pathway activation by vFLIP

The alternative pathway of NF-κB activation is considered to be distinct in a number of ways from the classical NF-κB pathway, and RelB:p52 complexes appear in the nucleus at later time points following NF-kB activation (Muller *et al.*, 2003; Saccani *et al.*, 2003). We set out to study the activation of the alternative NF-kB pathway induced by vFLIP independently, by specifically blocking the classical NF-κB pathway. To do this, we decided to use the IkB super-repressor (kindly provided by Dr. Neil Perkins), a dominant negative mutant of IκBα bearing serine to alanine substitutions in the amino-terminal amino acids Ser^{32} and Ser^{36}, which prevent its phosphorylation and dissociation from NF-κB (Baldwin, 2001). By preventing dissociation, NF-κB is unable to translocate to the nucleus and induce gene expression (Roff *et al.*, 1996).

293T cells were co-transfected with expression vectors encoding the IκB super-repressor (Sr) (1μg) and vFLIP (1μg), vFLIP (1μg) and empty vector, or empty vector alone. Cytoplasmic and nuclear fractions were prepared from these cells and were analysed by western blotting for endogenous p100 and p52, RelB, and RelA/p65. Immunoblotting for tubulin (cytoplasmic marker) and SP1 (nuclear marker) confirmed cell fractionation, while blotting for vFLIP and IkBα confirmed expression of the proteins of interest from the transfected expression vectors. Figure 3.5 shows that expression of vFLIP in 293T cells led to a significant increase in endogenous p100 expression levels and to the generation of the p52 processing product (Figure 3.5, cytoplasmic panel, lane 2). Moreover, vFLIP expression resulted in the translocation of p52, RelB, and RelA/p65 into the nucleus (Figure 3.5, nuclear panel, lane 5), consistent with our previous findings that indicate that vFLIP activates both classical and

alternative pathways of NF-κB. There was no detectable p52, very little RelB and RelA/p65 in the nuclear fraction of 293T cells transfected with the empty vector, but there were low levels of p100 present in the nucleus (Figure 3.5, nuclear panel, lane 4), possibly shuttling in and out of the nucleus for the constitutive processing of p100 (as explained previously). Co-expression of vFLIP and the super-repressor led to a significant reduction in the levels of p100 expression, as well as RelB, in the cytoplasm (Figure 3.5, cytoplasmic panel, lane 3), which were even lower than those detected in cells transfected with an empty vector. This result confirmed successful inhibition of the classical pathway through the action of the IκB super-repressor, and suggested that there is a basal level of constitutive NF-κB activation in control cells which is responsible for the increased levels of p100 observed (lane 1). However, p52 was successfully generated in cells expressing vFLIP and the IκB super-repressor, and its levels were comparable to those observed in cells transfected only with vFLIP (Figure 3.5, cytoplasmic panel, lane 3). This suggests that vFLIP-induced p100 processing is independent of classical pathway activation and does not require the degradation of IκBα. Nevertheless, nuclear accumulation of p52 and RelB was significantly reduced in the presence of the IκB super-repressor (Figure 3.5, nuclear panel, lane 6), while RelA/p65 levels in the nucleus were undetectable, as expected.

These results demonstrate that although the vFLIP-induced activation of the alternative NF-kB pathway is distinct from that of the classical NF-kB pathway, since it does not require IκBα degradation, but employs a separate mechanism to release active p52, the two pathways are still somehow interconnected. It appears that classical pathway activation by vFLIP occurs upstream of the alternative pathway, and it enhances the transcription of p100 (and possibly of RelB too), which is then more abundant and readily available to be processed during alternative pathway activation. This in turn results in more active p52: NF-kB dimers entering the nucleus during alternative pathway activation and delivering a stronger activation signal. Complete inhibition of the classical NF-kB pathway by the IκB super-repressor seems to dampen the activation of the alternative pathway mediated by vFLIP.

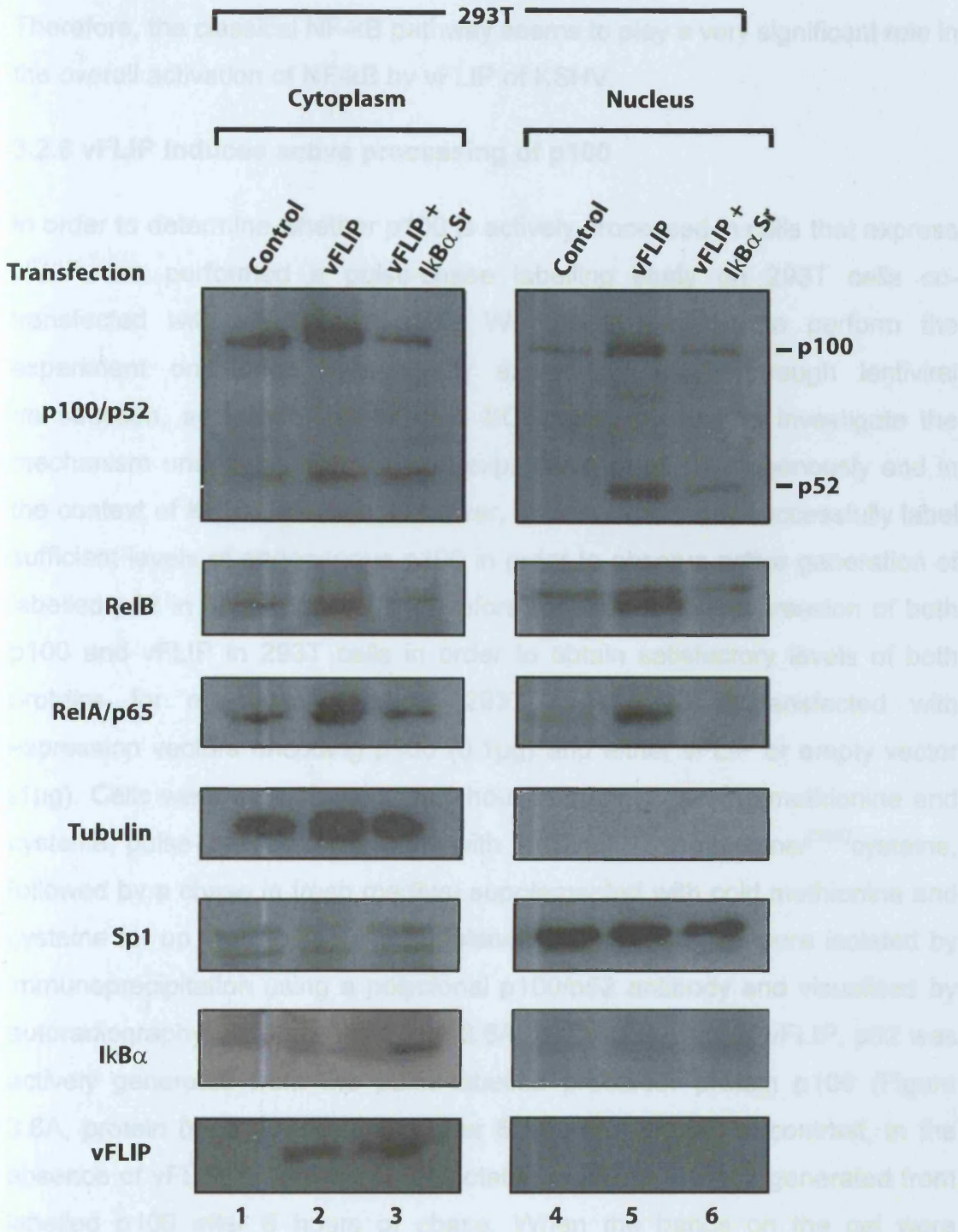

Figure 3.5 Inhibition of classical NF-κB pathway activation also results in the downregulation of the alternative pathway activation mediated by vFLIP

293T cells were co-transfected with expression vectors encoding vFLIP (1μg) and empty vector, vFLIP and IkBα super-repressor (Sr) (1μg), or empty vector alone (labelled control). 24 hours post transfection, nuclear and cytoplasmic extracts were prepared from these cells. 20μg of cytoplasmic extract (2%) and 30μg of nuclear extract (10%) were separated on a 12% SDS-polyacrylamide gel and analysed by immunoblotting using the monoclonal anti-p100/p52, anti-RelB, anti-RelA/p65, anti-Sp1, anti-tubulin, anti IkBα, and anti-vFLIP antibodies.

Therefore, the classical NF-kB pathway seems to play a very significant role in the overall activation of NF-kB by vFLIP of KSHV.

3.2.6 vFLIP induces active processing of p100

In order to determine whether p100 is actively processed in cells that express vFLIP, we performed a pulse-chase labelling study on 293T cells co-transfected with vFLIP and p100. We initially planned to perform the experiment on Jurkat cells stably expressing vFLIP through lentiviral transduction, and on KSHV-infected BC3 cells, in order to investigate the mechanism underlying the aberrant expression of p52 endogenously and in the context of KSHV infection. However, we were unable to successfully label sufficient levels of endogenous p100 in order to observe active generation of labelled p52 in these cells. We therefore resorted to overexpression of both p100 and vFLIP in 293T cells in order to obtain satisfactory levels of both proteins for metabolic labelling. 293T cells were co-transfected with expression vectors encoding p100 (0.1μg) and either vFLIP or empty vector (1μg). Cells were then starved for 1 hour in medium lacking methionine and cysteine, pulse-labelled for 2 hours with 1mCi/ml $^{[35S]}$methionine/$^{[35S]}$cysteine, followed by a chase in fresh medium supplemented with cold methionine and cysteine for up to 6 hours. The radiolabelled p100 and p52 were isolated by immunoprecipitation using a polyclonal p100/p52 antibody and visualised by autoradiography. As shown in figure 3.6A, in the presence of vFLIP, p52 was actively generated from the pulse-labelled precursor protein p100 (Figure 3.6A, protein band with asterisk) after 6 hours of chase. In contrast, in the absence of vFLIP, there was no detectable radiolabelled p52 generated from labelled p100 after 6 hours of chase. When the bands on the gel were quantified for the intensity of the radioactive signal in each one, there was an evident precursor-product relationship between p100 and p52 in the presence of vFLIP (Figure 3.6B, left graph), with p100 levels decreasing with time as p52 levels were increasing due to the active processing of p100 and subsequent accumulation of the p52 product. In contrast, in the absence of vFLIP, p100 levels slightly increased with time, but this was not associated with any significant generation of p52, as its levels remained constant and

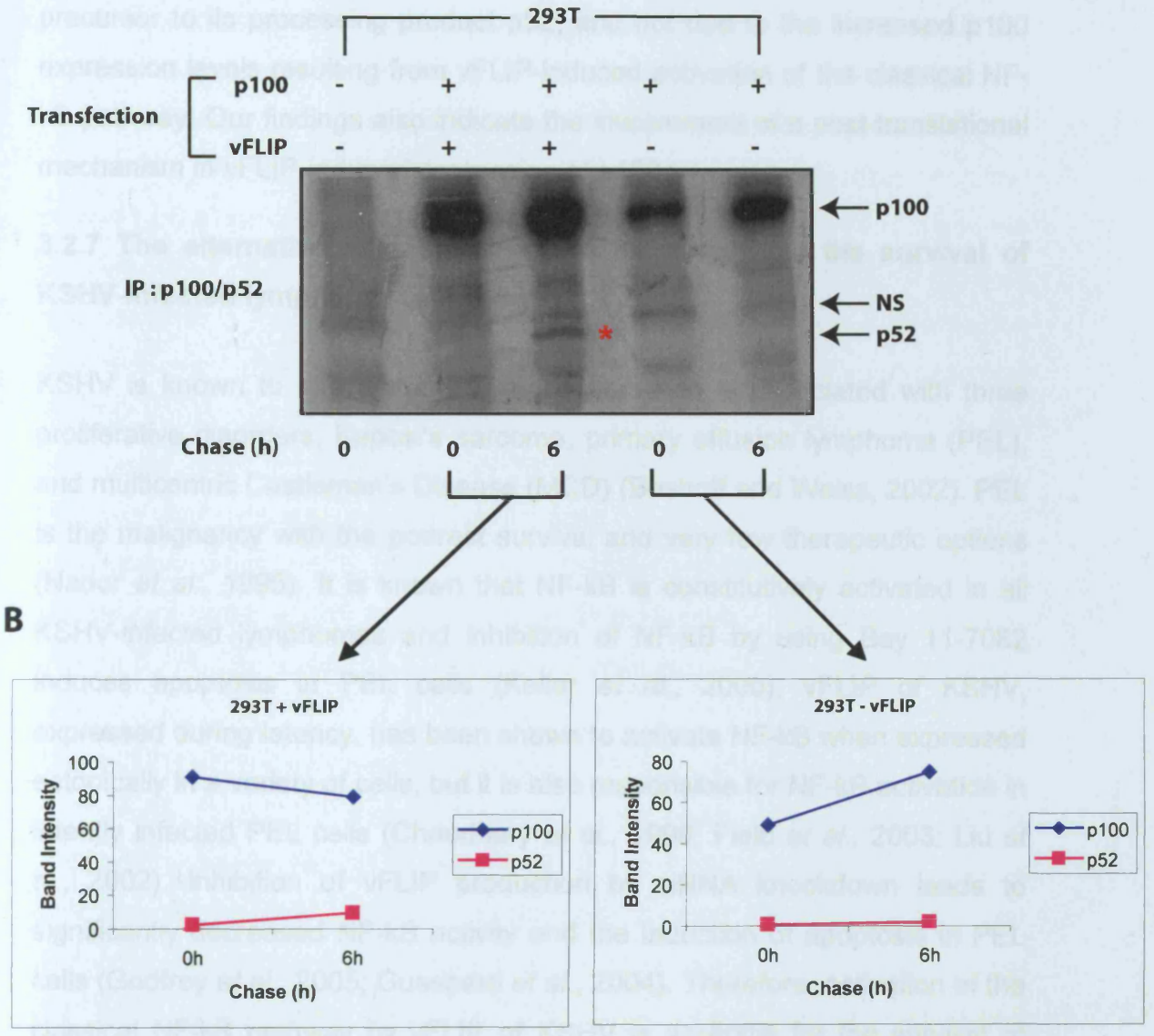

Figure 3.6 Active processing of p100 associated with vFLIP expression

Pulse chase labelling. **(A)** 293T cells were co-transfected with expression vectors encoding p100 (0.1µg) and either vFLIP or empty vector (1µg each). 24 hours post transfection, cells were pulse-labelled for 2h with 1mCi/ml [35S]methionine/[35S]cysteine in Eagle's Minimal Essential medium (-cysteine,-methionine), and chased in complete fresh DMEM, supplemented with 10mM cold methionine and cysteine, for 0h and 6h. Radiolabelled p100 and p52 were isolated by IP of whole cell lysates (RIPA) using a rabbit polyclonal p100/p52 antibody (Upstate), separated on a 12% SDS-polyacrylamide gel, and analysed by autoradiography. p100 and its processing product p52 are indicated. A non-specific band is indicated as NS. **(B)** Densitometry quantitation of the radiolabelled p100 and p52 bands presented in (A).

nearly undetectable throughout the 6 hours of chase (Figure 3.6B, right graph). These results clearly suggest that generation of p52 is a specific event for vFLIP-expressing cells, and is a result of the active processing of the p100 precursor to its processing product p52, and not due to the increased p100 expression levels resulting from vFLIP-induced activation of the classical NF-kB pathway. Our findings also indicate the involvement of a post-translational mechanism in vFLIP-induced processing of p100.

3.2.7 The alternative NF-kB pathway is necessary for the survival of KSHV-infected lymphoma cells

KSHV is known to infect human lymphocytes and is associated with three proliferative disorders, Kaposi's sarcoma, primary effusion lymphoma (PEL), and multicentric Castleman's Disease (MCD) (Boshoff and Weiss, 2002). PEL is the malignancy with the poorest survival and very few therapeutic options (Nador *et al.*, 1996). It is known that NF-kB is constitutively activated in all KSHV-infected lymphomas and inhibition of NF-kB by using Bay 11-7082 induces apoptosis in PEL cells (Keller *et al.*, 2000). vFLIP of KSHV, expressed during latency, has been shown to activate NF-kB when expressed ectopically in a variety of cells, but it is also responsible for NF-kB activation in latently infected PEL cells (Chaudhary *et al.*, 1999; Field *et al.*, 2003; Liu *et al.*, 2002). Inhibition of vFLIP production by siRNA knockdown leads to significantly decreased NF-kB activity and the induction of apoptosis in PEL cells (Godfrey *et al.*, 2005; Guasparri *et al.*, 2004). Therefore, activation of the classical NF-kB pathway by vFLIP of KSHV is essential for the survival of infected lymphoma cells.

We sought to determine the role of the vFLIP-induced alternative NF-kB pathway activation in the survival of PEL cells. To address this question, we decided to test whether elimination of endogenous p100 and p52 in by siRNA would lead to apoptosis in PEL cells. We therefore obtained a pool of four siRNA duplexes (Dharmacon Research) that target different regions of the *nfkb2* gene, which codes for p100/52 in cells, along with a control scramble siRNA duplex, which doesn't knock down any known genes, as a control for

non-sequence-specific effects. The BC3 PEL cell line was transfected with p100/p52 siRNA, scramble siRNA, or mock-transfected using Oligofectamine reagent (Invitrogen), and assayed for gene silencing by immunoblotting 72 hours post transfection. The induction of apoptosis following gene knockdown was measured by flow cytometry for Annexin V, and by Death Detection ELISA. Viability was assayed by trypan blue exclusion 72 hours after transfection. We decided to perform an extended time course study on these cells, as no significant cell death was seen within the initial 72 hours, and we assumed that a single transfection of siRNA would provide transient delivery and incomplete inhibition of the gene of interest. We therefore transfected BC3 cells with siRNA every 3 days (days 0, 3, 6, and 9), and apoptosis, and viability, were measured at 3-day intervals (days 3, 6, 9, and 12) before the next transfection, for a total of four transfections and a 12 day time course. Western blot analysis on cellular lysates prepared 72 hours after each transfection (days 3, 6, 9, and 12) demonstrated significant downregualtion of endogenous p52 levels, and a considerable decrease in p100 expression (Figure 3.7A). Immunoblotting for β-actin confirmed equal loading of proteins.

Figure 3.7B shows that over the course of 12 days, the number of PEL cells undergoing apoptosis increases when transfected with siRNA against p100/p52, and by day 12, over half of the cell population (58.6%) is expressing Annexin V on the cell surface. In contrast, PEL cells transfected with scramble non-specific siRNA, and mock-transfected cells, exhibit very low levels of apoptosis throughout the 12-day time course (<8%), and therefore seem to remain quite viable. In order to exclude the possibility that multiple transfections every 3 days might be inducing stress and leading to apoptosis, we decided to test whether the same level of apoptosis would occur in PEL cells that had only been transfected once at day 0 (Figure 3.7B, bars labelled 12 Days*), or twice at days 0 and 6 (Figure 3.7B, bars labelled 12 Days**). As seen in figure 3.7B, a similar proportion of cells underwent apoptosis when transfected once (55.4 %,), or twice (53.2 %), as in cells that had been transfected four times. In all separate experiments performed, it usually took over 6 days for any significant increase in apoptosis, due to p100/p52 knockdown, to become obvious.

A

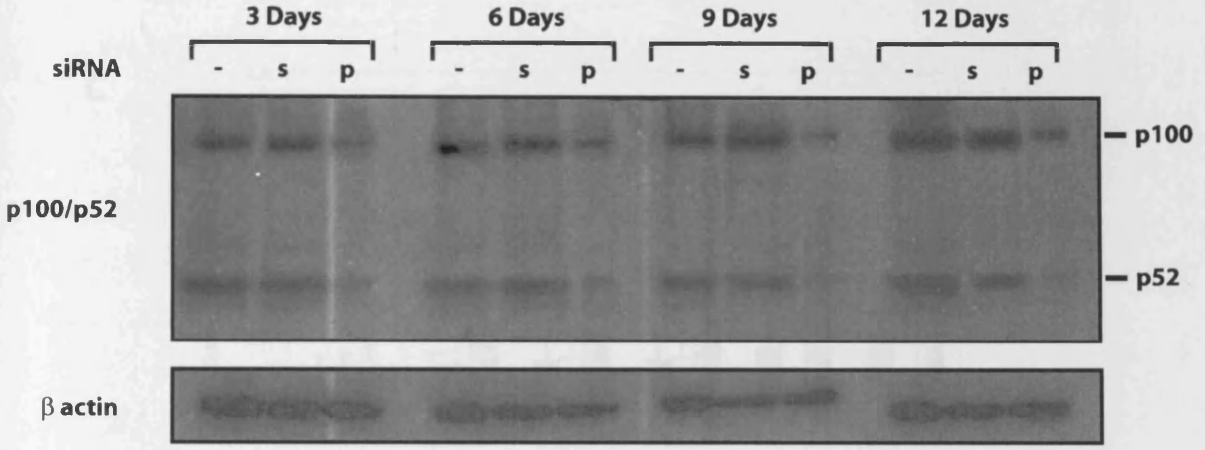

Figure 3.7 (A) Effects of siRNA-mediated p100 knockdown in a BC3 PEL cell line

(A) BC3 cells were transfected with a p100/p52 siRNA (p), scramble siRNA (s), or mock-transfected (-) at days 0, 3, 6, and 9. Approximately 72h after each transfection (indicated time points on the upper panel), cell lysates were prepared and used (40 μg) in Western blot analysis with a mouse monoclonal p100/p52 antibody (Upstate) to assess protein down-regulation. To confirm equal protein loading, β-actin reprobing was performed. Similar results were obtained in three independent experiments.

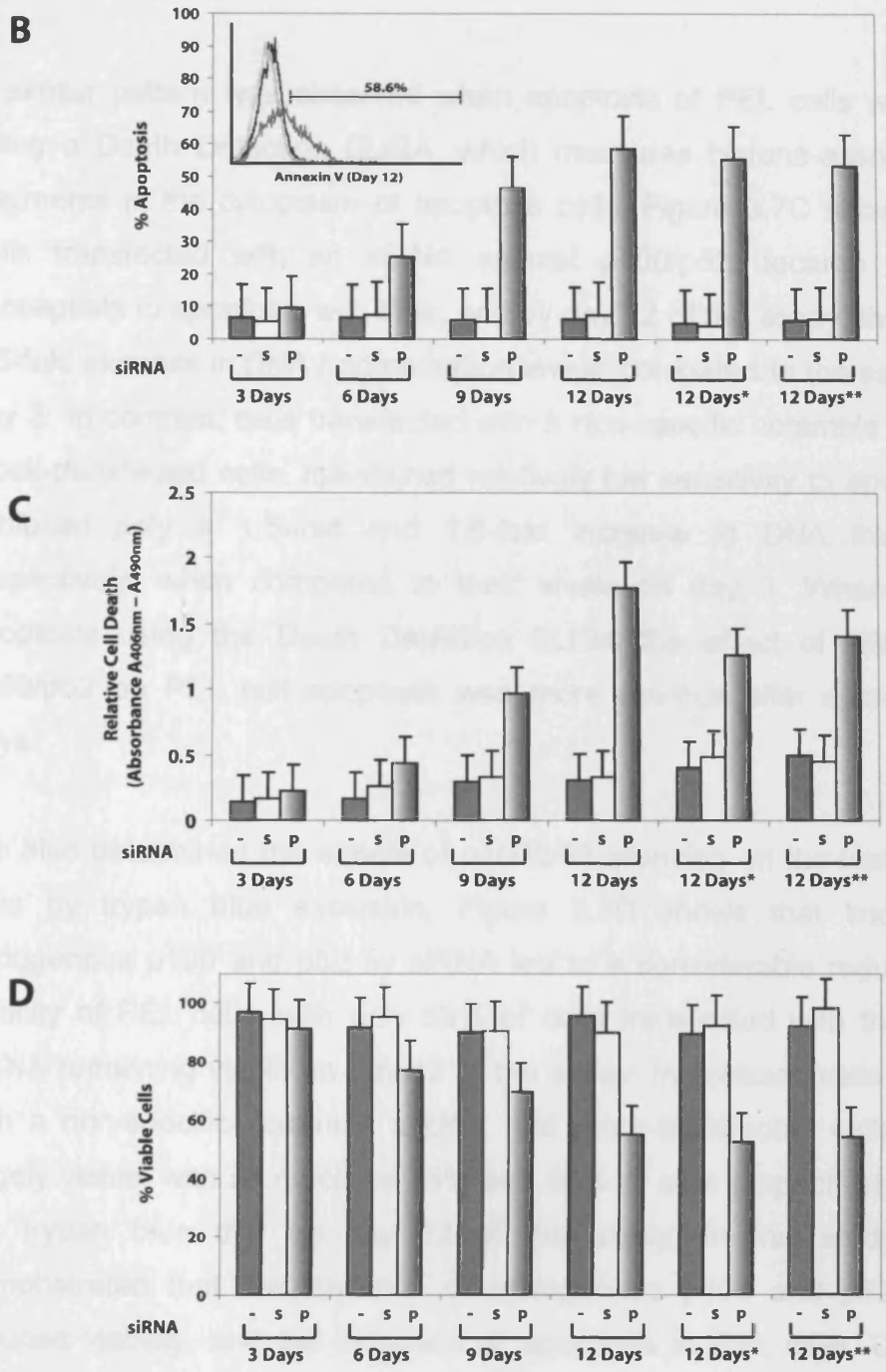

Figure 3.7 (B, C, D) Inhibition of endogenous p100/p52 by siRNA results in apoptosis of BC3 PEL cells

BC3 cells were were transfected with a p100/p52 siRNA (p), scramble siRNA (s), or mock-transfected (-) at days 0, 3, 6, and 9 and assessed for apoptosis and viability at the indicated time points. BC3 cells were also evaluated for apoptosis and viability at day 12 after being transfected only once at day 0 (*), and twice at days 0 and 6 (**). **(B)** Assessment of apoptosis was performed at the indicated time points by Annexin V staining (Trevigen) and measured by FACScan analysis. Inset shows a representative flow cytometric histogram plot at day 12 for Annexin analysis of mock-transfected BC3 cells (light grey line), cells transfected with scramble siRNA as a negative control (black line), and cells transfected with siRNA to p100/p52 (dark grey line with the shift). **(C)** Apoptosis was also measured by using a cell death detection ELISA kit (Roche), which measures DNA fragmentation. **(D)** Cell Viability was measured by Trypan Blue exclusion, as described in Materials and Methods. Bars represent the mean values from three independent experiments with error bars indicating the standard deviation between the three experiments. For each individual experiment, each transfection and analysis was performed in triplicate.

A similar pattern was observed when apoptosis of PEL cells was assayed using a Death Detection ELISA, which measures histone-associated DNA fragments in the cytoplasm of apoptotic cells. Figure 3.7C shows that PEL cells transfected with an siRNA against p100/p52 became increasingly susceptible to apoptosis with time, and by day 12 of the assay, they exhibited a 5-fold increase in DNA fragmentation levels, compared to the same cells on day 3. In contrast, cells transfected with a non-specific scramble siRNA, and mock-transfected cells, maintained relatively low sensitivity to apoptosis, and exhibited only a 1.5-fold and 1.6-fold increase in DNA fragmentation, respectively, when compared to their levels on day 3. When measuring apoptosis using the Death Detection ELISA the effect of siRNA against p100/p52 on PEL cell apoptosis was more obvious after approximately 9 days.

We also determined the effects of p100/p52 silencing on the viability of PEL cells by trypan blue exclusion. Figure 3.7D shows that knockdown of endogenous p100 and p52 by siRNA led to a considerable reduction in the viability of PEL cells, with only 53% of cells transfected with the p100/p52 siRNA remaining viable on day 12 of the assay. In contrast, cells transfected with a non-specific scramble siRNA, and mock-transfected cells, remained largely viable, with as much as 85% and 90% of cells respectively, excluding the trypan blue dye on day 12 of the assay. In this study we have demonstrated that the inhibition of endogenous p100 and p52 results in reduced viability, and the induction of apoptosis in PEL cells. Our findings suggest that the alternative pathway plays an important role in the survival and proliferation of KSHV-infected lymphoma cells.

3.3 Discussion

The processing of p100 and generation of p52 are essential to the development of the immune system. B cell maturation and the formation of secondary lymphoid structures do not occur in the absence of this pathway (Franzoso *et al.*, 1998; Caamano *et al.*, 1998), and a number of cellular receptors that stimulate this process have now been identified (Hacker and Karin, 2002). Two viruses, EBV and HTLV-1, encode proteins that modulate this pathway (Xiao *et al.*, 2001a; Saito *et al.*, 2003), and it is tempting to speculate that this has a specific role in allowing the viruses to regulate differentiation of infected cells to their own advantage.

In this chapter data have been presented suggesting that the vFLIP protein of KSHV also activates the alternative pathway of NF-κB. High-level expression of the precursor p100, as well as significant expression of the p52 subunit observed in KSHV-infected BC3 cells (Figure 3.1), indicated that the alternative NF-κB pathway is constitutively active in PEL cells. Expression of vFLIP by lentiviral-mediated gene transfer in Jurkat 3T8 cells, led to increased p100 levels and the accumulation of p52. This observation suggested that vFLIP not only activates the canonical NF-κB pathway, which leads to the upregulation of its transcriptional target p100 (Derudder *et al.*, 2003; Yilmaz *et al.*, 2003), but it also induces the processing of the p100 precursor to active p52, and hence activates the alternative NF-κB pathway in a haematopoietic cell line (Figure 3.1). To rule out the possibility that p52 accumulates constitutively as a direct result of the vFLIP-mediated increase in p100 expression levels, rather than through induced processing of p100, we performed a pulse-chase metabolic labelling study in 293T cells co-transfected with p100 and vFLIP. In the presence of vFLIP we observed active p100 processing and accumulation of radiolabelled p52 after 6 hours, which was not the case in the absence of vFLIP, indicating that this was a specific and direct result of vFLIP-induced activation of the alternative NF-κB pathway and the subsequent proteolytic processing of p100 (Figure 3.6). Analysis of nuclear and cytoplasmic cellular fractions revealed that in cells expressing vFLIP, there was significant translocation of p52 and RelB to the nucleus, in

contrast to the absence of any nuclear p52 and RelB from the nuclear fractions of untransduced cells, or cells transduced with a lentivector encoding only GFP (Figure 3.3). Mitogen stimulation of Jurkat cells transduced with the control GFP lentivector led to the activation of the canonical NF-κB pathway, as expected, and therefore upregulated the expression of p100. However, consistent with the inability of p100 to respond to cellular activation signals (Sun *et al.*, 1994), mitogen stimulation alone, failed to induce p100 processing to p52 and nuclear translocation of p52, which are indicative of alternative NF-κB activation (Figure, 3.4). This confirmed our hypothesis that the nuclear translocation of p52 and RelB observed in Jurkat cells expressing vFLIP is a specific event which is mediated by the activation of the alternative NF-κB pathway by vFLIP (Figure 3.4). These data are therefore consistent with the theory that vFLIP of KSHV can also activate the alternative NF-κB pathway, leading to p100 processing and generation of p52.

During the course of this study, Chaudhary and colleagues, published a report confirming the hypothesis we had been working on, which showed that vFLIP of KSHV activates the alternative NF-κB pathway (Matta and Chaudhary, 2004). Our respective studies have employed different approaches to arrive at the same conclusion, and therefore in Chapter 3 we have presented several findings which have not been published and are not included in the above mentioned report. These include the observation that vFLIP induces the nuclear translocation of p52 and RelB, and that vFLIP expression mediates the active processing of p100 and generation of p52. Together, our findings demonstrate that vFLIP of KSHV is the third viral protein capable of stimulating the processing of p100, along with Tax of HTLV-1 (Xiao *et al.*, 2001a) and LMP1 of EBV (Atkinson *et al.*, 2003). These observations not only demonstrate a novel function of the latently expressed vFLIP protein of KSHV, but also provide some insights into the general mechanism of p100 processing. Similar to the HTLV-1 oncoprotein Tax (Xiao *et al.*, 2001a), the alternative NF-κB activation through vFLIP depends on the catalytic activity of the IKKα subunit of the IKK complex, but is independent of the activity of IKKβ, and also seems to be able to bypass NIK when inducing the processing of 100 to p52 (Matta and Chaudhary, 2004). Moreover, vFLIP associates with

both p100 (Matta and Chaudhary, 2004) and the IKK complex, through its direct interaction with IKKγ (Chaudhary *et al.*, 1999; Field *et al.*, 2003). These interactions raised the intriguing possibility that vFLIP specifically recruits p100 to the IKK complex, triggering phosphorylation-dependent p100 processing. Indeed, vFLIP was shown to interact with endogenous p100 and IKKα, and this interaction enhanced the formation of a stable complex between p100 and IKKα (Matta and Chaudhary, 2004). Therefore, the association of vFLIP with p100, IKKα, and IKKγ may bridge an interaction between these proteins necessary for p100 phosphorylation and subsequent processing.

To further investigate the vFLIP-p100 complex we decided to define the domain of p100 required for its interaction with vFLIP. To this end we constructed deletion mutants of p100 lacking regions of the molecule that we speculated might be involved in this interaction (Figure 3.2). Specifically, we deleted a portion of the N terminus of p100, containing two α helices that have been shown to be important for Tax binding to p100 (Xiao *et al.*, 2001a), and a portion of the C terminus that contains the p100 death domain, which we believed might be instigating the association of p100 with vFLIP through homotypic interactions between itself and the Death Effector Domains (DEDs) of vFLIP. In section 3.2.2 of this chapter we showed that, unlike Tax of HTLV-1, vFLIP interacts with p100 via a region in its C-terminus that includes the Death Domain (DD), and truncation of p100 by removing the DD (amino acids 1-753) almost entirely abolishes the vFLIP-p100 interaction. In contrast to p100 mutants defective in Tax binding, which failed to respond to Tax-induced p100 processing (Xiao *et al.*, 2001a), the p100 ΔC mutant defective in vFLIP binding, was efficiently processed to p52 following induction by vFLIP expression. This might seem bizarre in light or recent findings that increased p100 processing is associated with the interaction of vFLIP with p100. However, we must take into account the fact that the region of p100 deleted in order to generate the p100 ΔC mutant used in this study, also contains the processing inhibitory domain (PID) of p100, which is located within the DD at the C-terminus. Deletion of the DD has been shown to be sufficient to trigger

constitutive processing of p100 (Xiao *et al.*, 2001b), and therefore our p100 ΔC mutant can be constitutively processed to p52 even in the absence of an interaction with vFLIP.

The observation that vFLIP associates with p100 via a region in p100 that contains a Death Domain, and the recently resolved structure of vFLIP MC159L from the *Molluscum contagiosum*, has allowed us to speculate on the composition of the vFLIP-p100-IKK multi-protein complex and the mechanism via which it mediates p100 processing. A recent study has demonstrated that although vFLIP has a TRAF-2 interacting motif, this is buried in the interface between the two DEDs of vFLIP, and it is not accessible for interaction with TRAF-2 or any other signalling proteins (Matta *et al.*, 2007). Therefore, it seems that vFLIP can bypass the function of upstream adapter proteins such as the TRAFs, to directly interact with IKK through its physical interaction with IKKγ (Chaudhary *et al.*, 1999; Field *et al.*, 2003). Moreover, structural analyses of the crystal structure of MC159 have revealed two distinctive surface features for tandem DED structures, presumably including those of vFLIP of KSHV, which might be important for protein interactions. They are a conserved hydrophobic patch on DED2, which is surface exposed and available for interactions, and a hydrogen-bonded charge triad on the surface of DED1 and DED2, which contributes to the highly charged features on one face of the structure and has been proposed to be a hot spot for protein-protein interactions (Yang *et al.*, 2005). Finally, the two DEDs of MC159 have been shown to rigidly associate with each other by folding to form a single compact dumbbell-shaped structure, and this association may reveal a mode for vFLIPs to mediate ternary complex interactions. Therefore, we propose a model whereby one of the DEDs of vFLIP of KSHV interacts with amino acids 150-272 of IKKγ (Field *et al.*, 2003), while the other DED domain associates by homotypic interactions with a region in p100 (amino acids 753-900) which contains the p100 DD (section 3.2.2). vFLIP therefore bridges an interaction between p100 and the IKK complex. Subsequently, the dumbbell-shaped folding of the two vFLIP DEDs recruits p100 to IKKα, which along with IKKβ is already associated with the N-terminus of IKKγ (Rothwarf *et al*, 1998; Mercurio *et al*, 1999; May *et al*, 2000; Poyet *et al*, 2000; Ye *et al*, 2000) via its

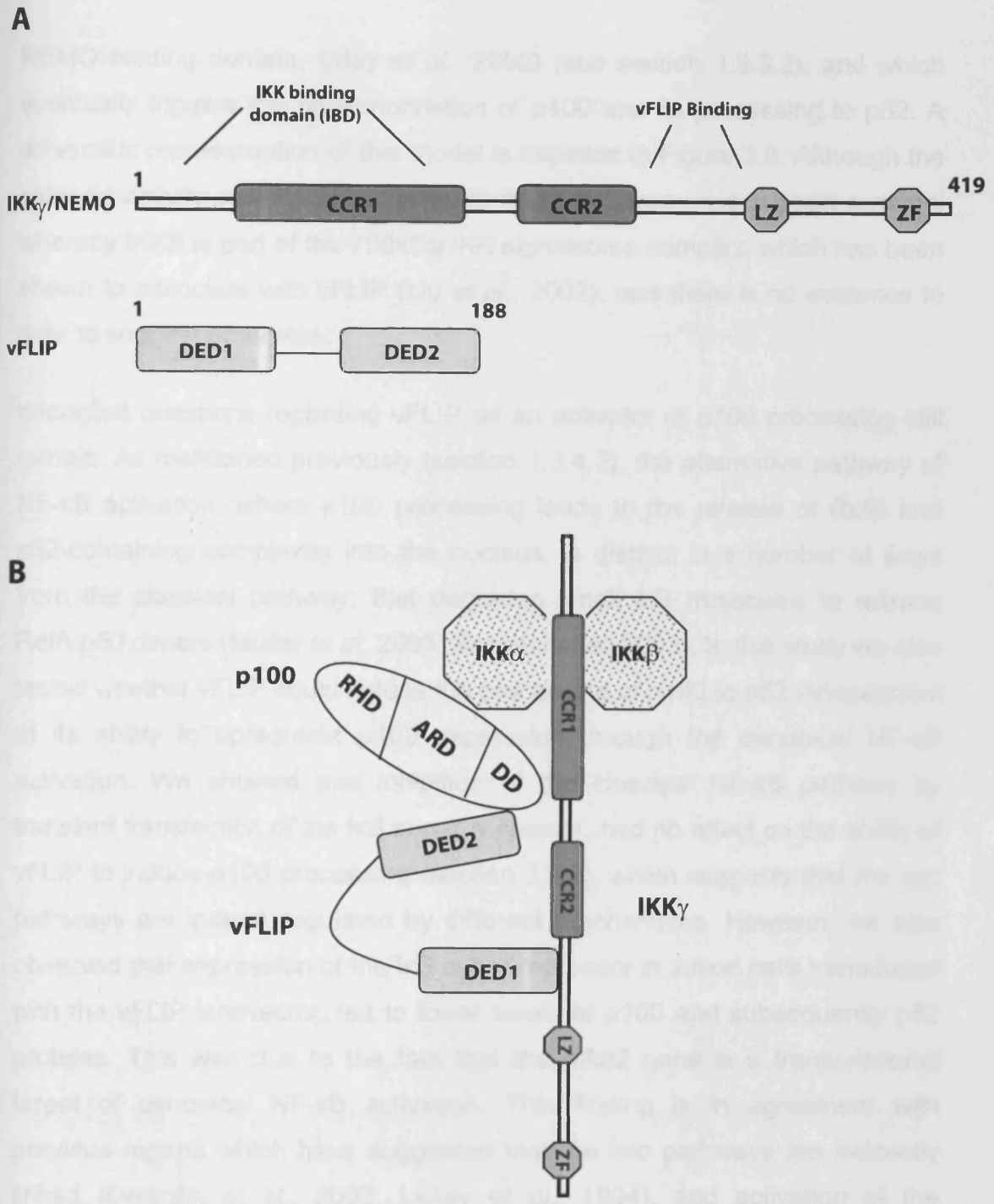

Figure 3.8 Model of the multi-protein complex between vFLIP, p100, and IKK

(A) Schematic diagrams of IKKγ/NEMO and vFLIP showing the principal structural motifs of both molecules. The IKK binding domain (region of association of IKKγ with IKKα and IKKβ and the region involved in vFLIP binding are highlighted on the IKKγ/NEMO diagram. The number of amino acids in each protein is shown on the right. **(B)** Hypothetical model of the the vFLIP-p100-IKK complex based on experimental evidence as described in section 3.3. It is proposed that vFLIP mediates an interaction between p100 and IKK via its two DEDs, whose folding brings p100 and the catalytic IKKα into close proximity, allowing IKKα to phosphorylate p100 and induce its processing to p52. A simplified version of p100 is shown with its major structural motifs for the purpose of presentation. CCR, coiled-coil region; LZ, leucine zipper; ZF, zinc finger; DED, death effector domain; RHD, Rel homology domain; ARD, ankyrin repeat domain; DD, death domain.

NEMO binding domain (May *et al.*, 2002) (see section 1.3.3.2), and which eventually triggers the phosphorylation of p100 and its processing to p52. A schematic representation of this model is depicted in Figure 3.8. Although the catalytic activity of IKKβ is dispensable for this process, we support a model whereby IKKβ is part of the 700kDa IKK signalsome complex, which has been shown to associate with vFLIP (Liu *et al.*, 2002), and there is no evidence to date to suggest otherwise.

Important questions regarding vFLIP as an activator of p100 processing still remain. As mentioned previously (section 1.3.4.3), the alternative pathway of NF-κB activation, where p100 processing leads to the release of RelB and p52-containing complexes into the nucleus, is distinct in a number of ways from the classical pathway, that degrades small IκB molecules to release RelA:p50 dimers (Muller *et al*, 2003; Saccani *et al*, 2003). In this study we also tested whether vFLIP could induce the processing of p100 to p52 independent of its ability to upregulate p100 expression through the canonical NF-κB activation. We showed that inhibition of the classical NF-κB pathway by transient transfection of the IκB super-repressor, had no effect on the ability of vFLIP to induce p100 processing (section 3.2.5), which suggests that the two pathways are indeed regulated by different mechanisms. However, we also observed that expression of the IκB super-repressor in Jurkat cells transduced with the vFLIP lentivector, led to lower levels of p100 and subsequently p52 proteins. This was due to the fact that the *nfkb2* gene is a transcriptional target of canonical NF-κB activation. This finding is in agreement with previous reports which have suggested that the two pathways are indirectly linked (Dejardin *et al.*, 2002; Liptay *et al.*, 1994), and activation of the canonical NF-κB pathway may influence the amplitude of the alternative pathway, through the transcription of *nfkb2*.

Deregulated p100 processing has been associated with a variety of T cell and B cell lymphomas (Demicco *et al.*, 2005; Ishikawa *et al.*, 1997; Kim *et al.*, 2000; Migliazza *et al.*, 1994; Neri *et al.*, 1991; Neri *et al.*, 1996; Neri *et al.*, 1995; Xiao *et al.*, 2001b). Therefore, we believe that that the alternative pathway plays a major role in the transforming ability of vFLIP. Consistent with

this hypothesis, siRNA-mediated knockdown of vFLIP expression results in a block in proliferation and the induction of apoptosis in PEL cells (Godfrey *et al.*, 2005; Guasparri *et al.*, 2004; Keller *et al.*, 2000; Matta and Chaudhary, 2004), which in one case was associated with the downregulation of p100 processing (Matta and Chaudhary, 2004). In this study we attempted to determine the relative contribution of the alternative NF-κB pathway in the survival and proliferation of PEL cells, by suppressing the expression of p52 using siRNA. In section 3.2.7, we showed that inhibition of p52 expression led to the induction of apoptosis in up to 60% of PEL cells, and a significant reduction of cell viability (section 3.2.7). These findings support our hypothesis that vFLIP-mediated p100 processing plays a key role in the proliferation and survival of KSHV-infected cells. However, the exact contribution of the alternative NF-κB pathway to the survival of PEL cells remains unclear, as it is possible that the vFLIP-mediated activation of the classical NF-κB pathway in these cells can counteract and compensate for some of the observed anti-proliferative effect. This hypothesis can probably explain the fact that, although the p100/p52 siRNA led to a decrease in p100 levels, this was not as significant as the decrease observed for p52 levels, suggesting that the vFLIP-mediated activation of the classical pathway might be maintaining the p100 expression levels. It would be interesting to examine the alternative pathway independently, by constructing a lentiviral vector that encodes the IκB super-repressor and expressing it in various cells of interest. This would prove invaluable in consolidating the existing data on vFLIP-mediated activation of the alternative NF-κB pathway, and might provide a clearer picture of the exact role of the alternative versus canonical pathway in vFLIP-mediated transformation.

Chapter 4

The Role of vFLIP in the Survival of Primary Endothelial Cells

4.1 Introduction

4.1.1 The Target Cell of KSHV

The biology of KS is poorly understood because the dominant cell type in KS lesions is not known (Regezi *et al.*, 1993). Moreover, the cellular origin of the spindle cells of KS lesions is poorly defined (Gallo, 1998; Ganem, 1997). While KS is considered to be a neoplasm of KSHV-infected lymphatic endothelium (Beckstead *et al.*, 1985; Jussila *et al.*, 1998; Weninger *et al.*, 1999), and KS spindle cells express endothelial cell markers, they also have features of other cell lineages, including smooth muscle cells, macrophages, and dendritic cells (Gallo, 1998; Kaaya *et al.*, 1995; Regezi *et al.*, 1993). Spindle cells ubiquitously express several lymphatic lineage-specific proteins, including VEGFR-3 and podoplanin (Beckstead *et al.*, 1985; Jussila *et al.*, 1998; Weninger *et al.*, 1999), but all spindle cells also express some blood endothelial cell (BEC) markers such as CD34 (Regezi *et al.*, 1993). Recently, three studies using gene expression microarrays of KSHV-infected endothelial, fibroblast and B cells showed that KSHV can induce transcriptional reprogramming of all these cell types (Hong *et al.*, 2004; Naranatt *et al.*, 2004; Wang *et al.*, 2004). By investigating a number of genes that discriminate between lymphatic endothelial cells (LECs) and blood endothelial cells (BECs), but are also present in the KS expression signature, one group found substantially more LEC markers, than BEC markers, overlapping with the KS expression signature (Wang *et al.*, 2004). Indeed, another group showed that infection of differentiated blood vascular endothelial cells with KSHV drove the cells to lymphatic reprogramming with induction of the main lymphatic lineage-specific genes, including *PROX1*, which play a major role in lymphatic development (Hong *et al.*, 2004). However, the finding that both LEC and BEC markers were present in the KS signature, indicated that KS spindle cells do not faithfully represent either cell type, implying that KSHV infection induces a transcriptional reprogramming of

both infected LECs and BECs, that causes them to move away from the uninfected populations and towards each other (Wang et al., 2004a). It seems that KSHV can infect both LECs and BECs *in vitro*, but LECs seem to be the favoured target of infection, since KSHV is not present in resident blood vessels (BECs) of KS lesions (Dupin *et al.*, 1999), despite the production of virions in such lesions (Orenstein *et al.*, 1997), and KS occurs most frequently at sites that are rich in LECs, such as skin, lymph nodes and mucosa, but not in organs without lymphatic vessels, like the brain. However, another hypothesis that has been addressed is that KSHV may infect endothelial-cell precursors and drive these cells towards a lymphatic endothelial-cell phenotype (Boshoff and Weiss, 2002; Jussila *et al.*, 1998).

Several cytokines and their cognate receptors were found to be upregulated in the KS expression signature, indicative of autocrine growth loops. Angiopoietin-2 (ANG2), which is involved in lymphangiogenesis (Gale *et al.*, 2002)(discussed below), was highly upregulated in KSHV-infected LECs and BECs (Wang et al., 2004a), as was VEGFR-3, a receptor for VEGF-D that upon ligation stimulates lymphangiogenesis (Stacker *et al.*, 2002). Other studies have shown that within minutes of target cell infection, KSHV can activate the phosphatidylinositol 3'-kinase (PI3K), protein kinase C-ζ (PKC- ζ), and mitogen-activated protein/ERK kinase signalling cascades (Naranatt *et al.*, 2003). Together these data give us an insight into the early modulation events during KSHV infection.

Microvascular endothelial cells (MVECs) represent a mixed population of LECs and BECs (Makinen *et al.*, 2001) and have been shown to be the most susceptible to KSHV infection, when compared to mesenchymal stem cells, smooth muscle cells, and fibroblasts (Wang et al., 2004a). KSHV is the first human pathogen capable of reprogramming endothelial cell transcriptomes and *in vitro*, it can infect both micro- and macrovascular endothelial cells, making them very useful for studying the role of KSHV in the pathogenesis of KS (Ciufo *et al.*, 2001; Flore *et al.*, 1998; Moses *et al.*, 1999).

4.1.2 Regulation of Endothelial Cell Survival

Survival of endothelial cells is critical for cellular processes such as angiogenesis. The process of angiogenesis plays an important role in many physiological (e.g. embryonic development) and pathological (e.g. tumour growth and metastasis) conditions. Inhibition of endothelial cell (EC) apoptosis, providing EC survival, is thought to be an essential mechanism during angiogenesis. Many angiogenic growth factors inhibit EC apoptosis. In addition, the adhesion of ECs to the extracellular matrix or intercellular adhesion promotes EC survival.

4.1.2.1 Angiogenic Growth Factors and Endothelial Cell survival

EC survival is maintained by proangiogenic growth factors and by contact to the extracellular matrix. Several endothelial growth factors, such as vascular endothelial growth factor (VEGF), basic fibroblast growth factor (bFGF), hepatocyte growth factor (HGF), and angiopoietin-1 are known to provide EC survival by inhibiting EC apoptosis. **Vascular endothelial growth factor** (VEGF) has been shown to be a potent mediator of angiogenesis that functions as a survival factor for ECs (Alon *et al.*, 1995). It exerts its angiogenic effects by binding to the VEGF-receptor tyrosine kinases VEGF-receptor 1 (VEGFR1) and VEGF-receptor 2 (VEGFR2). VEGF has been shown to induce EC migration and proliferation (Neufeld *et al.*, 1999). An important angiogenic and vasculoprotective property of VEGF is the promotion of EC survival by inhibiting apoptosis (Spyridopoulos *et al.*, 1997). The inhibition of VEGF leads to apoptosis of ECs and vessel regression in several models of tumour angiogenesis (Benjamin and Keshet, 1997; Jain *et al.*, 1998; Shaheen *et al.*, 1999). However, developmental investigations have indicated the VEGF-mediated survival is only required until the vessel comes in contact with pericytes, at which time the mature vessel is less sensitive to alterations of the VEGF level for proliferation or regression (Benjamin *et al.*, 1999).

VEGF inhibits EC apoptosis that is induced by growth factor deprivation (Fujio and Walsh, 1999; Gerber *et al.*, 1998) and tumour necrosis factor-(TNF- α)

stimulation (Spyridopoulos *et al.*, 1997). VEGF has been shown to induce the expression of antiapoptotic proteins such as Bcl-2, A1 (Gerber et al., 1998; Nor *et al.*, 1999), survivin (Tran *et al.*, 2002), and XIAP (Tran *et al.*, 1999). Up-regulation of Bcl-2 in microvascular ECs (MVECs) enhances intratumoural angiogenesis and accelerates tumour growth (Nor *et al.*, 2001). Although these results were initially attributed to Bcl-2-mediated endothelial cell survival, it was later shown that conditioned medium from Bcl-2-transduced human dermal microvascular ECs (HDMVECs) was sufficient to induce potent neovascularisation (Karl *et al.*, 2005). Gene expression arrays revealed that the expression of the proangiogenic chemokines IL-8 (CXCL8) and growth-related oncogene-alpha (CXCL1) was significantly higher in HDMVECs exposed to VEGF or transduced with Bcl-2, than in controls (Karl *et al.*, 2005). Moreover, NF-kB was also found to be highly activated in the same cells. These results demonstrated that VEGF induces expression of Bcl-2, which in turn acts in a proangiogenic signalling pathway through NF-kB and CXC chemokines (Karl *et al.*, 2005). In fact, NF-kB might prove to be a key molecule produced by transformed cells, which stimulates the secretion of different cytokines such as VEGF, IL-6, IL-8, and monocyte chemotactic protein-1 (MCP-1) (Lee *et al.*, 2003b; Stifter, 2006). MCP-1 secretion is reduced by 60% when blocking NF-kB production, which in turn leads to reduced production of IL-6 and VEGF, since MCP-1 upregulates VEGF and IL-6 (Stifter, 2006). Therefore, angiogenesis can potentially induce itself through NF-kB activation.

Furthermore, VEGF utilizes a PI3-kinase/Akt signalling pathway to protect ECs from apoptotic death (Fujio and Walsh, 1999). Inhibition of PI3K or a dominant-negative Akt mutant can abolish the antiapoptotic effect of VEGF on ECs (Fujio and Walsh, 1999). Interestingly, the survival effect of VEGF is dependent on the binding of VEGF on the VEGFR2 but not VEGFR1 (Gerber *et al.*, 1998). Therefore, VEGFR2 and the PI3K/Akt signal transduction pathway are crucial in the promotion of EC survival induced by VEGF. The downstream effector pathways mediating the antiapoptotic effect include Akt-dependent activation of the endothelial nitric oxide synthase (NOS), leading to enhanced synthesis of NO, which promotes EC survival by inhibiting the

cysteine protease activity of caspases (Dimmeler *et al.*, 1999). The PI3K/Akt pathway also upregulates the transcription of survivin (Papapetropoulos *et al.*, 2000), can inhibit p38 MAPK-dependent apoptosis (Gratton *et al.*, 2001), and stimulates the phosphorylation and thus inactivation of proapoptotic proteins such as Bad (Khwaja, 1999). Moreover, PI3K/Akt signalling can reverse EC sensitivity to Fas-mediated apoptosis via promoting the expression of the caspase-8 inhibitor FLIP (Suhara *et al.*, 2001). VEGF can also induce the activation of the MAPK/ERK pathway and inhibit the stress-activated protein kinase/c-Jun amino-terminal kinase pathway (JNK) to exert its antiapoptotic effect (Gupta *et al.*, 1999). More recently, VEGF was shown to activate the Raf-1 serine/threonine kinase via Src kinase, which resulted in the phosphorylation of Raf-1 and MEK-1-dependent protection of human endothelial cells from DR-mediated apoptosis (Alavi *et al.*, 2003).

Angiopoietin-1/Tie2 is another endothelial-specific growth factor/growth factor receptor system involved in angiogenesis. Angiopoietin-1 (Ang-1) and -2 (Ang-2) are the ligands for the Tie2 receptor tyrosine kinase (Davis *et al.*, 1996; Maisonpierre *et al.*, 1997). Angiopoietin-1 stimulation has no mitogenic effect on ECs. Angiopoietin-1 and the Tie2 receptor are important for the later steps of the angiogenic process, the remodelling, and the maturation of the newly formed vascular system, and have a stabilizing effect on capillaries (Suri *et al.*, 1996). In vitro, angiopoietin-1 activation of the Tie2 receptor inhibits EC apoptosis (Kwak *et al.*, 1999). This survival effect is dependent on the activation of PI3K and Akt (Fujikawa *et al.*, 1999). Angiopoietin-1 induces PI3K-dependent activation of Akt and upregulates the antiapoptotic protein survivin (Papapetropoulos *et al.*, 2000), whereas it has no effect on the transcription of Bcl-2. Another possible mechanism for the survival effect is the recruitment of pericytes (Jain, 2003). Angiopoietin-2 does not lead to the activation of the Tie2 receptor and it is believed to be a naturally occurring antagonist of the Tie2 receptor (Maisonpierre *et al.*, 1997). However, it has since been demonstrated that a high concentration of angiopoietin-2 can also act as an apoptosis survival factor for endothelial cells during serum deprivation-mediated apoptosis, through the activation of the Tie2 receptor and subsequent PI3K/Akt signal transduction (Kim *et al.*, 2000). Several lines

of evidence suggest that angiopoietin-2, in combination with VEGF, leads to sprouting angiogenesis, while angiopoietin-2 in the absence of growth-promoting signals renders vessels susceptible to regression (Carmeliet, 2003; Hanahan, 1997; Holash *et al.*, 1999; Jain, 2003).

Basic fibroblast growth factor (bFGF) is an important angiogenic factor, which inhibits apoptosis induced by radiation (Fuks *et al.*, 1994) or growth factor deprivation (Karsan *et al.*, 1997). bFGF also upregulates the expression of the antiapoptotic proteins Bcl-2 and surviving (O'Connor *et al.*, 2000), and activates the protein kinase Akt in ECs (Carmeliet et al., 1999).

Hepatocyte growth factor (HGF) is a potent mesenchyme-derived mitogen for a number of cell types, including epithelial and endothelial cells (Rosen *et al.*, 1997). HGF is also a known angiogenesis factor by its ability to promote endothelial cell growth, survival, and migration both *in vitro* and *in vivo* (Bussolino *et al.*, 1992; Grant *et al.*, 1993). Moreover, HGF has been shown to induce the production of VEGF by a variety of cells (Gille *et al.*, 1998; Van Belle *et al.*, 1998; Wojta *et al.*, 1999), and has been correlated with higher levels of IL-8 and VEGF in tumour cells from head and neck squamous cell carcinoma (HNSCC). HGF-induced IL-8 and VEGF production was associated with the phosphorylation of its high-affinity receptor c-Met, and the subsequent activation of MEK and PI3K pathways (Dong *et al.*, 2001). HGF can act in synergy with VEGF to promote endothelial cell survival and tubulogenesis *in vitro*, and enhance angiogenesis *in vivo*, and these morphogenic changes are accompanied by the synergistic induction of the anti-apoptotic genes Bcl-2 and A1(Xin *et al.*, 2001). Moreover, HGF has been shown to provide protection against detachment-induced apoptosis (anoikis) in HNSCC cells, and this effect is dependent on Erk and Akt signalling, but independent of NF-κB (Zeng *et al.*, 2002).

Finally, **TNF-α**, a macrophage/monocyte-derived polypeptide, modulates the expression of various genes in vascular ECs and induces angiogenesis. This effect seems to involve NF-kB and the up-regulation of IL-8, VEGF, bFGF, and their respective receptors (Yoshida *et al.*, 1997). Moreover, TNF-α and IL-

1 can also activate the PI3K/Akt pathway to inhibit apoptosis, and this effect is independent of the TNF-α-induced antiapoptotic effect of NF-kB (Madge and Pober, 2000). Taken together, many growth factors are involved in the initiation and promotion of angiogenesis. A common property of these growth factors is the induction of EC survival. The inhibition of EC apoptosis by the distinct growth factors is dependent on PI3K/Akt signalling but may also include the upregulation of apoptosis inhibiting proteins such as survivin and Bcl-2.

4.1.2.2 Adhesion and Endothelial Cell Survival

Adhesion of ECs to the extracellular matrix and intercellular adhesion are essential for EC survival and angiogenesis. **Cell-matrix interactions** and EC migration are both mediated by integrins (Stromblad and Cheresh, 1996). In the absence of any extracellular matrix (ECM) interactions, ECs rapidly undergo apoptosis (Meredith *et al.*, 1993), a phenomenon called anoikis. The interaction of cells via integrins with the ECM provides a potent survival signal. The vitronectin receptors $\alpha_v\beta_3$- and $\alpha_v\beta_5$ are expressed during in vivo angiogenesis and are markers of the angiogenic phenotype of ECs (Brooks *et al.*, 1994).

Various signalling cascades have been considered to mediate the antiapoptotic effect of integrins. Regarding the intracellular signalling mediated by the $\alpha_v\beta_3$-integrin, it has been demonstrated that signalling from the $\alpha_v\beta_3$-integrin leads to inhibition of p53 transcriptional activity, decreased expression of the cell cycle inhibitor $p21^{WAF1/CIP1}$, and suppression of the bax cell death pathway in endothelial cells, thereby promoting EC survival (Stromblad *et al.*, 1996). Moreover, attachment of ECs on vitronectin or osteopontin (ECM proteins that are known $\alpha_v\beta_3$-integrin ligands) induces NF-kB activity. This $\alpha_v\beta_3$-integrin-induced NF-kB activation is mediated by the small GTP-binding protein Ras and the tyrosine kinase Src, but not by MAPK or PI3K (Scatena *et al.*, 1998). The $\alpha_v\beta_3$-integrin-mediated EC survival effect depends on the osteopontin-induced, NF-kB-dependent gene, osteoprotegerin (Malyankar *et al.*, 2000). Inhibition of the $\alpha_v\beta_3$-integrin, and the subsequent antiangiogenic and apoptotic effect on ECs, has been shown

to be associated with an increase in the intracellular ceramide (a proapoptotic lipid second-messenger) level, which may induce apoptosis (Erdreich-Epstein *et al.*, 2005). Furthermore, various studies suggest an essential role for the PI3K/Akt pathway in the antiapoptotic signalling promoted by integrin-cell matrix interactions. It has been demonstrated that adhesion to the ECM induces PI3K/Akt, and overexpression of a constitutively active PI3K or Akt mutant can inhibit detachment-induced apoptosis of ECs (anoikis) (Khwaja *et al.*, 1997; Wary *et al.*, 1996). The association of other specific integrins such as the $\alpha_5\beta_1$-, the $\alpha_v\beta_3$-, and the $\alpha_1\beta_1$-integrin with the adaptor protein Shc can regulate cell survival and cell cycle progression via the Ras/MAPK/ERK pathway (Wary *et al.*, 1996).

Interestingly, integrin signalling can also affect and influence growth factor signalling. Angiopoietin-1 (Fujikawa *et al.*, 1999), bFGF (Fujikawa *et al.*, 1999), or VEGF (Fujio and Walsh, 1999) fail to prevent EC apoptosis (anoikis) in suspension culture. However, it has been demonstrated that during EC stimulation with VEGF, the $\alpha_v\beta_3$-integrin co-immunoprecipitates with the VEGFR2, and that anti -$\alpha_v\beta_3$-antibodies inhibit the VEGF-induced phosphorylation of VEGFR2 and the subsequent activation of PI3K (Soldi *et al.*, 1999). Consequently, this suggests that integrin ligation may enhance the antiapoptotic signalling mediated by VEGF. In conclusion, there seems to be a functional cross-talk between integrin- and growth factor-mediated signalling, which may act synergistically to promote EC survival.

4.1.2.3 Cell-Cell Adhesion and Endothelial Cell Survival

Recent evidence suggests that not only cell matrix contacts but also cell-cell contacts between ECs may support cell survival. VE-cadherin, an adhesive protein contained at endothelial adherens junctions that mediates inter-endothelial cell adhesion, has been shown to be essential for the VEGF-induced antiapoptotic effect (Carmeliet *et al.*, 1999). Inactivation of the VE-cadherin gene can abolish the VEGF-induced activation of the PI3K/Akt pathway, upregulation of Bcl-2, reduction of p53 and p21 expression, and the subsequent prevention of EC apoptosis (Carmeliet *et al.*, 1999). Therefore, VE-cadherin signalling is essential for the survival signalling mediated by

VEGF. Taken together, cell matrix and cell-cell interactions provide EC survival by inhibiting EC apoptosis that acts synergistically to growth factors. This survival signalling is essential for the promotion of angiogenesis.

4.1.3 KSHV and Endothelial Cell survival

Previous reports have demonstrated that KSHV preferentially infects B lymphocytes (Ambroziak *et al.*, 1995), but a recent study from Pellet *et al.* demonstrated that 50% of patients had circulating endothelial cells infected with KSHV (Pellet *et al.*, 2006). This is directly linked with the pathogenesis of KS since it is a complex angiogenic tumour characterised by both the presence of ectatic vessels and the proliferation of spindle cells, which may originate from endothelial cells (described in section 4.1.1). KSHV-infection of endothelial cells *in vitro* leads to transcriptional reprogramming of these cells (Hong *et al.*, 2004; Naranatt *et al.*, 2004; Wang *et al.*, 2004). Gene-expression microarray profiling of KSHV-infected endothelial cells, showed that a considerable number of the genes found upregulated in the KSHV expression signature encode growth factors, their receptors, and cytokines (Di Bartolo and Cesarman, 2004). Array data has demonstrated that the expression of numerous cytokines necessary for endothelial cell survival is induced by KSHV, including Ang-2, MCP-1, and VEGFC (Wang *et al.*, 2004). More recently, it was shown that KSHV infection of primary human umbilical vein endothelial cells (HUVECs) induced the expression of Ang-2, by activating the Ang-2 promoter via the AP-1 and Ets1 transcriptional factors, which were mediated by the ERK, JNK, and p38-MAPK pathways (Ye *et al.*, 2007). This release of Ang-2 was subsequently required for KSHV-induced angiogenesis *in vivo*, highlighting the importance of Ang-2 in KS angiogenesis as well (Ye *et al.*, 2007). Moreover, latent KSHV infection of HUVECs has been shown to result in the upregulation of several chemokines, such as MCP-1, NAP 2, and RANTES, as well as CXCL16 (Xu and Ganem, 2007), which has been associated with endothelial cell chemotaxis, growth, and proliferation (Zhuge *et al.*, 2005). A model of acute productive infection in endothelial cells, demonstrated that KSHV infection led to potent activation of the NF-κB pathway, which resulted in the production of high levels of MCP-1 and was

accompanied by virus-induced capillary-like structure formation during early stages of infection (Caselli *et al.*, 2007).

Several viral genes encoded by KSHV have been associated with cytokine release in KS lesions. vGPCR, through activating NF-κB, induces the expression of pro-angiogenic factors (VEGF, bFGF), proinflammatory cytokines (IL-1β, IL-6, IL-8, TNFα), and adhesion molecules (VCAM, ICAM-1, E-selectin) (Couty *et al.*, 2001; Montaner *et al.*, 2004; Pati *et al.*, 2001; Schwarz and Murphy, 2001). Moreover, vGPCR and vIL-6 were recently shown to cause upregulation of Ang-2 in LECs infected with KSHV (Vart *et al.*, 2007). Furthermore, lentiviral transduction of mature and progenitor ECs with a vector encoding the viral CC chemokine vMIP-II (viral macrophage inflammatory protein-II), demonstrated that vMIP-II expression can be angiogenic, and results in the upregulation of the expression of multiple proangiogenic factors, including VEGF, kinase insert domain receptor, neurophilin 2, carcinoembryonic antigen-related cell adhesion molecule 1, IL-1α, fibronectin, and integrins α3, α4, and α5 (Cherqui *et al.*, 2007).

Interestingly, the major function of vFLIP of KSHV is the activation of the NF-κB pathway (discussed in section 1.4.5). Therefore, the majority of biological effects of vFLIP-mediated NF-κB activation can be linked to endothelial cell survival, since angiogenesis can potentially induce itself through NF-kB activation (Stifter, 2006). Examples include the vFLIP-mediated, NF-κB-dependent constitutive upregulation of IL-8 in HUVECs (Sun *et al.*, 2006), which has been shown to stimulate angiogenesis and tumour growth (Koch *et al.*, 1992; Sparmann and Bar-Sagi, 2004), the induction of CXCL16 in KSHV-infected HUVECs, which was attributed to vFLIP and its ability to activate NF-κB (Xu and Ganem, 2007), and the fact that the vFLIP was responsible for the spindling phenotype observed in KSHV-infected primary ECs, as well as the production of proinflammatory cytokine IL-6 and the proangiogenic cytokine IL-8 (Grossmann *et al.*, 2006). Moreover, NF-kB regulates a number of anti-apoptotic genes, which include members of the anti-apoptotic Bcl-2 family, the IAP family, and cFLIP (Burstein and Duckett, 2003), and have been shown to promote EC survival (discussed in section 4.1.2.1). It seems therefore, that

vFLIP might be a key mediator of the transcriptional reprogramming observed in KSHV-infected ECs, and this effect potentially plays a major role in KS pathogenesis by promoting the survival and proliferation of KSHV-infected endothelial cells.

4.1.4 Aims

In this chapter we describe our studies on the effects of vFLIP expression on dermal microvascular endothelial cells (dMVECs), in order to gain some insight into its individual role in their survival and proliferation. We decided to use primary dermal microvascular endothelial cells (dMVECs), because we wanted to model the function of vFLIP in cells that were as close as possible to those targeted naturally for infection by KSHV. We therefore expressed vFLIP in dMVECs using lentiviral gene transfer and assessed its ability to activate NF-κB in these cells. Following this, we investigated whether vFLIP expression was capable of protecting these cells from detachment-induced apoptosis, and tried to determine the mechanism by which it does so.

4.2 Results

4.2.1 MVECs are efficiently transduced with the vFLIP_eGFP lentivector and express vFLIP and GFP *in vitro*

Figure 4.1 shows the map of the dual promoter vector, into which vFLIP was subcloned. vFLIP was inserted under the stronger SFFV promoter, and emerald GFP was expressed from the weaker human polyubiquitin C (Ub) promoter, since GFP was only used as a marker for transduction. We knew from the work of fellow lab members that the Ub promoter works well in primary cells, in particular murine dendritic cells, although GFP fluorescences can be up to one log lower, when compared to GFP expression driven by SFFV, as seen by the mean fluorescence intensities (MFIs) in Figure 4.2A. vFLIP was amplified (567bp) by PCR from the pcDNA3.1 vector plasmid, using primers designed to introduce a *BamHI* and a *NotI* site at the 5' and 3' ends respectively. The vFLIP dual promoter vector is referred to as the vFLIP_eGFP vector and was used to transduce MVECs for all the experiments described in Chapter 4. The GFP vector was used as a control in most experiments to test whether any of the activation effects seen could be due to the vector itself or GFP expression.

We decided to test the transduction efficiency and expression of the constructs from the dual promoter lentivector in MVECs. Cells were transduced at an MOI of 30 (instead of an MOI of 10 for Jurkat 3T8 or 293T cells, as primary cells are more resistant to transduction) on day 0, and were cultured for 48 hours before assaying for GFP expression by FACScan analysis and confocal microscopy, as we seem achieve strongest transgene expression 2 days post-infection. For FACS analysis, live cells were gated to exclude cell debris and transduction efficiency was measured by GFP expression. Figure 4.2A shows that MVECs were efficiently transduced by lentivectors, with 76% of cells in the cultures staining positive for GFP using the GFP lentivector, and 53% of cells expressing GFP using the vFLIP_eGFP lentivector. Cells were also analysed for GFP expression using a confocal microscope and Figure 4.2B shows that MVECs are

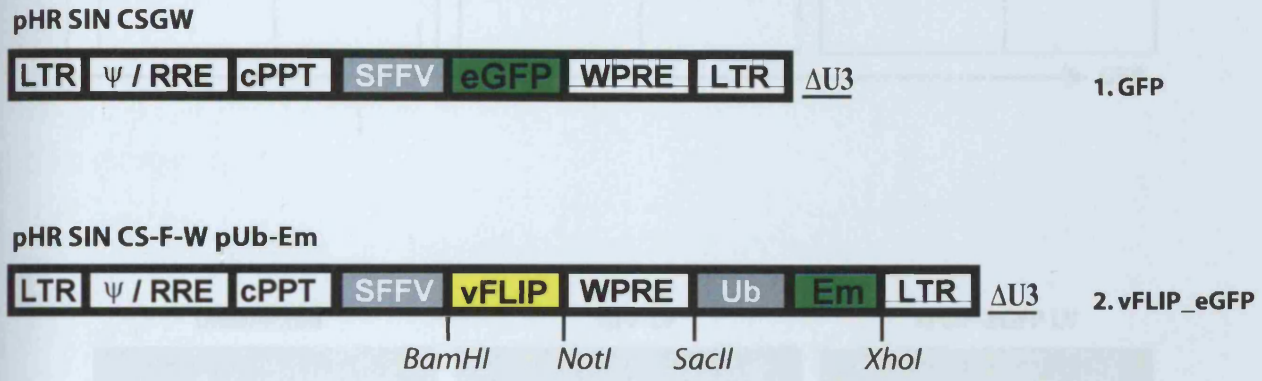

Figure 4.1 A dual promoter lentiviral vector for the expression vFLIP and the detection of transduction

The vFLIP_eGFP vector (2.), used to activate NF-κB, expresses vFLIP (567 bp) and emerald GFP (Em, 780 bp). The original GFP vector (1.) was used as a control. Unique restriction sites are shown. LTR, long terminal repeat; ψ, packaging signal; RRE, rev responsive element; cPPT, central polypurine tract; SFFV, spleen focus forming virus promoter; WPRE, wood chuck post transcriptional regulatory element; Ub, ubiquitin promoter; ΔU3, deletion in U3 region (SIN vector).

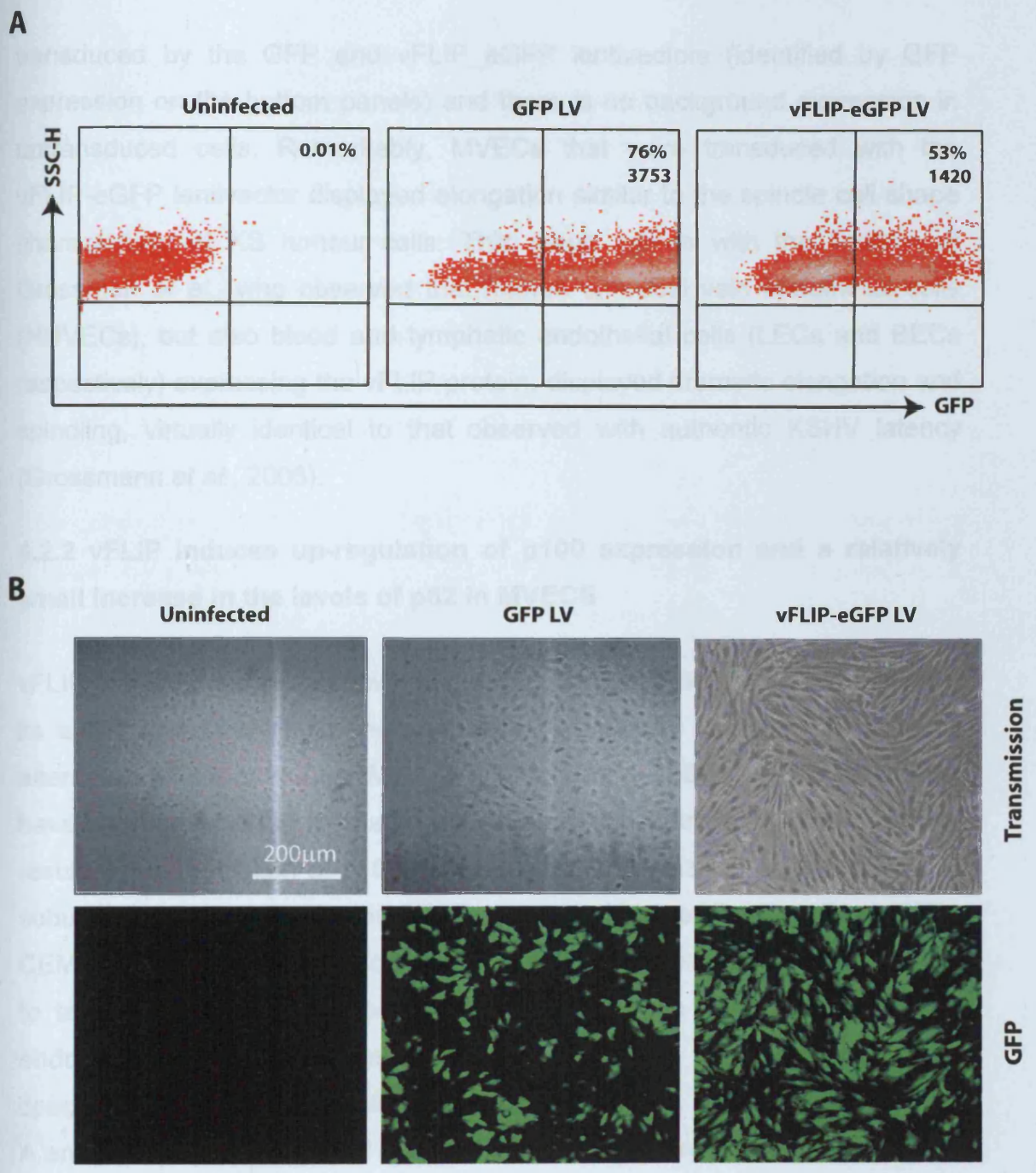

Figure 4.2 (A, B) Efficient *in vitro* transduction of MVECs and GFP expression using the vFLIP_eGFP and GFP lentiviral vectors

Human dermal microvascular endothelial cells (dMVECs) were either not transduced, or transduced with a lentiviral vector encoding GFP alone, or vFLIP and emerald GFP at an MOI=30. 48 hours post transduction, the transduction efficiency was assessed by FACScan analysis and confocal microscopy for GFP expression. **(A)** Live cells were gated (not shown) and expression of GFP was analysed by FACS analysis 48h post transduction. The top right quadrant in each plot shows transduced MVECs expressing GFP (10, 000 events recorded per sample). The mean percentage of transduced MVECs was 55% for vFLIP_eGFP (standard deviation, S.D. = 5.06) and 66.3% for GFP (S.D. = 4.33), out of three experiments. Values below the % transduced cells represent the mean fluorescence intensity (MFI). **(B)** Transduction efficiency and GFP expression were also measured using a BioRad confocal microscope 48h post-transduction.

transduced by the GFP and vFLIP_eGFP lentivectors (identified by GFP expression on the bottom panels) and there is no background expression in untransduced cells. Remarkably, MVECs that were transduced with the vFLIP-eGFP lentivector displayed elongation similar to the spindle cell shape characteristic of KS tumour cells. This result agrees with the findings of Grossman *et al.*, who observed that human umbilical vein endothelial cells (HUVECs), but also blood and lymphatic endothelial cells (LECs and BECs respectively) expressing the vFLIP protein, displayed dramatic elongation and spindling, virtually identical to that observed with authentic KSHV latency (Grossmann *et al.*, 2006).

4.2.2 vFLIP induces up-regulation of p100 expression and a relatively small increase in the levels of p52 in MVECS

vFLIP of KSHV has been shown to be unique among the viral FLIP proteins in its ability to activate both the canonical (Chaudhary et al., 1999) and the alternative NF-κB pathways (Matta and Chaudhary, 2004). Our lab and others have shown that vFLIP-mediated activation of the alternative NF-κB pathway results in up-regulation of p100 expression and generation of the active p52 subunit in multiple solid tumour and haematopoietic cell lines, such as HeLa, CEM, Jurkat 3T8, and 293T cells (Matta and Chaudhary, 2004). We decided to test whether vFLIP expression in primary human dermal microvascular endothelial cells (MVECs) also leads to activation of NF-κB, and more specifically activation of the alternative NF-κB pathway. As shown in figure 4.3 A and B, expression of vFLIP in MVECs led to higher levels of p100 precursor expression and generation of the p52 subunit. The up-regulation of p100 indicates activation of the classical NF-κB pathway by vFLIP in MVECS, as p100 is an NF-κB responsive gene (Dejardin *et al.*, 2002), while the accumulation of p52 suggests that the p100 precursor is being processed into p52, either by the activity of the alternative NF-κB pathway, or due to accumulation of excessive p100 which results in some constitutive processing into p52. Interestingly, the p100 and p52 levels observed in untransduced MVECs were quite high, as compared to those seen in uninfected Jurkats routinely used in such experiments (Figure 3.1, Chapter 3). This leads us to

believe that NF-κB, through the alternative pathway, is already activated in these cells, possibly in response to an external stimulus (e.g. growth factor) present in the growth medium, or due to increased constitutive p100 processing in these cells. Moreover, we observed that transduction with the control lentivector that expresses only GFP resulted in higher p100 expression levels (Figure 4.3A), when compared to uninfected cells. This means that transduction of the cells, or the vector itself, or GFP expression from the vector, can activate NF-κB to some degree in MVECs, although not to the extent of cells expressing vFLIP.

The cells were infected at an MOI of 30 using the vFLIP_eGFP lentivector (Figure 4.1), which resulted in 53% of MVECs being GFP positive after FACScan analysis for transduction efficiency. This vector, with two independent internal promoters driving expression of the transgenes, has been shown to induce high-level expression of multiple transgenes (Yu et al., 2003), and has been found by members of our lab to be more efficient at infecting primary cells (e.g. dendritic cells). Moreover, analysis of these cells by Western Blotting for vFLIP protein levels showed that a significant amount of vFLIP was being expressed in the cytoplasm of these cells (Figure 4.3 A, middle panel). In contrast, transduction of MVECs at an MOI of 30 using the vFLIP_IRES_eGFP lentivector, which can express both vFLIP and eGFP from the internal ribosome entry site (IRES) of encephalomyocarditis virus (EMCV) under the control of the human cytomegalovirus (hCMV) immediate early promoter, and was used for all the transductions of cell lines in Chapter 3 (Figure 2.1), resulted in only 24% of cells expressing GFP by FACScan analysis (data not shown). However, when cell lysates from the vFLIP_IRES_eGFP-transduced MVECs were analysed for NF-κB activation, we observed up-regulation of p100 expression and generation of p52 to similar levels as those seen in vFLIP_eGFP-transduced MVECs (figure 4.3B upper panel), although the expression levels of vFLIP were lower using this vector (Figure 4.3B middle panel). Therefore, we were able to confirm our observations about vFLIP-mediated p100 upregulation using two different lentivectors, and the two results were consistent irrespective of vFLIP expression levels.

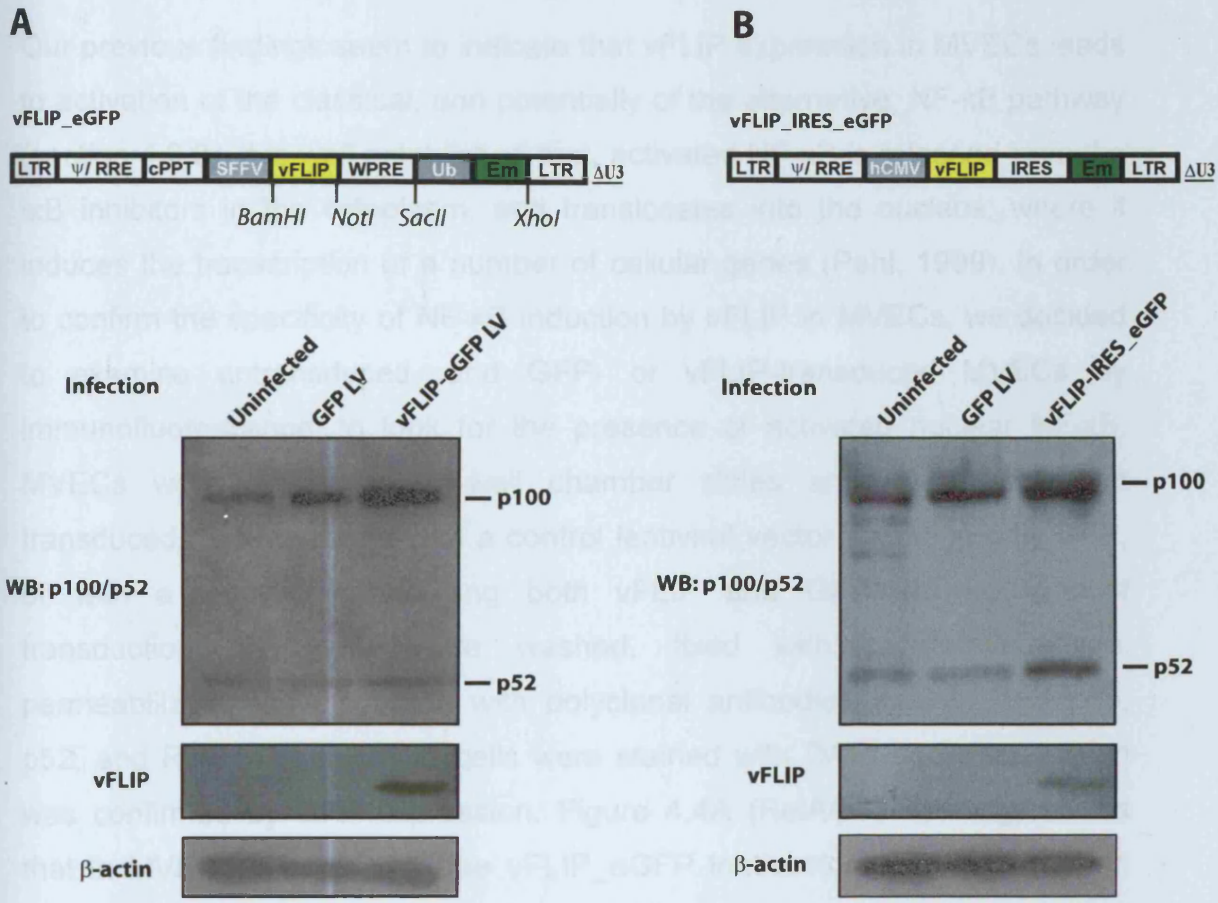

Figure 4.3 (A, B) Stable vFLIP expression from two different lentivectors induces upregulation of p100 expression and generation of more p52 in MVECs

Human dermal microvascular endothelial cells (dMVECs) were either not transduced, or transduced with a lentiviral vector encoding GFP alone, or vFLIP and GFP. 40μg of cell lysate, prepared from $5x10^6$ MVECs lysed in RIPA buffer 48 hours post transduction, was analysed on a 12% SDS-polyacrylamide gel by immunoblotting using a mouse monoclonal anti-p100/p52 antibody for endogenous p100/p52 expression, and the anti-vFLIP antibody to check the expression level of vFLIP. β-actin levels were visualised to ensure equal protein loading. **(A)** MVECs were transduced at an MOI of 30 with the double promoter lentivector vFLIP_eGFP for stable vFLIP expression. Transduction efficiency of the lentivector was measured by FACScan analysis of cells expressing GFP. 54% and 63% of cells expressed GFP after infection with the vFLIP_eGFP and GFP lentivirus respectively. **(B)** MVECs were transduced at an MOI of 30 with a lentivector that expresses both vFLIP and eGFP from an IRES, vFLIP_IRES_eGFP. Transduction efficiency of the lentivector was measured by FACScan analysis of cells expressing GFP. 24% and 40% of cells expressed GFP after infection with the vFLIP_IRES_eGFP and GFP lentivirus respectively.

4.2.3 vFLIP expression triggers the nuclear translocation of RelA/p65 and the upregulation of RelB expression in MVECs

Our previous findings seem to indicate that vFLIP expression in MVECs leads to activation of the classical, and potentially of the alternative, NF-κB pathway (section 4.2.2). It is well established that, activated NF-κB is released from the IκB inhibitors in the cytoplasm, and translocates into the nucleus, where it induces the transcription of a number of cellular genes (Pahl, 1999). In order to confirm the specificity of NF-κB induction by vFLIP in MVECs, we decided to examine untransduced, and GFP- or vFLIP-transduced MVECs by immunofluorescence, to look for the presence of activated nuclear NF-κB. MVECs were grown on 24-well chamber slides and were either not transduced, or transduced with a control lentiviral vector encoding only GFP, or with a lentivector encoding both vFLIP and GFP. 48 hours post transduction, the cells were washed, fixed with paraformaldehyde, permeabilized, and incubated with polyclonal antibodies against RelA/p65, p52, and RelB. The nuclei of cells were stained with DAPI and transduction was confirmed by GFP expression. Figure 4.4A (RelA/p65 staining) shows that in MVECs infected with the vFLIP_eGFP lentivector, vFLIP expression specifically induced the translocation of p65 into the nucleus. Cells staining positive for nuclear p65, observed when p65 staining was merged with the nuclear DAPI stain (panel F), were also positive for GFP staining (panels G and H, indicated by arrows), observed when p65 staining was merged with GFP staining (panel G). The co-localization of nuclear p65 and GFP indicates that p65 translocated into the nuclei of these cells as a result of vFLIP expression after transduction with the vFLIP_eGFP lentivector. On the same slide, no nuclear p65 was found in any of the cells that did not stain positive for GFP (panel H). In contrast, p65 was predominantly localized in the cytoplasm of untransduced cells (data not shown) and cells transduced with the control lentivector encoding only GFP, and we did not observe any nuclear p65 staining (panel B) in these cells. In this case, cells staining positive for GFP did not stain positive for nuclear p65, indicating that the control lentivector did not induce any active NF-κB-p65 nuclear translocation. These results confirm the specificity of NF-κB induction by vFLIP, and further support

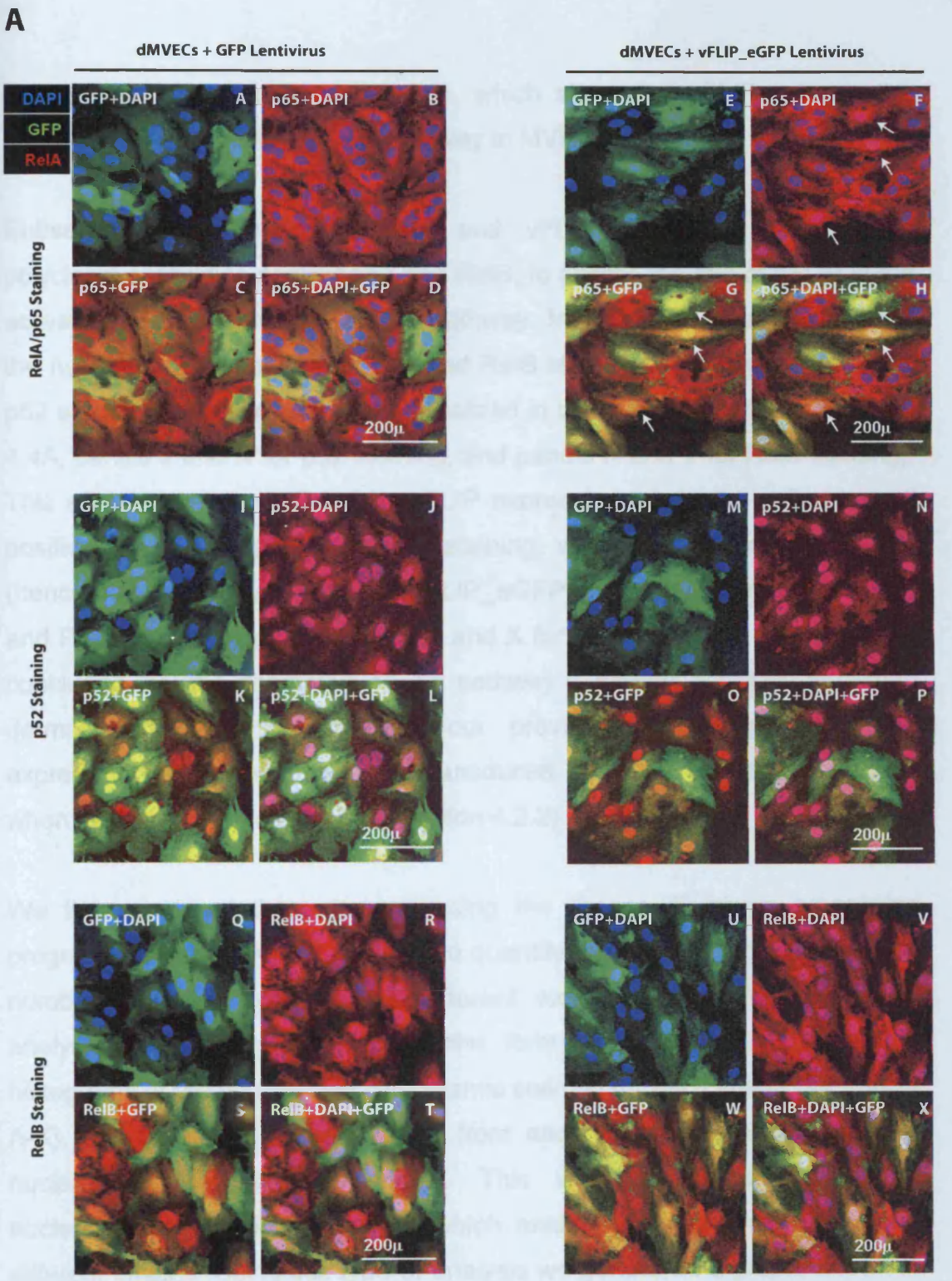

Figure 4.4 (A) vFLIP expression in MVECs induces the nuclear translocation of NF-κB-p65, but has no effect on p52 and RelB, which are predominantly nuclear irrespective of vFLIP expression

Human dermal microvascular endothelial cells (dMVECs) were grown on 24-well chamber slides, and were either not transduced, or transduced with a lentiviral vector encoding GFP alone, or vFLIP and GFP at an MOI of 30. **(A)** 48 hours post-transduction, the cells were washed, fixed, permeabilised, and stained with a rabbit polyclonal antibody against p65, p52, and RelB. DAPI staining was used as a nuclear stain, and GFP staining was used to confirm transduction by the lentivectors. DAPI-stained nuclei were merged with p65, p52, and RelB staining, (top right panels) to confirm nuclear translocation, and all stains were merged (bottom right panels) to indicate nuclear translocation of p65, p52, and RelB induced by the vFLIP or GFP lentivectors. The arrows indicate cells positive for p65 nuclear staining, which are also positive for vFLIP expression, as assayed by the presence of GFP in the nuclei.

our previous findings (section 4.2.2), which show that vFLIP induces the activation of the classical NF-κB pathway in MVECs.

Subsequently, we stained GFP-, and vFLIP-transduced MVECs with polyclonal antibodies against p52 and RelB, to assess the role of vFLIP in the activation of the alternative NF-κB pathway. Interestingly, when we merged the nuclear DAPI staining with p52 and RelB staining, we observed that both p52 and RelB were predominantly localized in the nuclei of these cells (figure 4.4A, panels J and N for p52 staining, and panels R and V for RelB staining). This effect was not mediated by vFLIP expression, since the cells were all positive for nuclear p52 and RelB staining, whether they expressed GFP (hence transduced by the GFP or vFLIP_eGFP lentivectors), or not (panels L and P for p52 staining, and panels T and X for RelB staining). Therefore, we concluded that the alternative NF-κB pathway is already activated in human dermal MVECs, which supports our previous observations that p52 expression levels were high in untransduced and GFP-transduced MVECs when assessed by Western Blot (section 4.2.2).

We then analysed these images using the "Image J" image processing program developed by NIH, in order to quantify the cell staining based on the number of pixels, compare the different experiments, perform statistical analysis, and generate results in the form of graphs. We generated histograms of the nuclear and cytoplasmic staining for each image (for panels A-X), and used the median values from each histogram to compare the nuclear and cytoplasmic staining. This way we came up with a nuclear:cytoplasmic staining ratio, which enabled us to compare between different images. Using this type of analysis we generated a graph, shown in figure 4.4B, which summarizes the results of this immunofluorescence study. Figure 4.4B shows that p52 staining is principally nuclear in these cells, irrespective of cells expressing GFP, or vFLIP and GFP. There is also much greater baseline RelB nuclear staining in untransduced cells, as compared to that seen with RelA/p65 nuclear staining of untransduced cells. Moreover, vFLIP expression does not seem to have any significant effect on RelB nuclear translocation. In contrast, the baseline localization of RelA/p65 is

B

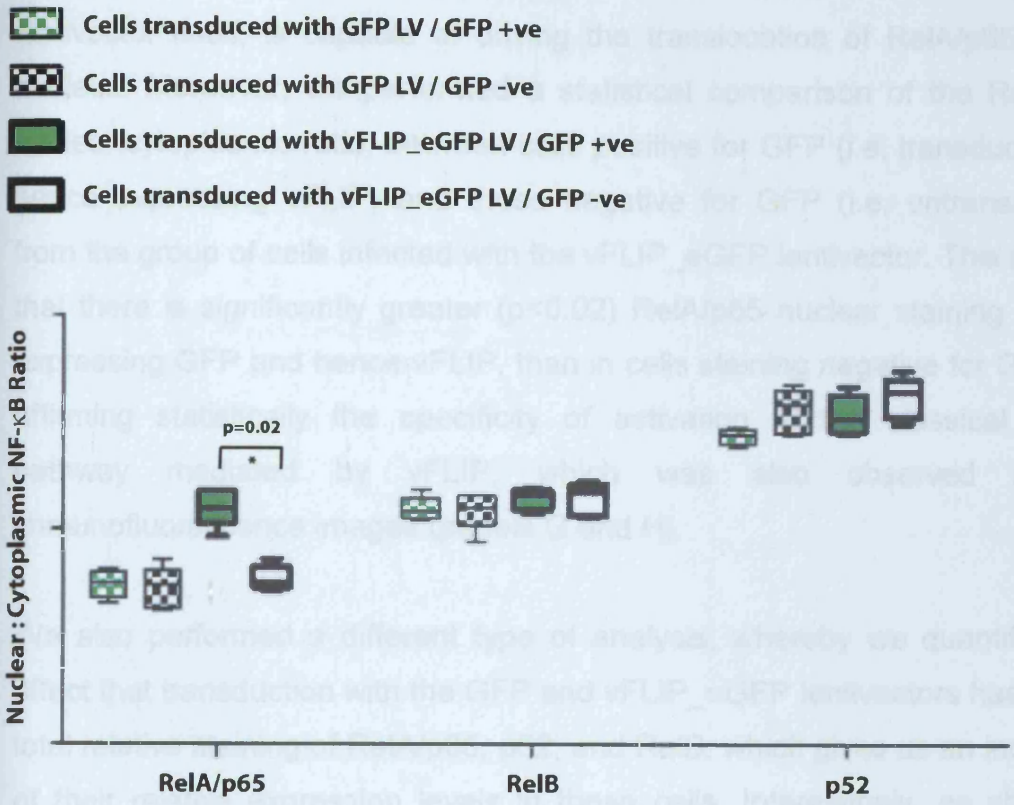

Nuclear:Cytoplasmic Ratios				
	GFP LV/GFP +ve	GFP LV/GFP -ve	vFLIP_eGFP LV/ GFP +ve	vFLIP_eGFP LV/ GFP -ve
RelA/p65	0,56	0,54	1,28	0,60
RelB	1,27	1,26	1,40	1,43
p52	2,79	3,77	3,58	4,32

Figure 4.4 (B) vFLIP expression in MVECs induces the nuclear translocation of NF-κB-p65, but has no effect on p52 and RelB, which are predominantly nuclear irrespective of vFLIP expression

(B) Comparison of nuclear:cytoplasmic NF-κB staining ratios between cells transduced with a lentivector encoding GFP alone, or vFLIP and GFP. Each high power field image seen in Figure 4.4 (A) (A-X) was analysed using "Image J" software from NIH, to generate quantitative fluorescence data for the cytoplasms and nuclei, in the form of histograms. These data were then exported from ImageJ into Graphpad Prism 5 software for further analysis and presentation. Nuclear:cytoplasmic ratios for each NF-κB subunit staining (RelA/p65, RelB, and p52) were then calculated by comparison of median values from the histogram data. The results of the analysis are summarised in the above graph. Differences were calculated using paired student *t* tests, where p=<0.05 was considered significant. * indicates p=<0.05. The values of the individual nuclear:cytoplasmic ratios are depicted in the table, and each value represents the mean ratio of 5 replicates for each NF-κB subunit staining.

mainly cytoplasmic for untransduced cells and cells transduced with the GFP lentivector, whereas vFLIP expression in these cells, but not the vFLIP_eGFP lentivector itself, is capable of driving the translocation of RelA/p65 to the nucleus. Moreover, we performed a statistical comparison of the RelA/p65 nuclear:cytoplasmic ratio, between cells positive for GFP (i.e. transduced and hence expressing vFLIP) and those negative for GFP (i.e. untransduced), from the group of cells infected with the vFLIP_eGFP lentivector. This showed that there is significantly greater ($p<0.02$) RelA/p65 nuclear staining in cells expressing GFP and hence vFLIP, than in cells staining negative for GFP, re-affirming statistically the specificity of activation of the classical NF-κB pathway mediated by vFLIP, which was also observed in the immunofluorescence images (panels G and H).

We also performed a different type of analysis, whereby we quantified the effect that transduction with the GFP and vFLIP_eGFP lentivectors has on the total relative staining of RelA/p65, p52, and RelB, which gives us an indication of their relative expression levels in these cells. Interestingly, as shown in figure 4.4C, we observed that in the case of total RelA/p65 staining in MVECs, successful lentiviral transduction and subsequent transgene expression induces an increase in total RelA/p65 levels (green line on the histograms, GFP+ve), irrespective of which transgene is expressed (GFP alone, or vFLIP and GFP). Therefore, it seems that transgene expression from the lentivector somehow activates the MVECs. This is in agreement with our previous observation, whereby transduction with the control lentivector that expresses only GFP, resulted in higher p100 expression levels in Western Blot (section 4.2.2, Figure 4.3A), when compared to uninfected cells. In the case of p52 staining (Figure 4.4C, p52 staining), neither transgene expression, nor vFLIP expression in particular, seemed to have any effect whatsoever on total p52 staining, and hence p52 expression levels, confirming that vFLIP does not appear to have any effect on the activation of the alternative NF-κB pathway in these cells. Finally, analysis of total relative RelB staining (Figure 4.4C, RelB staining) demonstrated that, like RelA/p65 staining, expression of both GFP and vFLIP/GFP led to greater levels of RelB staining, however, vFLIP expression was capable of inducing considerably higher levels of RelB.

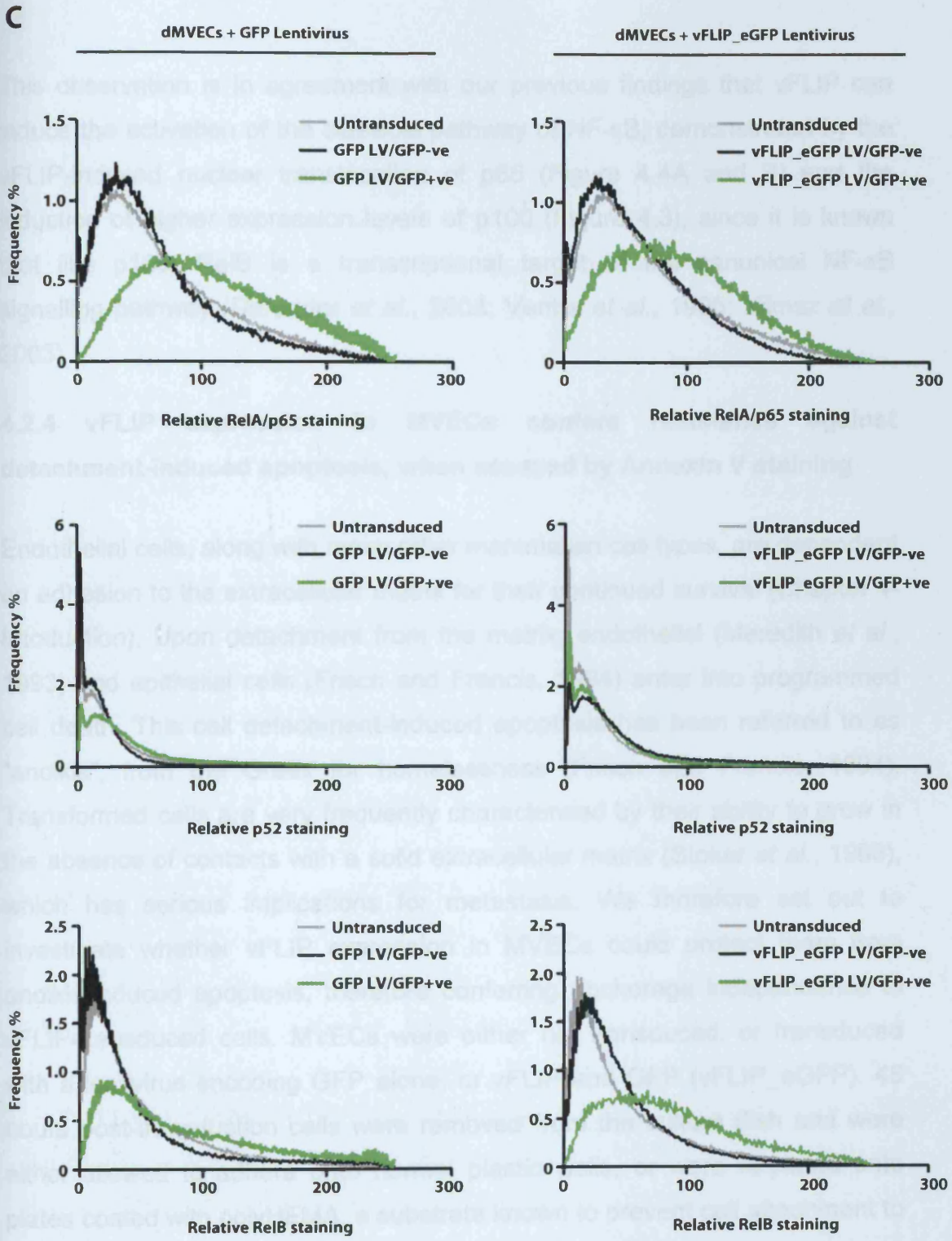

Figure 4.4 (C) vFLIP expression from the vFLIP_eGFP lentivector increases total RelB expression levels in MVECs

(C) Quantification of total relative NF-κB subunit cell staining. Each high power field image seen in Figure 4.4 (A) (A-X) was analysed using "Image J" software, to generate quantitative fluorescence data in the form of histograms. The histograms in this figure represent an analysis of total relative NF-κB subunit staining, derived from the sum of cytoplasmic and nuclear staining for each individual field. The results are plotted in the form of relative NF-κB subunit staining against frequency %, in order to normalise data for the different number of pixels in cytoplasmic and nuclear fractions. A shift in the histogram denotes an increase in the total relative NF-κB subunit staining, which in turn signifies an increase in the protein expression levels.

This observation is in agreement with our previous findings that vFLIP can induce the activation of the classical pathway of NF-κB, demonstrated by the vFLIP-induced nuclear translocation of p65 (Figure 4.4A and B) and the induction of higher expression levels of p100 (Figure 4.3), since it is known that like p100, RelB is a transcriptional target of the canonical NF-κB signalling pathway (Derudder *et al.*, 2003; Verma *et al.*, 1995; Yilmaz *et al.*, 2003).

4.2.4 vFLIP expression in MVECs confers resistance against detachment-induced apoptosis, when assayed by Annexin V staining

Endothelial cells, along with many other mammalian cell types, are dependent on adhesion to the extracellular matrix for their continued survival (Chapter 4-Intoduction). Upon detachment from the matrix, endothelial (Meredith *et al.*, 1993) and epithelial cells (Frisch and Francis, 1994) enter into programmed cell death. This cell detachment-induced apoptosis has been referred to as "anoikis", from the Greek for homelessness (Frisch and Francis, 1994). Transformed cells are very frequently characterised by their ability to grow in the absence of contacts with a solid extracellular matrix (Stoker *et al.*, 1968), which has serious implications for metastasis. We therefore set out to investigate whether vFLIP expression in MVECs could protect them from anoikis-induced apoptosis, therefore conferring anchorage independence to vFLIP-transduced cells. MVECs were either not transduced, or transduced with a lentivirus encoding GFP alone, or vFLIP and GFP (vFLIP_eGFP). 48 hours post-transduction cells were removed from the culture dish and were either allowed to adhere onto normal plastic wells, or were re-plated onto plates coated with polyHEMA, a substrate known to prevent cell attachment to the matrix, for 16 hours. To examine the effects of vFLIP expression on MVEC's anoikis, adherent and detached cells were then stained for Annexin V, which binds to phosphatidylserine (PS) and can therefore measure the translocation of PS (which is normally located exclusively at the inner side of the plasma membrane) to the outer layer or the external surface of the cell, and which is a marker for early apoptotic events. In adherent cultures the basal level for apoptosis was below 10% for untransduced and transduced

cells alike (Figure 4.5A left hand side dot plots/Attached), excluding the possibility that lentivector transduction was in any way toxic in these cells.

Figure 4.5A shows dot plots after FACS analysis, from one representative experiment out of three with similar results obtained, of attached and detached MVECs stained for Annexin V. Anoikis was successfully induced after 16 hours of detachment on polyHEMA-coated wells, and both uninfected (Figure 4.5A top right plot) and GFP-transduced cells (Figure 4.5A middle right plot) were susceptible to apoptosis following removal from the extracellular matrix, with 37% and 48% of cells staining positive for Annexin V expression respectively . However, cells expressing the vFLIP protein were resistant to anoikis, with only 6% of cells staining positive for Annexin V after detachment (Figure 4.5A bottom right plot), as compared to 4% of cells that were positive in the attached culture. We obtained similar results when staining cells with propidium iodide (PI), which is used to discriminate late apoptotic or necrotic cells that have lost membrane integrity from early apoptotic cells (stained with Annexin V) which still have intact membranes. 24% of uninfected cells and 26% of cells transduced with the GFP lentivector were necrotic (PI positive), in contrast to only 5% of cells transduced with the vFLIP_eGFP lentivector staining positive for PI (FACS plots not shown). The results obtained from three independent experiments are summarised in Figure 4.5C. In brief, MVECs attached to the culture plate, whether transduced or not, were >90% viable and lentiviral transduction did not seem to have any toxic effect on these cells. However, detachment from the matrix induced significant levels of cell death in MVECs, with 61% of untransduced cells, and 74% of GFP-transduced cells in total staining positive for either Annexin V (apoptotic) or PI (necrotic). In contrast, cells expressing vFLIP were rendered resistant to anoikis-induced apoptosis, since after detachment only 11% of vFLIP_eGFP-transduced MVECs were apoptotic /necrotic, and 89% of these cells remained viable even after the loss of contact with the matrix.

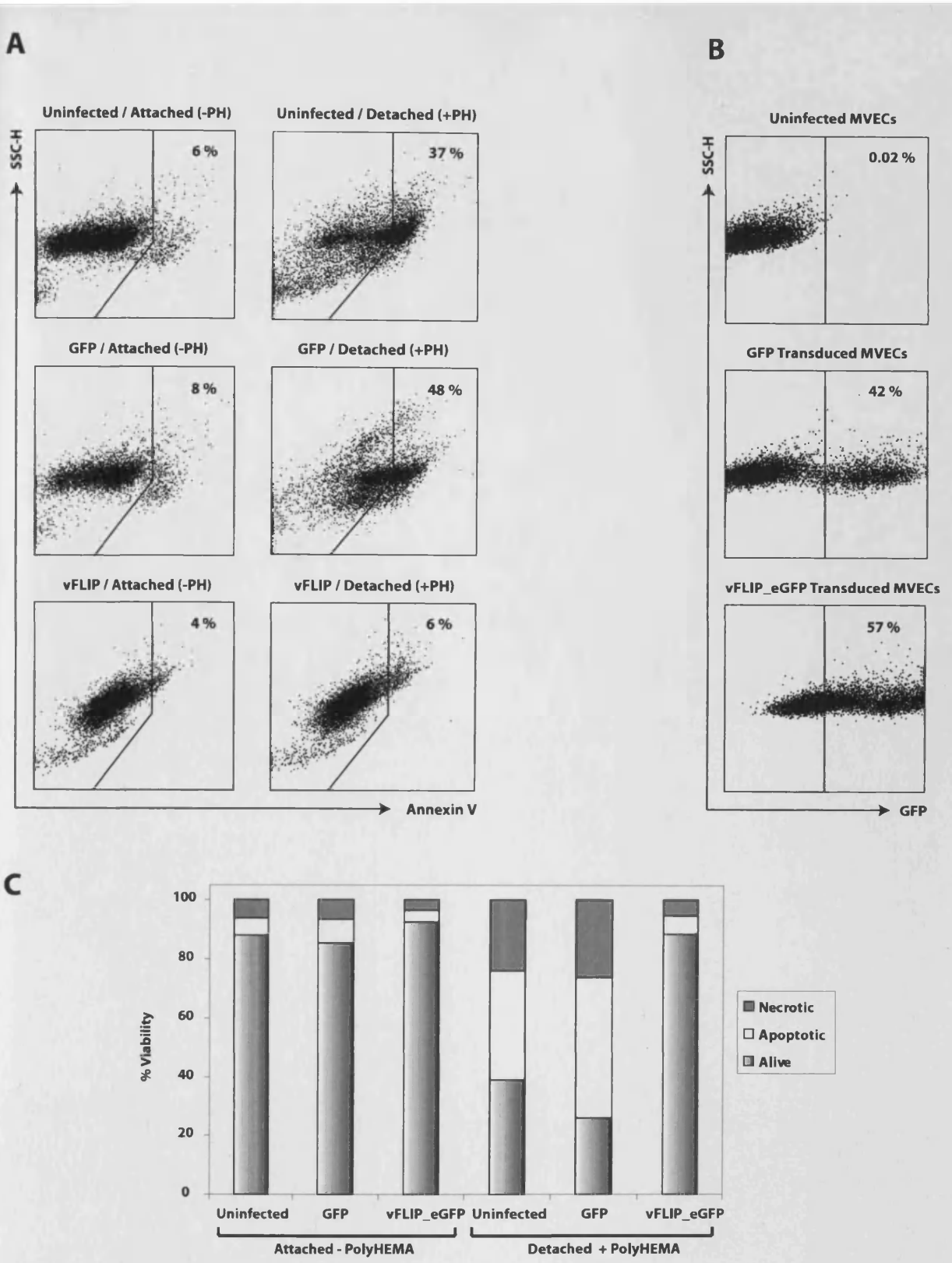

Figure 4.5 (A, B, C) Expression of vFLIP in MVECs rescues cells from detachment-induced apoptosis when assayed by Annexin V-Biotin binding

Human dermal microvascular endothelial cells (dMVECs) were either not transduced, or transduced with a lentiviral vector encoding GFP alone, or vFLIP and GFP. 48 hours post-transduction, cells were detached from the matrix by trypsinisation and either plated on control wells, or anoikis was induced by plating cells on polyHEMA-coated wells for 16h. Apoptosis was assayed by Annexin V-Biotin/PI staining. **(A)** Early apoptotic events were measured by labelling cells with Annexin V-Biotin (Trevigen), and detected with a secondary antibody binding to a red fluorescent-streptavidin. Annexin V staining is plotted against side scatter of cells. **(B)** Transduction efficiency was measured by FACScan analysis of cells expressing GFP. **(C)** Summary of results from Annexin V/PI staining. Cells staining positive for Annexin V are referred to as apoptotic, cells positive for PI as necrotic, and double negative cells as alive.

The cells were stained with Annexin V-Biotin and detected with a streptavidin –conjugated RPE-Cy5 red fluorescent secondary antibody (FL3 channel detection), instead of Annexin V-FITC (FL1 channel detection), as we wanted to check transduction efficiency by GFP expression, which is also detected by the FL1 channel. As seen in Figure 4.5A, single staining was performed for either Annexin V, or PI, and plotted against the side scatter, as opposed to Annexin V against PI, which is used to distinguish live, apoptotic and necrotic cell populations. This was due to the fact that triple staining was not possible due to overlap between the red and far red channels, which could not be overcome with any amount of instrument compensation. Nevertheless, this type of analysis means that we have probably overestimated the percentage of cells staining positive for Annexin V. Annexin V can detect apoptotic cells by being used as a sensitive probe for PS that is exposed on the outer leaflet of the cell membrane. However, due to the loss of membrane integrity in necrotic cells, Annexin V can enter the cells and also bind to the PS exposed on the inner leaflet of the cell membrane. Therefore, when we analysed cells undergoing anoikis-induced cell death using Annexin V, a fraction of the population that stained positive for Annexin V might have been necrotic cells, as they stain positive for both Annexin V and PI since the cell membrane is not intact. In contrast, PI positive cells are definitely only necrotic because the PI cannot cross the intact cell membrane. Simultaneous staining with Annexin V and PI is therefore recommended, when possible, to distinguish apoptotic cells from necrotic cells. In any event, we do not believe that this has any major bearing on our observation that vFLIP expression rescues MVECs from anoikis, since the difference in viability between cells expressing vFLIP and those that don't is still quite substantial.

4.2.5 vFLIP expression rescues MVECs from anoikis-induced apoptosis but not from growth factor removal, when assayed by DNA Fragmentation ELISA

In an effort to confirm our findings that vFLIP expression in MVECs confers protection against anoikis-induced apoptosis, uninfected MVECs, or MVECs transduced with the GFP lentivirus or the vFLIP_eGFP lentivirus, were removed from the plate, and were either allowed to re-adhere onto normal plates, or anoikis was induced by plating cells onto polyHEMA-coated wells for 16 hours. A fraction of the cells grown on control or polyHEMA-coated wells was also deprived of growth factors in the medium, in order to investigate whether the expression of vFLIP is able to suppress other forms of apoptosis in MVECs. The ability of these cells to undergo apoptosis upon detachment from the extracellular matrix and removal of growth factors was measured using a Death Detection ELISA (Roche) assay which specifically detects and quantitates mono- and oligonucleosomes (histone-associated DNA fragments) that are released into the cytoplasm of cells that die from apoptosis (Figure 4.6A). Cell metabolism was measured using an MTT cell proliferation assay, which is based on the cleavage of the yellow tetrazolium salt MTT to purple formazan crystal by metabolically active cells (Figure 4.6B).

As shown in figure 4.6A, uninfected cells, and cells transduced with the GFP lentivector, were highly susceptible to apoptosis following detachment from the extracellular matrix, and exhibited a 2-fold and 5-fold increase in DNA fragmentation respectively, which was significantly different ($p =< 0.01$) from their attached counterparts. However, MVECs expressing vFLIP were highly protected from apoptosis following detachment, with DNA fragmentation levels comparable to vFLIP-expressing cells grown on control plates (no significant difference observed), but significantly different ($p =< 0.01$) from uninfected and GFP-transduced MVECs.

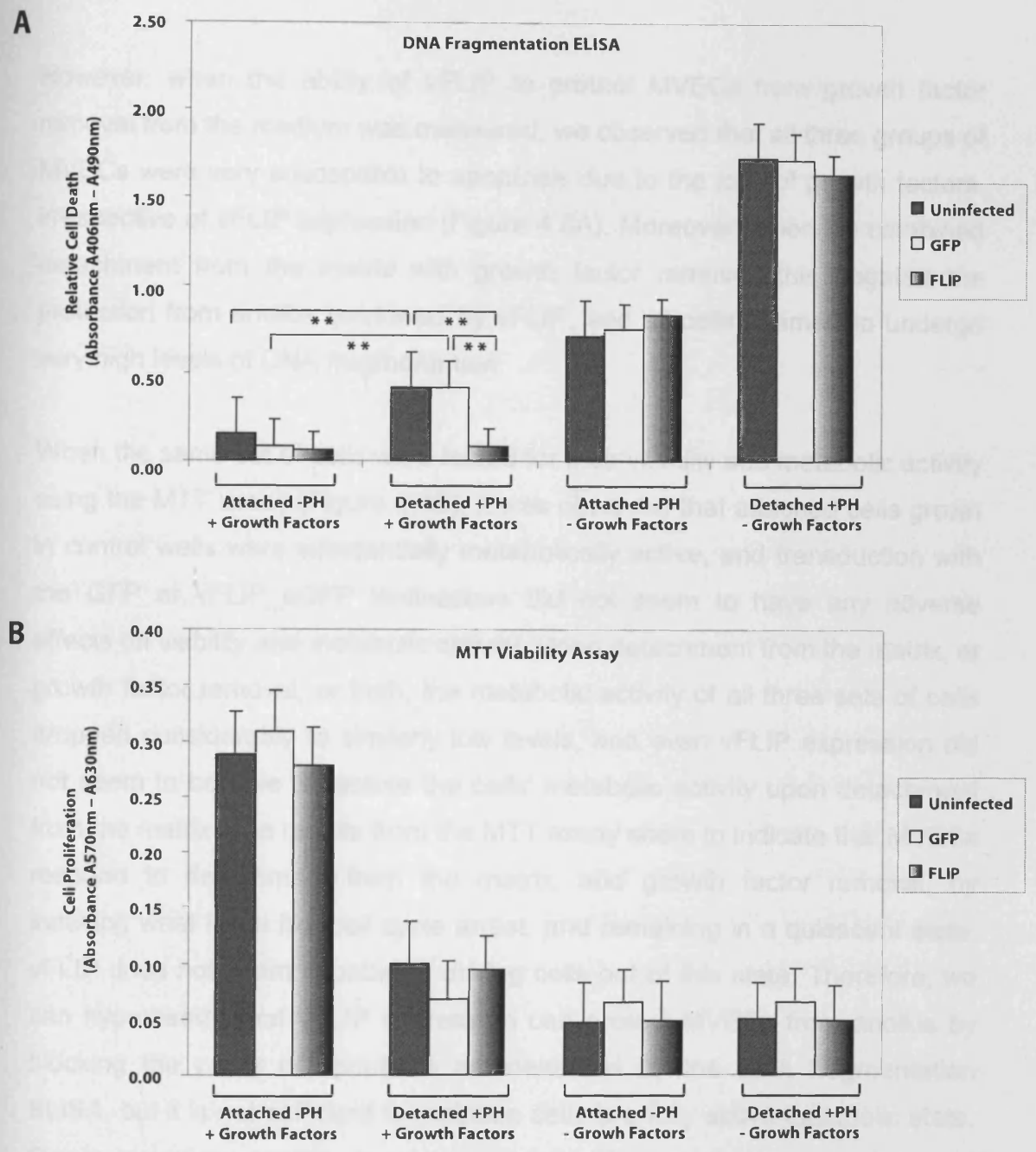

Figure 4.6 (A, B) Expression of vFLIP in MVECs confers resistance against detachment-induced apoptosis when assayed by DNA fragmentation ELISA, but does not rescue cells in the absence of growth factors

Human dermal microvascular endothelial cells (dMVECs) were either not transduced, or transduced with a lentiviral vector encoding GFP alone, or vFLIP and GFP. 48 hours post-transduction, cells were detached from the matrix by trypsinisation and either re-plated on control wells (Attached -PH), or anoikis was induced by plating cells on polyHEMA-coated wells for 16h (Detached +PH). A subset of cells was washed free of medium and plated on control or polyHEMA-coated wells in the absence of any growth factors (- Growth Factors). **(A)** Apoptosis was measured by using a cell death detection ELISA kit (Roche), which measures DNA fragmentation. Significant differences between the different samples are indicated on the graph. Differences were calculated using paired student t tests, where $p=<0.05$ was considered significant. ** indicate $p=<0.01$. **(B)** Cell viability was assessed using an MTT survival assay, which measures metabolic activity, as described in Materials and Methods. The results shown are the mean values from three independent experiments with error bars indicating the standard deviation between the three experiments. Transduction efficiency was assessed by FACScan analysis of cells expressing GFP. 57% of MVECs infected with the vFLIP lentivirus were GFP positive and 73% of MVECs infected with the GFP lentivirus were GFP positive.

However, when the ability of vFLIP to protect MVECs from growth factor removal from the medium was measured, we observed that all three groups of MVECs were very susceptible to apoptosis due to the loss of growth factors, irrespective of vFLIP expression (Figure 4.6A). Moreover, when we combined detachment from the matrix with growth factor removal, this negated the protection from anoikis bestowed by vFLIP, and all cells seemed to undergo very high levels of DNA fragmentation.

When the same set of cells were tested for their viability and metabolic activity using the MTT assay (Figure 4.6B), it was observed that attached cells grown in control wells were substantially metabolically active, and transduction with the GFP or vFLIP_eGFP lentivectors did not seem to have any adverse effects on viability and metabolic activity. Upon detachment from the matrix, or growth factor removal, or both, the metabolic activity of all three sets of cells dropped considerably to similarly low levels, and even vFLIP expression did not seem to be able to restore the cells' metabolic activity upon detachment from the matrix. The results from the MTT assay seem to indicate that MVECs respond to detachment from the matrix, and growth factor removal, by inducing what looks like cell cycle arrest, and remaining in a quiescent state. vFLIP does not seem capable of driving cells out of this state. Therefore, we can hypothesize that vFLIP expression can protect MVECs from anoikis by blocking the onset of apoptosis as measured by the DNA fragmentation ELISA, but it is not sufficient to maintain cells is a fully active metabolic state. Since surviving anoikis is a prerequisite for cancer progression and metastasis, these findings give us further insight into the important role that vFLIP plays in KSHV pathogenesis.

4.2.6 vFLIP protects MVECs against detachment-induced apoptosis via the NF-κB pathway

Our previous findings have demonstrated that vFLIP is capable of protecting MVECs from detachment-induced apoptosis. We were therefore interested to investigate the mechanism by which it does so. As discussed in section 1.4.5 of the Introduction, it seems that one of the main functions of vFLIP is to induce sustained NF-κB activation (Chaudhary *et al.*, 2000; Chaudhary *et al.*, 1999; Liu *et al.*, 2002; Matta *et al.*, 2003). Blocking NF-κB induces apoptosis in KSHV-infected PEL cells (Keller *et al.*, 2000), leads to the downregulation of NF-κB-inducible cytokines (Sun *et al.*, 2006), and reverses the vFLIP-mediated protection of cells against growth factor withdrawal-induced apoptosis (Sun *et al.*, 2003a). Since we previously demonstrated that vFLIP can activate NF-κB in MVECs (section 4.2.2 and 4.2.3), we formed the hypothesis that vFLIP could also protect MVECs against detachment-induced apoptosis via the activation of the NF-κB pathway. To test this hypothesis, we decided to inhibit NF-κB using a known inhibitor of this pathway, namely Bay 11-7082, which irreversibly blocks the phosphorylation of IκBα and the subsequent release of active NF-κB into the nucleus (Cahir-McFarland *et al.*, 2004). MVECs were grown to ~70% confluency and were either left untreated, or were pre-treated with 20μM of Bay 11-7082 for 1 hour at 37 °C. Cells were then washed free on the inhibitor, and were either not transduced, or transduced with a lentivector encoding GFP alone, or vFLIP and GFP. 48 hours post-transduction cells were removed from the culture dish and were either allowed to re-adhere onto normal plates, or anoikis was induced by plating cells onto polyHEMA-coated wells for 16 hours. Subsequently, apoptosis was assessed using a Death Detection ELISA (Roche), which quantifies the extent of DNA degradation in cells.

Figure 4.7 shows that, as expected, in the absence of Bay 11-7082, vFLIP expression rescued cells from detachment-induced apoptosis, whereas untransduced and GFP-transduced cells were very susceptible to apoptosis, displaying a 9-fold increase in DNA fragmentation levels. However, treatment of the cells with the Bay 11-7082 inhibitor, and the subsequent inhibition of

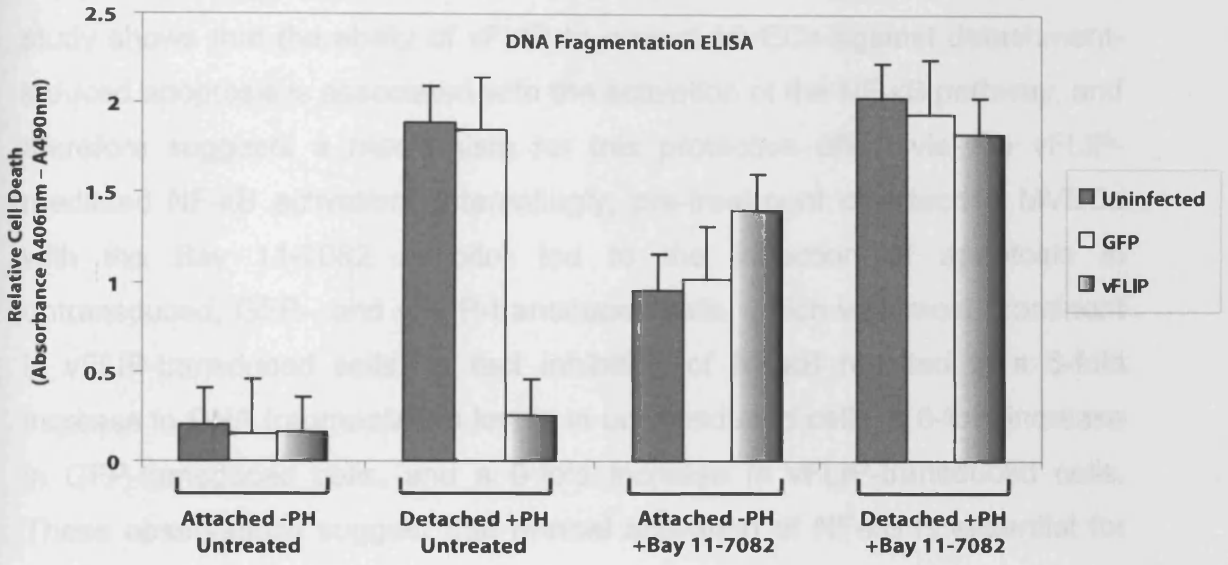

Figure 4.7 Inhibition of vFLIP-mediated NF-κB activation by Bay 11-7082 induces apoptosis in attached MVECs, and abolishes the vFLIP-mediated protection against anoikis

Human dermal microvascular endothelial cells (dMVECs) were either left untreated, or were pretreated with 20mM Bay 11-7082 for 1h. Untreated cells, and cells incubated with Bay 11-7082, were then washed twice with HBSS, and either not transduced (labelled Uninfected), or transduced with a lentiviral vector encoding GFP alone, or vFLIP and GFP. 48 hours post-transduction, cells were detached from the matrix by trypsinisation and either plated on control wells, or anoikis was induced by plating cells on polyHEMA-coated wells for 16h. Apoptosis was then measured using a cell death detection ELISA kit (Roche), which measures DNA fragmentation. The results shown are the mean values from three independent experiments with error bars indicating the standard deviation between the three experiments. Transduction efficiency was assessed by FACScan analysis of cells expressing GFP. 57% of MVECs infected with the vFLIP lentivirus were GFP positive, and 73% of MVECs infected with the GFP lentivirus were GFP positive.

NF-κB, led to a reversal of the protective effect mediated by vFLIP against detachment-induced apoptosis, and resulted in a 7-fold increase in DNA fragmentation levels, as compared to the levels observed in detached vFLIP-expressing cells in the absence of the Bay 11-7082 inhibitor. The present study shows that the ability of vFLIP to protect MVECs against detachment-induced apoptosis is associated with the activation of the NF-κB pathway, and therefore suggests a mechanism for this protective effect via the vFLIP-mediated NF-κB activation. Interestingly, pre-treatment of attached MVECs with the Bay 11-7082 inhibitor led to the induction of apoptosis in untransduced, GFP-, and vFLIP-transduced cells, which was most prominent in vFLIP-transduced cells. In fact inhibition of NF-κB resulted in a 5-fold increase in DNA fragmentation levels in untransduced cells, a 6-fold increase in GFP-transduced cells, and a 9-fold increase in vFLIP-transduced cells. These observations suggest that normal activation of NF-κB is essential for the survival of untransduced cells under physiological conditions.

4.2.7 Culture supernatant from vFLIP-expressing MVECs can rescue cells from anoikis

We set out to further investigate the mechanism by which vFLIP-mediated NF-κB can protect MVECS from detachment-induced apoptosis. Our previous findings in sections 4.2.4 and 4.2.5 (Figures 4.5 and 4.6) seem to suggest that expression of vFLIP by cells that have been successfully transduced with the vFLIP_eGFP lentivirus, does not only result in the protection of the cells which are positive for vFLIP expression, but can also rescue from anoikis most of the neighbouring cell population. This led us to believe that vFLIP expression, and the subsequent activation of NF-κB in MVECs, might induce the secretion of a survival factor into the medium, which can send survival signals to all of the cells growing within it.

KSHV infection of endothelial cells *in* vitro induces the expression of numerous cytokines (Di Bartolo and Cesarman, 2004), while in KS lesions several viral genes have been linked to cytokine release (An *et al.*, 2005; Montaner et al., 2004). For example, vFLIP not only activates NF-κB (Liu et

al., 2002), but it also induces IL-6 gene expression in a JNK- and AP1-dependent fashion (An *et al.*, 2003) and therefore contributes to the cytokine-rich milieu of KS lesions. For this reason we decided to test whether the culture supernatant from MVECs transduced with the vFLIP_eGFP lentivector was capable of mediating protection against anoikis. MVECs were either not transduced, or transduced with a lentivirus encoding GFP alone, or vFLIP and GFP (vFLIP_eGFP). 48 hours post-transduction cells were removed from the culture dish and were either allowed to re-adhere or anoikis was induced by plating cells on polyHEMA for 16 hours. A subset of cells from the three groups was washed free of growth medium following detachment, and was resuspended and plated on polyHEMA for 16 hours in 500µl of culture supernatant (diluted 1:2) derived from untransduced, GFP, and vFLIP-transduced MVECs, to assess the effect of the different supernatants on MVEC survival during anoikis. The extent of apoptosis was determined using the Death Detection ELISA (Roche).

As shown in Figure 4.8, untransduced and GFP-transduced MVECs were very susceptible to detachment-induced cell death, since we observed more than a 7-fold increase in the DNA fragmentation levels of both as determined by the Death Detection ELISA. However, cells transduced with the vFLIP_eGFP lentivector were protected from anoikis, confirming our previous findings (Figure 4.6A). Culture supernatant from uninfected cells did not protect untransduced or GFP-transduced MVECs from anoikis, and only the cells transduced with the vFLIP_eGFP lentivector were rescued. The same was observed when detached cells were incubated in culture supernatant from GFP-transduced cells, ruling out the possibility that lentiviral transduction or the vector itself induces any survival factor secretion. However, when detached MVECs were grown in culture supernatant derived from vFLIP expressing cells, untransduced and GFP-transduced cells were partially protected from anoikis, while vFLIP-transduced cells were fully protected. Indeed, untransduced and GFP-transduced cells exhibited an almost 2-fold decrease in DNA fragmentation levels and there was a significant difference ($p=<0.05$) between these levels and the DNA fragmentation levels of cells grown in the supernatant of untransduced, or GFP-transduced cells.

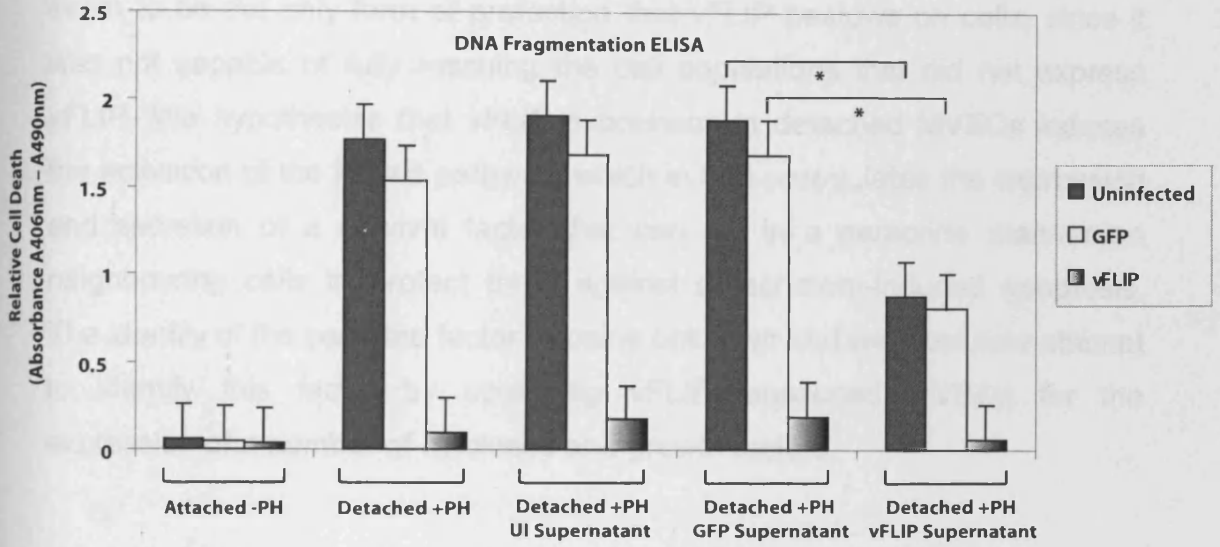

Figure 4.8 Supernatant from vFLIP-expressing MVECs, is capable of mediating resistance against detachment-induced apoptosis in untransduced and GFP-expressing MVECs

Human dermal microvascular endothelial cells (dMVECs) were either not transduced (labelled Uninfected, or UI on the graph), or transduced with a lentiviral vector encoding GFP alone, or vFLIP and GFP. 48 hours post-transduction, cells were detached from the matrix by trypsinisation and either plated on control wells, or anoikis was induced by plating cells on polyHEMA-coated wells for 16h. A subset of cells from all three groups was washed post-trypsinisation and plated in 500μl of supernatant, diluted 1:2 in normal medium, from untransduced, GFP, and vFLIP-transduced cells on polyHEMA-coated wells for 16h, to assess the effect of secreted factors in the respective supernatants on the survival of MVECs upon detachment. Apoptosis was measured using a cell death detection ELISA kit (Roche), which measures DNA fragmentation. The results shown are the mean values from three independent experiments with error bars indicating the standard deviation between the three experiments. Significant differences between the different samples are indicated on the graph. Differences were calculated using paired student *t* tests, where $p=<0.05$ was considered significant. * indicates $p=<0.05$. Transduction efficiency was assessed by FACScan analysis of cells expressing GFP. 63% of MVECs infected with the vFLIP lentivirus were GFP positive and 75% of MVECs infected with the GFP lentivirus were GFP positive. PH, polyHEMA.

This data suggests that vFLIP-mediated NF-κB activation induces the secretion of one or several soluble survival factors, which are sufficient to confer a level of protection to cells against detachment-induced cell death. However, this secreted survival factor in the culture supernatant does not seem to be the only form of protection that vFLIP bestows on cells, since it was not capable of fully rescuing the cell populations that did not express vFLIP. We hypothesize that vFLIP expression in detached MVECs induces the activation of the NF-κB pathway, which in turn upregulates the expression and secretion of a survival factor that can act in a paracrine manner on neighbouring cells to protect them against detachment-induced apoptosis. The identity of the secreted factor remains unknown and we must now attempt to identify this factor by screening vFLIP-transduced MVECs for the expression of a number of cytokines and growth factors.

4.3 Discussion

Kaposi's sarcoma is considered to be a neoplasm of KSHV-infected lymphatic endothelium (Beckstead *et al.*, 1985; Jussila *et al.*, 1998; Weninger *et al.*, 1999), as in most KS tumours KSHV infection is largely detected in the endothelial cell compartment. However, KSHV latency has been most extensively studied in B cells, which are considered to be the primary reservoir of infection. We therefore decided to individually examine the role of the latently-expressed vFLIP protein of KSHV in promoting cell survival and proliferation of KSHV-infected cells, by conducting our studies using human dermal microvascular endothelial cells (MVECs). These cells represent a mixed population of lymphatic and blood endothelial cells (Makinen *et al.*, 2001), and are therefore a good model for our studies by being closely related to those cells targeted naturally for infection by KSHV. In this chapter we have presented evidence suggesting a role for vFLIP in the modulation of the NF-κB pathway in MVECs, and we have demonstrated that ectopic expression of vFLIP confers MVECs with a survival advantage when challenged with an apoptotic stimulus.

We have previously shown that vFLIP expression in a variety of haematopoietic cell lines can induce the activation of both the canonical and alternative NF-κB pathways (Chapter 3). Since activated NF-κB is probably critical for the escape of immune surveillance and the prevention of apoptosis in KSHV-infected cells, we wanted to determine whether vFLIP is also capable of activating NF-κB in primary human MVECs. Indeed, lentiviral transduction of MVECs with a vector encoding vFLIP led to upregulation of p100 expression, suggesting canonical pathway activation, and generation of p52, indicating alternative pathway activation as well (Figure 4.3). However, levels of p100 and p52 were also quite high in untransduced cells and cells transduced with a control lentivector encoding only GFP, suggesting that the alternative NF-κB pathway is already activated in these cells, possibly through the action of an exogenous factor in the growth medium. This hypothesis was confirmed by an immunofluorescence assay examining the nuclear and cytoplasmic staining of RelA/p65, p52, and RelB in untransduced and

transduced cells, which showed that although vFLIP induces a significant nuclear translocation of p65, the subcellular localization of p52 and RelB is already nuclear in these cells, irrespective of vFLIP expression (Figure 4.4). These findings indicate that in MVECs, vFLIP is only inducing the canonical pathway of NF-κB activation. However, we cannot rule out the possibility that vFLIP can also activate the alternative NF-κB pathway, since the basal levels of nuclear p52 and RelB were so high in all the cells that they might have masked any significant upregulation mediated by vFLIP. This hypothesis is further supported by the Western Blot analysis performed on the same cells, which demonstrated higher expression levels of total p52 in cells expressing vFLIP, as compared to those that didn't (Figure 3.3 A and B). The elevated basal levels of nuclear p52 in untransduced cells and cells transduced with the control GFP lentivector can be explained by the fact that these cells are grown in a growth factor-rich medium, which apart from serum also contains VEGF, human fibroblast growth factor (hFGF), insulin-like growth factor (IGF), and human epidermal growth factor (hEGF), and some of these growth factors might be inducing downstream signalling cascades that lead to the activation of NF-κB. Indeed, NF-kB has been shown to be highly activated in MVECs exposed to VEGF, in conjunction with Bcl-2 anti-apoptotic signalling (Karl *et al.*, 2005). Moreover, serum in the growth medium of certain cells, such as U-2 OS human osteosarcoma cells, has been shown to stimulate p100 processing and generation of significant basal levels of p52 (Schumm *et al.*, 2006). MVECs transduced with the vFLIP lentivector, were examined for 48 hours post-transduction and most of the cells positive for vFLIP expression (as assayed by the expression of GFP) displayed p65 nuclear translocation. These findings demonstrate that vFLIP induces the persistent activation of NF-κB in MVECs, and are consistent with a previous report showing activation of NF-κB in KSHV-infected MVECs at later time points post infection (Sadagopan *et al.*, 2007), suggesting that vFLIP is responsible for the NF-κB activation observed during the late phase of infection with KSHV and probably for the NF-κB-dependent anti-apoptotic and pro-proliferative effects on KSHV-infected cell survival.

Many mammalian cells are dependent on adhesion to the extracellular matrix for the continuous supply of survival signals. Upon detachment from the matrix, endothelial (Meredith *et al.*, 1993), and epithelial cells (Frisch and Francis, 1994) undergo detachment-induced apoptosis, termed anoikis. These survival signals ensure that these types of cells cannot normally survive in the absence of cell-matrix interactions, and cells are therefore unable to proliferate in inappropriate sites or to survive in the absence of attachment, acting as a major defence against metastasis. Previous reports have shown that vFLIP is capable of rescuing haematopoietic cells from growth factor withdrawal-mediated apoptosis in an NF-κB-dependent manner (Sun *et al.*, 2003a), and Rat-1 cells transduced with a vFLIP retroviral vector displayed anchorage-independent growth and formation of colonies in soft agar, which was associated with the activation of NF-κB by vFLIP (Sun *et al.*, 2003b). We therefore decided to study the effect of vFLIP on detachment-induced apoptosis of MVECs, by plating cells on culture wells coated with the substance polyHEMA, which prevents cell adhesion to the matrix, and measuring apoptosis by Annexin V staining and DNA fragmentation ELISA, and viability of the cells using an MTT assay. In this chapter we have presented evidence showing that vFLIP has the ability to protect cells from detachment-induced apoptosis, since cells expressing vFLIP were resistant to anoikis, while untransduced cells and those transduced with the control lentivector were very susceptible to detachment-induced cell death (Figures 4.5 and 4.6). However, when we removed the growth factors from the culture medium of these cells and assessed the ability of vFLIP to protect cells from growth factor withdrawal-induced apoptosis, we failed to observe any protective effect against apoptosis mediated by vFLIP (Figure 4.6A), in contrast to previous findings which have observed so (Sun *et al.*, 2003a). This could be due to the fact that Sun *et al.* used a leukaemia cell line and removed only GM-CSF from the growth medium to induce apoptosis, whereas in our study we used primary cells, which are very sensitive and dependent on multiple growth factors for proliferation and survival, and we removed all the growth factors contained in the growth medium, perhaps exposing our cells to a much stronger apoptotic stimulus, which vFLIP was unable to counteract. It will be interesting to repeat this study in the future, by sequentially removing a

single growth factor at one time and assessing for protection against apoptosis mediated by vFLIP. Moreover, although vFLIP expression resulted in a strong protective effect against apoptosis, cells expressing vFLIP did not recover their full metabolic activity, as assayed by MTT, upon detachment from the matrix (Figure 4.6B). However, it has been shown that although some adherent cell types such as fibroblasts, which are specialized in tissue invasion, do not undergo anoikis in the absence of contact with the matrix, they do become quiescent (Ben-Ze'ev *et al.*, 1980; Folkman and Moscona, 1978), which might explain the loss of metabolic activity observed in vFLIP expressing cells.

Since we previously demonstrated that vFLIP induces NF-κB activation in MVECs, we hypothesized that the ability of vFLIP to protect cells against detachment-induced apoptosis might be attributed to its ability to activate the NF-κB pathway in these cells. Indeed, when we blocked NF-κB activation by using the Bay 11-7082 inhibitor, which blocks the degradation of IκB, we observed a near complete reversal of the protective effect afforded to cells by the expression of vFLIP (Figure 4.7). Subsequently, we tried to elucidate the mechanism via which vFLIP-mediated NF-κB might protect MVECs against anoikis. We speculated that this protective effect might be the result of autocrine and paracrine survival signals from a secreted factor induced by vFLIP-mediated NF-κB, since NF-κB regulates the expression of a great number of cytokines and growth factors, and it plays an important role in regulating cytokines in PEL cells with pro-proliferative and angiogenic effects (An et al., 2003; Matta *et al.*, 2007b; Polson *et al.*, 2002; Wang et al., 2004a). As a mater of fact, our hypothesis was confirmed by results demonstrating that the supernatant alone from vFLIP expressing cells, but not that from untransduced cells or those that were transduced with the control lentivector, was capable of partially rescuing cells from anoikis (Figure 4.8), suggesting that this protective effect could be attributed to the NF-κB-dependent secretion of a soluble survival factor.

The next step in dissecting the mechanism of vFLIP-mediated protection against anoikis would be to identify the secreted factor and assess its ability to

rescue MVECs from anoikis in the absence of vFLIP. However, time did not allow us to further investigate this experimentally, so we decided to come up with a list of likely candidates. This was achieved by analysing data from a gene expression microarray (GEM) of KSHV-infected lymphatic endothelial cells (KLECs), generated in the laboratory of our collaborator Prof. Boshoff and presented in a recent Blood paper by Lagos *et al* (Lagos *et al.*, 2007). This analysis was made possible by the kind permission of Prof. Boshoff to examine the data generated by his laboratory, and with invaluable help from Dimitrios Lagos, who planned and executed most of the data analysis. Our approach was to initially identify all the genes with NF-κB responsive elements, and this was achieved from searching publicly available databases, most notably the "Rel/NF-KB target genes" database (http://bioinfo.lifl.fr/NF-KB), and the "Rel/NF-KB Transcription Factors" website of TD Gilmore (http://people.bu.edu/gilmore/nf-kb/target/index.html). Subsequently, we narrowed down this list by examining which of these genes were significantly upregulated by KSHV after infection of LECs. Finally, the list was narrowed down even further by extracting only the secreted factors from the list of NF-κB responsive targets significantly upregulated after KSHV infection of LECs. The analysis and extraction of the secreted factors from the GEM was performed using the website http://www.affymetrix.com/analysis/index.affx, which is available from the manufacturer of the hg-u133+2 GeneChips (Affymetrix) used in this experiment. The final list is shown in Figure 4.9, in the form of a heat map of GEM data from 6 pairs of LECs and KLECs, and shows the NF-κB-responsive secreted factors significantly upregulated in KSHV-infected LECs.

Following examination of the list of secreted factors, a few of them stand out as the most likely candidates, such as IL-6, CXCL16, PDGFB, and BMP2, based on reports on their function in the literature. IL-6, has been shown to be secreted by KS tumour cells in culture and can stimulate KS tumour cell proliferation (Ensoli *et al.*, 1989). In addition IL-6 can act as an autocrine growth factor for endothelial cells immortalized with the middle-size Ag of polyomavirus (PmT), inducing significant proliferation in PmT-endothelial cells and promoting the progression of vascular tumours (Giraudo *et al.*, 1996).

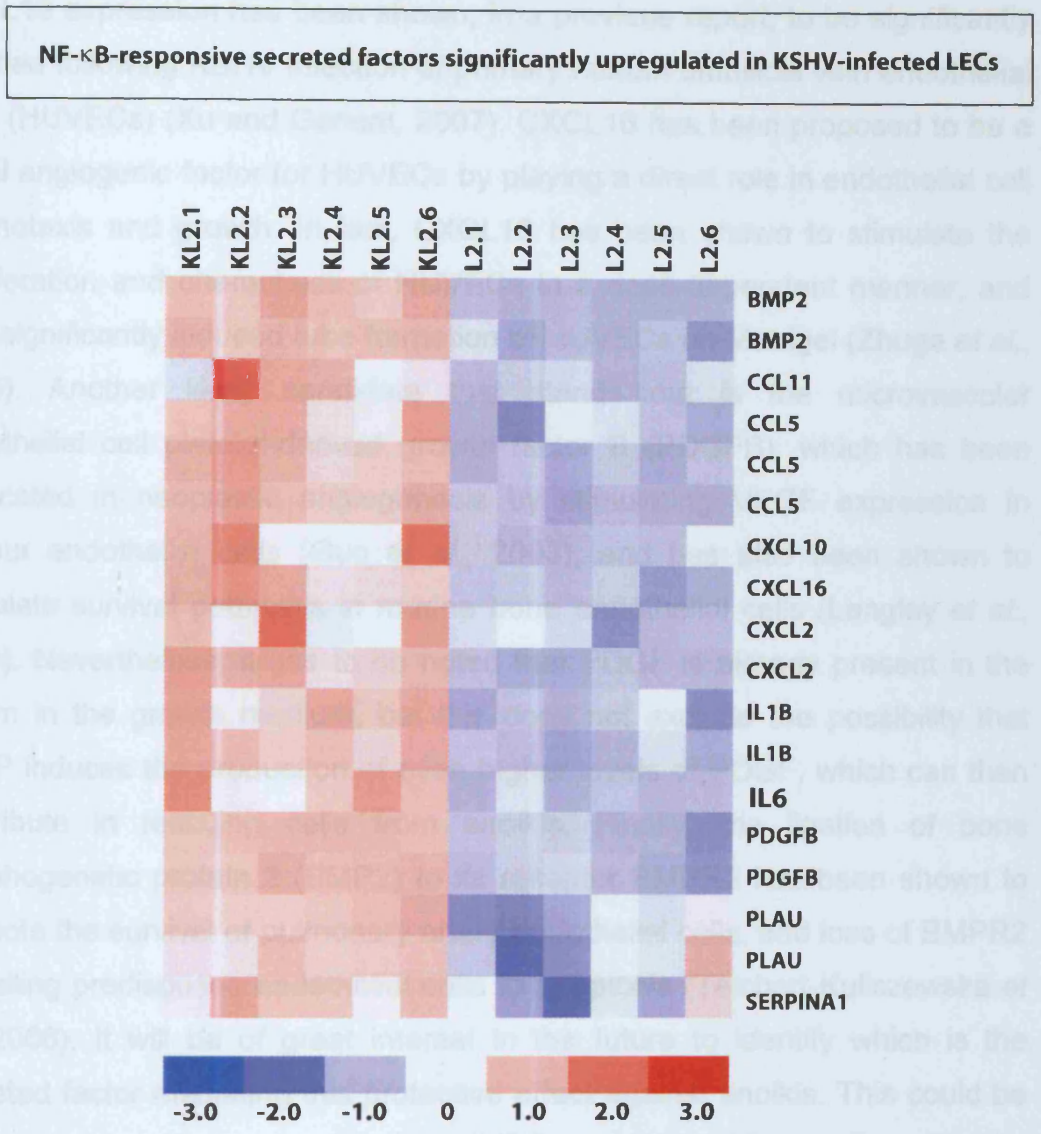

Figure 4.9 Secreted factors with NF-κB responsive elements in their promoters that are upregulated after KSHV infection of LECs

Heatmap of GEM data for NF-κB responsive secreted factors significantly upregulated upon infection of LECs (lymphatic endothelial cells) with KSHV. GEM profiles were obtained for 6 pairs of LECs and KLECs (KSHV-infected LECs) as described in Lagos *et al.* 2007, and the data used to perform this analysis was kindly provided by Dimitrios Lagos and Prof. Chris Boshoff (Viral Oncology Group, Wolfson Institute for Biomedical Research, Cruciform Building,). Downregulated genes are shown in blue and upregulated genes in red. The heat map color scale indicates units of standard deviation from the mean expression of each row (red high and blue low expression). The threshold for significant differential gene regulation after KSHV infection of LECs was set at $q<0.005$. The NF-κB responsive genes within the GEM data were identified using online resources listing NF-κB target genes, namely http://bioinfo.lifl.fr/NF-KB, and http://people.bu.edu/gilmore/nf-kb/target/index/html. The extraction of the secreted factors from the list of NF-κB targets, significantly upregulated after KSHV infection of LECs was performed using the website http://www.affymetrix.com/analysis/index.affx.

CXCL16 expression has been shown, in a previous report, to be significantly induced following KSHV infection of primary human umbilical vein endothelial cells (HUVECs) (Xu and Ganem, 2007). CXCL16 has been proposed to be a novel angiogenic factor for HUVECs by playing a direct role in endothelial cell chemotaxis and growth. In fact, CXCL16 has been shown to stimulate the proliferation and chemotaxis of HUVECs in a dose-dependent manner, and also significantly induced tube formation of HUVECs on Matrigel (Zhuge *et al.*, 2005). Another likely candidate that stands out is the microvascular endothelial cell platelet-derived growth factor B (PDGFB), which has been implicated in neoplastic angiogenesis by stimulating VEGF expression in tumour endothelial cells (Guo *et al.*, 2003), and has also been shown to stimulate survival pathways in murine bone endothelial cells (Langley *et al.*, 2004). Nevertheless, it has to be noted that PDGF is already present in the serum in the growth medium, but this does not exclude the possibility that vFLIP induces the production of even higher levels of PDGF, which can then contribute in rescuing cells from anoikis. Finally, the ligation of bone morphogenetic protein 2 (BMP2) to its receptor BMPR2 has been shown to promote the survival of pulmonary artery endothelial cells, and loss of BMPR2 signalling predisposes endothelial cells to apoptosis (Teichert-Kuliszewska *et al.*, 2006). It will be of great interest in the future to identify which is the secreted factor mediating this protective effect against anoikis. This could be achieved by inducing anoikis in MVECs and providing cells with the recombinant form of each of our target secreted factors, followed by assessing the ability of these factors to rescue cells from detachment-induced apoptosis, in the absence of vFLIP. A more complicated and sophisticated approach might involve a targeted RNAi screen.

Although the exact mechanism via which these secreted growth factors might protect against detachment induced apoptosis is not known, we suggest that this may be through the activation of the PI3K/Akt signalling pathway. As mentioned previously (section 4.1.2.2), numerous studies have suggested an essential role for the PI3K/Akt pathway in the antiapoptotic signalling promoted by integrin-cell matrix interactions. Cell-matrix interactions induce a PI3K/Akt cell survival pathway, and overexpression of constitutively active

PI3K or Akt mutants have been shown to have the ability to inhibit detachment-induced apoptosis of endothelial cells (Khwaja *et al.*, 1997; Wary *et al.*, 1996). Interestingly, CXCL16 has been shown to induce cellular proliferation in human aortic smooth muscle cell, and is capable of increasing cell-cell adhesion in these cells in an NF-κB-dependent manner (Chandrasekar *et al.*, 2004). Consequently, CXCL16-mediated NF-κB activation was shown to occur via heterotrimeric G proteins, PI3K, PDK-1, and Akt (Chandrasekar *et al.*, 2004). Therefore, the vFLIP-mediated CXCL16 secretion might mediate the protection of detached MVECs through a PI3K/Akt survival pathway, leading to the downstream activation of NF-κB, thereby maintaining long lasting activation and at the same time inducing the expression of anti-apoptotic genes regulated by NF-κB. Moreover, conditioned medium from multipotent stromal cells can inhibit hypoxia-induced apoptosis and cell death of primary human aortic endothelial cells (HAECs), and this anti-apoptotic function has been associated with its high content of anti-apoptotic and angiogenic factors, such as IL-6, VEGF and MCP-1. The effects of the conditioned medium on hypoxic HAECs could be reproduced by the addition of recombinant IL-6, and were attributed to its ability to activate the PI3K-Akt pathway (Hung *et al.*, 2007). In addition, the receptors for platelet-derived growth factor, the PDGFRs, have been shown to be critical for PI3K/Akt activation. Reduced PDGFR expression in cells of tuberous sclerosis complex, a benign tumour syndrome with hyperactivation of the negative feedback regulator of PDFGR, mTOR, results in the inhibition of the PI3K/Akt signalling pathway (Zhang *et al.*, 2007). As mentioned previously, PDGFB can stimulate survival pathways in murine bone endothelial cells, and this pro-proliferative effect has been associated with its ability to activate its downstream targets Akt and ERK1/2 (Langley *et al.*, 2004). Finally, BMP2 has been implicated in the development of lung cancer, since it is highly expressed in almost 98% of human lung carcinomas (Langenfeld et al., 2005). BMP-2 has been shown to enhance mobility, invasiveness, and metastasis of cancer cell lines (Langenfeld et al., 2005a; Langenfeld *et al.*, 2003; Langenfeld *et al.*, 2006; Langenfeld and Langenfeld, 2004; Rothhammer *et al.*, 2005; Valdimarsdottir *et al.*, 2002). Forced expression of BMP2 enhances metastatic growth in the lungs of nude mice (Langenfeld *et al.*, 2006), and this

has been shown to be associated with the ability of BMP2 to induce transformation through the activation of the PI3K/mTOR signalling pathway (Langenfeld *et al.*, 2005b). Collectively, these observations support our hypothesis that the candidate NF-κB-dependent secreted factors might be mediating the protection of MVECs against anoikis by signalling through the PI3K/Akt pathway. In light of our recent observation that the supernatant from vFLIP-expressing cells can partially rescue cells from anoikis, it would be very interesting to find out whether blocking of PI3K signalling in cells after exposure to vFLIP supernatant reverses the protective effect, which would indicate that the secreted factor prevents detachment-induced apoptosis by way of PI3K.

It is important to note that supernatant from vFLIP-expressing cells only partially rescued untransduced cells and cells transduced with the control GFP lentivector from anoikis (Figure 4.8), suggesting that additional genes induced by the NF-κB pathway might contribute to the protective effect of vFLIP against detachment-induced apoptosis. Anti-apoptotic genes regulated by NF-κB include Bcl-2, Bcl-X_L, Bfl-1, XIAP, cIAP1, cIAP2, and cFLIP (Burstein and Duckett, 2003), and many of them have also been shown to be regulated by vFLIP for the survival of KSHV-infected PEL cells, such as cIAP-1, cIAP-2, and cFLIP$_L$ (Guasparri *et al.*, 2004). Therefore, vFLIP might be mediating protection against anoikis by inducing the expression of a number of NF-κB target genes involved in the cell proliferation and the prevention of apoptosis.

Finally, Studies of X chromosome inactivation patterns in nodular KS lesions that contain latently infected spindle cells suggest that both monoclonal and polyclonal patterns of inactivation exist (Delabesse *et al.*, 1997; Rabkin *et al.*, 1995; Rabkin *et al.*, 1997). A study of size heterogeneity in KSHV terminal repeats in nodular lesions also demonstrated monoclonal, oligoclonal and polyclonal patterns of infection, implying that KSHV infection precedes tumour expansion (Judde *et al.*, 2000). As inhibition of anoikis is a prerequisite for metastasis (Douma *et al.*, 2004), we suggest that one of the actions of vFLIP in these latently infected cells is to inhibit anoikis and thereby contribute to the

metastasis recognised as a hallmark of epidemic KS (Buchbinder and Friedman-Kien, 1992).

CHAPTER 5

Discussion and Future Directions

5.1 The function of vFLIP

This thesis has presented evidence implicating vFLIP of KSHV in the persistent activation of the transcription factor NF-κB. We have demonstrated that vFLIP can not only activate the classical NF-κB pathway, but is also a potent inducer of the alternative NF-κB pathway in a variety of cell lines. Expression of vFLIP results in classical pathway activation and the subsequent upregulation of p100 expression, which then feeds into the alternative pathway and is actively processed to produce the cleaved p52 subunit. We have identified the region of p100 responsible for its association with vFLIP, which maps within the portion of the p100 C-terminus that contains the Death Domain. This has allowed us to speculate on the composition of the multi-protein complex responsible for mediating IKKα-dependent p100 processing, and the mechanism involved in vFLIP-mediated activation of the alternative NF-κB pathway. We now believe that the direct interaction of vFLIP with both IKKγ and p100 through its Death Effector Domains, mediates the recruitment of p100 to IKKα, which can in turn phosphorylate p100 and lead to its ubiquitin-dependent degradation, without the involvement of any upstream adapters or signalling molecules. Moreover, we have shown that expression of vFLIP in human primary microvascular endothelial cells (MVECs), which are potential target cells for KSHV infection, leads to the activation of NF-κB and the nuclear translocation of RelA/p65, suggesting an important role for vFLIP-mediated NF-κB activation in the establishment of latent infection by KSHV. In addition, our findings indicate that vFLIP-mediated activation of the alternative NF-κB pathway plays a major role in the survival of KSHV-infected PEL cells, since inhibition of p52 expression by siRNA leads to the induction of apoptosis and a decrease in viability of these cells. However, the exact contribution of the alternative versus the canonical NF-κB activation in the survival of KSHV-infected cells, and the subsequent transforming ability of vFLIP, still remains unclear.

Together, these data confirm the hypothesis that the major function of vFLIP in KSHV infection is the activation of NF-κB via IKK. Our studies on the role of vFLIP on MVEC survival have demonstrated that activation of NF-κB by vFLIP has new and significant consequences. It appears that vFLIP expression is capable of rescuing MVECs from detachment-induced apoptosis in an NF-κB-dependent fashion, through the induction of a secreted survival factor. This finding is in agreement with previous reports implicating vFLIP in the upregulation of a number of cytokines and chemokines (see section 1.4.5), and has important implications for vFLIP in KSHV metastasis. This chapter explores some of the other questions concerning the function of vFLIP that remain unanswered.

5.2 How does vFLIP activate NF-κB?

Even though recent studies have outlined the strategy employed by vFLIP to activate NF-κB (Field *et al.*, 2003; Liu *et al.*, 2002; Matta and Chaudhary, 2004; Matta *et al.*, 2007; Matta *et al.*, 2003), some issues have not been addressed yet. Therefore, although we now know that vFLIP activates the classical NF-κB pathway by being recruited to a 700kDa signalsome complex, which consists of IKKα, IKKβ, and IKKγ and has the ability to phosphorylate IκBα (Liu *et al.*, 2002), and the alternative pathway by recruiting p100 to IKKα via its interaction with IKKγ (Matta and Chaudhary, 2004), we still don't know how vFLIP activates the kinase activities of IKKβ and IKKα, respectively. Previous studies initially speculated that a possible mechanism of NF-κB activation by vFLIP was the recruitment of upstream kinases or regulatory proteins, and the first study to show that vFLIP associates with and activates IKK, actually found that vFLIP could interact with the protein kinase RIP (Liu *et al.*, 2002). However, since then the role of upstream kinases has been argued against and it is now clear that upstream activators of the NF-κB pathway such as RIP, NIK, and the TRAFs are dispensable for this process (Matta et al., 2007; Matta et al., 2003). The model that is currently supported is that vFLIP mediates NF-κB activation by directly binding to the IKK complex and activating it. It is possible then that vFLIP might activate IKK by directly binding to the complex and inducing a conformational change, which results in

the oligomerisation and autophosphorylation of the kinase subunits. This is in agreement with reports which have indicated that overexpression of IKKβ leads to the phosphorylation of IKKα and IKKβ itself in the activation loops (Woronicz *et al.*, 1997). Another possible mechanism, which could in fact work in synergy with the one mentioned above, involves the oligomerisation of the IKKγ regulatory subunit of the IKK complex, which also mediates the direct interaction of vFLIP with IKK (Field *et al.*, 2003). A recent study has shown that in unstimulated cells, IKKγ can exist largely as a monomer, while following stimulation by IL-1β, or Tax from HTLV-1, IKKγ dimerizes to form a high molecular weight complex with increased IKK activity (Fontan *et al.*, 2007). Moreover, another group recently suggested that in an inactive state, the helix-loop-helix 2 (HLH2) domain of IKKγ packs against the coiled-coil region 2 (CCR2) and the leucine zipper (LZ) domains, to form a compact helical bundle, which makes key residues inaccessible to potential interacting proteins (Hong *et al.*, 2007), and this conformation probably stabilizes the IKKγ monomer. Interestingly, this region (HLH2) of IKKγ partially overlaps with the vFLIP-binding motif on IKKγ, suggesting that in resting cells, helical bundle formation prevents vFLIP binding by sequestering the necessary region of interaction. In this scenario, vFLIP would activate IKK in a fashion very similar to that proposed for the Tax oncoprotein of HTLV-1 (Hong et al., 2007). Similar to Tax, it is possible that vFLIP stimulation initially induces the unfolding of IKKγ into a fully extended and open conformation, whereby the previously sequestered groups would become accessible, and vFLIP could bind to the C-terminus of IKKγ. Subsequently, binding of vFLIP to IKKγ might stimulate its dimerization (Fontan *et al.*, 2007). It is known that IKKα and IKKβ are associated with the N-terminus of IKKγ, which incidentally contains a region crucial for IKKγ dimerization and is necessary for NF-κB activation (Marienfeld *et al.*, 2006). Therefore, we speculate that stimulation and binding of vFLIP to the C-terminus of IKKγ, results in a fully extended and dimeric IKKγ molecule, which is an optimal conformation for the recruitment of the IKKα and IKKβ kinase subunits, bringing them to close proximity and allowing IKK trans-autophosphorylation, activation, and induction of NF-κB.

5.3 The implications of vFLIP-mediated NF-κB activation for KSHV

Many viruses carry limited genomic information and therefore heavily depend on host factors and processes for their survival, proliferation, and persistence. One of the most sophisticated strategies that viruses have developed is their ability to modulate cellular signalling pathways and transcription factors, and utilize them for their own survival advantage (Santoro *et al.*, 2003). A good example of this process is presented by EBV, the closest human relative of KSHV (Alba *et al.*, 2001; McGeoch and Davison, 1999; Montague and Hutchison, 2000), which expresses the viral oncoprotein that constitutively transmits signals that activate NF-kB and stimulate cell proliferation. LMP-1 mimics the action of TNFR members like CD40, and provides signals to infected B cells which drive their differentiation from naïve B cells towards a memory B cell phenotype (Thorley-Lawson, 2001). This way the virus establishes and maintains persistent latent infection in the host. It appears that KSHV might employ a similar strategy in order to overcome obstacles like apoptosis and host immune responses, through the sustained induction of NF-κB by vFLIP.

NF-κB can be induced very early during infection of host cells by KSHV, and this activation seems to be sustained for a long period of time, possibly contributing to the establishment of latency (Sadagopan *et al.*, 2007). The early phase of activation can probably be attributed to viral entry and the expression of lytic phase genes, such as K1 (Samaniego *et al.*, 2001; Prakash *et al.*, 2002) and vGPCR (Pati *et al.*, 2001), many of which have been shown to have roles in inducing NF-κB. This early phase activation can serve as a first line of defence against apoptosis and host immunity, but can also influence viral gene expression, for example by activating the ORF50 gene RTA (Lan *et al.*, 2004), which contributes to the establishment of latency by activating the transcription of the major latency antigen LANA (Lan *et al.*, 2005). Latency in KSHV-infected cells ensures the expression of viral proteins like vFLIP, which is probably the major factor responsible for maintaining the

sustained NF-κB activation, necessary for infected-cell survival in the later stages of infection.

The induction of NF-κB activation by vFLIP mediates survival of the KSHV-infected cells by activating various anti-apoptotic molecules, and by inducing the secretion of a number of cytokines. In fact, vFLIP has been shown to protect cells from growth factor withdrawal-induced apoptosis by upregulating the expression of the pro-survival Bcl-2 family member Bcl-x_L in an NF-κB-dependent manner (Sun *et al.*, 2003). Moreover, inhibition of vFLIP expression by siRNA results in a significant decrease in NF-κB activity and the subsequent downregulation of NF-κB-regulated cellular prosurvival factors, such as cFLIP, cIAP-1, cIAP-2 (Guasparri *et al.*, 2004). Activation of NF-κB signalling by vFLIP has also been associated with the release of numerous cytokines and growth factors, such as IL-8 (Sun *et al.*, 2006), IL-6 (An *et al.*, 2003), MCP-1, NAP-2, RANTES, and CXCL16 (Xu and Ganem, 2007), which play a pivotal role in the pathogenesis of KS. Indeed, several cytokines which are secreted by KS tumour cells in culture, have been shown to stimulate KS-cell proliferation (Ensoli *et al.*, 1989). Therefore, the activation of NF-κB-dependent cytokines and growth factors by vFLIP, is utilized by KSHV to protect infected cells from immune responses and apoptosis, and confers a growth advantage to the infected-cell population.

The delivery of these survival and pro-proliferative signals by vFLIP-mediated NF-κB activation requires sophisticated regulation of host gene expression, which would enable the virus to deliver the appropriate signal at the correct moment. We believe that this can be achieved by the ability of vFLIP to induce the activation of both the canonical and alternative NF-κB pathways. Classical pathway activation by vFLIP leads to the phosphorylation and subsequent ubiquitin-induced degradation of IκBα, releasing the so-called canonical NF-κB heterodimers, such as p50/RelA and p50/c-Rel (Pomerantz and Baltimore, 2002). The alternative NF-κB pathway regulates the processing of the p100 precursor, which preferentially sequesters RelB in the cytoplasm, and therefore the induction of the alternative NF-κB pathway by vFLIP results in the generation and release of p52/RelB heterodimers (Dejardin *et al.*, 1995).

However, p100 can also associate with other Rel molecules, and this interaction generates a pool of separate p52-containing dimers, such as p52/p65 and p52/c-Rel (Naumann *et al.*, 1993). These are retained in the cytoplasm by IκB inhibitors and require the activation of the IKK complex, through the induction of the classical pathway, to be released into the nucleus. Therefore, vFLIP also contributes to the formation of p52/p65 and p52/c-Rel dimers (through activation of the alternative NF-κB pathway), as well as their activation and release (through activation of the canonical NF-κB pathway). Each combination of Rel proteins shows differential specificity for DNA binding sites, and has its own transactivating potential (Verma *et al.*, 1995). Therefore, by releasing a wide and varying combination of Rel proteins into the nucleus, vFLIP is able to transmit a multitude of signals and can also regulate the transcription of different genes with great specificity, which allows for the fine-tuning of the different survival signals over time. In order to dissect the exact role and the mechanism of vFLIP-mediated NF-κB activation in the survival of KSHV-infected cells, it would be interesting in the future to use chromatin immunoprecipitation (ChIP) assays, in order to determine which gene promoters are engaged by which Rel molecules, in cells expressing vFLIP.

5.4 Role of the alternative NF-κB pathway in KSHV pathogenesis

In humans, aberrant processing of p100 has been found in various lymphomas, such as cutaneous T-cell lymphomas, B-cell non-Hodgkin lymphomas, chronic lymphocytic leukaemia, and myelomas (Rayet and Gelinas, 1999; Sun and Xiao, 2003). These lymphomas are always associated with the presence of C-terminal truncation mutants of p100 lacking the PID, which are capable of transforming fibroblasts, and therefore have a significant oncogenic potential (Ciana *et al.*, 1997). Overproduction of p52 in mice results in lymphoid hyperplasia, suggesting that p52 plays an important role in promoting the proliferation of cells and blocking apoptosis (Ishikawa *et al.*, 1997). Moreover, in human carcinomas of the breast, p52 is significantly overexpressed, and this upregulation is specific to tumour cells (Cogswell *et al.*, 2000). Several oncogenic viruses have also been shown to induce the

constitutive processing of p100, namely HTLV-1, which mediates the activation of p52 production by its transforming oncoprotein Tax (Xiao *et al.*, 2001), also the transforming protein LMP-1 of EBV can induce p100 processing (Atkinson *et al.*, 2003), and as described in this thesis and by others, vFLIP expression from KSHV results in the persistent activation of the alternative NF-κB pathway (Matta and Chaudhary, 2004). The fact that all of these oncogenic viruses have evolved the ability to induce constitutive p100 processing, suggests that the alternative NF-κB pathway must play an important role in infected-cell survival and transformation. Therefore, it is logical to wonder how p52 mediates its oncogenic potential, and what mechanisms it employs to transform virally-infected cells.

Recently, p100 was shown to have a pro-apoptotic function, which was associated with the DD of p100 and the activation of caspase-8 (Hacker and Karin, 2002; Wang *et al.*, 2002). Therefore, constitutive processing of p100 by a virus like KSHV would ensure the removal of the DD, and would abolish the pro-apoptotic potential of p100, facilitating cell transformation. Moreover, it has been demonstrated that p52 homodimers, in association with the Bcl-3 coactivator, can induce the expression of the anti-apoptotic factor Bcl-2, and in breast cancer cells, elevated levels of p52 are associated with the upregulation of endogenous Bcl-2 expression (Viatour *et al.*, 2003). In addition, a study on the role of stromal cells in the survival of non-Hodgkin's lymphoma cells, showed that adhesion of the two cell types resulted in p100 processing and generation of p52/RelA and p52/RelB dimers, which were associated with the upregulation NF-κB-dependent anti-apoptotic factors, such as XIAP, cIAP, and $cIAP_2$ (Lwin *et al.*, 2007). A different strategy of cell transformation by p52 might be the regulation of Cyclin D1 expression, as p52 and Bcl-3 have been shown to associate with the Cyclin D1 promoter (Rocha *et al.*, 2003; Romieu-Mourez *et al.*, 2003; Westerheide *et al.*, 2001), which would lead to progression through the G1-S phase of the cell cycle, thereby promoting the proliferation of virally-infected cells. Recently, a transgenic mouse model for ductal development in the formation of the mammary gland, demonstrated that overexpression of p100/p52 led to an increase in Cyclin D1 levels, which was responsible for an accelerated rate of proliferation in ductal

epithelium and the appearance of areas with hyperplastic growth (Connelly *et al.*, 2007). A recent study on the effects of p52 on cell proliferation and the cell cycle, presented compelling evidence implicating p52 as a regulator of the tumour suppressor p53 and its target genes (Schumm *et al.*, 2006). It appears that p53 recruits p52 to the promoters of its target genes, where p52 can regulate the recruitment of coactivators and corepressors to modulate p53-target gene expression. In this report, p52 was shown to downregulate the expression of the CDK inhibitor $p21^{WAF1/CIP1}$ in a p53-dependent manner, by being recruited to the p21 promoter by p53, and inducing the recruitment of the corepressor Histone Deacetylase 1 (HDAC1), thereby suppressing its expression (Schumm *et al.*, 2006). Collectively, these data suggest that p52 plays a major role in tumourigenesis by inducing the expression of anti-apoptotic genes and regulating the cell cycle, and provide a possible explanation as to why oncogenic viruses have evolved the ability to persistently activate the alternative NF-κB pathway.

References

Acehan, D., Jiang, X., Morgan, D. G., Heuser, J. E., Wang, X. and Akey, C. W. (2002). Three-dimensional structure of the apoptosome: implications for assembly, procaspase-9 binding, and activation. *Mol Cell* **9**, 423-32.

Agou, F., Ye, F., Goffinont, S., Courtois, G., Yamaoka, S., Israel, A. and Veron, M. (2002). NEMO trimerizes through its coiled-coil C-terminal domain. *J Biol Chem* **277**, 17464-75.

Alavi, A., Hood, J. D., Frausto, R., Stupack, D. G. and Cheresh, D. A. (2003). Role of Raf in vascular protection from distinct apoptotic stimuli. *Science* **301**, 94-6.

Alba, M. M., Das, R., Orengo, C. A. and Kellam, P. (2001). Genomewide function conservation and phylogeny in the Herpesviridae. *Genome Res* **11**, 43-54.

Alkalay, I., Yaron, A., Hatzubai, A., Jung, S., Avraham, A., Gerlitz, O., Pashut-Lavon, I. and Ben-Neriah, Y. (1995a). In vivo stimulation of I kappa B phosphorylation is not sufficient to activate NF-kappa B. *Mol Cell Biol* **15**, 1294-301.

Alkalay, I., Yaron, A., Hatzubai, A., Orian, A., Ciechanover, A. and Ben-Neriah, Y. (1995b). Stimulation-dependent I kappa B alpha phosphorylation marks the NF-kappa B inhibitor for degradation via the ubiquitin-proteasome pathway. *Proc Natl Acad Sci U S A* **92**, 10599-603.

Alon, T., Hemo, I., Itin, A., Pe'er, J., Stone, J. and Keshet, E. (1995). Vascular endothelial growth factor acts as a survival factor for newly formed retinal vessels and has implications for retinopathy of prematurity. *Nat Med* **1**, 1024-8.

Ambroziak, J. A., Blackbourn, D. J., Herndier, B. G., Glogau, R. G., Gullett, J. H., McDonald, A. R., Lennette, E. T. and Levy, J. A. (1995). Herpes-like sequences in HIV-infected and uninfected Kaposi's sarcoma patients. *Science* **268**, 582-3.

Amir, R. E., Haecker, H., Karin, M. and Ciechanover, A. (2004). Mechanism of processing of the NF-kappa B2 p100 precursor: identification of the specific polyubiquitin chain-anchoring lysine residue and analysis of the role of NEDD8-modification on the SCF(beta-TrCP) ubiquitin ligase. *Oncogene* **23**, 2540-7.

An, F. Q., Compitello, N., Horwitz, E., Sramkoski, M., Knudsen, E. S. and Renne, R. (2005). The latency-associated nuclear antigen of Kaposi's sarcoma-associated herpesvirus modulates cellular gene expression and protects lymphoid cells from p16 INK4A-induced cell cycle arrest. *J Biol Chem* **280**, 3862-74.

An, J., Lichtenstein, A. K., Brent, G. and Rettig, M. B. (2002). The Kaposi sarcoma-associated herpesvirus (KSHV) induces cellular interleukin 6 expression: role of the KSHV latency-associated nuclear antigen and the AP1 response element. *Blood* **99**, 649-54.

An, J., Sun, Y., Sun, R. and Rettig, M. B. (2003). Kaposi's sarcoma-associated herpesvirus encoded vFLIP induces cellular IL-6 expression: the role of the NF-kappaB and JNK/AP1 pathways. *Oncogene* **22**, 3371-85.

Anest, V., Hanson, J. L., Cogswell, P. C., Steinbrecher, K. A., Strahl, B. D. and Baldwin, A. S. (2003). A nucleosomal function for IkappaB kinase-alpha in NF-kappaB-dependent gene expression. *Nature* **423**, 659-63.

Aoki, Y., Jaffe, E. S., Chang, Y., Jones, K., Teruya-Feldstein, J., Moore, P. S. and Tosato, G. (1999). Angiogenesis and hematopoiesis induced by Kaposi's sarcoma-associated herpesvirus-encoded interleukin-6. *Blood* **93**, 4034-43.

Aoki, Y., Yarchoan, R., Braun, J., Iwamoto, A. and Tosato, G. (2000). Viral and cellular cytokines in AIDS-related malignant lymphomatous effusions. *Blood* **96**, 1599-601.

Arvanitakis, L., Geras-Raaka, E., Varma, A., Gershengorn, M. C. and Cesarman, E. (1997). Human herpesvirus KSHV encodes a constitutively active G-protein-coupled receptor linked to cell proliferation. *Nature* **385**, 347-50.

Arvanitakis, L., Mesri, E. A., Nador, R. G., Said, J. W., Asch, A. S., Knowles, D. M. and Cesarman, E. (1996). Establishment and characterization of a primary effusion (body cavity-based) lymphoma cell line (BC-3) harboring kaposi's sarcoma-associated herpesvirus (KSHV/HHV-8) in the absence of Epstein-Barr virus. *Blood* **88**, 2648-54.

Atkinson, P. G., Coope, H. J., Rowe, M. and Ley, S. C. (2003). Latent membrane protein 1 of Epstein-Barr virus stimulates processing of NF-kappa B2 p100 to p52. *J Biol Chem* **278**, 51134-42.

AuCoin, D. P., Colletti, K. S., Cei, S. A., Papouskova, I., Tarrant, M. and Pari, G. S. (2004). Amplification of the Kaposi's sarcoma-associated herpesvirus/human herpesvirus 8 lytic origin of DNA replication is dependent upon a cis-acting AT-rich region and an ORF50 response element and the trans-acting factors ORF50 (K-Rta) and K8 (K-bZIP). *Virology* **318**, 542-55.

Bais, C., Santomasso, B., Coso, O., Arvanitakis, L., Raaka, E. G., Gutkind, J. S., Asch, A. S., Cesarman, E., Gershengorn, M. C. and Mesri, E. A. (1998). G-protein-coupled receptor of Kaposi's sarcoma-associated herpesvirus is a viral oncogene and angiogenesis activator. *Nature* **391**, 86-9.

Bais, C., Van Geelen, A., Eroles, P., Mutlu, A., Chiozzini, C., Dias, S., Silverstein, R. L., Rafii, S. and Mesri, E. A. (2003). Kaposi's sarcoma associated herpesvirus G protein-coupled receptor immortalizes human endothelial cells by activation of the VEGF receptor-2/ KDR. *Cancer Cell* **3**, 131-43.

Baldwin, A. S. (2001). Control of oncogenesis and cancer therapy resistance by the transcription factor NF-kappaB. *J Clin Invest* **107**, 241-6.

Ballestas, M. E., Chatis, P. A. and Kaye, K. M. (1999). Efficient persistence of extrachromosomal KSHV DNA mediated by latency-associated nuclear antigen. *Science* **284**, 641-4.

Ballestas, M. E. and Kaye, K. M. (2001). Kaposi's sarcoma-associated herpesvirus latency-associated nuclear antigen 1 mediates episome persistence through cis-acting terminal repeat (TR) sequence and specifically binds TR DNA. *J Virol* **75**, 3250-8.

Barbera, A. J., Chodaparambil, J. V., Kelley-Clarke, B., Luger, K. and Kaye, K. M. (2006). Kaposi's sarcoma-associated herpesvirus LANA hitches a ride on the chromosome. *Cell Cycle* **5**, 1048-52.

Bayley, A. C. (1984). Aggressive Kaposi's sarcoma in Zambia, 1983. *Lancet* **1**, 1318-20.

Beckstead, J. H., Wood, G. S. and Fletcher, V. (1985). Evidence for the origin of Kaposi's sarcoma from lymphatic endothelium. *Am J Pathol* **119**, 294-300.

Belanger, C., Gravel, A., Tomoiu, A., Janelle, M. E., Gosselin, J., Tremblay, M. J. and Flamand, L. (2001). Human herpesvirus 8 viral FLICE-inhibitory protein inhibits Fas-mediated apoptosis through binding and prevention of procaspase-8 maturation. *J Hum Virol* **4**, 62-73.

Ben-Neriah, Y. (2002). Regulatory functions of ubiquitination in the immune system. *Nat Immunol* **3**, 20-6.

Ben-Ze'ev, A., Farmer, S. R. and Penman, S. (1980). Protein synthesis requires cell-surface contact while nuclear events respond to cell shape in anchorage-dependent fibroblasts. *Cell* **21**, 365-72.

Benjamin, L. E., Golijanin, D., Itin, A., Pode, D. and Keshet, E. (1999). Selective ablation of immature blood vessels in established human tumors follows vascular endothelial growth factor withdrawal. *J Clin Invest* **103**, 159-65.

Benjamin, L. E. and Keshet, E. (1997). Conditional switching of vascular endothelial growth factor (VEGF) expression in tumors: induction of endothelial cell shedding and regression of hemangioblastoma-like vessels by VEGF withdrawal. *Proc Natl Acad Sci U S A* **94**, 8761-6.

Beral, V., Peterman, T. A., Berkelman, R. L. and Jaffe, H. W. (1990). Kaposi's sarcoma among persons with AIDS: a sexually transmitted infection? *Lancet* **335**, 123-8.

Beraud, C., Sun, S. C., Ganchi, P., Ballard, D. W. and Greene, W. C. (1994). Human T-cell leukemia virus type I Tax associates with and is negatively regulated by the NF-kappa B2 p100 gene product: implications for viral latency. *Mol Cell Biol* **14**, 1374-82.

Bertin, J., Armstrong, R. C., Ottilie, S., Martin, D. A., Wang, Y., Banks, S., Wang, G. H., Senkevich, T. G., Alnemri, E. S., Moss, B. *et al.* (1997). Death effector domain-containing herpesvirus and poxvirus proteins inhibit both Fas- and TNFR1-induced apoptosis. *Proc Natl Acad Sci U S A* **94**, 1172-6.

Bertin, J., Wang, L., Guo, Y., Jacobson, M. D., Poyet, J. L., Srinivasula, S. M., Merriam, S., DiStefano, P. S. and Alnemri, E. S. (2001). CARD11 and CARD14 are novel caspase recruitment domain (CARD)/membrane-associated guanylate kinase (MAGUK) family members that interact with BCL10 and activate NF-kappa B. *J Biol Chem* **276**, 11877-82.

Besnier, C., Takeuchi, Y. and Towers, G. (2002). Restriction of lentivirus in monkeys. *Proc Natl Acad Sci U S A* **99**, 11920-5.

Betts, J. C. and Nabel, G. J. (1996). Differential regulation of NF-kappaB2(p100) processing and control by amino-terminal sequences. *Mol Cell Biol* **16**, 6363-71.

Bieleski, L. and Talbot, S. J. (2001). Kaposi's sarcoma-associated herpesvirus vCyclin open reading frame contains an internal ribosome entry site. *J Virol* **75**, 1864-9.

Bin, L., Li, X., Xu, L. G. and Shu, H. B. (2002). The short splice form of Casper/c-FLIP is a major cellular inhibitor of TRAIL-induced apoptosis. *FEBS Lett* **510**, 37-40.

Bishop, G. A. (2004). The multifaceted roles of TRAFs in the regulation of B-cell function. *Nat Rev Immunol* **4**, 775-86.

Blair, W. S., Bogerd, H. P., Madore, S. J. and Cullen, B. R. (1994). Mutational analysis of the transcription activation domain of RelA: identification of a highly synergistic minimal acidic activation module. *Mol Cell Biol* **14**, 7226-34.

Blobel, G. A. (2000). CREB-binding protein and p300: molecular integrators of hematopoietic transcription. *Blood* **95**, 745-55.

Boatright, K. M. and Salvesen, G. S. (2003). Mechanisms of caspase activation. *Curr Opin Cell Biol* **15**, 725-31.

Bonizzi, G. and Karin, M. (2004). The two NF-kappaB activation pathways and their role in innate and adaptive immunity. *Trends Immunol* **25**, 280-8.

Bonneau, A. M. and Sonenberg, N. (1987). Involvement of the 24-kDa cap-binding protein in regulation of protein synthesis in mitosis. *J Biol Chem* **262**, 11134-9.

Booy, F. P., Newcomb, W. W., Trus, B. L., Brown, J. C., Baker, T. S. and Steven, A. C. (1991). Liquid-crystalline, phage-like packing of encapsidated DNA in herpes simplex virus. *Cell* **64**, 1007-15.

Borkovic, S. P. and Schwartz, R. A. (1981). Kaposi's sarcoma presenting in the homosexual man -- a new and striking phenomenon! *Ariz Med* **38**, 902-4.

Boshoff, C., Gao, S. J., Healy, L. E., Matthews, S., Thomas, A. J., Coignet, L., Warnke, R. A., Strauchen, J. A., Matutes, E., Kamel, O. W. *et al.* (1998). Establishing a KSHV+ cell line (BCP-1) from peripheral blood and characterizing its growth in Nod/SCID mice. *Blood* **91**, 1671-9.

Boshoff, C., Schulz, T. F., Kennedy, M. M., Graham, A. K., Fisher, C., Thomas, A., McGee, J. O., Weiss, R. A. and O'Leary, J. J. (1995). Kaposi's sarcoma-associated herpesvirus infects endothelial and spindle cells. *Nat Med* **1**, 1274-8.

Boshoff, C. and Weiss, R. (2002). AIDS-related malignancies. *Nat Rev Cancer* **2**, 373-82.

Boshoff, C. and Weiss, R. A. (1998). Kaposi's sarcoma-associated herpesvirus. *Adv Cancer Res* **75**, 57-86.

Boshoff, C. and Weiss, R. A. (2001). Epidemiology and pathogenesis of Kaposi's sarcoma-associated herpesvirus. *Philos Trans R Soc Lond B Biol Sci* **356**, 517-34.

Bours, V., Franzoso, G., Azarenko, V., Park, S., Kanno, T., Brown, K. and Siebenlist, U. (1993). The oncoprotein Bcl-3 directly transactivates through kappa B motifs via association with DNA-binding p50B homodimers. *Cell* **72**, 729-39.

Bradford, M. M. (1976). A rapid and sensitive method for the quantitation of microgram quantities of protein utilizing the principle of protein-dye binding. *Anal Biochem* **72**, 248-54.

Bratton, S. B., MacFarlane, M., Cain, K. and Cohen, G. M. (2000). Protein complexes activate distinct caspase cascades in death receptor and stress-induced apoptosis. *Exp Cell Res* **256**, 27-33.

Brinkmann, M. M., Glenn, M., Rainbow, L., Kieser, A., Henke-Gendo, C. and Schulz, T. F. (2003). Activation of mitogen-activated protein kinase and NF-kappaB pathways by a Kaposi's sarcoma-associated herpesvirus K15 membrane protein. *J Virol* **77**, 9346-58.

Brinkmann, M. M., Pietrek, M., Dittrich-Breiholz, O., Kracht, M. and Schulz, T. F. (2007). Modulation of host gene expression by the K15 protein of Kaposi's sarcoma-associated herpesvirus. *J Virol* **81**, 42-58.

Brinkmann, M. M. and Schulz, T. F. (2006). Regulation of intracellular signalling by the terminal membrane proteins of members of the Gammaherpesvirinae. *J Gen Virol* **87**, 1047-74.

Brooks, P. C., Clark, R. A. and Cheresh, D. A. (1994). Requirement of vascular integrin alpha v beta 3 for angiogenesis. *Science* **264**, 569-71.

Brown, A. M., Linhoff, M. W., Stein, B., Wright, K. L., Baldwin, A. S., Jr., Basta, P. V. and Ting, J. P. (1994). Function of NF-kappa B/Rel binding sites in the major histocompatibility complex class II invariant chain promoter is dependent on cell-specific binding of different NF-kappa B/Rel subunits. *Mol Cell Biol* **14**, 2926-35.

Brown, H. J., Song, M. J., Deng, H., Wu, T. T., Cheng, G. and Sun, R. (2003). NF-kappaB inhibits gammaherpesvirus lytic replication. *J Virol* **77**, 8532-40.

Brown, K., Gerstberger, S., Carlson, L., Franzoso, G. and Siebenlist, U. (1995). Control of I kappa B-alpha proteolysis by site-specific, signal-induced phosphorylation. *Science* **267**, 1485-8.

Brummelkamp, T. R., Nijman, S. M., Dirac, A. M. and Bernards, R. (2003). Loss of the cylindromatosis tumour suppressor inhibits apoptosis by activating NF-kappaB. *Nature* **424**, 797-801.

Bubman, D., Guasparri, I. and Cesarman, E. (2007). Deregulation of c-Myc in primary effusion lymphoma by Kaposi's sarcoma herpesvirus latency-associated nuclear antigen. *Oncogene* **26**, 4979-86.

Buchbinder, A. and Friedman-Kien, A. E. (1992). Clinical aspects of Kaposi's sarcoma. *Curr Opin Oncol* **4**, 867-74.

Bull, P., Morley, K. L., Hoekstra, M. F., Hunter, T. and Verma, I. M. (1990). The mouse c-rel protein has an N-terminal regulatory domain and a C-terminal transcriptional transactivation domain. *Mol Cell Biol* **10**, 5473-85.

Burns, K. A. and Martinon, F. (2004). Inflammatory diseases: is ubiquitinated NEMO at the hub? *Curr Biol* **14**, R1040-2.

Burstein, E. and Duckett, C. S. (2003). Dying for NF-kappaB? Control of cell death by transcriptional regulation of the apoptotic machinery. *Curr Opin Cell Biol* **15**, 732-7.

Burysek, L. and Pitha, P. M. (2001). Latently expressed human herpesvirus 8-encoded interferon regulatory factor 2 inhibits double-stranded RNA-activated protein kinase. *J Virol* **75**, 2345-52.

Burysek, L., Yeow, W. S., Lubyova, B., Kellum, M., Schafer, S. L., Huang, Y. Q. and Pitha, P. M. (1999a). Functional analysis of human herpesvirus 8-encoded viral interferon regulatory factor 1 and its association with cellular interferon regulatory factors and p300. *J Virol* **73**, 7334-42.

Burysek, L., Yeow, W. S. and Pitha, P. M. (1999b). Unique properties of a second human herpesvirus 8-encoded interferon regulatory factor (vIRF-2). *J Hum Virol* **2**, 19-32.

Bussolino, F., Di Renzo, M. F., Ziche, M., Bocchietto, E., Olivero, M., Naldini, L., Gaudino, G., Tamagnone, L., Coffer, A. and Comoglio, P. M. (1992). Hepatocyte growth factor is a potent angiogenic factor which stimulates endothelial cell motility and growth. *J Cell Biol* **119**, 629-41.

Caamano, J. H., Rizzo, C. A., Durham, S. K., Barton, D. S., Raventos-Suarez, C., Snapper, C. M. and Bravo, R. (1998). Nuclear factor (NF)-kappa B2 (p100/p52) is required for normal splenic microarchitecture and B cell-mediated immune responses. *J Exp Med* **187**, 185-96.

Cahir-McFarland, E. D., Carter, K., Rosenwald, A., Giltnane, J. M., Henrickson, S. E., Staudt, L. M. and Kieff, E. (2004). Role of NF-kappa B in cell survival and transcription of latent membrane protein 1-expressing or Epstein-Barr virus latency III-infected cells. *J Virol* **78**, 4108-19.

Cai, Q. L., Knight, J. S., Verma, S. C., Zald, P. and Robertson, E. S. (2006). EC5S ubiquitin complex is recruited by KSHV latent antigen LANA for degradation of the VHL and p53 tumor suppressors. *PLoS Pathog* **2**, e116.

Cai, X. and Cullen, B. R. (2006). Transcriptional origin of Kaposi's sarcoma-associated herpesvirus microRNAs. *J Virol* **80**, 2234-42.

Cai, X., Lu, S., Zhang, Z., Gonzalez, C. M., Damania, B. and Cullen, B. R. (2005). Kaposi's sarcoma-associated herpesvirus expresses an array of viral microRNAs in latently infected cells. *Proc Natl Acad Sci U S A* **102**, 5570-5.

Calderhead, D. M., Kosaka, Y., Manning, E. M. and Noelle, R. J. (2000). CD40-CD154 interactions in B-cell signaling. *Curr Top Microbiol Immunol* **245**, 73-99.

Callahan, J., Pai, S., Cotter, M. and Robertson, E. S. (1999). Distinct patterns of viral antigen expression in Epstein-Barr virus and Kaposi's sarcoma-associated herpesvirus coinfected body-cavity-based lymphoma cell lines: potential switches in latent gene expression due to coinfection. *Virology* **262**, 18-30.

Cannon, M., Cesarman, E. and Boshoff, C. (2006). KSHV G protein-coupled receptor inhibits lytic gene transcription in primary-effusion lymphoma cells via p21-mediated inhibition of Cdk2. *Blood* **107**, 277-84.

Cannon, M., Philpott, N. J. and Cesarman, E. (2003). The Kaposi's sarcoma-associated herpesvirus G protein-coupled receptor has broad signaling effects in primary effusion lymphoma cells. *J Virol* **77**, 57-67.

Carbone, A., Cilia, A. M., Gloghini, A., Capello, D., Perin, T., Bontempo, D., Canzonieri, V., Tirelli, U., Volpe, R. and Gaidano, G. (2000). Primary effusion lymphoma cell lines harbouring human herpesvirus type-8. *Leuk Lymphoma* **36**, 447-56.

Carbone, A., Cilia, A. M., Gloghini, A., Capello, D., Todesco, M., Quattrone, S., Volpe, R. and Gaidano, G. (1998). Establishment and characterization of EBV-positive and EBV-negative primary effusion lymphoma cell lines harbouring human herpesvirus type-8. *Br J Haematol* **102**, 1081-9.

Carbone, A., Gloghini, A., Vaccher, E., Zagonel, V., Pastore, C., Dalla Palma, P., Branz, F., Saglio, G., Volpe, R., Tirelli, U. *et al.* (1996). Kaposi's sarcoma-associated herpesvirus DNA sequences in AIDS-related and AIDS-unrelated lymphomatous effusions. *Br J Haematol* **94**, 533-43.

Carmeliet, P. (2003). Angiogenesis in health and disease. *Nat Med* **9**, 653-60.

Carmeliet, P., Lampugnani, M. G., Moons, L., Breviario, F., Compernolle, V., Bono, F., Balconi, G., Spagnuolo, R., Oostuyse, B., Dewerchin, M. *et al.* (1999). Targeted deficiency or cytosolic truncation of the VE-cadherin gene in mice impairs VEGF-mediated endothelial survival and angiogenesis. *Cell* **98**, 147-57.

Caselli, E., Fiorentini, S., Amici, C., Di Luca, D., Caruso, A. and Santoro, M. G. (2007). Human herpesvirus 8 acute infection of endothelial cells induces monocyte chemoattractant protein 1-dependent capillary-like structure formation: role of the IKK/NF-kappaB pathway. *Blood* **109**, 2718-26.

Castelman, B., Iverson, L., and Menendez, V. P. . (1956). Localised mediastinal lymph-node hyperplasia resembling thymoma. *Cancer*, 822-830.

Cesarman, E., Chang, Y., Moore, P. S., Said, J. W. and Knowles, D. M. (1995a). Kaposi's sarcoma-associated herpesvirus-like DNA sequences in AIDS-related body-cavity-based lymphomas. *N Engl J Med* **332**, 1186-91.

Cesarman, E., Moore, P. S., Rao, P. H., Inghirami, G., Knowles, D. M. and Chang, Y. (1995b). In vitro establishment and characterization of two acquired immunodeficiency syndrome-related lymphoma cell lines (BC-1 and BC-2) containing Kaposi's sarcoma-associated herpesvirus-like (KSHV) DNA sequences. *Blood* **86**, 2708-14.

Cesarman, E., Nador, R. G., Bai, F., Bohenzky, R. A., Russo, J. J., Moore, P. S., Chang, Y. and Knowles, D. M. (1996). Kaposi's sarcoma-associated herpesvirus contains G protein-

coupled receptor and cyclin D homologs which are expressed in Kaposi's sarcoma and malignant lymphoma. *J Virol* **70**, 8218-23.

Chadburn, A., Cesarman, E., Nador, R. G., Liu, Y. F. and Knowles, D. M. (1997). Kaposi's sarcoma-associated herpesvirus sequences in benign lymphoid proliferations not associated with human immunodeficiency virus. *Cancer* **80**, 788-97.

Chandrasekar, B., Bysani, S. and Mummidi, S. (2004). CXCL16 signals via Gi, phosphatidylinositol 3-kinase, Akt, I kappa B kinase, and nuclear factor-kappa B and induces cell-cell adhesion and aortic smooth muscle cell proliferation. *J Biol Chem* **279**, 3188-96.

Chang, C. C., Zhang, J., Lombardi, L., Neri, A. and Dalla-Favera, R. (1995). Rearranged NFKB-2 genes in lymphoid neoplasms code for constitutively active nuclear transactivators. *Mol Cell Biol* **15**, 5180-7.

Chang, D. W., Claassen, G. F., Hann, S. R. and Cole, M. D. (2000a). The c-Myc transactivation domain is a direct modulator of apoptotic versus proliferative signals. *Mol Cell Biol* **20**, 4309-19.

Chang, D. W., Xing, Z., Pan, Y., Algeciras-Schimnich, A., Barnhart, B. C., Yaish-Ohad, S., Peter, M. E. and Yang, X. (2002a). c-FLIP(L) is a dual function regulator for caspase-8 activation and CD95-mediated apoptosis. *Embo J* **21**, 3704-14.

Chang, J., Renne, R., Dittmer, D. and Ganem, D. (2000b). Inflammatory cytokines and the reactivation of Kaposi's sarcoma-associated herpesvirus lytic replication. *Virology* **266**, 17-25.

Chang, P. J., Shedd, D., Gradoville, L., Cho, M. S., Chen, L. W., Chang, J. and Miller, G. (2002b). Open reading frame 50 protein of Kaposi's sarcoma-associated herpesvirus directly activates the viral PAN and K12 genes by binding to related response elements. *J Virol* **76**, 3168-78.

Chang, Y., Cesarman, E., Pessin, M. S., Lee, F., Culpepper, J., Knowles, D. M. and Moore, P. S. (1994). Identification of herpesvirus-like DNA sequences in AIDS-associated Kaposi's sarcoma. *Science* **266**, 1865-9.

Chang, Y. and Moore, P. S. (1996). Kaposi's Sarcoma (KS)-associated herpesvirus and its role in KS. *Infect Agents Dis* **5**, 215-22.

Chang, Y., Moore, P. S., Talbot, S. J., Boshoff, C. H., Zarkowska, T., Godden, K., Paterson, H., Weiss, R. A. and Mittnacht, S. (1996). Cyclin encoded by KS herpesvirus. *Nature* **382**, 410.

Chao, D. T. and Korsmeyer, S. J. (1998). BCL-2 family: regulators of cell death. *Annu Rev Immunol* **16**, 395-419.

Chatterjee, M., Osborne, J., Bestetti, G., Chang, Y. and Moore, P. S. (2002). Viral IL-6-induced cell proliferation and immune evasion of interferon activity. *Science* **298**, 1432-5.

Chaudhary, P. M., Eby, M. T., Jasmin, A., Kumar, A., Liu, L. and Hood, L. (2000). Activation of the NF-kappaB pathway by caspase 8 and its homologs. *Oncogene* **19**, 4451-60.

Chaudhary, P. M., Jasmin, A., Eby, M. T. and Hood, L. (1999). Modulation of the NF-kappa B pathway by virally encoded death effector domains-containing proteins. *Oncogene* **18**, 5738-46.

Chen, G., Cao, P. and Goeddel, D. V. (2002). TNF-induced recruitment and activation of the IKK complex require Cdc37 and Hsp90. *Mol Cell* **9**, 401-10.

Chen, Z., Hagler, J., Palombella, V. J., Melandri, F., Scherer, D., Ballard, D. and Maniatis, T. (1995). Signal-induced site-specific phosphorylation targets I kappa B alpha to the ubiquitin-proteasome pathway. *Genes Dev* **9**, 1586-97.

Chen, Z. J. (2005). Ubiquitin signalling in the NF-kappaB pathway. *Nat Cell Biol* **7**, 758-65.

Chen, Z. J., Bhoj, V. and Seth, R. B. (2006). Ubiquitin, TAK1 and IKK: is there a connection? *Cell Death Differ* **13**, 687-92.

Chen, Z. J., Parent, L. and Maniatis, T. (1996). Site-specific phosphorylation of IkappaBalpha by a novel ubiquitination-dependent protein kinase activity. *Cell* **84**, 853-62.

Cherqui, S., Kingdon, K. M., Thorpe, C., Kurian, S. M. and Salomon, D. R. (2007). Lentiviral Gene Delivery of vMIP-II to Transplanted Endothelial Cells and Endothelial Progenitors Is Proangiogenic In Vivo. *Mol Ther* **15**, 1264-72.

Chinnaiyan, A. M., O'Rourke, K., Tewari, M. and Dixit, V. M. (1995). FADD, a novel death domain-containing protein, interacts with the death domain of Fas and initiates apoptosis. *Cell* **81**, 505-12.

Cho, I. R., Jeong, S., Jhun, B. H., An, W. G., Lee, B., Kwak, Y. T., Lee, S. H., Jung, J. U. and Chung, Y. H. (2007). Activation of non-canonical NF-kappaB pathway mediated by STP-A11, an oncoprotein of Herpesvirus saimiri. *Virology* **359**, 37-45.

Choi, J., Means, R. E., Damania, B. and Jung, J. U. (2001). Molecular piracy of Kaposi's sarcoma associated herpesvirus. *Cytokine Growth Factor Rev* **12**, 245-57.

Choi, J. K., Lee, B. S., Shim, S. N., Li, M. and Jung, J. U. (2000). Identification of the novel K15 gene at the rightmost end of the Kaposi's sarcoma-associated herpesvirus genome. *J Virol* **74**, 436-46.

Chou, J. J., Matsuo, H., Duan, H. and Wagner, G. (1998). Solution structure of the RAIDD CARD and model for CARD/CARD interaction in caspase-2 and caspase-9 recruitment. *Cell* **94**, 171-80.

Chu, Z. L., DiDonato, J. A., Hawiger, J. and Ballard, D. W. (1998). The tax oncoprotein of human T-cell leukemia virus type 1 associates with and persistently activates IkappaB kinases containing IKKalpha and IKKbeta. *J Biol Chem* **273**, 15891-4.

Chu, Z. L., Shin, Y. A., Yang, J. M., DiDonato, J. A. and Ballard, D. W. (1999). IKKgamma mediates the interaction of cellular IkappaB kinases with the tax transforming protein of human T cell leukemia virus type 1. *J Biol Chem* **274**, 15297-300.

Chugh, P., Matta, H., Schamus, S., Zachariah, S., Kumar, A., Richardson, J. A., Smith, A. L. and Chaudhary, P. M. (2005). Constitutive NF-kappaB activation, normal Fas-induced apoptosis, and increased incidence of lymphoma in human herpes virus 8 K13 transgenic mice. *Proc Natl Acad Sci U S A* **102**, 12885-90.

Ciana, P., Neri, A., Cappellini, C., Cavallo, F., Pomati, M., Chang, C. C., Maiolo, A. T. and Lombardi, L. (1997). Constitutive expression of lymphoma-associated NFKB-2/Lyt-10 proteins is tumorigenic in murine fibroblasts. *Oncogene* **14**, 1805-10.

Ciufo, D. M., Cannon, J. S., Poole, L. J., Wu, F. Y., Murray, P., Ambinder, R. F. and Hayward, G. S. (2001). Spindle cell conversion by Kaposi's sarcoma-associated herpesvirus: formation of colonies and plaques with mixed lytic and latent gene expression in infected primary dermal microvascular endothelial cell cultures. *J Virol* **75**, 5614-26.

Claudio, E., Brown, K., Park, S., Wang, H. and Siebenlist, U. (2002). BAFF-induced NEMO-independent processing of NF-kappa B2 in maturing B cells. *Nat Immunol* **3**, 958-65.

Clemens, M. J. and Elia, A. (1997). The double-stranded RNA-dependent protein kinase PKR: structure and function. *J Interferon Cytokine Res* **17**, 503-24.

Cockerell, C. J. (1991). Histopathological features of Kaposi's sarcoma in HIV infected individuals. *Cancer Surv* **10**, 73-89.

Cogswell, P. C., Guttridge, D. C., Funkhouser, W. K. and Baldwin, A. S., Jr. (2000). Selective activation of NF-kappa B subunits in human breast cancer: potential roles for NF-kappa B2/p52 and for Bcl-3. *Oncogene* **19**, 1123-31.

Cohrs, R. J. and Gilden, D. H. (2001). Human herpesvirus latency. *Brain Pathol* **11**, 465-74.

Connelly, L., Robinson-Benion, C., Chont, M., Saint-Jean, L., Li, H., Polosukhin, V. V., Blackwell, T. S. and Yull, F. E. (2007). A transgenic model reveals important roles for the NF-kappa B alternative pathway (p100/p52) in mammary development and links to tumorigenesis. *J Biol Chem* **282**, 10028-35.

Connelly, M. A. and Marcu, K. B. (1995). CHUK, a new member of the helix-loop-helix and leucine zipper families of interacting proteins, contains a serine-threonine kinase catalytic domain. *Cell Mol Biol Res* **41**, 537-49.

Conzen, S. D., Gottlob, K., Kandel, E. S., Khanduri, P., Wagner, A. J., O'Leary, M. and Hay, N. (2000). Induction of cell cycle progression and acceleration of apoptosis are two separable functions of c-Myc: transrepression correlates with acceleration of apoptosis. *Mol Cell Biol* **20**, 6008-18.

Cook, P. M., Whitby, D., Calabro, M. L., Luppi, M., Kakoola, D. N., Hjalgrim, H., Ariyoshi, K., Ensoli, B., Davison, A. J. and Schulz, T. F. (1999). Variability and evolution of Kaposi's sarcoma-associated herpesvirus in Europe and Africa. International Collaborative Group. *Aids* **13**, 1165-76.

Coope, H. J., Atkinson, P. G., Huhse, B., Belich, M., Janzen, J., Holman, M. J., Klaus, G. G., Johnston, L. H. and Ley, S. C. (2002). CD40 regulates the processing of NF-kappaB2 p100 to p52. *Embo J* **21**, 5375-85.

Cotter, M. A., 2nd and Robertson, E. S. (1999). The latency-associated nuclear antigen tethers the Kaposi's sarcoma-associated herpesvirus genome to host chromosomes in body cavity-based lymphoma cells. *Virology* **264**, 254-64.

Cotter, M. A., 2nd, Subramanian, C. and Robertson, E. S. (2001). The Kaposi's sarcoma-associated herpesvirus latency-associated nuclear antigen binds to specific sequences at the left end of the viral genome through its carboxy-terminus. *Virology* **291**, 241-59.

Couty, J. P., Geras-Raaka, E., Weksler, B. B. and Gershengorn, M. C. (2001). Kaposi's sarcoma-associated herpesvirus G protein-coupled receptor signals through multiple pathways in endothelial cells. *J Biol Chem* **276**, 33805-11.

Cramer, P., Larson, C. J., Verdine, G. L. and Muller, C. W. (1997). Structure of the human NF-kappaB p52 homodimer-DNA complex at 2.1 A resolution. *Embo J* **16**, 7078-90.

Cunningham, C., Barnard, S., Blackbourn, D. J. and Davison, A. J. (2003). Transcription mapping of human herpesvirus 8 genes encoding viral interferon regulatory factors. *J Gen Virol* **84**, 1471-83.

D'Oliveira, J. J. and Torres, F. O. (1972). Kaposi's sarcoma in the Bantu of Mozambique. *Cancer* **30**, 553-61.

Damania, B., Choi, J. K. and Jung, J. U. (2000). Signaling activities of gammaherpesvirus membrane proteins. *J Virol* **74**, 1593-601.

Davis, S., Aldrich, T. H., Jones, P. F., Acheson, A., Compton, D. L., Jain, V., Ryan, T. E., Bruno, J., Radziejewski, C., Maisonpierre, P. C. *et al.* (1996). Isolation of angiopoietin-1, a ligand for the TIE2 receptor, by secretion-trap expression cloning. *Cell* **87**, 1161-9.

Davison, A. (2002). Comments on the phylogenetics and evolution of herpesviruses and other large DNA viruses. *Virus Res* **82**, 127-32.

Dejardin, E., Bonizzi, G., Bellahcene, A., Castronovo, V., Merville, M. P. and Bours, V. (1995). Highly-expressed p100/p52 (NFKB2) sequesters other NF-kappa B-related proteins in the cytoplasm of human breast cancer cells. *Oncogene* **11**, 1835-41.

Dejardin, E., Droin, N. M., Delhase, M., Haas, E., Cao, Y., Makris, C., Li, Z. W., Karin, M., Ware, C. F. and Green, D. R. (2002). The lymphotoxin-beta receptor induces different patterns of gene expression via two NF-kappaB pathways. *Immunity* **17**, 525-35.

Delabesse, E., Oksenhendler, E., Lebbe, C., Verola, O., Varet, B. and Turhan, A. G. (1997). Molecular analysis of clonality in Kaposi's sarcoma. *J Clin Pathol* **50**, 664-8.

Delhase, M., Hayakawa, M., Chen, Y. and Karin, M. (1999). Positive and negative regulation of IkappaB kinase activity through IKKbeta subunit phosphorylation. *Science* **284**, 309-13.

Demaison, C., Parsley, K., Brouns, G., Scherr, M., Battmer, K., Kinnon, C., Grez, M. and Thrasher, A. J. (2002). High-level transduction and gene expression in hematopoietic repopulating cells using a human immunodeficiency [correction of imunodeficiency] virus type 1-based lentiviral vector containing an internal spleen focus forming virus promoter. *Hum Gene Ther* **13**, 803-13.

Demicco, E. G., Kavanagh, K. T., Romieu-Mourez, R., Wang, X., Shin, S. R., Landesman-Bollag, E., Seldin, D. C. and Sonenshein, G. E. (2005). RelB/p52 NF-kappaB complexes rescue an early delay in mammary gland development in transgenic mice with targeted superrepressor IkappaB-alpha expression and promote carcinogenesis of the mammary gland. *Mol Cell Biol* **25**, 10136-47.

Deng, H., Chu, J. T., Rettig, M. B., Martinez-Maza, O. and Sun, R. (2002). Rta of the human herpesvirus 8/Kaposi sarcoma-associated herpesvirus up-regulates human interleukin-6 gene expression. *Blood* **100**, 1919-21.

Deng, H., Young, A. and Sun, R. (2000a). Auto-activation of the rta gene of human herpesvirus-8/Kaposi's sarcoma-associated herpesvirus. *J Gen Virol* **81**, 3043-8.

Deng, L., Wang, C., Spencer, E., Yang, L., Braun, A., You, J., Slaughter, C., Pickart, C. and Chen, Z. J. (2000b). Activation of the IkappaB kinase complex by TRAF6 requires a dimeric ubiquitin-conjugating enzyme complex and a unique polyubiquitin chain. *Cell* **103**, 351-61.

Derudder, E., Dejardin, E., Pritchard, L. L., Green, D. R., Korner, M. and Baud, V. (2003). RelB/p50 dimers are differentially regulated by tumor necrosis factor-alpha and lymphotoxin-beta receptor activation: critical roles for p100. *J Biol Chem* **278**, 23278-84.

Desrosiers, R. C., Sasseville, V. G., Czajak, S. C., Zhang, X., Mansfield, K. G., Kaur, A., Johnson, R. P., Lackner, A. A. and Jung, J. U. (1997). A herpesvirus of rhesus monkeys related to the human Kaposi's sarcoma-associated herpesvirus. *J Virol* **71**, 9764-9.

Devergne, O., Hatzivassiliou, E., Izumi, K. M., Kaye, K. M., Kleijnen, M. F., Kieff, E. and Mosialos, G. (1996). Association of TRAF1, TRAF2, and TRAF3 with an Epstein-Barr virus LMP1 domain important for B-lymphocyte transformation: role in NF-kappaB activation. *Mol Cell Biol* **16**, 7098-108.

Devin, A., Cook, A., Lin, Y., Rodriguez, Y., Kelliher, M. and Liu, Z. (2000). The distinct roles of TRAF2 and RIP in IKK activation by TNF-R1: TRAF2 recruits IKK to TNF-R1 while RIP mediates IKK activation. *Immunity* **12**, 419-29.

Di Bartolo, D. and Cesarman, E. (2004). Uncovering the complexities of Kaposi's sarcoma through genome-wide expression analysis. *Genome Biol* **5**, 247.

DiDonato, J. A., Hayakawa, M., Rothwarf, D. M., Zandi, E. and Karin, M. (1997). A cytokine-responsive IkappaB kinase that activates the transcription factor NF-kappaB. *Nature* **388**, 548-54.

DiDonato, J. A., Mercurio, F. and Karin, M. (1995). Phosphorylation of I kappa B alpha precedes but is not sufficient for its dissociation from NF-kappa B. *Mol Cell Biol* **15**, 1302-11.

Dimmeler, S., Fleming, I., Fisslthaler, B., Hermann, C., Busse, R. and Zeiher, A. M. (1999). Activation of nitric oxide synthase in endothelial cells by Akt-dependent phosphorylation. *Nature* **399**, 601-5.

Dittmer, D., Lagunoff, M., Renne, R., Staskus, K., Haase, A. and Ganem, D. (1998). A cluster of latently expressed genes in Kaposi's sarcoma-associated herpesvirus. *J Virol* **72**, 8309-15.

Djerbi, M., Screpanti, V., Catrina, A. I., Bogen, B., Biberfeld, P. and Grandien, A. (1999). The inhibitor of death receptor signaling, FLICE-inhibitory protein defines a new class of tumor progression factors. *J Exp Med* **190**, 1025-32.

Dobrzanski, P., Ryseck, R. P. and Bravo, R. (1995). Specific inhibition of RelB/p52 transcriptional activity by the C-terminal domain of p100. *Oncogene* **10**, 1003-7.

Dong, G., Chen, Z., Li, Z. Y., Yeh, N. T., Bancroft, C. C. and Van Waes, C. (2001). Hepatocyte growth factor/scatter factor-induced activation of MEK and PI3K signal pathways contributes to expression of proangiogenic cytokines interleukin-8 and vascular endothelial growth factor in head and neck squamous cell carcinoma. *Cancer Res* **61**, 5911-8.

Douglas, J., Dutia, B., Rhind, S., Stewart, J. P. and Talbot, S. J. (2004). Expression in a recombinant murid herpesvirus 4 reveals the in vivo transforming potential of the K1 open reading frame of Kaposi's sarcoma-associated herpesvirus. *J Virol* **78**, 8878-84.

Douma, S., Van Laar, T., Zevenhoven, J., Meuwissen, R., Van Garderen, E. and Peeper, D. S. (2004). Suppression of anoikis and induction of metastasis by the neurotrophic receptor TrkB. *Nature* **430**, 1034-9.

Du, M. Q., Liu, H., Diss, T. C., Ye, H., Hamoudi, R. A., Dupin, N., Meignin, V., Oksenhendler, E., Boshoff, C. and Isaacson, P. G. (2001). Kaposi sarcoma-associated herpesvirus infects monotypic (IgM lambda) but polyclonal naive B cells in Castleman disease and associated lymphoproliferative disorders. *Blood* **97**, 2130-6.

Ducut Sigala, J. L., Bottero, V., Young, D. B., Shevchenko, A., Mercurio, F. and Verma, I. M. (2004). Activation of transcription factor NF-kappaB requires ELKS, an IkappaB kinase regulatory subunit. *Science* **304**, 1963-7.

Dupin, N., Diss, T. L., Kellam, P., Tulliez, M., Du, M. Q., Sicard, D., Weiss, R. A., Isaacson, P. G. and Boshoff, C. (2000). HHV-8 is associated with a plasmablastic variant of Castleman disease that is linked to HHV-8-positive plasmablastic lymphoma. *Blood* **95**, 1406-12.

Dupin, N., Fisher, C., Kellam, P., Ariad, S., Tulliez, M., Franck, N., van Marck, E., Salmon, D., Gorin, I., Escande, J. P. *et al.* (1999). Distribution of human herpesvirus-8 latently infected cells in Kaposi's sarcoma, multicentric Castleman's disease, and primary effusion lymphoma. *Proc Natl Acad Sci U S A* **96**, 4546-51.

Ea, C. K., Deng, L., Xia, Z. P., Pineda, G. and Chen, Z. J. (2006). Activation of IKK by TNFalpha requires site-specific ubiquitination of RIP1 and polyubiquitin binding by NEMO. *Mol Cell* **22**, 245-57.

Eberstadt, M., Huang, B., Chen, Z., Meadows, R. P., Ng, S. C., Zheng, L., Lenardo, M. J. and Fesik, S. W. (1998). NMR structure and mutagenesis of the FADD (Mort1) death-effector domain. *Nature* **392**, 941-5.

Eliopoulos, A. G., Caamano, J. H., Flavell, J., Reynolds, G. M., Murray, P. G., Poyet, J. L. and Young, L. S. (2003). Epstein-Barr virus-encoded latent infection membrane protein 1 regulates the processing of p100 NF-kappaB2 to p52 via an IKKgamma/NEMO-independent signalling pathway. *Oncogene* **22**, 7557-69.

Eliopoulos, A. G. and Young, L. S. (2001). LMP1 structure and signal transduction. *Semin Cancer Biol* **11**, 435-44.

Ellis, M., Chew, Y. P., Fallis, L., Freddersdorf, S., Boshoff, C., Weiss, R. A., Lu, X. and Mittnacht, S. (1999). Degradation of p27(Kip) cdk inhibitor triggered by Kaposi's sarcoma virus cyclin-cdk6 complex. *Embo J* **18**, 644-53.

Ensoli, B., Nakamura, S., Salahuddin, S. Z., Biberfeld, P., Larsson, L., Beaver, B., Wong-Staal, F. and Gallo, R. C. (1989). AIDS-Kaposi's sarcoma-derived cells express cytokines with autocrine and paracrine growth effects. *Science* **243**, 223-6.

Ensoli, B., Sturzl, M. and Monini, P. (2000). Cytokine-mediated growth promotion of Kaposi's sarcoma and primary effusion lymphoma. *Semin Cancer Biol* **10**, 367-81.

Erdreich-Epstein, A., Tran, L. B., Cox, O. T., Huang, E. Y., Laug, W. E., Shimada, H. and Millard, M. (2005). Endothelial apoptosis induced by inhibition of integrins alphavbeta3 and alphavbeta5 involves ceramide metabolic pathways. *Blood* **105**, 4353-61.

Esteban, M., Garcia, M. A., Domingo-Gil, E., Arroyo, J., Nombela, C. and Rivas, C. (2003). The latency protein LANA2 from Kaposi's sarcoma-associated herpesvirus inhibits apoptosis induced by dsRNA-activated protein kinase but not RNase L activation. *J Gen Virol* **84**, 1463-70.

Fakhari, F. D. and Dittmer, D. P. (2002). Charting latency transcripts in Kaposi's sarcoma-associated herpesvirus by whole-genome real-time quantitative PCR. *J Virol* **76**, 6213-23.

Fan, C. M. and Maniatis, T. (1991). Generation of p50 subunit of NF-kappa B by processing of p105 through an ATP-dependent pathway. *Nature* **354**, 395-8.

Feng, P., Park, J., Lee, B. S., Lee, S. H., Bram, R. J. and Jung, J. U. (2002). Kaposi's sarcoma-associated herpesvirus mitochondrial K7 protein targets a cellular calcium-modulating cyclophilin ligand to modulate intracellular calcium concentration and inhibit apoptosis. *J Virol* **76**, 11491-504.

Fickenscher, H. and Fleckenstein, B. (2001). Herpesvirus saimiri. *Philos Trans R Soc Lond B Biol Sci* **356**, 545-67.

Field, N., Low, W., Daniels, M., Howell, S., Daviet, L., Boshoff, C. and Collins, M. (2003). KSHV vFLIP binds to IKK-gamma to activate IKK. *J Cell Sci* **116**, 3721-8.

Fiorelli, V., Gendelman, R., Sirianni, M. C., Chang, H. K., Colombini, S., Markham, P. D., Monini, P., Sonnabend, J., Pintus, A., Gallo, R. C. *et al.* (1998). gamma-Interferon produced by CD8+ T cells infiltrating Kaposi's sarcoma induces spindle cells with angiogenic phenotype and synergy with human immunodeficiency virus-1 Tat protein: an immune response to human herpesvirus-8 infection? *Blood* **91**, 956-67.

Flore, O., Rafii, S., Ely, S., O'Leary, J. J., Hyjek, E. M. and Cesarman, E. (1998). Transformation of primary human endothelial cells by Kaposi's sarcoma-associated herpesvirus. *Nature* **394**, 588-92.

Folkman, J. and Moscona, A. (1978). Role of cell shape in growth control. *Nature* **273**, 345-9.

Fong, A. and Sun, S. C. (2002). Genetic evidence for the essential role of beta-transducin repeat-containing protein in the inducible processing of NF-kappa B2/p100. *J Biol Chem* **277**, 22111-4.

Fong, A., Zhang, M., Neely, J. and Sun, S. C. (2002). S9, a 19 S proteasome subunit interacting with ubiquitinated NF-kappaB2/p100. *J Biol Chem* **277**, 40697-702.

Fontan, E., Traincard, F., Levy, S. G., Yamaoka, S., Veron, M. and Agou, F. (2007). NEMO oligomerization in the dynamic assembly of the IkappaB kinase core complex. *Febs J* **274**, 2540-51.

Foussat, A., Wijdenes, J., Bouchet, L., Gaidano, G., Neipel, F., Balabanian, K., Galanaud, P., Couderc, J. and Emilie, D. (1999). Human interleukin-6 is in vivo an autocrine growth factor for human herpesvirus-8-infected malignant B lymphocytes. *Eur Cytokine Netw* **10**, 501-8.

Fracchiolla, N. S., Lombardi, L., Salina, M., Migliazza, A., Baldini, L., Berti, E., Cro, L., Polli, E., Maiolo, A. T. and Neri, A. (1993). Structural alterations of the NF-kappa B transcription factor lyt-10 in lymphoid malignancies. *Oncogene* **8**, 2839-45.

Frances, C., Mouquet, C., Marcelin, A. G., Barete, S., Agher, R., Charron, D., Benalia, H., Dupin, N., Piette, J. C., Bitker, M. O. *et al.* (2000). Outcome of kidney transplant recipients with previous human herpesvirus-8 infection. *Transplantation* **69**, 1776-9.

Franceschi, S. and Serraino, D. (1995). Kaposi's sarcoma and KSHV. *Lancet* **346**, 1360-1.

Franzoso, G., Carlson, L., Poljak, L., Shores, E. W., Epstein, S., Leonardi, A., Grinberg, A., Tran, T., Scharton-Kersten, T., Anver, M. *et al.* (1998). Mice deficient in nuclear factor (NF)-kappa B/p52 present with defects in humoral responses, germinal center reactions, and splenic microarchitecture. *J Exp Med* **187**, 147-59.

Friborg, J., Jr., Kong, W., Hottiger, M. O. and Nabel, G. J. (1999). p53 inhibition by the LANA protein of KSHV protects against cell death. *Nature* **402**, 889-94.

Frisch, S. M. and Francis, H. (1994). Disruption of epithelial cell-matrix interactions induces apoptosis. *J Cell Biol* **124**, 619-26.

Frizzera, G., Banks, P. M., Massarelli, G. and Rosai, J. (1983). A systemic lymphoproliferative disorder with morphologic features of Castleman's disease. Pathological findings in 15 patients. *Am J Surg Pathol* **7**, 211-31.

Fuchs, S. Y., Chen, A., Xiong, Y., Pan, Z. Q. and Ronai, Z. (1999). HOS, a human homolog of Slimb, forms an SCF complex with Skp1 and Cullin1 and targets the phosphorylation-dependent degradation of IkappaB and beta-catenin. *Oncogene* **18**, 2039-46.

Fujikawa, K., de Aos Scherpenseel, I., Jain, S. K., Presman, E., Christensen, R. A. and Varticovski, L. (1999). Role of PI 3-kinase in angiopoietin-1-mediated migration and attachment-dependent survival of endothelial cells. *Exp Cell Res* **253**, 663-72.

Fujimuro, M., Wu, F. Y., ApRhys, C., Kajumbula, H., Young, D. B., Hayward, G. S. and Hayward, S. D. (2003). A novel viral mechanism for dysregulation of beta-catenin in Kaposi's sarcoma-associated herpesvirus latency. *Nat Med* **9**, 300-6.

Fujio, Y. and Walsh, K. (1999). Akt mediates cytoprotection of endothelial cells by vascular endothelial growth factor in an anchorage-dependent manner. *J Biol Chem* **274**, 16349-54.

Fujita, T., Nolan, G. P., Liou, H. C., Scott, M. L. and Baltimore, D. (1993). The candidate proto-oncogene bcl-3 encodes a transcriptional coactivator that activates through NF-kappa B p50 homodimers. *Genes Dev* **7**, 1354-63.

Fukazawa, H., Mizuno, S. and Uehara, Y. (1995). A microplate assay for quantitation of anchorage-independent growth of transformed cells. *Anal Biochem* **228**, 83-90.

Fukazawa, H., Nakano, S., Mizuno, S. and Uehara, Y. (1996). Inhibitors of anchorage-independent growth affect the growth of transformed cells on poly(2-hydroxyethyl methacrylate)-coated surfaces. *Int J Cancer* **67**, 876-82.

Fuld, S., Cunningham, C., Klucher, K., Davison, A. J. and Blackbourn, D. J. (2006). Inhibition of interferon signaling by the Kaposi's sarcoma-associated herpesvirus full-length viral interferon regulatory factor 2 protein. *J Virol* **80**, 3092-7.

Gaidano, G., Capello, D., Cilia, A. M., Gloghini, A., Perin, T., Quattrone, S., Migliazza, A., Lo Coco, F., Saglio, G., Ascoli, V. *et al.* (1999). Genetic characterization of HHV-8/KSHV-positive primary effusion lymphoma reveals frequent mutations of BCL6: implications for disease pathogenesis and histogenesis. *Genes Chromosomes Cancer* **24**, 16-23.

Gaidano, G., Pastore, C., Gloghini, A., Cusini, M., Nomdedeu, J., Volpe, G., Capello, D., Vaccher, E., Bordes, R., Tirelli, U. *et al.* (1996). Distribution of human herpesvirus-8 sequences throughout the spectrum of AIDS-related neoplasia. *Aids* **10**, 941-9.

Gaide, O., Favier, B., Legler, D. F., Bonnet, D., Brissoni, B., Valitutti, S., Bron, C., Tschopp, J. and Thome, M. (2002). CARMA1 is a critical lipid raft-associated regulator of TCR-induced NF-kappa B activation. *Nat Immunol* **3**, 836-43.

Gaide, O., Martinon, F., Micheau, O., Bonnet, D., Thome, M. and Tschopp, J. (2001). Carma1, a CARD-containing binding partner of Bcl10, induces Bcl10 phosphorylation and NF-kappaB activation. *FEBS Lett* **496**, 121-7.

Gale, N. W., Thurston, G., Hackett, S. F., Renard, R., Wang, Q., McClain, J., Martin, C., Witte, C., Witte, M. H., Jackson, D. *et al.* (2002). Angiopoietin-2 is required for postnatal angiogenesis and lymphatic patterning, and only the latter role is rescued by Angiopoietin-1. *Dev Cell* **3**, 411-23.

Gallo, R. C. (1998). The enigmas of Kaposi's sarcoma. *Science* **282**, 1837-9.

Ganchi, P. A., Sun, S. C., Greene, W. C. and Ballard, D. W. (1993). A novel NF-kappa B complex containing p65 homodimers: implications for transcriptional control at the level of subunit dimerization. *Mol Cell Biol* **13**, 7826-35.

Ganem, D. (1997). KSHV and Kaposi's sarcoma: the end of the beginning? *Cell* **91**, 157-60.

Gao, S. J., Boshoff, C., Jayachandra, S., Weiss, R. A., Chang, Y. and Moore, P. S. (1997). KSHV ORF K9 (vIRF) is an oncogene which inhibits the interferon signaling pathway. *Oncogene* **15**, 1979-85.

Gao, S. J., Kingsley, L., Hoover, D. R., Spira, T. J., Rinaldo, C. R., Saah, A., Phair, J., Detels, R., Parry, P., Chang, Y. *et al.* (1996). Seroconversion to antibodies against Kaposi's sarcoma-associated herpesvirus-related latent nuclear antigens before the development of Kaposi's sarcoma. *N Engl J Med* **335**, 233-41.

Garber, A. C., Hu, J. and Renne, R. (2002). Latency-associated nuclear antigen (LANA) cooperatively binds to two sites within the terminal repeat, and both sites contribute to the

ability of LANA to suppress transcription and to facilitate DNA replication. *J Biol Chem* **277**, 27401-11.

Garber, A. C., Shu, M. A., Hu, J. and Renne, R. (2001). DNA binding and modulation of gene expression by the latency-associated nuclear antigen of Kaposi's sarcoma-associated herpesvirus. *J Virol* **75**, 7882-92.

Garvey, T. L., Bertin, J., Siegel, R. M., Wang, G. H., Lenardo, M. J. and Cohen, J. I. (2002). Binding of FADD and caspase-8 to molluscum contagiosum virus MC159 v-FLIP is not sufficient for its antiapoptotic function. *J Virol* **76**, 697-706.

Geleziunas, R., Ferrell, S., Lin, X., Mu, Y., Cunningham, E. T., Jr., Grant, M., Connelly, M. A., Hambor, J. E., Marcu, K. B. and Greene, W. C. (1998). Human T-cell leukemia virus type 1 Tax induction of NF-kappaB involves activation of the IkappaB kinase alpha (IKKalpha) and IKKbeta cellular kinases. *Mol Cell Biol* **18**, 5157-65.

Geras-Raaka, E., Varma, A., Ho, H., Clark-Lewis, I. and Gershengorn, M. C. (1998). Human interferon-gamma-inducible protein 10 (IP-10) inhibits constitutive signaling of Kaposi's sarcoma-associated herpesvirus G protein-coupled receptor. *J Exp Med* **188**, 405-8.

Gerber, H. P., Dixit, V. and Ferrara, N. (1998). Vascular endothelial growth factor induces expression of the antiapoptotic proteins Bcl-2 and A1 in vascular endothelial cells. *J Biol Chem* **273**, 13313-6.

Gershengorn, M. C., Geras-Raaka, E., Varma, A. and Clark-Lewis, I. (1998). Chemokines activate Kaposi's sarcoma-associated herpesvirus G protein-coupled receptor in mammalian cells in culture. *J Clin Invest* **102**, 1469-72.

Gessain, A., Briere, J., Angelin-Duclos, C., Valensi, F., Beral, H. M., Davi, F., Nicola, M. A., Sudaka, A., Fouchard, N., Gabarre, J. *et al.* (1997). Human herpes virus 8 (Kaposi's sarcoma herpes virus) and malignant lymphoproliferations in France: a molecular study of 250 cases including two AIDS-associated body cavity based lymphomas. *Leukemia* **11**, 266-72.

Ghosh, G., van Duyne, G., Ghosh, S. and Sigler, P. B. (1995). Structure of NF-kappa B p50 homodimer bound to a kappa B site. *Nature* **373**, 303-10.

Ghosh, S. and Karin, M. (2002). Missing pieces in the NF-kappaB puzzle. *Cell* **109 Suppl**, S81-96.

Ghosh, S., May, M. J. and Kopp, E. B. (1998). NF-kappa B and Rel proteins: evolutionarily conserved mediators of immune responses. *Annu Rev Immunol* **16**, 225-60.

Gibson, W. (1996). Structure and assembly of the virion. *Intervirology* **39**, 389-400.

Gille, J., Khalik, M., Konig, V. and Kaufmann, R. (1998). Hepatocyte growth factor/scatter factor (HGF/SF) induces vascular permeability factor (VPF/VEGF) expression by cultured keratinocytes. *J Invest Dermatol* **111**, 1160-5.

Giraudo, E., Arese, M., Toniatti, C., Strasly, M., Primo, L., Mantovani, A., Ciliberto, G. and Bussolini, F. (1996). IL-6 is an in vitro and in vivo autocrine growth factor for middle T antigen-transformed endothelial cells. *J Immunol* **157**, 2618-23.

Gires, O., Zimber-Strobl, U., Gonnella, R., Ueffing, M., Marschall, G., Zeidler, R., Pich, D. and Hammerschmidt, W. (1997). Latent membrane protein 1 of Epstein-Barr virus mimics a constitutively active receptor molecule. *Embo J* **16**, 6131-40.

Glenn, M., Rainbow, L., Aurade, F., Davison, A. and Schulz, T. F. (1999). Identification of a spliced gene from Kaposi's sarcoma-associated herpesvirus encoding a protein with similarities to latent membrane proteins 1 and 2A of Epstein-Barr virus. *J Virol* **73**, 6953-63.

Godden-Kent, D., Talbot, S. J., Boshoff, C., Chang, Y., Moore, P., Weiss, R. A. and Mittnacht, S. (1997). The cyclin encoded by Kaposi's sarcoma-associated herpesvirus stimulates cdk6 to phosphorylate the retinoblastoma protein and histone H1. *J Virol* **71**, 4193-8.

Godfrey, A., Anderson, J., Papanastasiou, A., Takeuchi, Y. and Boshoff, C. (2005). Inhibiting primary effusion lymphoma by lentiviral vectors encoding short hairpin RNA. *Blood* **105**, 2510-8.

Goltsev, Y. V., Kovalenko, A. V., Arnold, E., Varfolomeev, E. E., Brodianskii, V. M. and Wallach, D. (1997). CASH, a novel caspase homologue with death effector domains. *J Biol Chem* **272**, 19641-4.

Gommerman, J. L. and Browning, J. L. (2003). Lymphotoxin/light, lymphoid microenvironments and autoimmune disease. *Nat Rev Immunol* **3**, 642-55.

Gottlieb, G. J., Ragaz, A., Vogel, J. V., Friedman-Kien, A., Rywlin, A. M., Weiner, E. A. and Ackerman, A. B. (1981). A preliminary communication on extensively disseminated Kaposi's sarcoma in young homosexual men. *Am J Dermatopathol* **3**, 111-4.

Gottwein, E., Cai, X. and Cullen, B. R. (2006). Expression and function of microRNAs encoded by Kaposi's sarcoma-associated herpesvirus. *Cold Spring Harb Symp Quant Biol* **71**, 357-64.

Grammer, A. C. and Lipsky, P. E. (2000). CD40-mediated regulation of immune responses by TRAF-dependent and TRAF-independent signaling mechanisms. *Adv Immunol* **76**, 61-178.

Grandadam, M., Dupin, N., Calvez, V., Gorin, I., Blum, L., Kernbaum, S., Sicard, D., Buisson, Y., Agut, H., Escande, J. P. *et al.* (1997). Exacerbations of clinical symptoms in human immunodeficiency virus type 1-infected patients with multicentric Castleman's disease are associated with a high increase in Kaposi's sarcoma herpesvirus DNA load in peripheral blood mononuclear cells. *J Infect Dis* **175**, 1198-201.

Grant, D. S., Kleinman, H. K., Goldberg, I. D., Bhargava, M. M., Nickoloff, B. J., Kinsella, J. L., Polverini, P. and Rosen, E. M. (1993). Scatter factor induces blood vessel formation in vivo. *Proc Natl Acad Sci U S A* **90**, 1937-41.

Gratton, J. P., Morales-Ruiz, M., Kureishi, Y., Fulton, D., Walsh, K. and Sessa, W. C. (2001). Akt down-regulation of p38 signaling provides a novel mechanism of vascular endothelial growth factor-mediated cytoprotection in endothelial cells. *J Biol Chem* **276**, 30359-65.

Greensill, J., Sheldon, J. A., Renwick, N. M., Beer, B. E., Norley, S., Goudsmit, J. and Schulz, T. F. (2000). Two distinct gamma-2 herpesviruses in African green monkeys: a second gamma-2 herpesvirus lineage among old world primates? *J Virol* **74**, 1572-7.

Gross, J. A., Dillon, S. R., Mudri, S., Johnston, J., Littau, A., Roque, R., Rixon, M., Schou, O., Foley, K. P., Haugen, H. *et al.* (2001). TACI-Ig neutralizes molecules critical for B cell development and autoimmune disease. impaired B cell maturation in mice lacking BLyS. *Immunity* **15**, 289-302.

Gross, J. A., Johnston, J., Mudri, S., Enselman, R., Dillon, S. R., Madden, K., Xu, W., Parrish-Novak, J., Foster, D., Lofton-Day, C. *et al.* (2000). TACI and BCMA are receptors for a TNF homologue implicated in B-cell autoimmune disease. *Nature* **404**, 995-9.

Grossmann, C., Podgrabinska, S., Skobe, M. and Ganem, D. (2006). Activation of NF-kappaB by the latent vFLIP gene of Kaposi's sarcoma-associated herpesvirus is required for the spindle shape of virus-infected endothelial cells and contributes to their proinflammatory phenotype. *J Virol* **80**, 7179-85.

Grundhoff, A. and Ganem, D. (2001). Mechanisms governing expression of the v-FLIP gene of Kaposi's sarcoma-associated herpesvirus. *J Virol* **75**, 1857-63.

Guasparri, I., Keller, S. A. and Cesarman, E. (2004). KSHV vFLIP is essential for the survival of infected lymphoma cells. *J Exp Med* **199**, 993-1003.

Guasparri, I., Wu, H. and Cesarman, E. (2006). The KSHV oncoprotein vFLIP contains a TRAF-interacting motif and requires TRAF2 and TRAF3 for signalling. *EMBO Rep* **7**, 114-9.

Guo, H. G., Sadowska, M., Reid, W., Tschachler, E., Hayward, G. and Reitz, M. (2003a). Kaposi's sarcoma-like tumors in a human herpesvirus 8 ORF74 transgenic mouse. *J Virol* **77**, 2631-9.

Guo, P., Hu, B., Gu, W., Xu, L., Wang, D., Huang, H. J., Cavenee, W. K. and Cheng, S. Y. (2003b). Platelet-derived growth factor-B enhances glioma angiogenesis by stimulating vascular endothelial growth factor expression in tumor endothelia and by promoting pericyte recruitment. *Am J Pathol* **162**, 1083-93.

Gupta, K., Kshirsagar, S., Li, W., Gui, L., Ramakrishnan, S., Gupta, P., Law, P. Y. and Hebbel, R. P. (1999). VEGF prevents apoptosis of human microvascular endothelial cells via opposing effects on MAPK/ERK and SAPK/JNK signaling. *Exp Cell Res* **247**, 495-504.

Hacker, H. and Karin, M. (2002). Is NF-kappaB2/p100 a direct activator of programmed cell death? *Cancer Cell* **2**, 431-3.

Han, D. K., Chaudhary, P. M., Wright, M. E., Friedman, C., Trask, B. J., Riedel, R. T., Baskin, D. G., Schwartz, S. M. and Hood, L. (1997). MRIT, a novel death-effector domain-containing protein, interacts with caspases and BclXL and initiates cell death. *Proc Natl Acad Sci U S A* **94**, 11333-8.

Hanahan, D. (1997). Signaling vascular morphogenesis and maintenance. *Science* **277**, 48-50.

Hansen, M. B., Nielsen, S. E. and Berg, K. (1989). Re-examination and further development of a precise and rapid dye method for measuring cell growth/cell kill. *J Immunol Methods* **119**, 203-10.

Hansen, S. K., Baeuerle, P. A. and Blasi, F. (1994a). Purification, reconstitution, and I kappa B association of the c-Rel-p65 (RelA) complex, a strong activator of transcription. *Mol Cell Biol* **14**, 2593-603.

Hansen, S. K., Guerrini, L. and Blasi, F. (1994b). Differential DNA sequence specificity and regulation of HIV-1 enhancer activity by cRel-RelA transcription factor. *J Biol Chem* **269**, 22230-7.

Hara, H., Wada, T., Bakal, C., Kozieradzki, I., Suzuki, S., Suzuki, N., Nghiem, M., Griffiths, E. K., Krawczyk, C., Bauer, B. *et al.* (2003). The MAGUK family protein CARD11 is essential for lymphocyte activation. *Immunity* **18**, 763-75.

Harhaj, E. W. and Sun, S. C. (1999). IKKgamma serves as a docking subunit of the IkappaB kinase (IKK) and mediates interaction of IKK with the human T-cell leukemia virus Tax protein. *J Biol Chem* **274**, 22911-4.

Harwood, A. R., Osoba, D., Hofstader, S. L., Goldstein, M. B., Cardella, C. J., Holecek, M. J., Kunynetz, R. and Giammarco, R. A. (1979). Kaposi's sarcoma in recipients of renal transplants. *Am J Med* **67**, 759-65.

Hatakeyama, S., Kitagawa, M., Nakayama, K., Shirane, M., Matsumoto, M., Hattori, K., Higashi, H., Nakano, H., Okumura, K., Onoe, K. *et al.* (1999). Ubiquitin-dependent

degradation of IkappaBalpha is mediated by a ubiquitin ligase Skp1/Cul 1/F-box protein FWD1. *Proc Natl Acad Sci U S A* **96**, 3859-63.

Hauer, J., Puschner, S., Ramakrishnan, P., Simon, U., Bongers, M., Federle, C. and Engelmann, H. (2005). TNF receptor (TNFR)-associated factor (TRAF) 3 serves as an inhibitor of TRAF2/5-mediated activation of the noncanonical NF-kappaB pathway by TRAF-binding TNFRs. *Proc Natl Acad Sci U S A* **102**, 2874-9.

Hayward, G. S. (1999). KSHV strains: the origins and global spread of the virus. *Semin Cancer Biol* **9**, 187-99.

Henkel, T., Machleidt, T., Alkalay, I., Kronke, M., Ben-Neriah, Y. and Baeuerle, P. A. (1993). Rapid proteolysis of I kappa B-alpha is necessary for activation of transcription factor NF-kappa B. *Nature* **365**, 182-5.

Henriksson, M., Bakardjiev, A., Klein, G. and Luscher, B. (1993). Phosphorylation sites mapping in the N-terminal domain of c-myc modulate its transforming potential. *Oncogene* **8**, 3199-209.

Herndier, B. and Ganem, D. (2001). The biology of Kaposi's sarcoma. *Cancer Treat Res* **104**, 89-126.

Heusch, M., Lin, L., Geleziunas, R. and Greene, W. C. (1999). The generation of nfkb2 p52: mechanism and efficiency. *Oncogene* **18**, 6201-8.

Hiller, S., Kohl, A., Fiorito, F., Herrmann, T., Wider, G., Tschopp, J., Grutter, M. G. and Wuthrich, K. (2003). NMR structure of the apoptosis- and inflammation-related NALP1 pyrin domain. *Structure* **11**, 1199-205.

Holash, J., Wiegand, S. J. and Yancopoulos, G. D. (1999). New model of tumor angiogenesis: dynamic balance between vessel regression and growth mediated by angiopoietins and VEGF. *Oncogene* **18**, 5356-62.

Holzerlandt, R., Orengo, C., Kellam, P. and Alba, M. M. (2002). Identification of new herpesvirus gene homologs in the human genome. *Genome Res* **12**, 1739-48.

Homa, F. L. and Brown, J. C. (1997). Capsid assembly and DNA packaging in herpes simplex virus. *Rev Med Virol* **7**, 107-122.

Hong, S., Wang, L. C., Gao, X., Kuo, Y. L., Liu, B., Merling, R., Kung, H. J., Shih, H. M. and Giam, C. Z. (2007). Heptad repeats regulate protein phosphatase 2a recruitment to I-kappaB kinase gamma/NF-kappaB essential modulator and are targeted by human T-lymphotropic virus type 1 tax. *J Biol Chem* **282**, 12119-26.

Hong, Y. K., Foreman, K., Shin, J. W., Hirakawa, S., Curry, C. L., Sage, D. R., Libermann, T., Dezube, B. J., Fingeroth, J. D. and Detmar, M. (2004). Lymphatic reprogramming of blood vascular endothelium by Kaposi sarcoma-associated herpesvirus. *Nat Genet* **36**, 683-5.

Horenstein, M. G., Nador, R. G., Chadburn, A., Hyjek, E. M., Inghirami, G., Knowles, D. M. and Cesarman, E. (1997). Epstein-Barr virus latent gene expression in primary effusion lymphomas containing Kaposi's sarcoma-associated herpesvirus/human herpesvirus-8. *Blood* **90**, 1186-91.

Hu, S., Vincenz, C., Buller, M. and Dixit, V. M. (1997a). A novel family of viral death effector domain-containing molecules that inhibit both CD-95- and tumor necrosis factor receptor-1-induced apoptosis. *J Biol Chem* **272**, 9621-4.

Hu, S., Vincenz, C., Ni, J., Gentz, R. and Dixit, V. M. (1997b). I-FLICE, a novel inhibitor of tumor necrosis factor receptor-1- and CD-95-induced apoptosis. *J Biol Chem* **272**, 17255-7.

Hu, W. H., Johnson, H. and Shu, H. B. (2000). Activation of NF-kappaB by FADD, Casper, and caspase-8. *J Biol Chem* **275**, 10838-44.

Hu, Y., Baud, V., Delhase, M., Zhang, P., Deerinck, T., Ellisman, M., Johnson, R. and Karin, M. (1999). Abnormal morphogenesis but intact IKK activation in mice lacking the IKKalpha subunit of IkappaB kinase. *Science* **284**, 316-20.

Huang, B., Eberstadt, M., Olejniczak, E. T., Meadows, R. P. and Fesik, S. W. (1996). NMR structure and mutagenesis of the Fas (APO-1/CD95) death domain. *Nature* **384**, 638-41.

Huang, J. T. and Schneider, R. J. (1991). Adenovirus inhibition of cellular protein synthesis involves inactivation of cap-binding protein. *Cell* **65**, 271-80.

Huang, T. T., Wuerzberger-Davis, S. M., Wu, Z. H. and Miyamoto, S. (2003). Sequential modification of NEMO/IKKgamma by SUMO-1 and ubiquitin mediates NF-kappaB activation by genotoxic stress. *Cell* **115**, 565-76.

Huen, D. S., Henderson, S. A., Croom-Carter, D. and Rowe, M. (1995). The Epstein-Barr virus latent membrane protein-1 (LMP1) mediates activation of NF-kappa B and cell surface phenotype via two effector regions in its carboxy-terminal cytoplasmic domain. *Oncogene* **10**, 549-60.

Hung, S. C., Pochampally, R. R., Chen, S. C., Hsu, S. C. and Prockop, D. J. (2007). Angiogenic Effects of Human Multipotent Stromal Cells (MSCs). Conditioned Medium Activates the PI3K-Akt Pathway in Hypoxic Endothelial Cells to Inhibit Apoptosis, Increase Survival, and Stimulate Angiogenesis. *Stem Cells.*

Hyun, T. S., Subramanian, C., Cotter, M. A., 2nd, Thomas, R. A. and Robertson, E. S. (2001). Latency-associated nuclear antigen encoded by Kaposi's sarcoma-associated herpesvirus interacts with Tat and activates the long terminal repeat of human immunodeficiency virus type 1 in human cells. *J Virol* **75**, 8761-71.

Iha, H., Kibler, K. V., Yedavalli, V. R., Peloponese, J. M., Haller, K., Miyazato, A., Kasai, T. and Jeang, K. T. (2003). Segregation of NF-kappaB activation through NEMO/IKKgamma by Tax and TNFalpha: implications for stimulus-specific interruption of oncogenic signaling. *Oncogene* **22**, 8912-23.

Inohara, N., Koseki, T., Lin, J., del Peso, L., Lucas, P. C., Chen, F. F., Ogura, Y. and Nunez, G. (2000). An induced proximity model for NF-kappa B activation in the Nod1/RICK and RIP signaling pathways. *J Biol Chem* **275**, 27823-31.

Irmler, M., Thome, M., Hahne, M., Schneider, P., Hofmann, K., Steiner, V., Bodmer, J. L., Schroter, M., Burns, K., Mattmann, C. *et al.* (1997). Inhibition of death receptor signals by cellular FLIP. *Nature* **388**, 190-5.

Ishikawa, H., Carrasco, D., Claudio, E., Ryseck, R. P. and Bravo, R. (1997). Gastric hyperplasia and increased proliferative responses of lymphocytes in mice lacking the COOH-terminal ankyrin domain of NF-kappaB2. *J Exp Med* **186**, 999-1014.

Jain, R. K. (2003). Molecular regulation of vessel maturation. *Nat Med* **9**, 685-93.

Jain, R. K., Safabakhsh, N., Sckell, A., Chen, Y., Jiang, P., Benjamin, L., Yuan, F. and Keshet, E. (1998). Endothelial cell death, angiogenesis, and microvascular function after castration in an androgen-dependent tumor: role of vascular endothelial growth factor. *Proc Natl Acad Sci U S A* **95**, 10820-5.

Jarviluoma, A., Child, E. S., Sarek, G., Sirimongkolkasem, P., Peters, G., Ojala, P. M. and Mann, D. J. (2006). Phosphorylation of the cyclin-dependent kinase inhibitor p21Cip1 on serine 130 is essential for viral cyclin-mediated bypass of a p21Cip1-imposed G1 arrest. *Mol Cell Biol* **26**, 2430-40.

Jeang, K. T. (2001). Functional activities of the human T-cell leukemia virus type I Tax oncoprotein: cellular signaling through NF-kappa B. *Cytokine Growth Factor Rev* **12**, 207-17.

Jenkins, F. J., Hoffman, L. J. and Liegey-Dougall, A. (2002). Reactivation of and primary infection with human herpesvirus 8 among solid-organ transplant recipients. *J Infect Dis* **185**, 1238-43.

Jenner, R. G., Alba, M. M., Boshoff, C. and Kellam, P. (2001). Kaposi's sarcoma-associated herpesvirus latent and lytic gene expression as revealed by DNA arrays. *J Virol* **75**, 891-902.

Jenner, R. G. and Boshoff, C. (2002). The molecular pathology of Kaposi's sarcoma-associated herpesvirus. *Biochim Biophys Acta* **1602**, 1-22.

Jenner, R. G., Maillard, K., Cattini, N., Weiss, R. A., Boshoff, C., Wooster, R. and Kellam, P. (2003). Kaposi's sarcoma-associated herpesvirus-infected primary effusion lymphoma has a plasma cell gene expression profile. *Proc Natl Acad Sci U S A* **100**, 10399-404.

Jiang, Y., Woronicz, J. D., Liu, W. and Goeddel, D. V. (1999). Prevention of constitutive TNF receptor 1 signaling by silencer of death domains. *Science* **283**, 543-6.

Jin, D. Y., Giordano, V., Kibler, K. V., Nakano, H. and Jeang, K. T. (1999). Role of adapter function in oncoprotein-mediated activation of NF-kappaB. Human T-cell leukemia virus type I Tax interacts directly with IkappaB kinase gamma. *J Biol Chem* **274**, 17402-5.

Jones, K. D., Aoki, Y., Chang, Y., Moore, P. S., Yarchoan, R. and Tosato, G. (1999). Involvement of interleukin-10 (IL-10) and viral IL-6 in the spontaneous growth of Kaposi's sarcoma herpesvirus-associated infected primary effusion lymphoma cells. *Blood* **94**, 2871-9.

Joo, C. H., Shin, Y. C., Gack, M., Wu, L., Levy, D. and Jung, J. U. (2007). Inhibition of interferon regulatory factor 7 (IRF7)-mediated interferon signal transduction by the Kaposi's sarcoma-associated herpesvirus viral IRF homolog vIRF3. *J Virol* **81**, 8282-92.

Jope, R. S. and Johnson, G. V. (2004). The glamour and gloom of glycogen synthase kinase-3. *Trends Biochem Sci* **29**, 95-102.

Judde, J. G., Lacoste, V., Briere, J., Kassa-Kelembho, E., Clyti, E., Couppie, P., Buchrieser, C., Tulliez, M., Morvan, J. and Gessain, A. (2000). Monoclonality or oligoclonality of human herpesvirus 8 terminal repeat sequences in Kaposi's sarcoma and other diseases. *J Natl Cancer Inst* **92**, 729-36.

Jung, J. U., Choi, J. K., Ensser, A. and Biesinger, B. (1999). Herpesvirus saimiri as a model for gammaherpesvirus oncogenesis. *Semin Cancer Biol* **9**, 231-9.

Jung, J. U. and Desrosiers, R. C. (1995). Association of the viral oncoprotein STP-C488 with cellular ras. *Mol Cell Biol* **15**, 6506-12.

Jussila, L., Valtola, R., Partanen, T. A., Salven, P., Heikkila, P., Matikainen, M. T., Renkonen, R., Kaipainen, A., Detmar, M., Tschachler, E. *et al.* (1998). Lymphatic endothelium and Kaposi's sarcoma spindle cells detected by antibodies against the vascular endothelial growth factor receptor-3. *Cancer Res* **58**, 1599-604.

Kaaya, E. E., Parravicini, C., Ordonez, C., Gendelman, R., Berti, E., Gallo, R. C. and Biberfeld, P. (1995). Heterogeneity of spindle cells in Kaposi's sarcoma: comparison of cells in lesions and in culture. *J Acquir Immune Defic Syndr Hum Retrovirol* **10**, 295-305.

Kaisho, T., Takeda, K., Tsujimura, T., Kawai, T., Nomura, F., Terada, N. and Akira, S. (2001). IkappaB kinase alpha is essential for mature B cell development and function. *J Exp Med* **193**, 417-26.

Kang, S. M., Tran, A. C., Grilli, M. and Lenardo, M. J. (1992). NF-kappa B subunit regulation in nontransformed CD4+ T lymphocytes. *Science* **256**, 1452-6.

Kaposi, M. (1872). Idiopathisches multiplespigmentsarcom der haut. *Arch. Dermatologie Syphillis* 265-273.

Karcher, D. S. and Alkan, S. (1997). Human herpesvirus-8-associated body cavity-based lymphoma in human immunodeficiency virus-infected patients: a unique B-cell neoplasm. *Hum Pathol* **28**, 801-8.

Karl, E., Warner, K., Zeitlin, B., Kaneko, T., Wurtzel, L., Jin, T., Chang, J., Wang, S., Wang, C. Y., Strieter, R. M. *et al.* (2005). Bcl-2 acts in a proangiogenic signaling pathway through nuclear factor-kappaB and CXC chemokines. *Cancer Res* **65**, 5063-9.

Karsan, A., Yee, E., Poirier, G. G., Zhou, P., Craig, R. and Harlan, J. M. (1997). Fibroblast growth factor-2 inhibits endothelial cell apoptosis by Bcl-2-dependent and independent mechanisms. *Am J Pathol* **151**, 1775-84.

Kataoka, T., Budd, R. C., Holler, N., Thome, M., Martinon, F., Irmler, M., Burns, K., Hahne, M., Kennedy, N., Kovacsovics, M. *et al.* (2000). The caspase-8 inhibitor FLIP promotes activation of NF-kappaB and Erk signaling pathways. *Curr Biol* **10**, 640-8.

Kaufmann, M., Bozic, D., Briand, C., Bodmer, J. L., Zerbe, O., Kohl, A., Tschopp, J. and Grutter, M. G. (2002). Identification of a basic surface area of the FADD death effector domain critical for apoptotic signaling. *FEBS Lett* **527**, 250-4.

Kayagaki, N., Yan, M., Seshasayee, D., Wang, H., Lee, W., French, D. M., Grewal, I. S., Cochran, A. G., Gordon, N. C., Yin, J. *et al.* (2002). BAFF/BLyS receptor 3 binds the B cell survival factor BAFF ligand through a discrete surface loop and promotes processing of NF-kappaB2. *Immunity* **17**, 515-24.

Kaye, K. M., Izumi, K. M., Mosialos, G. and Kieff, E. (1995). The Epstein-Barr virus LMP1 cytoplasmic carboxy terminus is essential for B-lymphocyte transformation; fibroblast cocultivation complements a critical function within the terminal 155 residues. *J Virol* **69**, 675-83.

Keller, S. A., Hernandez-Hopkins, D., Vider, J., Ponomarev, V., Hyjek, E., Schattner, E. J. and Cesarman, E. (2006). NF-kappaB is essential for the progression of KSHV- and EBV-infected lymphomas in vivo. *Blood* **107**, 3295-302.

Keller, S. A., Schattner, E. J. and Cesarman, E. (2000). Inhibition of NF-kappaB induces apoptosis of KSHV-infected primary effusion lymphoma cells. *Blood* **96**, 2537-42.

Kelliher, M. A., Grimm, S., Ishida, Y., Kuo, F., Stanger, B. Z. and Leder, P. (1998). The death domain kinase RIP mediates the TNF-induced NF-kappaB signal. *Immunity* **8**, 297-303.

Kerr, J. F., Wyllie, A. H. and Currie, A. R. (1972). Apoptosis: a basic biological phenomenon with wide-ranging implications in tissue kinetics. *Br J Cancer* **26**, 239-57.

Khare, S. D., Sarosi, I., Xia, X. Z., McCabe, S., Miner, K., Solovyev, I., Hawkins, N., Kelley, M., Chang, D., Van, G. *et al.* (2000). Severe B cell hyperplasia and autoimmune disease in TALL-1 transgenic mice. *Proc Natl Acad Sci U S A* **97**, 3370-5.

Khoshnan, A., Bae, D., Tindell, C. A. and Nel, A. E. (2000). The physical association of protein kinase C theta with a lipid raft-associated inhibitor of kappa B factor kinase (IKK) complex plays a role in the activation of the NF-kappa B cascade by TCR and CD28. *J Immunol* **165**, 6933-40.

Khwaja, A. (1999). Akt is more than just a Bad kinase. *Nature* **401**, 33-4.

Khwaja, A., Rodriguez-Viciana, P., Wennstrom, S., Warne, P. H. and Downward, J. (1997). Matrix adhesion and Ras transformation both activate a phosphoinositide 3-OH kinase and protein kinase B/Akt cellular survival pathway. *Embo J* **16**, 2783-93.

Kilger, E., Kieser, A., Baumann, M. and Hammerschmidt, W. (1998). Epstein-Barr virus-mediated B-cell proliferation is dependent upon latent membrane protein 1, which simulates an activated CD40 receptor. *Embo J* **17**, 1700-9.

Kim, I., Kim, J. H., Moon, S. O., Kwak, H. J., Kim, N. G. and Koh, G. Y. (2000a). Angiopoietin-2 at high concentration can enhance endothelial cell survival through the phosphatidylinositol 3'-kinase/Akt signal transduction pathway. *Oncogene* **19**, 4549-52.

Kim, K. E., Gu, C., Thakur, S., Vieira, E., Lin, J. C. and Rabson, A. B. (2000b). Transcriptional regulatory effects of lymphoma-associated NFKB2/lyt10 protooncogenes. *Oncogene* **19**, 1334-45.

Kirshner, J. R., Staskus, K., Haase, A., Lagunoff, M. and Ganem, D. (1999). Expression of the open reading frame 74 (G-protein-coupled receptor) gene of Kaposi's sarcoma (KS)-associated herpesvirus: implications for KS pathogenesis. *J Virol* **73**, 6006-14.

Kischkel, F. C., Lawrence, D. A., Tinel, A., LeBlanc, H., Virmani, A., Schow, P., Gazdar, A., Blenis, J., Arnott, D. and Ashkenazi, A. (2001). Death receptor recruitment of endogenous caspase-10 and apoptosis initiation in the absence of caspase-8. *J Biol Chem* **276**, 46639-46.

Kliche, S., Nagel, W., Kremmer, E., Atzler, C., Ege, A., Knorr, T., Koszinowski, U., Kolanus, W. and Haas, J. (2001). Signaling by human herpesvirus 8 kaposin A through direct membrane recruitment of cytohesin-1. *Mol Cell* **7**, 833-43.

Klouche, M., Brockmeyer, N., Knabbe, C. and Rose-John, S. (2002). Human herpesvirus 8-derived viral IL-6 induces PTX3 expression in Kaposi's sarcoma cells. *Aids* **16**, F9-18.

Knight, J. S., Cotter, M. A., 2nd and Robertson, E. S. (2001). The latency-associated nuclear antigen of Kaposi's sarcoma-associated herpesvirus transactivates the telomerase reverse transcriptase promoter. *J Biol Chem* **276**, 22971-8.

Knowles, D. M., Inghirami, G., Ubriaco, A. and Dalla-Favera, R. (1989). Molecular genetic analysis of three AIDS-associated neoplasms of uncertain lineage demonstrates their B-cell derivation and the possible pathogenetic role of the Epstein-Barr virus. *Blood* **73**, 792-9.

Koch, A. E., Polverini, P. J., Kunkel, S. L., Harlow, L. A., DiPietro, L. A., Elner, V. M., Elner, S. G. and Strieter, R. M. (1992). Interleukin-8 as a macrophage-derived mediator of angiogenesis. *Science* **258**, 1798-801.

Kohl, A. and Grutter, M. G. (2004). Fire and death: the pyrin domain joins the death-domain superfamily. *C R Biol* **327**, 1077-86.

Koike, R., Nishimura, T., Yasumizu, R., Tanaka, H., Hataba, Y., Hataba, Y., Watanabe, T., Miyawaki, S. and Miyasaka, M. (1996). The splenic marginal zone is absent in alymphoplastic aly mutant mice. *Eur J Immunol* **26**, 669-75.

Komatsu, T., Ballestas, M. E., Barbera, A. J., Kelley-Clarke, B. and Kaye, K. M. (2004). KSHV LANA1 binds DNA as an oligomer and residues N-terminal to the oligomerization domain are essential for DNA binding, replication, and episome persistence. *Virology* **319**, 225-36.

Kovalenko, A., Chable-Bessia, C., Cantarella, G., Israel, A., Wallach, D. and Courtois, G. (2003). The tumour suppressor CYLD negatively regulates NF-kappaB signalling by deubiquitination. *Nature* **424**, 801-5.

Krappmann, D. and Scheidereit, C. (2005). A pervasive role of ubiquitin conjugation in activation and termination of IkappaB kinase pathways. *EMBO Rep* **6**, 321-6.

Krithivas, A., Fujimuro, M., Weidner, M., Young, D. B. and Hayward, S. D. (2002). Protein interactions targeting the latency-associated nuclear antigen of Kaposi's sarcoma-associated herpesvirus to cell chromosomes. *J Virol* **76**, 11596-604.

Krithivas, A., Young, D. B., Liao, G., Greene, D. and Hayward, S. D. (2000). Human herpesvirus 8 LANA interacts with proteins of the mSin3 corepressor complex and negatively regulates Epstein-Barr virus gene expression in dually infected PEL cells. *J Virol* **74**, 9637-45.

Kroll, M., Margottin, F., Kohl, A., Renard, P., Durand, H., Concordet, J. P., Bachelerie, F., Arenzana-Seisdedos, F. and Benarous, R. (1999). Inducible degradation of IkappaBalpha by the proteasome requires interaction with the F-box protein h-betaTrCP. *J Biol Chem* **274**, 7941-5.

Krueger, A., Schmitz, I., Baumann, S., Krammer, P. H. and Kirchhoff, S. (2001). Cellular FLICE-inhibitory protein splice variants inhibit different steps of caspase-8 activation at the CD95 death-inducing signaling complex. *J Biol Chem* **276**, 20633-40.

Kunsch, C., Ruben, S. M. and Rosen, C. A. (1992). Selection of optimal kappa B/Rel DNA-binding motifs: interaction of both subunits of NF-kappa B with DNA is required for transcriptional activation. *Mol Cell Biol* **12**, 4412-21.

Kwak, H. J., So, J. N., Lee, S. J., Kim, I. and Koh, G. Y. (1999). Angiopoietin-1 is an apoptosis survival factor for endothelial cells. *FEBS Lett* **448**, 249-53.

Lacoste, V., Mauclere, P., Dubreuil, G., Lewis, J., Georges-Courbot, M. C. and Gessain, A. (2000). KSHV-like herpesviruses in chimps and gorillas. *Nature* **407**, 151-2.

Lagos, D., Trotter, M. W., Vart, R. J., Wang, H. W., Matthews, N. C., Hansen, A., Flore, O., Gotch, F. and Boshoff, C. (2007). Kaposi sarcoma herpesvirus-encoded vFLIP and vIRF1 regulate antigen presentation in lymphatic endothelial cells. *Blood* **109**, 1550-8.

Lagunoff, M. and Ganem, D. (1997). The structure and coding organization of the genomic termini of Kaposi's sarcoma-associated herpesvirus. *Virology* **236**, 147-54.

Lagunoff, M., Lukac, D. M. and Ganem, D. (2001). Immunoreceptor tyrosine-based activation motif-dependent signaling by Kaposi's sarcoma-associated herpesvirus K1 protein: effects on lytic viral replication. *J Virol* **75**, 5891-8.

Lagunoff, M., Majeti, R., Weiss, A. and Ganem, D. (1999). Deregulated signal transduction by the K1 gene product of Kaposi's sarcoma-associated herpesvirus. *Proc Natl Acad Sci U S A* **96**, 5704-9.

Lallena, M. J., Diaz-Meco, M. T., Bren, G., Paya, C. V. and Moscat, J. (1999). Activation of IkappaB kinase beta by protein kinase C isoforms. *Mol Cell Biol* **19**, 2180-8.

Lan, K., Kuppers, D. A., Verma, S. C. and Robertson, E. S. (2004). Kaposi's sarcoma-associated herpesvirus-encoded latency-associated nuclear antigen inhibits lytic replication by targeting Rta: a potential mechanism for virus-mediated control of latency. *J Virol* **78**, 6585-94.

Lan, K., Kuppers, D. A., Verma, S. C., Sharma, N., Murakami, M. and Robertson, E. S. (2005). Induction of Kaposi's sarcoma-associated herpesvirus latency-associated nuclear antigen by the lytic transactivator RTA: a novel mechanism for establishment of latency. *J Virol* **79**, 7453-65.

Langenfeld, E. M., Bojnowski, J., Perone, J. and Langenfeld, J. (2005a). Expression of bone morphogenetic proteins in human lung carcinomas. *Ann Thorac Surg* **80**, 1028-32.

Langenfeld, E. M., Calvano, S. E., Abou-Nukta, F., Lowry, S. F., Amenta, P. and Langenfeld, J. (2003). The mature bone morphogenetic protein-2 is aberrantly expressed in non-small cell lung carcinomas and stimulates tumor growth of A549 cells. *Carcinogenesis* **24**, 1445-54.

Langenfeld, E. M., Kong, Y. and Langenfeld, J. (2005b). Bone morphogenetic protein-2-induced transformation involves the activation of mammalian target of rapamycin. *Mol Cancer Res* **3**, 679-84.

Langenfeld, E. M., Kong, Y. and Langenfeld, J. (2006). Bone morphogenetic protein 2 stimulation of tumor growth involves the activation of Smad-1/5. *Oncogene* **25**, 685-92.

Langenfeld, E. M. and Langenfeld, J. (2004). Bone morphogenetic protein-2 stimulates angiogenesis in developing tumors. *Mol Cancer Res* **2**, 141-9.

Langley, R. R., Fan, D., Tsan, R. Z., Rebhun, R., He, J., Kim, S. J. and Fidler, I. J. (2004). Activation of the platelet-derived growth factor-receptor enhances survival of murine bone endothelial cells. *Cancer Res* **64**, 3727-30.

Lee, B. S., Alvarez, X., Ishido, S., Lackner, A. A. and Jung, J. U. (2000). Inhibition of intracellular transport of B cell antigen receptor complexes by Kaposi's sarcoma-associated herpesvirus K1. *J Exp Med* **192**, 11-21.

Lee, B. S., Connole, M., Tang, Z., Harris, N. L. and Jung, J. U. (2003a). Structural analysis of the Kaposi's sarcoma-associated herpesvirus K1 protein. *J Virol* **77**, 8072-86.

Lee, B. S., Lee, S. H., Feng, P., Chang, H., Cho, N. H. and Jung, J. U. (2005). Characterization of the Kaposi's sarcoma-associated herpesvirus K1 signalosome. *J Virol* **79**, 12173-84.

Lee, B. S., Paulose-Murphy, M., Chung, Y. H., Connlole, M., Zeichner, S. and Jung, J. U. (2002). Suppression of tetradecanoyl phorbol acetate-induced lytic reactivation of Kaposi's sarcoma-associated herpesvirus by K1 signal transduction. *J Virol* **76**, 12185-99.

Lee, H., Choi, J. K., Li, M., Kaye, K., Kieff, E. and Jung, J. U. (1999). Role of cellular tumor necrosis factor receptor-associated factors in NF-kappaB activation and lymphocyte transformation by herpesvirus Saimiri STP. *J Virol* **73**, 3913-9.

Lee, H., Guo, J., Li, M., Choi, J. K., DeMaria, M., Rosenzweig, M. and Jung, J. U. (1998a). Identification of an immunoreceptor tyrosine-based activation motif of K1 transforming protein of Kaposi's sarcoma-associated herpesvirus. *Mol Cell Biol* **18**, 5219-28.

Lee, H., Veazey, R., Williams, K., Li, M., Guo, J., Neipel, F., Fleckenstein, B., Lackner, A., Desrosiers, R. C. and Jung, J. U. (1998b). Deregulation of cell growth by the K1 gene of Kaposi's sarcoma-associated herpesvirus. *Nat Med* **4**, 435-40.

Lee, T. H., Avraham, H. K., Jiang, S. and Avraham, S. (2003b). Vascular endothelial growth factor modulates the transendothelial migration of MDA-MB-231 breast cancer cells through regulation of brain microvascular endothelial cell permeability. *J Biol Chem* **278**, 5277-84.

Leger-Ravet, M. B., Peuchmaur, M., Devergne, O., Audouin, J., Raphael, M., Van Damme, J., Galanaud, P., Diebold, J. and Emilie, D. (1991). Interleukin-6 gene expression in Castleman's disease. *Blood* **78**, 2923-30.

Leitges, M., Sanz, L., Martin, P., Duran, A., Braun, U., Garcia, J. F., Camacho, F., Diaz-Meco, M. T., Rennert, P. D. and Moscat, J. (2001). Targeted disruption of the zetaPKC gene results in the impairment of the NF-kappaB pathway. *Mol Cell* **8**, 771-80.

Li, F. Y., Jeffrey, P. D., Yu, J. W. and Shi, Y. (2006). Crystal structure of a viral FLIP: insights into FLIP-mediated inhibition of death receptor signaling. *J Biol Chem* **281**, 2960-8.

Li, H., Komatsu, T., Dezube, B. J. and Kaye, K. M. (2002). The Kaposi's sarcoma-associated herpesvirus K12 transcript from a primary effusion lymphoma contains complex repeat elements, is spliced, and initiates from a novel promoter. *J Virol* **76**, 11880-8.

Li, H. P. and Chang, Y. S. (2003). Epstein-Barr virus latent membrane protein 1: structure and functions. *J Biomed Sci* **10**, 490-504.

Li, M., Damania, B., Alvarez, X., Ogryzko, V., Ozato, K. and Jung, J. U. (2000). Inhibition of p300 histone acetyltransferase by viral interferon regulatory factor. *Mol Cell Biol* **20**, 8254-63.

Li, M., Lee, H., Guo, J., Neipel, F., Fleckenstein, B., Ozato, K. and Jung, J. U. (1998). Kaposi's sarcoma-associated herpesvirus viral interferon regulatory factor. *J Virol* **72**, 5433-40.

Li, M., Lee, H., Yoon, D. W., Albrecht, J. C., Fleckenstein, B., Neipel, F. and Jung, J. U. (1997). Kaposi's sarcoma-associated herpesvirus encodes a functional cyclin. *J Virol* **71**, 1984-91.

Li, Q., Van Antwerp, D., Mercurio, F., Lee, K. F. and Verma, I. M. (1999a). Severe liver degeneration in mice lacking the IkappaB kinase 2 gene. *Science* **284**, 321-5.

Li, X. H., Fang, X. and Gaynor, R. B. (2001). Role of IKKgamma/nemo in assembly of the Ikappa B kinase complex. *J Biol Chem* **276**, 4494-500.

Li, Z., Zhang, J., Chen, D. and Shu, H. B. (2003). Casper/c-FLIP is physically and functionally associated with NF-kappaB1 p105. *Biochem Biophys Res Commun* **309**, 980-5.

Li, Z. W., Chu, W., Hu, Y., Delhase, M., Deerinck, T., Ellisman, M., Johnson, R. and Karin, M. (1999b). The IKKbeta subunit of IkappaB kinase (IKK) is essential for nuclear factor kappaB activation and prevention of apoptosis. *J Exp Med* **189**, 1839-45.

Liang, C., Zhang, M. and Sun, S. C. (2006). beta-TrCP binding and processing of NF-kappaB2/p100 involve its phosphorylation at serines 866 and 870. *Cell Signal* **18**, 1309-17.

Liao, G. and Sun, S. C. (2003). Regulation of NF-kappaB2/p100 processing by its nuclear shuttling. *Oncogene* **22**, 4868-74.

Liao, G., Zhang, M., Harhaj, E. W. and Sun, S. C. (2004). Regulation of the NF-kappaB-inducing kinase by tumor necrosis factor receptor-associated factor 3-induced degradation. *J Biol Chem* **279**, 26243-50.

Lim, C., Gwack, Y., Hwang, S., Kim, S. and Choe, J. (2001). The transcriptional activity of cAMP response element-binding protein-binding protein is modulated by the latency associated nuclear antigen of Kaposi's sarcoma-associated herpesvirus. *J Biol Chem* **276**, 31016-22.

Lim, C., Sohn, H., Gwack, Y. and Choe, J. (2000). Latency-associated nuclear antigen of Kaposi's sarcoma-associated herpesvirus (human herpesvirus-8) binds ATF4/CREB2 and inhibits its transcriptional activation activity. *J Gen Virol* **81**, 2645-52.

Lim, C., Sohn, H., Lee, D., Gwack, Y. and Choe, J. (2002). Functional dissection of latency-associated nuclear antigen 1 of Kaposi's sarcoma-associated herpesvirus involved in latent DNA replication and transcription of terminal repeats of the viral genome. *J Virol* **76**, 10320-31.

Lin, C. L., Li, H., Wang, Y., Zhu, F. X., Kudchodkar, S. and Yuan, Y. (2003). Kaposi's sarcoma-associated herpesvirus lytic origin (ori-Lyt)-dependent DNA replication: identification of the ori-Lyt and association of K8 bZip protein with the origin. *J Virol* **77**, 5578-88.

Liptay, S., Schmid, R. M., Nabel, E. G. and Nabel, G. J. (1994). Transcriptional regulation of NF-kappa B2: evidence for kappa B-mediated positive and negative autoregulation. *Mol Cell Biol* **14**, 7695-703.

Liu, C., Okruzhnov, Y., Li, H. and Nicholas, J. (2001). Human herpesvirus 8 (HHV-8)-encoded cytokines induce expression of and autocrine signaling by vascular endothelial growth factor (VEGF) in HHV-8-infected primary-effusion lymphoma cell lines and mediate VEGF-independent antiapoptotic effects. *J Virol* **75**, 10933-40.

Liu, L., Eby, M. T., Rathore, N., Sinha, S. K., Kumar, A. and Chaudhary, P. M. (2002). The human herpes virus 8-encoded viral FLICE inhibitory protein physically associates with and persistently activates the Ikappa B kinase complex. *J Biol Chem* **277**, 13745-51.

Low, W., Harries, M., Ye, H., Du, M. Q., Boshoff, C. and Collins, M. (2001). Internal ribosome entry site regulates translation of Kaposi's sarcoma-associated herpesvirus FLICE inhibitory protein. *J Virol* **75**, 2938-45.

Lubyova, B. and Pitha, P. M. (2000). Characterization of a novel human herpesvirus 8-encoded protein, vIRF-3, that shows homology to viral and cellular interferon regulatory factors. *J Virol* **74**, 8194-201.

Lucas, P. C., McAllister-Lucas, L. M. and Nunez, G. (2004). NF-kappaB signaling in lymphocytes: a new cast of characters. *J Cell Sci* **117**, 31-9.

Lucas, P. C., Yonezumi, M., Inohara, N., McAllister-Lucas, L. M., Abazeed, M. E., Chen, F. F., Yamaoka, S., Seto, M. and Nunez, G. (2001). Bcl10 and MALT1, independent targets of chromosomal translocation in malt lymphoma, cooperate in a novel NF-kappa B signaling pathway. *J Biol Chem* **276**, 19012-9.

Luftig, M., Prinarakis, E., Yasui, T., Tsichritzis, T., Cahir-McFarland, E., Inoue, J., Nakano, H., Mak, T. W., Yeh, W. C., Li, X. *et al.* (2003). Epstein-Barr virus latent membrane protein 1 activation of NF-kappaB through IRAK1 and TRAF6. *Proc Natl Acad Sci U S A* **100**, 15595-600.

Lukac, D. M., Renne, R., Kirshner, J. R. and Ganem, D. (1998). Reactivation of Kaposi's sarcoma-associated herpesvirus infection from latency by expression of the ORF 50 transactivator, a homolog of the EBV R protein. *Virology* **252**, 304-12.

Lwin, T., Hazlehurst, L. A., Li, Z., Dessureault, S., Sotomayor, E., Moscinski, L. C., Dalton, W. S. and Tao, J. (2007). Bone marrow stromal cells prevent apoptosis of lymphoma cells by upregulation of anti-apoptotic proteins associated with activation of NF-kappaB (RelB/p52) in non-Hodgkin's lymphoma cells. *Leukemia* **21**, 1521-31.

Mackay, F., Schneider, P., Rennert, P. and Browning, J. (2003). BAFF AND APRIL: a tutorial on B cell survival. *Annu Rev Immunol* **21**, 231-64.

Mackay, F., Woodcock, S. A., Lawton, P., Ambrose, C., Baetscher, M., Schneider, P., Tschopp, J. and Browning, J. L. (1999). Mice transgenic for BAFF develop lymphocytic disorders along with autoimmune manifestations. *J Exp Med* **190**, 1697-710.

MacPhail, L. A., Dekker, N. P. and Regezi, J. A. (1996). Macrophages and vascular adhesion molecules in oral Kaposi's sarcoma. *J Cutan Pathol* **23**, 464-72.

Madge, L. A. and Pober, J. S. (2000). A phosphatidylinositol 3-kinase/Akt pathway, activated by tumor necrosis factor or interleukin-1, inhibits apoptosis but does not activate NFkappaB in human endothelial cells. *J Biol Chem* **275**, 15458-65.

Maisonpierre, P. C., Suri, C., Jones, P. F., Bartunkova, S., Wiegand, S. J., Radziejewski, C., Compton, D., McClain, J., Aldrich, T. H., Papadopoulos, N. *et al.* (1997). Angiopoietin-2, a natural antagonist for Tie2 that disrupts in vivo angiogenesis. *Science* **277**, 55-60.

Makinen, T., Veikkola, T., Mustjoki, S., Karpanen, T., Catimel, B., Nice, E. C., Wise, L., Mercer, A., Kowalski, H., Kerjaschki, D. *et al.* (2001). Isolated lymphatic endothelial cells transduce growth, survival and migratory signals via the VEGF-C/D receptor VEGFR-3. *Embo J* **20**, 4762-73.

Makris, C., Godfrey, V. L., Krahn-Senftleben, G., Takahashi, T., Roberts, J. L., Schwarz, T., Feng, L., Johnson, R. S. and Karin, M. (2000). Female mice heterozygous for IKK gamma/NEMO deficiencies develop a dermatopathy similar to the human X-linked disorder incontinentia pigmenti. *Mol Cell* **5**, 969-79.

Makris, C., Roberts, J. L. and Karin, M. (2002). The carboxyl-terminal region of IkappaB kinase gamma (IKKgamma) is required for full IKK activation. *Mol Cell Biol* **22**, 6573-81.

Malyankar, U. M., Scatena, M., Suchland, K. L., Yun, T. J., Clark, E. A. and Giachelli, C. M. (2000). Osteoprotegerin is an alpha vbeta 3-induced, NF-kappa B-dependent survival factor for endothelial cells. *J Biol Chem* **275**, 20959-62.

Mann, D. J., Child, E. S., Swanton, C., Laman, H. and Jones, N. (1999). Modulation of p27(Kip1) levels by the cyclin encoded by Kaposi's sarcoma-associated herpesvirus. *Embo J* **18**, 654-63.

Marienfeld, R. B., Palkowitsch, L. and Ghosh, S. (2006). Dimerization of the I kappa B kinase-binding domain of NEMO is required for tumor necrosis factor alpha-induced NF-kappa B activity. *Mol Cell Biol* **26**, 9209-19.

Martin, D. F., Kuppermann, B. D., Wolitz, R. A., Palestine, A. G., Li, H. and Robinson, C. A. (1999). Oral ganciclovir for patients with cytomegalovirus retinitis treated with a ganciclovir implant. Roche Ganciclovir Study Group. *N Engl J Med* **340**, 1063-70.

Matloubian, M., David, A., Engel, S., Ryan, J. E. and Cyster, J. G. (2000). A transmembrane CXC chemokine is a ligand for HIV-coreceptor Bonzo. *Nat Immunol* **1**, 298-304.

Matta, H. and Chaudhary, P. M. (2004). Activation of alternative NF-kappa B pathway by human herpes virus 8-encoded Fas-associated death domain-like IL-1 beta-converting enzyme inhibitory protein (vFLIP). *Proc Natl Acad Sci U S A* **101**, 9399-404.

Matta, H., Eby, M. T., Gazdar, A. F. and Chaudhary, P. M. (2002). Role of MRIT/cFLIP in protection against chemotherapy-induced apoptosis. *Cancer Biol Ther* **1**, 652-60.

Matta, H., Mazzacurati, L., Schamus, S., Yang, T., Sun, Q. and Chaudhary, P. M. (2007a). KSHV oncoprotein K13 bypasses TRAFs and directly interacts with the Ikappa B kinase complex to selectively activate NF-kappa B without JNK activation. *J Biol Chem.*

Matta, H., Sun, Q., Moses, G. and Chaudhary, P. M. (2003). Molecular genetic analysis of human herpes virus 8-encoded viral FLICE inhibitory protein-induced NF-kappaB activation. *J Biol Chem* **278**, 52406-11.

Matta, H., Surabhi, R. M., Zhao, J., Punj, V., Sun, Q., Schamus, S., Mazzacurati, L. and Chaudhary, P. M. (2007b). Induction of spindle cell morphology in human vascular endothelial cells by human herpesvirus 8-encoded viral FLICE inhibitory protein K13. *Oncogene* **26**, 1656-60.

May, M. J., D'Acquisto, F., Madge, L. A., Glockner, J., Pober, J. S. and Ghosh, S. (2000). Selective inhibition of NF-kappaB activation by a peptide that blocks the interaction of NEMO with the IkappaB kinase complex. *Science* **289**, 1550-4.

May, M. J. and Ghosh, S. (1997). Rel/NF-kappa B and I kappa B proteins: an overview. *Semin Cancer Biol* **8**, 63-73.

May, M. J., Marienfeld, R. B. and Ghosh, S. (2002). Characterization of the Ikappa B-kinase NEMO binding domain. *J Biol Chem* **277**, 45992-6000.

McCormick, C. and Ganem, D. (2005). The kaposin B protein of KSHV activates the p38/MK2 pathway and stabilizes cytokine mRNAs. *Science* **307**, 739-41.

McGeoch, D. J. (2001). Molecular evolution of the gamma-Herpesvirinae. *Philos Trans R Soc Lond B Biol Sci* **356**, 421-35.

McGeoch, D. J. and Davison, A. J. (1999). The descent of human herpesvirus 8. *Semin Cancer Biol* **9**, 201-9.

Mercurio, F., DiDonato, J. A., Rosette, C. and Karin, M. (1993). p105 and p98 precursor proteins play an active role in NF-kappa B-mediated signal transduction. *Genes Dev* **7**, 705-18.

Mercurio, F., Murray, B. W., Shevchenko, A., Bennett, B. L., Young, D. B., Li, J. W., Pascual, G., Motiwala, A., Zhu, H., Mann, M. *et al.* (1999). IkappaB kinase (IKK)-associated protein 1, a common component of the heterogeneous IKK complex. *Mol Cell Biol* **19**, 1526-38.

Mercurio, F., Zhu, H., Murray, B. W., Shevchenko, A., Bennett, B. L., Li, J., Young, D. B., Barbosa, M., Mann, M., Manning, A. *et al.* (1997). IKK-1 and IKK-2: cytokine-activated IkappaB kinases essential for NF-kappaB activation. *Science* **278**, 860-6.

Meredith, J. E., Jr., Fazeli, B. and Schwartz, M. A. (1993). The extracellular matrix as a cell survival factor. *Mol Biol Cell* **4**, 953-61.

Micheau, O., Thome, M., Schneider, P., Holler, N., Tschopp, J., Nicholson, D. W., Briand, C. and Grutter, M. G. (2002). The long form of FLIP is an activator of caspase-8 at the Fas death-inducing signaling complex. *J Biol Chem* **277**, 45162-71.

Migliazza, A., Lombardi, L., Rocchi, M., Trecca, D., Chang, C. C., Antonacci, R., Fracchiolla, N. S., Ciana, P., Maiolo, A. T. and Neri, A. (1994). Heterogeneous chromosomal aberrations generate 3' truncations of the NFKB2/lyt-10 gene in lymphoid malignancies. *Blood* **84**, 3850-60.

Miles, S. A., Rezai, A. R., Salazar-Gonzalez, J. F., Vander Meyden, M., Stevens, R. H., Logan, D. M., Mitsuyasu, R. T., Taga, T., Hirano, T., Kishimoto, T. *et al.* (1990). AIDS Kaposi sarcoma-derived cells produce and respond to interleukin 6. *Proc Natl Acad Sci U S A* **87**, 4068-72.

Miller, B. S. and Zandi, E. (2001). Complete reconstitution of human IkappaB kinase (IKK) complex in yeast. Assessment of its stoichiometry and the role of IKKgamma on the complex activity in the absence of stimulation. *J Biol Chem* **276**, 36320-6.

Mitchell, T. and Sugden, B. (1995). Stimulation of NF-kappa B-mediated transcription by mutant derivatives of the latent membrane protein of Epstein-Barr virus. *J Virol* **69**, 2968-76.

Molden, J., Chang, Y., You, Y., Moore, P. S. and Goldsmith, M. A. (1997). A Kaposi's sarcoma-associated herpesvirus-encoded cytokine homolog (vIL-6) activates signaling through the shared gp130 receptor subunit. *J Biol Chem* **272**, 19625-31.

Molitor, J. A., Walker, W. H., Doerre, S., Ballard, D. W. and Greene, W. C. (1990). NF-kappa B: a family of inducible and differentially expressed enhancer-binding proteins in human T cells. *Proc Natl Acad Sci U S A* **87**, 10028-32.

Montague, M. G. and Hutchison, C. A., 3rd. (2000). Gene content phylogeny of herpesviruses. *Proc Natl Acad Sci U S A* **97**, 5334-9.

Montaner, S., Sodhi, A., Molinolo, A., Bugge, T. H., Sawai, E. T., He, Y., Li, Y., Ray, P. E. and Gutkind, J. S. (2003). Endothelial infection with KSHV genes in vivo reveals that vGPCR initiates Kaposi's sarcomagenesis and can promote the tumorigenic potential of viral latent genes. *Cancer Cell* **3**, 23-36.

Montaner, S., Sodhi, A., Pece, S., Mesri, E. A. and Gutkind, J. S. (2001). The Kaposi's sarcoma-associated herpesvirus G protein-coupled receptor promotes endothelial cell survival through the activation of Akt/protein kinase B. *Cancer Res* **61**, 2641-8.

Montaner, S., Sodhi, A., Servitja, J. M., Ramsdell, A. K., Barac, A., Sawai, E. T. and Gutkind, J. S. (2004). The small GTPase Rac1 links the Kaposi sarcoma-associated herpesvirus vGPCR to cytokine secretion and paracrine neoplasia. *Blood* **104**, 2903-11.

Moore, P. S., Boshoff, C., Weiss, R. A. and Chang, Y. (1996). Molecular mimicry of human cytokine and cytokine response pathway genes by KSHV. *Science* **274**, 1739-44.

Moore, P. S. and Chang, Y. (1998). Antiviral activity of tumor-suppressor pathways: clues from molecular piracy by KSHV. *Trends Genet* **14**, 144-50.

Moore, P. S. and Chang, Y. (2001). Molecular virology of Kaposi's sarcoma-associated herpesvirus. *Philos Trans R Soc Lond B Biol Sci* **356**, 499-516.

Moorthy, R. K. and Thorley-Lawson, D. A. (1993). Biochemical, genetic, and functional analyses of the phosphorylation sites on the Epstein-Barr virus-encoded oncogenic latent membrane protein LMP-1. *J Virol* **67**, 2637-45.

Mordmuller, B., Krappmann, D., Esen, M., Wegener, E. and Scheidereit, C. (2003). Lymphotoxin and lipopolysaccharide induce NF-kappaB-p52 generation by a co-translational mechanism. *EMBO Rep* **4**, 82-7.

Moses, A. V., Fish, K. N., Ruhl, R., Smith, P. P., Strussenberg, J. G., Zhu, L., Chandran, B. and Nelson, J. A. (1999). Long-term infection and transformation of dermal microvascular endothelial cells by human herpesvirus 8. *J Virol* **73**, 6892-902.

Muller, C. W. and Harrison, S. C. (1995). The structure of the NF-kappa B p50:DNA-complex: a starting point for analyzing the Rel family. *FEBS Lett* **369**, 113-7.

Muller, J. R. and Siebenlist, U. (2003). Lymphotoxin beta receptor induces sequential activation of distinct NF-kappa B factors via separate signaling pathways. *J Biol Chem* **278**, 12006-12.

Munshi, N., Ganju, R. K., Avraham, S., Mesri, E. A. and Groopman, J. E. (1999). Kaposi's sarcoma-associated herpesvirus-encoded G protein-coupled receptor activation of c-jun amino-terminal kinase/stress-activated protein kinase and lyn kinase is mediated by related adhesion focal tyrosine kinase/proline-rich tyrosine kinase 2. *J Biol Chem* **274**, 31863-7.

Munshi, N., Merika, M., Yie, J., Senger, K., Chen, G. and Thanos, D. (1998). Acetylation of HMG I(Y) by CBP turns off IFN beta expression by disrupting the enhanceosome. *Mol Cell* **2**, 457-67.

Muralidhar, S., Pumfery, A. M., Hassani, M., Sadaie, M. R., Kishishita, M., Brady, J. N., Doniger, J., Medveczky, P. and Rosenthal, L. J. (1998). Identification of kaposin (open reading frame K12) as a human herpesvirus 8 (Kaposi's sarcoma-associated herpesvirus) transforming gene. *J Virol* **72**, 4980-8.

Nador, R. G., Cesarman, E., Chadburn, A., Dawson, D. B., Ansari, M. Q., Sald, J. and Knowles, D. M. (1996). Primary effusion lymphoma: a distinct clinicopathologic entity associated with the Kaposi's sarcoma-associated herpes virus. *Blood* **88**, 645-56.

Nakamura, H., Li, M., Zarycki, J. and Jung, J. U. (2001). Inhibition of p53 tumor suppressor by viral interferon regulatory factor. *J Virol* **75**, 7572-82.

Naldini, L., Blomer, U., Gallay, P., Ory, D., Mulligan, R., Gage, F. H., Verma, I. M. and Trono, D. (1996). In vivo gene delivery and stable transduction of nondividing cells by a lentiviral vector. *Science* **272**, 263-7.

Naranatt, P. P., Akula, S. M., Zien, C. A., Krishnan, H. H. and Chandran, B. (2003). Kaposi's sarcoma-associated herpesvirus induces the phosphatidylinositol 3-kinase-PKC-zeta-MEK-ERK signaling pathway in target cells early during infection: implications for infectivity. *J Virol* **77**, 1524-39.

Naranatt, P. P., Krishnan, H. H., Svojanovsky, S. R., Bloomer, C., Mathur, S. and Chandran, B. (2004). Host gene induction and transcriptional reprogramming in Kaposi's sarcoma-associated herpesvirus (KSHV/HHV-8)-infected endothelial, fibroblast, and B cells: insights into modulation events early during infection. *Cancer Res* **64**, 72-84.

Naumann, M., Nieters, A., Hatada, E. N. and Scheidereit, C. (1993). NF-kappa B precursor p100 inhibits nuclear translocation and DNA binding of NF-kappa B/rel-factors. *Oncogene* **8**, 2275-81.

Neipel, F., Albrecht, J. C. and Fleckenstein, B. (1997). Cell-homologous genes in the Kaposi's sarcoma-associated rhadinovirus human herpesvirus 8: determinants of its pathogenicity? *J Virol* **71**, 4187-92.

Neipel, F., Albrecht, J. C. and Fleckenstein, B. (1998). Human herpesvirus 8--the first human Rhadinovirus. *J Natl Cancer Inst Monogr*, 73-7.

Nelson, D. E., Ihekwaba, A. E., Elliott, M., Johnson, J. R., Gibney, C. A., Foreman, B. E., Nelson, G., See, V., Horton, C. A., Spiller, D. G. *et al.* (2004). Oscillations in NF-kappaB signaling control the dynamics of gene expression. *Science* **306**, 704-8.

Neri, A., Chang, C. C., Lombardi, L., Salina, M., Corradini, P., Maiolo, A. T., Chaganti, R. S. and Dalla-Favera, R. (1991). B cell lymphoma-associated chromosomal translocation involves candidate oncogene lyt-10, homologous to NF-kappa B p50. *Cell* **67**, 1075-87.

Neri, A., Fracchiolla, N. S., Migliazza, A., Trecca, D. and Lombardi, L. (1996). The involvement of the candidate proto-oncogene NFKB2/lyt-10 in lymphoid malignancies. *Leuk Lymphoma* **23**, 43-8.

Neri, A., Fracchiolla, N. S., Roscetti, E., Garatti, S., Trecca, D., Boletini, A., Perletti, L., Baldini, L., Maiolo, A. T. and Berti, E. (1995). Molecular analysis of cutaneous B- and T-cell lymphomas. *Blood* **86**, 3160-72.

Neufeld, G., Cohen, T., Gengrinovitch, S. and Poltorak, Z. (1999). Vascular endothelial growth factor (VEGF) and its receptors. *Faseb J* **13**, 9-22.

Nicholas, J. (2003). Human herpesvirus-8-encoded signalling ligands and receptors. *J Biomed Sci* **10**, 475-89.

Nicholas, J., Ruvolo, V. R., Burns, W. H., Sandford, G., Wan, X., Ciufo, D., Hendrickson, S. B., Guo, H. G., Hayward, G. S. and Reitz, M. S. (1997). Kaposi's sarcoma-associated human herpesvirus-8 encodes homologues of macrophage inflammatory protein-1 and interleukin-6. *Nat Med* **3**, 287-92.

Nickoloff, B. J. and Griffiths, C. E. (1989). Factor XIIIa-expressing dermal dendrocytes in AIDS-associated cutaneous Kaposi's sarcomas. *Science* **243**, 1736-7.

Nor, J. E., Christensen, J., Liu, J., Peters, M., Mooney, D. J., Strieter, R. M. and Polverini, P. J. (2001). Up-Regulation of Bcl-2 in microvascular endothelial cells enhances intratumoral angiogenesis and accelerates tumor growth. *Cancer Res* **61**, 2183-8.

Nor, J. E., Christensen, J., Mooney, D. J. and Polverini, P. J. (1999). Vascular endothelial growth factor (VEGF)-mediated angiogenesis is associated with enhanced endothelial cell survival and induction of Bcl-2 expression. *Am J Pathol* **154**, 375-84.

Novack, D. V., Yin, L., Hagen-Stapleton, A., Schreiber, R. D., Goeddel, D. V., Ross, F. P. and Teitelbaum, S. L. (2003). The IkappaB function of NF-kappaB2 p100 controls stimulated osteoclastogenesis. *J Exp Med* **198**, 771-81.

O'Connor, D. S., Schechner, J. S., Adida, C., Mesri, M., Rothermel, A. L., Li, F., Nath, A. K., Pober, J. S. and Altieri, D. C. (2000). Control of apoptosis during angiogenesis by survivin expression in endothelial cells. *Am J Pathol* **156**, 393-8.

Ojala, P. M., Tiainen, M., Salven, P., Veikkola, T., Castanos-Velez, E., Sarid, R., Biberfeld, P. and Makela, T. P. (1999). Kaposi's sarcoma-associated herpesvirus-encoded v-cyclin triggers apoptosis in cells with high levels of cyclin-dependent kinase 6. *Cancer Res* **59**, 4984-9.

Ojala, P. M., Yamamoto, K., Castanos-Velez, E., Biberfeld, P., Korsmeyer, S. J. and Makela, T. P. (2000). The apoptotic v-cyclin-CDK6 complex phosphorylates and inactivates Bcl-2. *Nat Cell Biol* **2**, 819-25.

Orenstein, J. M., Alkan, S., Blauvelt, A., Jeang, K. T., Weinstein, M. D., Ganem, D. and Herndier, B. (1997). Visualization of human herpesvirus type 8 in Kaposi's sarcoma by light and transmission electron microscopy. *Aids* **11**, F35-45.

Pahl, H. L. (1999). Activators and target genes of Rel/NF-kappaB transcription factors. *Oncogene* **18**, 6853-66.

Papapetropoulos, A., Fulton, D., Mahboubi, K., Kalb, R. G., O'Connor, D. S., Li, F., Altieri, D. C. and Sessa, W. C. (2000). Angiopoietin-1 inhibits endothelial cell apoptosis via the Akt/survivin pathway. *J Biol Chem* **275**, 9102-5.

Parry, G. C. and Mackman, N. (1994). A set of inducible genes expressed by activated human monocytic and endothelial cells contain kappa B-like sites that specifically bind c-Rel-p65 heterodimers. *J Biol Chem* **269**, 20823-5.

Pastore, C., Gloghini, A., Volpe, G., Nomdedeu, J., Leonardo, E., Mazza, U., Saglio, G., Carbone, A. and Gaidano, G. (1995). Distribution of Kaposi's sarcoma herpesvirus sequences among lymphoid malignancies in Italy and Spain. *Br J Haematol* **91**, 918-20.

Pati, S., Cavrois, M., Guo, H. G., Foulke, J. S., Jr., Kim, J., Feldman, R. A. and Reitz, M. (2001). Activation of NF-kappaB by the human herpesvirus 8 chemokine receptor ORF74: evidence for a paracrine model of Kaposi's sarcoma pathogenesis. *J Virol* **75**, 8660-73.

Pati, S., Foulke, J. S., Jr., Barabitskaya, O., Kim, J., Nair, B. C., Hone, D., Smart, J., Feldman, R. A. and Reitz, M. (2003). Human herpesvirus 8-encoded vGPCR activates nuclear factor of activated T cells and collaborates with human immunodeficiency virus type 1 Tat. *J Virol* **77**, 5759-73.

Paulose-Murphy, M., Ha, N. K., Xiang, C., Chen, Y., Gillim, L., Yarchoan, R., Meltzer, P., Bittner, M., Trent, J. and Zeichner, S. (2001). Transcription program of human herpesvirus 8 (kaposi's sarcoma-associated herpesvirus). *J Virol* **75**, 4843-53.

Pellet, C., Kerob, D., Dupuy, A., Carmagnat, M. V., Mourah, S., Podgorniak, M. P., Toledano, C., Morel, P., Verola, O., Dosquet, C. *et al.* (2006). Kaposi's sarcoma-associated

herpesvirus viremia is associated with the progression of classic and endemic Kaposi's sarcoma. *J Invest Dermatol* **126**, 621-7.

Perkins, N. D., Felzien, L. K., Betts, J. C., Leung, K., Beach, D. H. and Nabel, G. J. (1997). Regulation of NF-kappaB by cyclin-dependent kinases associated with the p300 coactivator. *Science* **275**, 523-7.

Peter, M. E. and Krammer, P. H. (2003). The CD95(APO-1/Fas) DISC and beyond. *Cell Death Differ* **10**, 26-35.

Pfeffer, S., Sewer, A., Lagos-Quintana, M., Sheridan, R., Sander, C., Grasser, F. A., van Dyk, L. F., Ho, C. K., Shuman, S., Chien, M. *et al.* (2005). Identification of microRNAs of the herpesvirus family. *Nat Methods* **2**, 269-76.

Piolot, T., Tramier, M., Coppey, M., Nicolas, J. C. and Marechal, V. (2001). Close but distinct regions of human herpesvirus 8 latency-associated nuclear antigen 1 are responsible for nuclear targeting and binding to human mitotic chromosomes. *J Virol* **75**, 3948-59.

Plaksin, D., Baeuerle, P. A. and Eisenbach, L. (1993). KBF1 (p50 NF-kappa B homodimer) acts as a repressor of H-2Kb gene expression in metastatic tumor cells. *J Exp Med* **177**, 1651-62.

Platt, G. M., Simpson, G. R., Mittnacht, S. and Schulz, T. F. (1999). Latent nuclear antigen of Kaposi's sarcoma-associated herpesvirus interacts with RING3, a homolog of the Drosophila female sterile homeotic (fsh) gene. *J Virol* **73**, 9789-95.

Poiesz, B. J., Ruscetti, F. W., Gazdar, A. F., Bunn, P. A., Minna, J. D. and Gallo, R. C. (1980). Detection and isolation of type C retrovirus particles from fresh and cultured lymphocytes of a patient with cutaneous T-cell lymphoma. *Proc Natl Acad Sci U S A* **77**, 7415-9.

Poison, A. G., Wang, D., DeRisi, J. and Ganem, D. (2002). Modulation of host gene expression by the constitutively active G protein-coupled receptor of Kaposi's sarcoma-associated herpesvirus. *Cancer Res* **62**, 4525-30.

Pomerantz, J. L. and Baltimore, D. (2002). Two pathways to NF-kappaB. *Mol Cell* **10**, 693-5.

Poole, L. J., Zong, J. C., Ciufo, D. M., Alcendor, D. J., Cannon, J. S., Ambinder, R., Orenstein, J. M., Reitz, M. S. and Hayward, G. S. (1999). Comparison of genetic variability at multiple loci across the genomes of the major subtypes of Kaposi's sarcoma-associated herpesvirus reveals evidence for recombination and for two distinct types of open reading frame K15 alleles at the right-hand end. *J Virol* **73**, 6646-60.

Poyet, J. L., Srinivasula, S. M., Lin, J. H., Fernandes-Alnemri, T., Yamaoka, S., Tsichlis, P. N. and Alnemri, E. S. (2000). Activation of the Ikappa B kinases by RIP via IKKgamma /NEMO-mediated oligomerization. *J Biol Chem* **275**, 37966-77.

Prakash, O., Tang, Z. Y., Peng, X., Coleman, R., Gill, J., Farr, G. and Samaniego, F. (2002). Tumorigenesis and aberrant signaling in transgenic mice expressing the human herpesvirus-8 K1 gene. *J Natl Cancer Inst* **94**, 926-35.

Pulverer, B. J., Fisher, C., Vousden, K., Littlewood, T., Evan, G. and Woodgett, J. R. (1994). Site-specific modulation of c-Myc cotransformation by residues phosphorylated in vivo. *Oncogene* **9**, 59-70.

Qin, H., Srinivasula, S. M., Wu, G., Fernandes-Alnemri, T., Alnemri, E. S. and Shi, Y. (1999). Structural basis of procaspase-9 recruitment by the apoptotic protease-activating factor 1. *Nature* **399**, 549-57.

Qing, G., Qu, Z. and Xiao, G. (2005). Regulation of NF-kappa B2 p100 processing by its cis-acting domain. *J Biol Chem* **280**, 18-27.

Qing, G., Qu, Z. and Xiao, G. (2007). Endoproteolytic processing of C-terminally truncated NF-kappaB2 precursors at kappaB-containing promoters. *Proc Natl Acad Sci U S A* **104**, 5324-9.

Qing, G. and Xiao, G. (2005). Essential role of IkappaB kinase alpha in the constitutive processing of NF-kappaB2 p100. *J Biol Chem* **280**, 9765-8.

Qu, Z., Qing, G., Rabson, A. and Xiao, G. (2004). Tax deregulation of NF-kappaB2 p100 processing involves both beta-TrCP-dependent and -independent mechanisms. *J Biol Chem* **279**, 44563-72.

Rabkin, C. S., Bedi, G., Musaba, E., Sunkutu, R., Mwansa, N., Sidransky, D. and Biggar, R. J. (1995). AIDS-related Kaposi's sarcoma is a clonal neoplasm. *Clin Cancer Res* **1**, 257-60.

Rabkin, C. S., Janz, S., Lash, A., Coleman, A. E., Musaba, E., Liotta, L., Biggar, R. J. and Zhuang, Z. (1997). Monoclonal origin of multicentric Kaposi's sarcoma lesions. *N Engl J Med* **336**, 988-93.

Radkov, S. A., Kellam, P. and Boshoff, C. (2000). The latent nuclear antigen of Kaposi sarcoma-associated herpesvirus targets the retinoblastoma-E2F pathway and with the oncogene Hras transforms primary rat cells. *Nat Med* **6**, 1121-7.

Ragoczy, T. and Miller, G. (2001). Autostimulation of the Epstein-Barr virus BRLF1 promoter is mediated through consensus Sp1 and Sp3 binding sites. *J Virol* **75**, 5240-51.

Rasper, D. M., Vaillancourt, J. P., Hadano, S., Houtzager, V. M., Seiden, I., Keen, S. L., Tawa, P., Xanthoudakis, S., Nasir, J., Martindale, D. *et al.* (1998). Cell death attenuation by 'Usurpin', a mammalian DED-caspase homologue that precludes caspase-8 recruitment and activation by the CD-95 (Fas, APO-1) receptor complex. *Cell Death Differ* **5**, 271-88.

Rayet, B. and Gelinas, C. (1999). Aberrant rel/nfkb genes and activity in human cancer. *Oncogene* **18**, 6938-47.

Reed, J. C., Doctor, K. S. and Godzik, A. (2004). The domains of apoptosis: a genomics perspective. *Sci STKE* **2004**, re9.

Regezi, J. A., MacPhail, L. A., Daniels, T. E., DeSouza, Y. G., Greenspan, J. S. and Greenspan, D. (1993). Human immunodeficiency virus-associated oral Kaposi's sarcoma. A heterogeneous cell population dominated by spindle-shaped endothelial cells. *Am J Pathol* **143**, 240-9.

Regnier, C. H., Song, H. Y., Gao, X., Goeddel, D. V., Cao, Z. and Rothe, M. (1997). Identification and characterization of an IkappaB kinase. *Cell* **90**, 373-83.

Renne, R., Barry, C., Dittmer, D., Compitello, N., Brown, P. O. and Ganem, D. (2001). Modulation of cellular and viral gene expression by the latency-associated nuclear antigen of Kaposi's sarcoma-associated herpesvirus. *J Virol* **75**, 458-68.

Renne, R., Lagunoff, M., Zhong, W. and Ganem, D. (1996a). The size and conformation of Kaposi's sarcoma-associated herpesvirus (human herpesvirus 8) DNA in infected cells and virions. *J Virol* **70**, 8151-4.

Renne, R., Zhong, W., Herndier, B., McGrath, M., Abbey, N., Kedes, D. and Ganem, D. (1996b). Lytic growth of Kaposi's sarcoma-associated herpesvirus (human herpesvirus 8) in culture. *Nat Med* **2**, 342-6.

Ressler, S., Connor, L. M. and Marriott, S. J. (1996). Cellular transformation by human T-cell leukemia virus type I. *FEMS Microbiol Lett* **140**, 99-109.

Rice, N. R., MacKichan, M. L. and Israel, A. (1992). The precursor of NF-kappa B p50 has I kappa B-like functions. *Cell* **71**, 243-53.

Riedl, S. J. and Shi, Y. (2004). Molecular mechanisms of caspase regulation during apoptosis. *Nat Rev Mol Cell Biol* **5**, 897-907.

Rivas, C., Thlick, A. E., Parravicini, C., Moore, P. S. and Chang, Y. (2001). Kaposi's sarcoma-associated herpesvirus LANA2 is a B-cell-specific latent viral protein that inhibits p53. *J Virol* **75**, 429-38.

Rocha, S., Martin, A. M., Meek, D. W. and Perkins, N. D. (2003). p53 represses cyclin D1 transcription through down regulation of Bcl-3 and inducing increased association of the p52 NF-kappaB subunit with histone deacetylase 1. *Mol Cell Biol* **23**, 4713-27.

Roff, M., Thompson, J., Rodriguez, M. S., Jacque, J. M., Baleux, F., Arenzana-Seisdedos, F. and Hay, R. T. (1996). Role of IkappaBalpha ubiquitination in signal-induced activation of NFkappaB in vivo. *J Biol Chem* **271**, 7844-50.

Romieu-Mourez, R., Kim, D. W., Shin, S. M., Demicco, E. G., Landesman-Bollag, E., Seldin, D. C., Cardiff, R. D. and Sonenshein, G. E. (2003). Mouse mammary tumor virus c-rel transgenic mice develop mammary tumors. *Mol Cell Biol* **23**, 5738-54.

Rose, T. M., Strand, K. B., Schultz, E. R., Schaefer, G., Rankin, G. W., Jr., Thouless, M. E., Tsai, C. C. and Bosch, M. L. (1997). Identification of two homologs of the Kaposi's sarcoma-associated herpesvirus (human herpesvirus 8) in retroperitoneal fibromatosis of different macaque species. *J Virol* **71**, 4138-44.

Rosen, E. M., Lamszus, K., Laterra, J., Polverini, P. J., Rubin, J. S. and Goldberg, I. D. (1997). HGF/SF in angiogenesis. *Ciba Found Symp* **212**, 215-26; discussion 227-9.

Rosenkilde, M. M., Kledal, T. N., Brauner-Osborne, H. and Schwartz, T. W. (1999). Agonists and inverse agonists for the herpesvirus 8-encoded constitutively active seven-transmembrane oncogene product, ORF-74. *J Biol Chem* **274**, 956-61.

Rothhammer, T., Poser, I., Soncin, F., Bataille, F., Moser, M. and Bosserhoff, A. K. (2005). Bone morphogenic proteins are overexpressed in malignant melanoma and promote cell invasion and migration. *Cancer Res* **65**, 448-56.

Rothwarf, D. M. and Karin, M. (1999). The NF-kappa B activation pathway: a paradigm in information transfer from membrane to nucleus. *Sci STKE* **1999**, RE1.

Rothwarf, D. M., Zandi, E., Natoli, G. and Karin, M. (1998). IKK-gamma is an essential regulatory subunit of the IkappaB kinase complex. *Nature* **395**, 297-300.

Rowe, M., Khanna, R., Jacob, C. A., Argaet, V., Kelly, A., Powis, S., Belich, M., Croom-Carter, D., Lee, S., Burrows, S. R. *et al.* (1995). Restoration of endogenous antigen processing in Burkitt's lymphoma cells by Epstein-Barr virus latent membrane protein-1: coordinate up-regulation of peptide transporters and HLA-class I antigen expression. *Eur J Immunol* **25**, 1374-84.

Rudolph, D., Yeh, W. C., Wakeham, A., Rudolph, B., Nallainathan, D., Potter, J., Elia, A. J. and Mak, T. W. (2000). Severe liver degeneration and lack of NF-kappaB activation in NEMO/IKKgamma-deficient mice. *Genes Dev* **14**, 854-62.

Ruland, J., Duncan, G. S., Elia, A., del Barco Barrantes, I., Nguyen, L., Plyte, S., Millar, D. G., Bouchard, D., Wakeham, A., Ohashi, P. S. *et al.* (2001). Bcl10 is a positive regulator of antigen receptor-induced activation of NF-kappaB and neural tube closure. *Cell* **104**, 33-42.

Russo, J. J., Bohenzky, R. A., Chien, M. C., Chen, J., Yan, M., Maddalena, D., Parry, J. P., Peruzzi, D., Edelman, I. S., Chang, Y. *et al.* (1996). Nucleotide sequence of the Kaposi sarcoma-associated herpesvirus (HHV8). *Proc Natl Acad Sci U S A* **93**, 14862-7.

Ryseck, R. P., Bull, P., Takamiya, M., Bours, V., Siebenlist, U., Dobrzanski, P. and Bravo, R. (1992). RelB, a new Rel family transcription activator that can interact with p50-NF-kappa B. *Mol Cell Biol* **12**, 674-84.

Ryseck, R. P., Novotny, J. and Bravo, R. (1995). Characterization of elements determining the dimerization properties of RelB and p50. *Mol Cell Biol* **15**, 3100-9.

Saccani, S., Pantano, S., Natoli, G. 11, 1563-1574. (2003). Modulation of NF-kappaB activity by exchange of dimers. *Mol. Cell*

Sadagopan, S., Sharma-Walia, N., Veettil, M. V., Raghu, H., Sivakumar, R., Bottero, V. and Chandran, B. (2007). Kaposi's sarcoma-associated herpesvirus induces sustained NF-kappaB activation during de novo infection of primary human dermal microvascular endothelial cells that is essential for viral gene expression. *J Virol* **81**, 3949-68.

Sadler, R., Wu, L., Forghani, B., Renne, R., Zhong, W., Herndier, B. and Ganem, D. (1999). A complex translational program generates multiple novel proteins from the latently expressed kaposin (K12) locus of Kaposi's sarcoma-associated herpesvirus. *J Virol* **73**, 5722-30.

Said, W., Chien, K., Takeuchi, S., Tasaka, T., Asou, H., Cho, S. K., de Vos, S., Cesarman, E., Knowles, D. M. and Koeffler, H. P. (1996). Kaposi's sarcoma-associated herpesvirus (KSHV or HHV8) in primary effusion lymphoma: ultrastructural demonstration of herpesvirus in lymphoma cells. *Blood* **87**, 4937-43.

Saito, K., Kigawa, T., Koshiba, S., Sato, K., Matsuo, Y., Sakamoto, A., Takagi, T., Shirouzu, M., Yabuki, T., Nunokawa, E. *et al.* (2004). The CAP-Gly domain of CYLD associates with the proline-rich sequence in NEMO/IKKgamma. *Structure* **12**, 1719-28.

Saito, N., Courtois, G., Chiba, A., Yamamoto, N., Nitta, T., Hironaka, N., Rowe, M., Yamamoto, N. and Yamaoka, S. (2003). Two carboxyl-terminal activation regions of Epstein-Barr virus latent membrane protein 1 activate NF-kappaB through distinct signaling pathways in fibroblast cell lines. *J Biol Chem* **278**, 46565-75.

Saitoh, T., Nakano, H., Yamamoto, N. and Yamaoka, S. (2002). Lymphotoxin-beta receptor mediates NEMO-independent NF-kappaB activation. *FEBS Lett* **532**, 45-51.

Saitoh, T., Nakayama, M., Nakano, H., Yagita, H., Yamamoto, N. and Yamaoka, S. (2003). TWEAK induces NF-kappaB2 p100 processing and long lasting NF-kappaB activation. *J Biol Chem* **278**, 36005-12.

Salahuddin, S. Z., Nakamura, S., Biberfeld, P., Kaplan, M. H., Markham, P. D., Larsson, L. and Gallo, R. C. (1988). Angiogenic properties of Kaposi's sarcoma-derived cells after long-term culture in vitro. *Science* **242**, 430-3.

Samaniego, F., Pati, S., Karp, J. E., Prakash, O. and Bose, D. (2001). Human herpesvirus 8 K1-associated nuclear factor-kappa B-dependent promoter activity: role in Kaposi's sarcoma inflammation? *J Natl Cancer Inst Monogr*, 15-23.

Samols, M. A., Hu, J., Skalsky, R. L. and Renne, R. (2005). Cloning and identification of a microRNA cluster within the latency-associated region of Kaposi's sarcoma-associated herpesvirus. *J Virol* **79**, 9301-5.

Santoro, M. G., Rossi, A. and Amici, C. (2003). NF-kappaB and virus infection: who controls whom. *Embo J* **22**, 2552-60.

Sanz, L., Diaz-Meco, M. T., Nakano, H. and Moscat, J. (2000). The atypical PKC-interacting protein p62 channels NF-kappaB activation by the IL-1-TRAF6 pathway. *Embo J* **19**, 1576-86.

Sarek, G., Jarviluoma, A. and Ojala, P. M. (2006). KSHV viral cyclin inactivates p27KIP1 through Ser10 and Thr187 phosphorylation in proliferating primary effusion lymphomas. *Blood* **107**, 725-32.

Sarid, R., Flore, O., Bohenzky, R. A., Chang, Y. and Moore, P. S. (1998). Transcription mapping of the Kaposi's sarcoma-associated herpesvirus (human herpesvirus 8) genome in a body cavity-based lymphoma cell line (BC-1). *J Virol* **72**, 1005-12.

Sarid, R., Sato, T., Bohenzky, R. A., Russo, J. J. and Chang, Y. (1997). Kaposi's sarcoma-associated herpesvirus encodes a functional bcl-2 homologue. *Nat Med* **3**, 293-8.

Sarid, R., Wiezorek, J. S., Moore, P. S. and Chang, Y. (1999). Characterization and cell cycle regulation of the major Kaposi's sarcoma-associated herpesvirus (human herpesvirus 8) latent genes and their promoter. *J Virol* **73**, 1438-46.

Scaffidi, C., Schmitz, I., Krammer, P. H. and Peter, M. E. (1999). The role of c-FLIP in modulation of CD95-induced apoptosis. *J Biol Chem* **274**, 1541-8.

Scatena, M., Almeida, M., Chaisson, M. L., Fausto, N., Nicosia, R. F. and Giachelli, C. M. (1998). NF-kappaB mediates alphavbeta3 integrin-induced endothelial cell survival. *J Cell Biol* **141**, 1083-93.

Schiemann, B., Gommerman, J. L., Vora, K., Cachero, T. G., Shulga-Morskaya, S., Dobles, M., Frew, E. and Scott, M. L. (2001). An essential role for BAFF in the normal development of B cells through a BCMA-independent pathway. *Science* **293**, 2111-4.

Schmidt-Supprian, M., Bloch, W., Courtois, G., Addicks, K., Israel, A., Rajewsky, K. and Pasparakis, M. (2000). NEMO/IKK gamma-deficient mice model incontinentia pigmenti. *Mol Cell* **5**, 981-92.

Schmitz, M. L. and Baeuerle, P. A. (1991). The p65 subunit is responsible for the strong transcription activating potential of NF-kappa B. *Embo J* **10**, 3805-17.

Schmitz, M. L., dos Santos Silva, M. A., Altmann, H., Czisch, M., Holak, T. A. and Baeuerle, P. A. (1994). Structural and functional analysis of the NF-kappa B p65 C terminus. An acidic and modular transactivation domain with the potential to adopt an alpha-helical conformation. *J Biol Chem* **269**, 25613-20.

Schmitz, M. L., Stelzer, G., Altmann, H., Meisterernst, M. and Baeuerle, P. A. (1995). Interaction of the COOH-terminal transactivation domain of p65 NF-kappa B with TATA-binding protein, transcription factor IIB, and coactivators. *J Biol Chem* **270**, 7219-26.

Schneider, P., Thome, M., Burns, K., Bodmer, J. L., Hofmann, K., Kataoka, T., Holler, N. and Tschopp, J. (1997). TRAIL receptors 1 (DR4) and 2 (DR5) signal FADD-dependent apoptosis and activate NF-kappaB. *Immunity* **7**, 831-6.

Schomer-Miller, B., Higashimoto, T., Lee, Y. K. and Zandi, E. (2006). Regulation of IkappaB kinase (IKK) complex by IKKgamma-dependent phosphorylation of the T-loop and C terminus of IKKbeta. *J Biol Chem* **281**, 15268-76.

Schulz, T. F. (1998). Kaposi's sarcoma-associated herpesvirus (human herpesvirus-8). *J Gen Virol* **79 (Pt 7)**, 1573-91.

Schulz, T. F. (2001). KSHV/HHV8-associated lymphoproliferations in the AIDS setting. *Eur J Cancer* **37**, 1217-26.

Schumm, K., Rocha, S., Caamano, J. and Perkins, N. D. (2006). Regulation of p53 tumour suppressor target gene expression by the p52 NF-kappaB subunit. *Embo J* **25**, 4820-32.

Schwam, D. R., Luciano, R. L., Mahajan, S. S., Wong, L. and Wilson, A. C. (2000). Carboxy terminus of human herpesvirus 8 latency-associated nuclear antigen mediates dimerization, transcriptional repression, and targeting to nuclear bodies. *J Virol* **74**, 8532-40.

Schwarz, M. and Murphy, P. M. (2001). Kaposi's sarcoma-associated herpesvirus G protein-coupled receptor constitutively activates NF-kappa B and induces proinflammatory cytokine and chemokine production via a C-terminal signaling determinant. *J Immunol* **167**, 505-13.

Searles, R. P., Bergquam, E. P., Axthelm, M. K. and Wong, S. W. (1999). Sequence and genomic analysis of a Rhesus macaque rhadinovirus with similarity to Kaposi's sarcoma-associated herpesvirus/human herpesvirus 8. *J Virol* **73**, 3040-53.

Sen, R. and Baltimore, D. (1986a). Inducibility of kappa immunoglobulin enhancer-binding protein Nf-kappa B by a posttranslational mechanism. *Cell* **47**, 921-8.

Sen, R. and Baltimore, D. (1986b). Multiple nuclear factors interact with the immunoglobulin enhancer sequences. *Cell* **46**, 705-16.

Senftleben, U., Cao, Y., Xiao, G., Greten, F. R., Krahn, G., Bonizzi, G., Chen, Y., Hu, Y., Fong, A., Sun, S. C. *et al.* (2001). Activation by IKKalpha of a second, evolutionary conserved, NF-kappa B signaling pathway. *Science* **293**, 1495-9.

Seo, T., Lee, D., Lee, B., Chung, J. H. and Choe, J. (2000). Viral interferon regulatory factor 1 of Kaposi's sarcoma-associated herpesvirus (human herpesvirus 8) binds to, and inhibits transactivation of, CREB-binding protein. *Biochem Biophys Res Commun* **270**, 23-7.

Seo, T., Park, J., Lim, C. and Choe, J. (2004). Inhibition of nuclear factor kappaB activity by viral interferon regulatory factor 3 of Kaposi's sarcoma-associated herpesvirus. *Oncogene* **23**, 6146-55.

Service, P. H. (1981). Kaposi's sarcoma and *Pneumocystis* pneumonia among homosexual men in New York City and California. *MMWR Morbidity and Mortality Weekly Report* **30**, 305-308.

Shaheen, R. M., Davis, D. W., Liu, W., Zebrowski, B. K., Wilson, M. R., Bucana, C. D., McConkey, D. J., McMahon, G. and Ellis, L. M. (1999). Antiangiogenic therapy targeting the tyrosine kinase receptor for vascular endothelial growth factor receptor inhibits the growth of colon cancer liver metastasis and induces tumor and endothelial cell apoptosis. *Cancer Res* **59**, 5412-6.

Shakhov, A. N. and Nedospasov, S. A. (2001). Expression profiling in knockout mice: lymphotoxin versus tumor necrosis factor in the maintenance of splenic microarchitecture. *Cytokine Growth Factor Rev* **12**, 107-19.

Sharp, D. A., Lawrence, D. A. and Ashkenazi, A. (2005). Selective knockdown of the long variant of cellular FLICE inhibitory protein augments death receptor-mediated caspase-8 activation and apoptosis. *J Biol Chem* **280**, 19401-9.

Sharp, T. V., Wang, H. W., Koumi, A., Hollyman, D., Endo, Y., Ye, H., Du, M. Q. and Boshoff, C. (2002). K15 protein of Kaposi's sarcoma-associated herpesvirus is latently expressed and binds to HAX-1, a protein with antiapoptotic function. *J Virol* **76**, 802-16.

Shaw, G. and Kamen, R. (1986). A conserved AU sequence from the 3' untranslated region of GM-CSF mRNA mediates selective mRNA degradation. *Cell* **46**, 659-67.

Shisler, J. L. and Moss, B. (2001). Molluscum contagiosum virus inhibitors of apoptosis: The MC159 v-FLIP protein blocks Fas-induced activation of procaspases and degradation of the related MC160 protein. *Virology* **282**, 14-25.

Siebenlist, U., Franzoso, G. and Brown, K. (1994). Structure, regulation and function of NF-kappa B. *Annu Rev Cell Biol* **10**, 405-55.

Simeoni, L., Kliche, S., Lindquist, J. and Schraven, B. (2004). Adaptors and linkers in T and B cells. *Curr Opin Immunol* **16**, 304-13.

Sirianni, M. C., Vincenzi, L., Fiorelli, V., Topino, S., Scala, E., Uccini, S., Angeloni, A., Faggioni, A., Cerimele, D., Cottoni, F. *et al.* (1998). gamma-Interferon production in peripheral blood mononuclear cells and tumor infiltrating lymphocytes from Kaposi's sarcoma patients: correlation with the presence of human herpesvirus-8 in peripheral blood mononuclear cells and lesional macrophages. *Blood* **91**, 968-76.

Smit, M. J., Verzijl, D., Casarosa, P., Navis, M., Timmerman, H. and Leurs, R. (2002). Kaposi's sarcoma-associated herpesvirus-encoded G protein-coupled receptor ORF74 constitutively activates p44/p42 MAPK and Akt via G(i) and phospholipase C-dependent signaling pathways. *J Virol* **76**, 1744-52.

Sodhi, A., Montaner, S., Patel, V., Zohar, M., Bais, C., Mesri, E. A. and Gutkind, J. S. (2000). The Kaposi's sarcoma-associated herpes virus G protein-coupled receptor up-regulates vascular endothelial growth factor expression and secretion through mitogen-activated protein kinase and p38 pathways acting on hypoxia-inducible factor 1alpha. *Cancer Res* **60**, 4873-80.

Solan, N. J., Miyoshi, H., Carmona, E. M., Bren, G. D. and Paya, C. V. (2002). RelB cellular regulation and transcriptional activity are regulated by p100. *J Biol Chem* **277**, 1405-18.

Soldi, R., Mitola, S., Strasly, M., Defilippi, P., Tarone, G. and Bussolino, F. (1999). Role of alphavbeta3 integrin in the activation of vascular endothelial growth factor receptor-2. *Embo J* **18**, 882-92.

Song, M. J., Deng, H. and Sun, R. (2003). Comparative study of regulation of RTA-responsive genes in Kaposi's sarcoma-associated herpesvirus/human herpesvirus 8. *J Virol* **77**, 9451-62.

Soulier, J., Grollet, L., Oksenhendler, E., Cacoub, P., Cazals-Hatem, D., Babinet, P., d'Agay, M. F., Clauvel, J. P., Raphael, M., Degos, L. *et al.* (1995). Kaposi's sarcoma-associated herpesvirus-like DNA sequences in multicentric Castleman's disease. *Blood* **86**, 1276-80.

Sozzani, S., Luini, W., Bianchi, G., Allavena, P., Wells, T. N., Napolitano, M., Bernardini, G., Vecchi, A., D'Ambrosio, D., Mazzeo, D. *et al.* (1998). The viral chemokine macrophage inflammatory protein-II is a selective Th2 chemoattractant. *Blood* **92**, 4036-9.

Sparmann, A. and Bar-Sagi, D. (2004). Ras-induced interleukin-8 expression plays a critical role in tumor growth and angiogenesis. *Cancer Cell* **6**, 447-58.

Spencer, E., Jiang, J. and Chen, Z. J. (1999). Signal-induced ubiquitination of IkappaBalpha by the F-box protein Slimb/beta-TrCP. *Genes Dev* **13**, 284-94.

Spyridopoulos, I., Brogi, E., Kearney, M., Sullivan, A. B., Cetrulo, C., Isner, J. M. and Losordo, D. W. (1997). Vascular endothelial growth factor inhibits endothelial cell apoptosis induced by tumor necrosis factor-alpha: balance between growth and death signals. *J Mol Cell Cardiol* **29**, 1321-30.

Srinivasula, S. M., Ahmad, M., Ottilie, S., Bullrich, F., Banks, S., Wang, Y., Fernandes-Alnemri, T., Croce, C. M., Litwack, G., Tomaselli, K. J. *et al.* (1997). FLAME-1, a novel

FADD-like anti-apoptotic molecule that regulates Fas/TNFR1-induced apoptosis. *J Biol Chem* **272**, 18542-5.

Stacker, S. A., Achen, M. G., Jussila, L., Baldwin, M. E. and Alitalo, K. (2002). Lymphangiogenesis and cancer metastasis. *Nat Rev Cancer* **2**, 573-83.

Staskus, K. A., Sun, R., Miller, G., Racz, P., Jaslowski, A., Metroka, C., Brett-Smith, H. and Haase, A. T. (1999). Cellular tropism and viral interleukin-6 expression distinguish human herpesvirus 8 involvement in Kaposi's sarcoma, primary effusion lymphoma, and multicentric Castleman's disease. *J Virol* **73**, 4181-7.

Staskus, K. A., Zhong, W., Gebhard, K., Herndier, B., Wang, H., Renne, R., Beneke, J., Pudney, J., Anderson, D. J., Ganem, D. *et al.* (1997). Kaposi's sarcoma-associated herpesvirus gene expression in endothelial (spindle) tumor cells. *J Virol* **71**, 715-9.

Stebbing, J., Bourboulia, D., Johnson, M., Henderson, S., Williams, I., Wilder, N., Tyrer, M., Youle, M., Imami, N., Kobu, T. *et al.* (2003). Kaposi's sarcoma-associated herpesvirus cytotoxic T lymphocytes recognize and target Darwinian positively selected autologous K1 epitopes. *J Virol* **77**, 4306-14.

Steven, A. C. a. S., P. G. . (1997). Herpesvirus capsid assembly and development.In Structural biology of viruses. New York: Oxford University Press.

Stifter, S. (2006). The role of nuclear factor kappaB on angiogenesis regulation through monocyte chemotactic protein-1 in myeloma. *Med Hypotheses* **66**, 384-6.

Stine, J. T., Wood, C., Hill, M., Epp, A., Raport, C. J., Schweickart, V. L., Endo, Y., Sasaki, T., Simmons, G., Boshoff, C. *et al.* (2000). KSHV-encoded CC chemokine vMIP-III is a CCR4 agonist, stimulates angiogenesis, and selectively chemoattracts TH2 cells. *Blood* **95**, 1151-7.

Stoker, M., O'Neill, C., Berryman, S. and Waxman, V. (1968). Anchorage and growth regulation in normal and virus-transformed cells. *Int J Cancer* **3**, 683-93.

Strasser, A., O'Connor, L. and Dixit, V. M. (2000). Apoptosis signaling. *Annu Rev Biochem* **69**, 217-45.

Stromblad, S., Becker, J. C., Yebra, M., Brooks, P. C. and Cheresh, D. A. (1996). Suppression of p53 activity and p21WAF1/CIP1 expression by vascular cell integrin alphaVbeta3 during angiogenesis. *J Clin Invest* **98**, 426-33.

Stromblad, S. and Cheresh, D. A. (1996). Integrins, angiogenesis and vascular cell survival. *Chem Biol* **3**, 881-5.

Sturzl, M., Brandstetter, H. and Roth, W. K. (1992). Kaposi's sarcoma: a review of gene expression and ultrastructure of KS spindle cells in vivo. *AIDS Res Hum Retroviruses* **8**, 1753-63.

Sturzl, M., Brandstetter, H., Zietz, C., Eisenburg, B., Raivich, G., Gearing, D. P., Brockmeyer, N. H. and Hofschneider, P. H. (1995). Identification of interleukin-1 and platelet-derived growth factor-B as major mitogens for the spindle cells of Kaposi's sarcoma: a combined in vitro and in vivo analysis. *Oncogene* **10**, 2007-16.

Sturzl, M., Hohenadl, C., Zietz, C., Castanos-Velez, E., Wunderlich, A., Ascherl, G., Biberfeld, P., Monini, P., Browning, P. J. and Ensoli, B. (1999). Expression of K13/v-FLIP gene of human herpesvirus 8 and apoptosis in Kaposi's sarcoma spindle cells. *J Natl Cancer Inst* **91**, 1725-33.

Suhara, T., Mano, T., Oliveira, B. E. and Walsh, K. (2001). Phosphatidylinositol 3-kinase/Akt signaling controls endothelial cell sensitivity to Fas-mediated apoptosis via regulation of FLICE-inhibitory protein (FLIP). *Circ Res* **89**, 13-9.

Sullivan, C. S. (2007). High conservation of Kaposi sarcoma--associated herpesvirus microRNAs implies important function. *J Infect Dis* **195**, 618-20.

Sun, L., Deng, L., Ea, C. K., Xia, Z. P. and Chen, Z. J. (2004). The TRAF6 ubiquitin ligase and TAK1 kinase mediate IKK activation by BCL10 and MALT1 in T lymphocytes. *Mol Cell* **14**, 289-301.

Sun, Q., Matta, H. and Chaudhary, P. M. (2003a). The human herpes virus 8-encoded viral FLICE inhibitory protein protects against growth factor withdrawal-induced apoptosis via NF-kappa B activation. *Blood* **101**, 1956-61.

Sun, Q., Matta, H., Lu, G. and Chaudhary, P. M. (2006). Induction of IL-8 expression by human herpesvirus 8 encoded vFLIP K13 via NF-kappaB activation. *Oncogene*.

Sun, Q., Zachariah, S. and Chaudhary, P. M. (2003b). The human herpes virus 8-encoded viral FLICE-inhibitory protein induces cellular transformation via NF-kappaB activation. *J Biol Chem* **278**, 52437-45.

Sun, R., Lin, S. F., Gradoville, L., Yuan, Y., Zhu, F. and Miller, G. (1998). A viral gene that activates lytic cycle expression of Kaposi's sarcoma-associated herpesvirus. *Proc Natl Acad Sci U S A* **95**, 10866-71.

Sun, S. C. and Ballard, D. W. (1999). Persistent activation of NF-kappaB by the tax transforming protein of HTLV-1: hijacking cellular IkappaB kinases. *Oncogene* **18**, 6948-58.

Sun, S. C., Ganchi, P. A., Beraud, C., Ballard, D. W. and Greene, W. C. (1994). Autoregulation of the NF-kappa B transactivator RelA (p65) by multiple cytoplasmic inhibitors containing ankyrin motifs. *Proc Natl Acad Sci U S A* **91**, 1346-50.

Sun, S. C. and Xiao, G. (2003). Deregulation of NF-kappaB and its upstream kinases in cancer. *Cancer Metastasis Rev* **22**, 405-22.

Sun, Z., Arendt, C. W., Ellmeier, W., Schaeffer, E. M., Sunshine, M. J., Gandhi, L., Annes, J., Petrzilka, D., Kupfer, A., Schwartzberg, P. L. *et al.* (2000). PKC-theta is required for TCR-induced NF-kappaB activation in mature but not immature T lymphocytes. *Nature* **404**, 402-7.

Suri, C., Jones, P. F., Patan, S., Bartunkova, S., Maisonpierre, P. C., Davis, S., Sato, T. N. and Yancopoulos, G. D. (1996). Requisite role of angiopoietin-1, a ligand for the TIE2 receptor, during embryonic angiogenesis. *Cell* **87**, 1171-80.

Suzuki, H., Chiba, T., Kobayashi, M., Takeuchi, M., Suzuki, T., Ichiyama, A., Ikenoue, T., Omata, M., Furuichi, K. and Tanaka, K. (1999). IkappaBalpha ubiquitination is catalyzed by an SCF-like complex containing Skp1, cullin-1, and two F-box/WD40-repeat proteins, betaTrCP1 and betaTrCP2. *Biochem Biophys Res Commun* **256**, 127-32.

Swanton, C., Mann, D. J., Fleckenstein, B., Neipel, F., Peters, G. and Jones, N. (1997). Herpes viral cyclin/Cdk6 complexes evade inhibition by CDK inhibitor proteins. *Nature* **390**, 184-7.

Szekely, L., Chen, F., Teramoto, N., Ehlin-Henriksson, B., Pokrovskaja, K., Szeles, A., Manneborg-Sandlund, A., Lowbeer, M., Lennette, E. T. and Klein, G. (1998). Restricted expression of Epstein-Barr virus (EBV)-encoded, growth transformation-associated antigens in an EBV- and human herpesvirus type 8-carrying body cavity lymphoma line. *J Gen Virol* **79 (Pt 6)**, 1445-52.

Tada, K., Okazaki, T., Sakon, S., Kobarai, T., Kurosawa, K., Yamaoka, S., Hashimoto, H., Mak, T. W., Yagita, H., Okumura, K. *et al.* (2001). Critical roles of TRAF2 and TRAF5 in tumor necrosis factor-induced NF-kappa B activation and protection from cell death. *J Biol Chem* **276**, 36530-4.

Taga, T. and Kishimoto, T. (1997). Gp130 and the interleukin-6 family of cytokines. *Annu Rev Immunol* **15**, 797-819.

Takaesu, G., Kishida, S., Hiyama, A., Yamaguchi, K., Shibuya, H., Irie, K., Ninomiya-Tsuji, J. and Matsumoto, K. (2000). TAB2, a novel adaptor protein, mediates activation of TAK1 MAPKKK by linking TAK1 to TRAF6 in the IL-1 signal transduction pathway. *Mol Cell* **5**, 649-58.

Takaesu, G., Surabhi, R. M., Park, K. J., Ninomiya-Tsuji, J., Matsumoto, K. and Gaynor, R. B. (2003). TAK1 is critical for IkappaB kinase-mediated activation of the NF-kappaB pathway. *J Mol Biol* **326**, 105-15.

Takeda, K., Takeuchi, O., Tsujimura, T., Itami, S., Adachi, O., Kawai, T., Sanjo, H., Yoshikawa, K., Terada, N. and Akira, S. (1999). Limb and skin abnormalities in mice lacking IKKalpha. *Science* **284**, 313-6.

Talbot, S. J., Weiss, R. A., Kellam, P. and Boshoff, C. (1999). Transcriptional analysis of human herpesvirus-8 open reading frames 71, 72, 73, K14, and 74 in a primary effusion lymphoma cell line. *Virology* **257**, 84-94.

Tanaka, M., Fuentes, M. E., Yamaguchi, K., Durnin, M. H., Dalrymple, S. A., Hardy, K. L. and Goeddel, D. V. (1999). Embryonic lethality, liver degeneration, and impaired NF-kappa B activation in IKK-beta-deficient mice. *Immunity* **10**, 421-9.

Tang, E. D., Wang, C. Y., Xiong, Y. and Guan, K. L. (2003). A role for NF-kappaB essential modifier/IkappaB kinase-gamma (NEMO/IKKgamma) ubiquitination in the activation of the IkappaB kinase complex by tumor necrosis factor-alpha. *J Biol Chem* **278**, 37297-305.

Tegethoff, S., Behlke, J. and Scheidereit, C. (2003). Tetrameric oligomerization of IkappaB kinase gamma (IKKgamma) is obligatory for IKK complex activity and NF-kappaB activation. *Mol Cell Biol* **23**, 2029-41.

Teichert-Kuliszewska, K., Kutryk, M. J., Kuliszewski, M. A., Karoubi, G., Courtman, D. W., Zucco, L., Granton, J. and Stewart, D. J. (2006). Bone morphogenetic protein receptor-2 signaling promotes pulmonary arterial endothelial cell survival: implications for loss-of-function mutations in the pathogenesis of pulmonary hypertension. *Circ Res* **98**, 209-17.

Teitelbaum, S. L. (2000). Bone resorption by osteoclasts. *Science* **289**, 1504-8.

Thanos, D., Du, W. and Maniatis, T. (1993). The high mobility group protein HMG I(Y) is an essential structural component of a virus-inducible enhancer complex. *Cold Spring Harb Symp Quant Biol* **58**, 73-81.

Thanos, D. and Maniatis, T. (1992). The high mobility group protein HMG I(Y) is required for NF-kappa B-dependent virus induction of the human IFN-beta gene. *Cell* **71**, 777-89.

Thanos, D. and Maniatis, T. (1995). Virus induction of human IFN beta gene expression requires the assembly of an enhanceosome. *Cell* **83**, 1091-100.

Thome, M. (2004). CARMA1, BCL-10 and MALT1 in lymphocyte development and activation. *Nat Rev Immunol* **4**, 348-59.

Thome, M., Schneider, P., Hofmann, K., Fickenscher, H., Meinl, E., Neipel, F., Mattmann, C., Burns, K., Bodmer, J. L., Schroter, M. *et al.* (1997). Viral FLICE-inhibitory proteins (FLIPs) prevent apoptosis induced by death receptors. *Nature* **386**, 517-21.

Thome, M. and Tschopp, J. (2001). Regulation of lymphocyte proliferation and death by FLIP. *Nat Rev Immunol* **1**, 50-8.

Thorley-Lawson, D. A. (2001). Epstein-Barr virus: exploiting the immune system. *Nat Rev Immunol* **1**, 75-82.

Thurau, M., Everett, H., Tapernoux, M., Tschopp, J. and Thome, M. (2006). The TRAF3-binding site of human molluscipox virus FLIP molecule MC159 is critical for its capacity to inhibit Fas-induced apoptosis. *Cell Death Differ.*

Tomkowicz, B., Singh, S. P., Cartas, M. and Srinivasan, A. (2002). Human herpesvirus-8 encoded Kaposin: subcellular localization using immunofluorescence and biochemical approaches. *DNA Cell Biol* **21**, 151-62.

Tomlinson, C. C. and Damania, B. (2004). The K1 protein of Kaposi's sarcoma-associated herpesvirus activates the Akt signaling pathway. *J Virol* **78**, 1918-27.

Tran, J., Master, Z., Yu, J. L., Rak, J., Dumont, D. J. and Kerbel, R. S. (2002). A role for survivin in chemoresistance of endothelial cells mediated by VEGF. *Proc Natl Acad Sci U S A* **99**, 4349-54.

Tran, J., Rak, J., Sheehan, C., Saibil, S. D., LaCasse, E., Korneluk, R. G. and Kerbel, R. S. (1999). Marked induction of the IAP family antiapoptotic proteins survivin and XIAP by VEGF in vascular endothelial cells. *Biochem Biophys Res Commun* **264**, 781-8.

Trompouki, E., Hatzivassiliou, E., Tsichritzis, T., Farmer, H., Ashworth, A. and Mosialos, G. (2003). CYLD is a deubiquitinating enzyme that negatively regulates NF-kappaB activation by TNFR family members. *Nature* **424**, 793-6.

Uccini, S., Ruco, L. P., Monardo, F., Stoppacciaro, A., Dejana, E., La Parola, I. L., Cerimele, D. and Baroni, C. D. (1994). Co-expression of endothelial cell and macrophage antigens in Kaposi's sarcoma cells. *J Pathol* **173**, 23-31.

Uhlik, M., Good, L., Xiao, G., Harhaj, E. W., Zandi, E., Karin, M. and Sun, S. C. (1998). NF-kappaB-inducing kinase and IkappaB kinase participate in human T-cell leukemia virus I Tax-mediated NF-kappaB activation. *J Biol Chem* **273**, 21132-6.

Valdimarsdottir, G., Goumans, M. J., Rosendahl, A., Brugman, M., Itoh, S., Lebrin, F., Sideras, P. and ten Dijke, P. (2002). Stimulation of Id1 expression by bone morphogenetic protein is sufficient and necessary for bone morphogenetic protein-induced activation of endothelial cells. *Circulation* **106**, 2263-70.

Van Belle, E., Witzenbichler, B., Chen, D., Silver, M., Chang, L., Schwall, R. and Isner, J. M. (1998). Potentiated angiogenic effect of scatter factor/hepatocyte growth factor via induction of vascular endothelial growth factor: the case for paracrine amplification of angiogenesis. *Circulation* **97**, 381-90.

Vart, R. J., Nikitenko, L. L., Lagos, D., Trotter, M. W., Cannon, M., Bourboulia, D., Gratrix, F., Takeuchi, Y. and Boshoff, C. (2007). Kaposi's sarcoma-associated herpesvirus-encoded interleukin-6 and G-protein-coupled receptor regulate angiopoietin-2 expression in lymphatic endothelial cells. *Cancer Res* **67**, 4042-51.

Verma, I. M., Stevenson, J. K., Schwarz, E. M., Van Antwerp, D. and Miyamoto, S. (1995). Rel/NF-kappa B/I kappa B family: intimate tales of association and dissociation. *Genes Dev* **9**, 2723-35.

Verma, S. C., Choudhuri, T., Kaul, R. and Robertson, E. S. (2006a). Latency-associated nuclear antigen (LANA) of Kaposi's sarcoma-associated herpesvirus interacts with origin recognition complexes at the LANA binding sequence within the terminal repeats. *J Virol* **80**, 2243-56.

Verma, S. C., Lan, K., Choudhuri, T. and Robertson, E. S. (2006b). Kaposi's sarcoma-associated herpesvirus-encoded latency-associated nuclear antigen modulates K1 expression through its cis-acting elements within the terminal repeats. *J Virol* **80**, 3445-58.

Verma, S. C., Lan, K. and Robertson, E. (2007). Structure and function of latency-associated nuclear antigen. *Curr Top Microbiol Immunol* **312**, 101-36.

Verma, U. N., Yamamoto, Y., Prajapati, S. and Gaynor, R. B. (2004). Nuclear role of I kappa B Kinase-gamma/NF-kappa B essential modulator (IKK gamma/NEMO) in NF-kappa B-dependent gene expression. *J Biol Chem* **279**, 3509-15.

Verschuren, E. W., Jones, N. and Evan, G. I. (2004). The cell cycle and how it is steered by Kaposi's sarcoma-associated herpesvirus cyclin. *J Gen Virol* **85**, 1347-61.

Verschuren, E. W., Klefstrom, J., Evan, G. I. and Jones, N. (2002). The oncogenic potential of Kaposi's sarcoma-associated herpesvirus cyclin is exposed by p53 loss in vitro and in vivo. *Cancer Cell* **2**, 229-41.

Viatour, P., Bentires-Alj, M., Chariot, A., Deregowski, V., de Leval, L., Merville, M. P. and Bours, V. (2003). NF- kappa B2/p100 induces Bcl-2 expression. *Leukemia* **17**, 1349-56.

Viejo-Borbolla, A., Kati, E., Sheldon, J. A., Nathan, K., Mattsson, K., Szekely, L. and Schulz, T. F. (2003). A Domain in the C-terminal region of latency-associated nuclear antigen 1 of Kaposi's sarcoma-associated Herpesvirus affects transcriptional activation and binding to nuclear heterochromatin. *J Virol* **77**, 7093-100.

Wadgaonkar, R., Phelps, K. M., Haque, Z., Williams, A. J., Silverman, E. S. and Collins, T. (1999). CREB-binding protein is a nuclear integrator of nuclear factor-kappaB and p53 signaling. *J Biol Chem* **274**, 1879-82.

Walts, A. E., Shintaku, I. P. and Said, J. W. (1990). Diagnosis of malignant lymphoma in effusions from patients with AIDS by gene rearrangement. *Am J Clin Pathol* **94**, 170-5.

Wan, X., Wang, H. and Nicholas, J. (1999). Human herpesvirus 8 interleukin-6 (vIL-6) signals through gp130 but has structural and receptor-binding properties distinct from those of human IL-6. *J Virol* **73**, 8268-78.

Wang, C., Deng, L., Hong, M., Akkaraju, G. R., Inoue, J. and Chen, Z. J. (2001). TAK1 is a ubiquitin-dependent kinase of MKK and IKK. *Nature* **412**, 346-51.

Wang, H. W., Sharp, T. V., Koumi, A., Koentges, G. and Boshoff, C. (2002a). Characterization of an anti-apoptotic glycoprotein encoded by Kaposi's sarcoma-associated herpesvirus which resembles a spliced variant of human survivin. *Embo J* **21**, 2602-15.

Wang, H. W., Trotter, M. W., Lagos, D., Bourboulia, D., Henderson, S., Makinen, T., Elliman, S., Flanagan, A. M., Alitalo, K. and Boshoff, C. (2004a). Kaposi sarcoma herpesvirus-induced cellular reprogramming contributes to the lymphatic endothelial gene expression in Kaposi sarcoma. *Nat Genet* **36**, 687-93.

Wang, J. F., Liu, Z. Y., Anand, A. R., Zhang, X., Brown, L. F., Dezube, B. J., Gill, P. and Ganju, R. K. (2004b). Alpha-chemokine-mediated signal transduction in human Kaposi's sarcoma spindle cells. *Biochim Biophys Acta* **1691**, 129-39.

Wang, L., Wakisaka, N., Tomlinson, C. C., DeWire, S. M., Krall, S., Pagano, J. S. and Damania, B. (2004c). The Kaposi's sarcoma-associated herpesvirus (KSHV/HHV-8) K1 protein induces expression of angiogenic and invasion factors. *Cancer Res* **64**, 2774-81.

Wang, Y., Cui, H., Schroering, A., Ding, J. L., Lane, W. S., McGill, G., Fisher, D. E. and Ding, H. F. (2002b). NF-kappa B2 p100 is a pro-apoptotic protein with anti-oncogenic function. *Nat Cell Biol* **4**, 888-93.

Wary, K. K., Mainiero, F., Isakoff, S. J., Marcantonio, E. E. and Giancotti, F. G. (1996). The adaptor protein Shc couples a class of integrins to the control of cell cycle progression. *Cell* **87**, 733-43.

Weber, C. H. and Vincenz, C. (2001). The death domain superfamily: a tale of two interfaces? *Trends Biochem Sci* **26**, 475-81.

Weich, H. A., Salahuddin, S. Z., Gill, P., Nakamura, S., Gallo, R. C. and Folkmann, J. (1991). AIDS-associated Kaposi's sarcoma-derived cells in long-term culture express and synthesize smooth muscle alpha-actin. *Am J Pathol* **139**, 1251-8.

Weninger, W., Partanen, T. A., Breiteneder-Geleff, S., Mayer, C., Kowalski, H., Mildner, M., Pammer, J., Sturzl, M., Kerjaschki, D., Alitalo, K. *et al.* (1999). Expression of vascular endothelial growth factor receptor-3 and podoplanin suggests a lymphatic endothelial cell origin of Kaposi's sarcoma tumor cells. *Lab Invest* **79**, 243-51.

Westerheide, S. D., Mayo, M. W., Anest, V., Hanson, J. L. and Baldwin, A. S., Jr. (2001). The putative oncoprotein Bcl-3 induces cyclin D1 to stimulate G(1) transition. *Mol Cell Biol* **21**, 8428-36.

Whiteside, S. T. and Israel, A. (1997). I kappa B proteins: structure, function and regulation. *Semin Cancer Biol* **8**, 75-82.

Wilkinson, J., Cope, A., Gill, J., Bourboulia, D., Hayes, P., Imami, N., Kubo, T., Marcelin, A., Calvez, V., Weiss, R. *et al.* (2002). Identification of Kaposi's sarcoma-associated herpesvirus (KSHV)-specific cytotoxic T-lymphocyte epitopes and evaluation of reconstitution of KSHV-specific responses in human immunodeficiency virus type 1-Infected patients receiving highly active antiretroviral therapy. *J Virol* **76**, 2634-40.

Winston, J. T., Strack, P., Beer-Romero, P., Chu, C. Y., Elledge, S. J. and Harper, J. W. (1999). The SCFbeta-TRCP-ubiquitin ligase complex associates specifically with phosphorylated destruction motifs in IkappaBalpha and beta-catenin and stimulates IkappaBalpha ubiquitination in vitro. *Genes Dev* **13**, 270-83.

Wojta, J., Kaun, C., Breuss, J. M., Koshelnick, Y., Beckmann, R., Hattey, E., Mildner, M., Weninger, W., Nakamura, T., Tschachler, E. *et al.* (1999). Hepatocyte growth factor increases expression of vascular endothelial growth factor and plasminogen activator inhibitor-1 in human keratinocytes and the vascular endothelial growth factor receptor flk-1 in human endothelial cells. *Lab Invest* **79**, 427-38.

Woods, A., Sherwin, T., Sasse, R., MacRae, T. H., Baines, A. J. and Gull, K. (1989). Definition of individual components within the cytoskeleton of Trypanosoma brucei by a library of monoclonal antibodies. *J Cell Sci* **93 (Pt 3)**, 491-500.

Woronicz, J. D., Gao, X., Cao, Z., Rothe, M. and Goeddel, D. V. (1997). IkappaB kinase-beta: NF-kappaB activation and complex formation with IkappaB kinase-alpha and NIK. *Science* **278**, 866-9.

Wu, C. and Ghosh, S. (1999). beta-TrCP mediates the signal-induced ubiquitination of IkappaBbeta. *J Biol Chem* **274**, 29591-4.

Wu, C. J., Conze, D. B., Li, T., Srinivasula, S. M. and Ashwell, J. D. (2006a). Sensing of Lys 63-linked polyubiquitination by NEMO is a key event in NF-kappaB activation [corrected]. *Nat Cell Biol* **8**, 398-406.

Wu, L., Lo, P., Yu, X., Stoops, J. K., Forghani, B. and Zhou, Z. H. (2000). Three-dimensional structure of the human herpesvirus 8 capsid. *J Virol* **74**, 9646-54.

Wu, Z. H., Shi, Y., Tibbetts, R. S. and Miyamoto, S. (2006b). Molecular linkage between the kinase ATM and NF-kappaB signaling in response to genotoxic stimuli. *Science* **311**, 1141-6.

Xiao, G., Cvijic, M. E., Fong, A., Harhaj, E. W., Uhlik, M. T., Waterfield, M. and Sun, S. C. (2001a). Retroviral oncoprotein Tax induces processing of NF-kappaB2/p100 in T cells: evidence for the involvement of IKKalpha. *Embo J* **20**, 6805-15.

Xiao, G., Fong, A. and Sun, S. C. (2004). Induction of p100 processing by NF-kappaB-inducing kinase involves docking IkappaB kinase alpha (IKKalpha) to p100 and IKKalpha-mediated phosphorylation. *J Biol Chem* **279**, 30099-105.

Xiao, G., Harhaj, E. W. and Sun, S. C. (2000). Domain-specific interaction with the I kappa B kinase (IKK)regulatory subunit IKK gamma is an essential step in tax-mediated activation of IKK. *J Biol Chem* **275**, 34060-7.

Xiao, G., Harhaj, E. W. and Sun, S. C. (2001b). NF-kappaB-inducing kinase regulates the processing of NF-kappaB2 p100. *Mol Cell* **7**, 401-9.

Xiao, G. and Sun, S. C. (2000). Activation of IKKalpha and IKKbeta through their fusion with HTLV-I tax protein. *Oncogene* **19**, 5198-203.

Xie, P., Hostager, B. S. and Bishop, G. A. (2004). Requirement for TRAF3 in signaling by LMP1 but not CD40 in B lymphocytes. *J Exp Med* **199**, 661-71.

Xin, X., Yang, S., Ingle, G., Zlot, C., Rangell, L., Kowalski, J., Schwall, R., Ferrara, N. and Gerritsen, M. E. (2001). Hepatocyte growth factor enhances vascular endothelial growth factor-induced angiogenesis in vitro and in vivo. *Am J Pathol* **158**, 1111-20.

Xu, Y. and Ganem, D. (2007). Induction of chemokine production by latent Kaposi's sarcoma-associated herpesvirus infection of endothelial cells. *J Gen Virol* **88**, 46-50.

Yamada, T., Mitani, T., Yorita, K., Uchida, D., Matsushima, A., Iwamasa, K., Fujita, S. and Matsumoto, M. (2000). Abnormal immune function of hemopoietic cells from alymphoplasia (aly) mice, a natural strain with mutant NF-kappa B-inducing kinase. *J Immunol* **165**, 804-12.

Yamamoto, Y., Verma, U. N., Prajapati, S., Kwak, Y. T. and Gaynor, R. B. (2003). Histone H3 phosphorylation by IKK-alpha is critical for cytokine-induced gene expression. *Nature* **423**, 655-9.

Yamaoka, S., Courtois, G., Bessia, C., Whiteside, S. T., Weil, R., Agou, F., Kirk, H. E., Kay, R. J. and Israel, A. (1998). Complementation cloning of NEMO, a component of the IkappaB kinase complex essential for NF-kappaB activation. *Cell* **93**, 1231-40.

Yang, J., Lin, Y., Guo, Z., Cheng, J., Huang, J., Deng, L., Liao, W., Chen, Z., Liu, Z. and Su, B. (2001). The essential role of MEKK3 in TNF-induced NF-kappaB activation. *Nat Immunol* **2**, 620-4.

Yang, J., Xu, Z. P., Huang, Y., Hamrick, H. E., Duerksen-Hughes, P. J. and Yu, Y. N. (2004). ATM and ATR: sensing DNA damage. *World J Gastroenterol* **10**, 155-60.

Yang, J. K., Wang, L., Zheng, L., Wan, F., Ahmed, M., Lenardo, M. J. and Wu, H. (2005). Crystal structure of MC159 reveals molecular mechanism of DISC assembly and FLIP inhibition. *Mol Cell* **20**, 939-49.

Yang, T. Y., Chen, S. C., Leach, M. W., Manfra, D., Homey, B., Wiekowski, M., Sullivan, L., Jenh, C. H., Narula, S. K., Chensue, S. W. *et al.* (2000). Transgenic expression of the chemokine receptor encoded by human herpesvirus 8 induces an angioproliferative disease resembling Kaposi's sarcoma. *J Exp Med* **191**, 445-54.

Yang, Z. and Wood, C. (2007). The transcriptional repressor K-RBP modulates RTA-mediated transactivation and lytic replication of Kaposi's sarcoma-associated herpesvirus. *J Virol* **81**, 6294-306.

Yaron, A., Gonen, H., Alkalay, I., Hatzubai, A., Jung, S., Beyth, S., Mercurio, F., Manning, A. M., Ciechanover, A. and Ben-Neriah, Y. (1997). Inhibition of NF-kappa-B cellular function via specific targeting of the I-kappa-B-ubiquitin ligase. *Embo J* **16**, 6486-94.

Yaron, A., Hatzubai, A., Davis, M., Lavon, I., Amit, S., Manning, A. M., Andersen, J. S., Mann, M., Mercurio, F. and Ben-Neriah, Y. (1998). Identification of the receptor component of the IkappaBalpha-ubiquitin ligase. *Nature* **396**, 590-4.

Ye, F. C., Blackbourn, D. J., Mengel, M., Xie, J. P., Qian, L. W., Greene, W., Yeh, I. T., Graham, D. and Gao, S. J. (2007). Kaposi's sarcoma-associated herpesvirus promotes angiogenesis by inducing angiopoietin-2 expression via AP-1 and Ets1. *J Virol* **81**, 3980-91.

Ye, J., Xie, X., Tarassishin, L. and Horwitz, M. S. (2000). Regulation of the NF-kappaB activation pathway by isolated domains of FIP3/IKKgamma, a component of the IkappaB-alpha kinase complex. *J Biol Chem* **275**, 9882-9.

Yeh, W. C., Itie, A., Elia, A. J., Ng, M., Shu, H. B., Wakeham, A., Mirtsos, C., Suzuki, N., Bonnard, M., Goeddel, D. V. *et al.* (2000). Requirement for Casper (c-FLIP) in regulation of death receptor-induced apoptosis and embryonic development. *Immunity* **12**, 633-42.

Yie, J., Merika, M., Munshi, N., Chen, G. and Thanos, D. (1999). The role of HMG I(Y) in the assembly and function of the IFN-beta enhanceosome. *Embo J* **18**, 3074-89.

Yilmaz, Z. B., Weih, D. S., Sivakumar, V. and Weih, F. (2003). RelB is required for Peyer's patch development: differential regulation of p52-RelB by lymphotoxin and TNF. *Embo J* **22**, 121-30.

Yin, L., Wu, L., Wesche, H., Arthur, C. D., White, J. M., Goeddel, D. V. and Schreiber, R. D. (2001). Defective lymphotoxin-beta receptor-induced NF-kappaB transcriptional activity in NIK-deficient mice. *Science* **291**, 2162-5.

Yin, M. J., Christerson, L. B., Yamamoto, Y., Kwak, Y. T., Xu, S., Mercurio, F., Barbosa, M., Cobb, M. H. and Gaynor, R. B. (1998). HTLV-I Tax protein binds to MEKK1 to stimulate IkappaB kinase activity and NF-kappaB activation. *Cell* **93**, 875-84.

Yin, X. M., Oltvai, Z. N. and Korsmeyer, S. J. (1994). BH1 and BH2 domains of Bcl-2 are required for inhibition of apoptosis and heterodimerization with Bax. *Nature* **369**, 321-3.

Yoshida, M., Miyoshi, I. and Hinuma, Y. (1982). Isolation and characterization of retrovirus from cell lines of human adult T-cell leukemia and its implication in the disease. *Proc Natl Acad Sci U S A* **79**, 2031-5.

Yoshida, S., Ono, M., Shono, T., Izumi, H., Ishibashi, T., Suzuki, H. and Kuwano, M. (1997). Involvement of interleukin-8, vascular endothelial growth factor, and basic fibroblast growth factor in tumor necrosis factor alpha-dependent angiogenesis. *Mol Cell Biol* **17**, 4015-23.

Yoshizaki, K., Matsuda, T., Nishimoto, N., Kuritani, T., Taeho, L., Aozasa, K., Nakahata, T., Kawai, H., Tagoh, H., Komori, T. *et al.* (1989). Pathogenic significance of interleukin-6 (IL-6/BSF-2) in Castleman's disease. *Blood* **74**, 1360-7.

Yu, F., Harada, J. N., Brown, H. J., Deng, H., Song, M. J., Wu, T. T., Kato-Stankiewicz, J., Nelson, C. G., Vieira, J., Tamanoi, F. *et al.* (2007). Systematic identification of cellular signals reactivating Kaposi sarcoma-associated herpesvirus. *PLoS Pathog* **3**, e44.

Yu, X., Zhan, X., D'Costa, J., Tanavde, V. M., Ye, Z., Peng, T., Malehorn, M. T., Yang, X., Civin, C. I. and Cheng, L. (2003). Lentiviral vectors with two independent internal promoters transfer high-level expression of multiple transgenes to human hematopoietic stem-progenitor cells. *Mol Ther* **7**, 827-38.

Zandi, E., Chen, Y. and Karin, M. (1998). Direct phosphorylation of IkappaB by IKKalpha and IKKbeta: discrimination between free and NF-kappaB-bound substrate. *Science* **281**, 1360-3.

Zandi, E., Rothwarf, D. M., Delhase, M., Hayakawa, M. and Karin, M. (1997). The IkappaB kinase complex (IKK) contains two kinase subunits, IKKalpha and IKKbeta, necessary for IkappaB phosphorylation and NF-kappaB activation. *Cell* **91**, 243-52.

Zarnegar, B., He, J. Q., Oganesyan, G., Hoffmann, A., Baltimore, D. and Cheng, G. (2004). Unique CD40-mediated biological program in B cell activation requires both type 1 and type 2 NF-kappaB activation pathways. *Proc Natl Acad Sci U S A* **101**, 8108-13.

Zeng, Q., Chen, S., You, Z., Yang, F., Carey, T. E., Saims, D. and Wang, C. Y. (2002). Hepatocyte growth factor inhibits anoikis in head and neck squamous cell carcinoma cells by activation of ERK and Akt signaling independent of NFkappa B. *J Biol Chem* **277**, 25203-8.

Zhang, H., Bajraszewski, N., Wu, E., Wang, H., Moseman, A. P., Dabora, S. L., Griffin, J. D. and Kwiatkowski, D. J. (2007). PDGFRs are critical for PI3K/Akt activation and negatively regulated by mTOR. *J Clin Invest* **117**, 730-8.

Zhang, S. Q., Kovalenko, A., Cantarella, G. and Wallach, D. (2000). Recruitment of the IKK signalosome to the p55 TNF receptor: RIP and A20 bind to NEMO (IKKgamma) upon receptor stimulation. *Immunity* **12**, 301-11.

Zhong, H., May, M. J., Jimi, E. and Ghosh, S. (2002). The phosphorylation status of nuclear NF-kappa B determines its association with CBP/p300 or HDAC-1. *Mol Cell* **9**, 625-36.

Zhong, W., Wang, H., Herndier, B. and Ganem, D. (1996). Restricted expression of Kaposi sarcoma-associated herpesvirus (human herpesvirus 8) genes in Kaposi sarcoma. *Proc Natl Acad Sci U S A* **93**, 6641-6.

Zhou, H., Wertz, I., O'Rourke, K., Ultsch, M., Seshagiri, S., Eby, M., Xiao, W. and Dixit, V. M. (2004). Bcl10 activates the NF-kappaB pathway through ubiquitination of NEMO. *Nature* **427**, 167-71.

Zhuge, X., Murayama, T., Arai, H., Yamauchi, R., Tanaka, M., Shimaoka, T., Yonehara, S., Kume, N., Yokode, M. and Kita, T. (2005). CXCL16 is a novel angiogenic factor for human umbilical vein endothelial cells. *Biochem Biophys Res Commun* **331**, 1295-300.

Zimber-Strobl, U., Kempkes, B., Marschall, G., Zeidler, R., Van Kooten, C., Banchereau, J., Bornkamm, G. W. and Hammerschmidt, W. (1996). Epstein-Barr virus latent membrane protein (LMP1) is not sufficient to maintain proliferation of B cells but both it and activated CD40 can prolong their survival. *Embo J* **15**, 7070-8.

Zong, J. C., Ciufo, D. M., Alcendor, D. J., Wan, X., Nicholas, J., Browning, P. J., Rady, P. L., Tyring, S. K., Orenstein, J. M., Rabkin, C. S. *et al.* (1999). High-level variability in the ORF-K1 membrane protein gene at the left end of the Kaposi's sarcoma-associated herpesvirus genome defines four major virus subtypes and multiple variants or clades in different human populations. *J Virol* **73**, 4156-70.

Zufferey, R., Nagy, D., Mandel, R. J., Naldini, L. and Trono, D. (1997). Multiply attenuated lentiviral vector achieves efficient gene delivery in vivo. *Nat Biotechnol* **15**, 871-5.